# Seismic loss modelling in insurance industry : towards a new model for better claims management

Adrien Pothon

# THÈSE

Pour obtenir le grade de

**DOCTEUR DE L'UNIVERSITÉ GRENOBLE ALPES**
Spécialité : **Sciences de la Terre, l'Univers et l'Environnement**

Arrêté ministériel : 25 mai 2016

Présentée par


## Adrien POTHON


Thèse dirigée par **Philippe GUEGUEN** et
codirigée par **Pierre-Yves BARD**

préparée au sein de l'**Institut des Sciences de la Terre**
dans **l'École Doctorale Terre, Univers, Environnement**

# Seismic loss modelling in insurance industry: towards a new model for better claims management

Thèse soutenue publiquement le **29 Janvier 2019**,
devant le jury composé de :

**M. Christian ROBERT**
Université Lyon 1/ISFA, Rapporteur
**M. Fabrice COTTON**
Université Potsdam/GFZ Germany, Rapporteur
**Mme. Oona SCOTTI**
Institut de Radio Protection et Sureté Nucléaire – France, Examinateur
**M. Stéphane GARAMBOIS**
Université de Grenoble/ISTerre, Président du jury
**M. Sylvain BUISINE**
AXA GIE – Group Risk Management, Invité
**M. Philippe GUEGUEN**
IFSTTAR – ISTerre – CNRS, Directeur de thèse
**M. Pierre-Yves BARD**
IFSTTAR – ISTerre – CNRS, Directeur de thèse

*Le paresseux est celui qui,*

*ayant un shaker à cocktail dans la main,*

*attend le prochain tremblement de terre.*

*Danny Kaye (1911-1987)*

# REMERCIEMENTS

Lorsque j'ai débuté cette thèse le 1er octobre 2016, je travaillais déjà depuis quatre ans dans le secteur des assurances, dont les deux dernières au Group Risk Management d'AXA. Le choix de m'engager dans un travail de recherche en parallèle de mes missions d'actuaire a été un vrai défi, autant pour ma hiérarchie que pour moi. Ainsi, je tiens à ouvrir ces remerciements en adressant toute ma gratitude à mon manager Sylvain BUISINE pour m'avoir encadré durant la thèse et encouragé dans les moments les plus difficiles, à Mathieu CHOUX, mon ancien manager, qui m'a aidé à réunir les conditions pour que ce projet de thèse puisse être lancé, et plus généralement à AXA pour la confiance que l'entreprise a placée en moi.

Je suis également très reconnaissant à Philippe GUEGUEN et Pierre Yves BARD, mes deux directeurs de thèse, pour la qualité de leur encadrement. Pour eux aussi cette thèse était une vraie prise de risque : du fait de mon cursus académique et professionnel, j'avais tout à apprendre du travail d'un scientifique, que ce soit la rigueur, la démarche ou encore la restitution des travaux. A leur côté, j'ai beaucoup progressé et c'est avant tout grâce à eux que j'ai pu soutenir cette thèse et en publier certaines parties dans deux journaux scientifiques.

Ensuite, j'adresse mes remerciements les plus chaleureux à Fabrice COTTON, Oona SCOTTI, Christian ROBERT, et Stéphane GARAMBOIS pour avoir accepté de constituer mon jury de thèse. Leur différent champ d'expertise est représentatif de l'interdisciplinarité de cette thèse.

Un grand merci aussi à mes collègues d'AXA qui m'ont apporté une aide précieuse chacun dans leur domaine respectif : ma responsable Madeleine-Sophie DEROCHE, Mathis JOFFRAIN, analyste sénior des risques de catastrophes naturelles, et Jérémie BONNEFOY, responsable des risques liées à l'épargne en assurance.

Je voudrais chaleureusement remercier l'ensemble des personnes qui ont alimenté ma passion pour le risque de tremblement de terre, et plus particulièrement Pierre MOUROUX, Christophe SIRA et Antoine SCHLUPP qui ont été et resteront pour moi des mentors et des modèles à suivre.

Enfin, le soutien familial est indispensable au bon déroulement d'une thèse. Je voudrais donc clore ces remerciements en déclarant à ma femme, ma famille et mes proches toute l'affection que je leur porte pour m'avoir aimé, encouragé et entouré durant toutes ces années.

# ABSTRACT

Several scientific studies highlight that earthquake is the natural disasters causing the highest uninsured loss, whether considering historical events or the expected annual average loss for the next years. In this context, my PhD topic is: “Seismic loss modelling in the insurance industry: towards a new model for better claims management”. Works can be divided in three parts: 1° review of current earthquake insurance models in different countries; 2° identify the main challenges for improving earthquake risk modelling; 3° introduce a new earthquake insurance model.

Two countries have been selected for the existing earthquake insurance models review: France and California. By cross-analysing risk perception indicators and economic variables a maturity scale dedicated to earthquake risk has been proposed. This tool allows to identify any decline or development in insurance market. Among the two countries studied, it shows that none of them has a sustainable earthquake insurance model.

In France, earthquake risk is covered since 1982 by a public-private insurance scheme called the CAT-NAT plan. Analysing all the historical CAT-NAT statements published after an earthquake in metropolitan France, an empirical probabilistic model for CAT-NAT statement has been developed. The model has been tested on two scenarios characterizing the consequences of a severe earthquake in metropolitan France and results show that the State could be struggled to pay its loss share as defined in the CAT-NAT plan.

About California, earthquake risk is covered by private insurance companies. Despite a high-risk level, only 15% of people are insured. To understand this low attractiveness, a study has been made to differentiate the contribution of the risk perception from the insurance cost. Results show that most of California households do not buy earthquake insurance because of the price and not because of risk underestimate. This study indicates also that most people would buy such an insurance if the price was divided by a factor of three.

The maturity scale introduced in this thesis also indicates that improving current insurance solutions requires to improve risk modelling. Therefore, we have developed a new method for comparing probabilistic seismic hazard maps with the estimated footprints of past events. Moreover, better stochastic loss models for earthquake risk necessitate to improve damage to

loss ratio relationships. To do so, a database about economic damage caused by past earthquakes and an economic model have been created. This model allows to test existing damage to loss ratio relationships with data from this new earthquake damage database.

The last part of this PhD work is dedicated to introduce a new earthquake insurance model. As long as no damaging earthquake occurs, the premium amount is invested on financial markets and the profits made are used to increase to capital for paying the future claims. Furthermore, in the proposed model, the insurance company takes over the repairing or reconstruction works after a damaging earthquake. If no damaging event occurs during a predetermined period, the capital is used to seismic retrofit the insured building. The capital decrease corresponding to the cost of works is counterbalanced by the decrease of the building seismic vulnerability. This allows to decrease the premium amount and to create a virtuous circle of earthquake risk mitigation.

# RESUME

Plusieurs rapports scientifiques ont mis en évidence que, tant sur l'historique des pertes liées aux catastrophes naturelles, que sur le coût moyen attendu pour les années à venir, le risque sismique est celui pour lequel la perte non-assurée est la plus forte parmi l'ensemble des catastrophes naturelles. Dans ce contexte, le sujet retenu pour ma thèse est : « Modélisation du risque sismique en assurance : étude d'un nouveau modèle pour une meilleure gestion assurantielle ». Les travaux s'organisent en trois parties : 1° présentation des différents systèmes assurantiels contre le risque sismique à travers le monde ; 2° identification des principaux axes d'amélioration de la modélisation du risque ; 3° propositions pour un nouveau modèle assurantiel.

La revue des systèmes d'assurance a porté principalement sur les deux pays suivants: la France et la Californie. En combinant plusieurs variables liées au niveau de risque, mis en perspective avec différents indicateurs économiques, nous avons créé une échelle de maturité dédiée à l'assurance sismique. Cet outil permet de mesurer l'évolution, à la hausse comme à la baisse, d'un marché d'assurance. En l'appliquant aux deux pays étudiés, il en ressort qu'aucun d'eux n'est équipé d'un système assurantiel durable.

En France, le risque de tremblement de terre est couvert par le régime CAT-NAT depuis 1982. En étudiant l'ensemble des communes reconnues en état de catastrophe naturelle à la suite d'un séisme, un modèle probabiliste de reconnaissance d'état de catastrophe naturelle a été développé. En l'appliquant à deux scénarios représentatifs d'un séisme majeur en France métropolitaine, les résultats montrent que l'Etat pourrait être mis en difficulté pour payer la charge des sinistres qui lui incombe dans le cadre du régime CAT-NAT.

En Californie, malgré que le risque soit important, seulement 15% de la population est assurée. Nous avons mené une étude différenciant l'effet de la perception du risque sismique par les Californiens de celui du prix de l'assurance. Les résultats montrent que les Californiens n'adhèrent pas aux offres d'assurance à cause de leur prix, et non par sous-estimation du risque. Ce modèle démontre aussi que la majorité des Californiens achèteraient une assurance tremblement de terre si son prix était divisé par trois.

D’après l’échelle de maturité préalablement développée, l’évolution de ce système assurantiel demande une meilleure modélisation du risque. Pour cela, nous avons élaboré une nouvelle méthode de comparaison entre des cartes d’aléas probabilistes et les modélisations d’empreintes d’aléa. Le perfectionnement des modèles stochastiques de pertes liées à un tremblement de terre nécessite également de renforcer la relation entre l’échelle de dommages utilisée et les coûts de réparation associés. Pour cela, une base de données des conséquences économiques des séismes passés a été constituée. En outre, un modèle économique a été élaboré pour tester les modèles dommages-coût existants avec les données historiques précédemment collectées.

Enfin, la dernière partie de mon travail de thèse porte sur l’étude d’un nouveau modèle assurantiel dans lequel le montant des primes est alloué à chaque bâtiment. Tant qu’un séisme n’endommage pas un bâtiment assuré, le montant des primes est investi pour accroître les ressources disponibles. Quand un séisme survient et endommage un bâtiment assuré, la compagnie d’assurance prend en charge les travaux de réparation ou de reconstruction. Si les ressources accumulées sont suffisamment importantes avant qu’un séisme survienne, celles-ci sont utilisées pour financer des travaux de renforcement parasismique. Le coût associé est alors compensé par le gain de résistance du bâtiment. Cela permet ainsi de diminuer la prime payée par l’assuré et créer un cercle vertueux de prévention des risques.

# TABLE OF CONTENTS

# CHAPTER 1: GENERAL INTRODUCTION

## 1.1. Problématique

Aucune catastrophe naturelle n'a eu plus d'impact dans l'Histoire de l'Humanité que le tremblement de terre de 1755 à Lisbonne (Molesky 2016). Alors que la chute de l'Empire Romain a montré qu'aucune civilisation n'est éternelle, cet événement a mis un terme à la croyance de l'époque que la Science pouvait maîtriser la Nature (Molesky 2016). Ce séisme fut d'une ampleur dramatique, causant entre 10,000 et 30,000 morts (Mullin 1992) et une perte économique estimée entre 32% et 48% du PIB du Portugal à l'époque (Pereira 2009). Il n'en demeure pas moins que les réformes économiques prises lors de la reconstruction ont permis que cette catastrophe ait un impact positif à long terme sur l'économie du Portugal (Pereira 2009). En outre, cela a été l'occasion de reconstruire une ville plus adaptée aux besoins du commerce (routes droites, plus larges et dédiées à différents types de commerces) et plus résiliente face au risque sismique (des bâtiments en matériaux plus ductiles et des rues plus larges pour limiter le risque d'entrechoquement des bâtiments).

Le financement de la reconstruction a été possible grâce à l'aide de plusieurs Etats Européens ainsi que le Brésil, colonie Portugaise au moment du séisme (Mullin 1992). Un protectionnisme économique a également été mis en place pour favoriser le développement de l'industrie portugaise. De plus, une taxe de 4% sur les importations et transactions commerciales a été instaurée pour lever des fonds supplémentaires.

De nos jours, les besoins financiers nécessaires à la reconstruction post-séisme peuvent être en partie pris en charge par l'assurance. Si le séisme de 1755 était survenu en 2008, la perte économique directe aurait été de €146.1bn (Tang et al. 2012), correspondant à 82% du PIB du Portugal. Toutefois, la perte assurantielle n'était estimée qu'à hauteur de €12bn (Franco et Shen-Tu 2009), soit moins de 8% de la perte économique directe. Or, un rapport de la Banque Mondiale (Melecky et Raddatz 2011) a montré que l'évolution du PIB d'un pays touché par

une catastrophe dépendait du niveau de couverture de l'assurance : dans le cas des pays à faible couverture assurantielle, l'étude montre que le PIB diminue en moyenne de 8% au cours des 10 années qui suivent la survenance d'une catastrophe naturelle ; alors qu'il augmente de 10% sur la même période dans le cas contraire. Ainsi, augmenter la couverture d'assurance pour les catastrophes naturelles représente un enjeu majeur pour la résilience des pays face à ce risque.

Depuis le développement de ce type d'assurance en Californie au début du XX$^{e}$ siècle (Goltz 1985), les mécanismes d'assurances n'ont cessé d'évoluer pour proposer une couverture toujours mieux adaptée à ce risque. Jusqu'au milieu des années 1990, les assurances calculaient les pertes assurantielles que pouvait causer un séisme avec une approche empirique : les tremblements de terre et les pertes associées des décennies précédentes étaient considérées comme représentatives du risque qui pouvait se produire (Grossi et al. 2008). Les séismes de Northridge en 1994, puis de Kobe en 1995 causèrent des pertes assurantielles au-delà des estimations faites à l'époque. Cela amena les compagnies d'assurance à utiliser des modèles stochastiques de pertes pour modéliser le risque de tremblement de terre. En 2012, l'entreprise leader sur le marché de cette modélisation est Risk Management Solutions (RMS), avec plus de 50% des sociétés d'assurance et réassurance utilisant leurs logiciels (Ericson et Mitas 2012). Un modèle stochastique de pertes peut se décomposer en cinq étapes, comme illustré par la Figure 1.1.

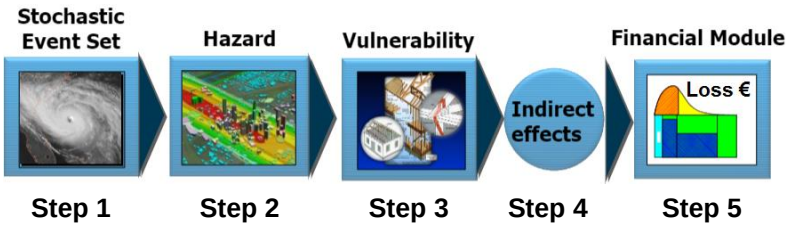


Figure 1.1: Principales étapes d'un modèle stochastique de pertes liées à une catastrophe naturelle (par exemple le tremblement de terre). Les "Indirect effects" regroupent l'ensemble des effets économiques qui peuvent faire augmenter le montant des dégâts (par exemple l'inflation des coûts de reconstruction). Source : Risk Management Solutions (Patmore 2008).

La première étape appelée "Stochastic Event Set" consiste à définir l'ensemble des événements possibles (ici des séismes) qui peuvent survenir dans la zone étudiée. L'enjeu de cette étape est d'associer la bonne fréquence de survenance à chaque type de séisme. La difficulté que cela représente peut s'apprécier à la lumière des séismes extrêmes : avant la survenance du séisme de Tohoku (2011, Mw9) au Japon, le modèle stochastique de pertes produit par RMS (Tabucchi

et Grossi 2012) considérait que la magnitude d'un séisme dans cette zone ne pouvait pas dépasser Mw8.3 (c'est-à-dire que les séismes de magnitude supérieure avaient une fréquence nulle). Cette problématique de la magnitude maximale est toujours d'actualité via le concept des Low Probability/High Consequences events, par exemple pour un séisme similaire à celui de Lisbonne en 1755 dont l'estimation de la magnitude varie entre Mw8.6 et Mw9 (Rodrigues et Craig 2008).

La deuxième étape consiste à modéliser l'empreinte du mouvement du sol que peut générer chaque événement sismique définit dans la première étape. Cela peut être illustré par le programme ShakeMap (Allen et al. 2009), développé par l'USGS, qui produit une estimation de l'empreinte du mouvement du sol pour les séismes majeurs passés. La modélisation repose principalement sur l'utilisation d'équations de prédiction du mouvement du sol (GMPE). Néanmoins, résumer la propagation d'ondes sismiques par une équation est un travail sujet à beaucoup d'incertitudes. Douglas (2019) a recensé 462 équations différentes publiées entre 1964 et 2019 pour la seule mesure de l'accélération maximale au sol (PGA). Malgré un nombre grandissant d'observations (Fig. 1.2a ; Bommer et al. 2010) et donc de variables explicatives pour calculer le mouvement du sol (Fig. 1.2b; Bommer et al. 2010), l'écart-type du terme d'erreur (définit comme la différence entre la valeur observée et la valeur modélisée) reste constant (Fig. 1.2c ; Strasser et al. 2009).

La troisième et la quatrième étape consistent à calculer une perte économique à partir du niveau du mouvement du sol pour chaque bâtiment assuré. La complexité de cette opération vient de la nature même d'un portefeuille d'assurance : le nombre de bâtiments assurés est très important (généralement en centaines de milliers), ils sont répartis sur un vaste territoire et chacun d'eux a une importance à la hauteur de la perte financière qu'il peut générer en cas de séisme. Dès lors, le calcul des pertes doit être à la fois précis pour estimer une perte au niveau d'un bâtiment et simple pour être appliqué à l'ensemble du portefeuille d'assurance. Cependant, la plupart des modèles de pertes existants dans la littérature scientifique sont soit au niveau du bâtiment (par exemple RISK-UE ; Milutinovic et Trendafiloski 2003 ou HAZUS ; Federal Emergency Management Agency 2010), soit au niveau d'une région (par exemple PAGER ; Jaiswal et Wald 2011). Par ailleurs les modèles à l'échelle du bâtiment requièrent un large éventail d'informations (comme les matériaux de construction utilisés dans les murs porteurs) qui sont difficilement accessibles à une large échelle (Riedel et al. 2015).

Dans la cinquième étape, les conditions financières, propres à chaque contrat d'assurance, sont

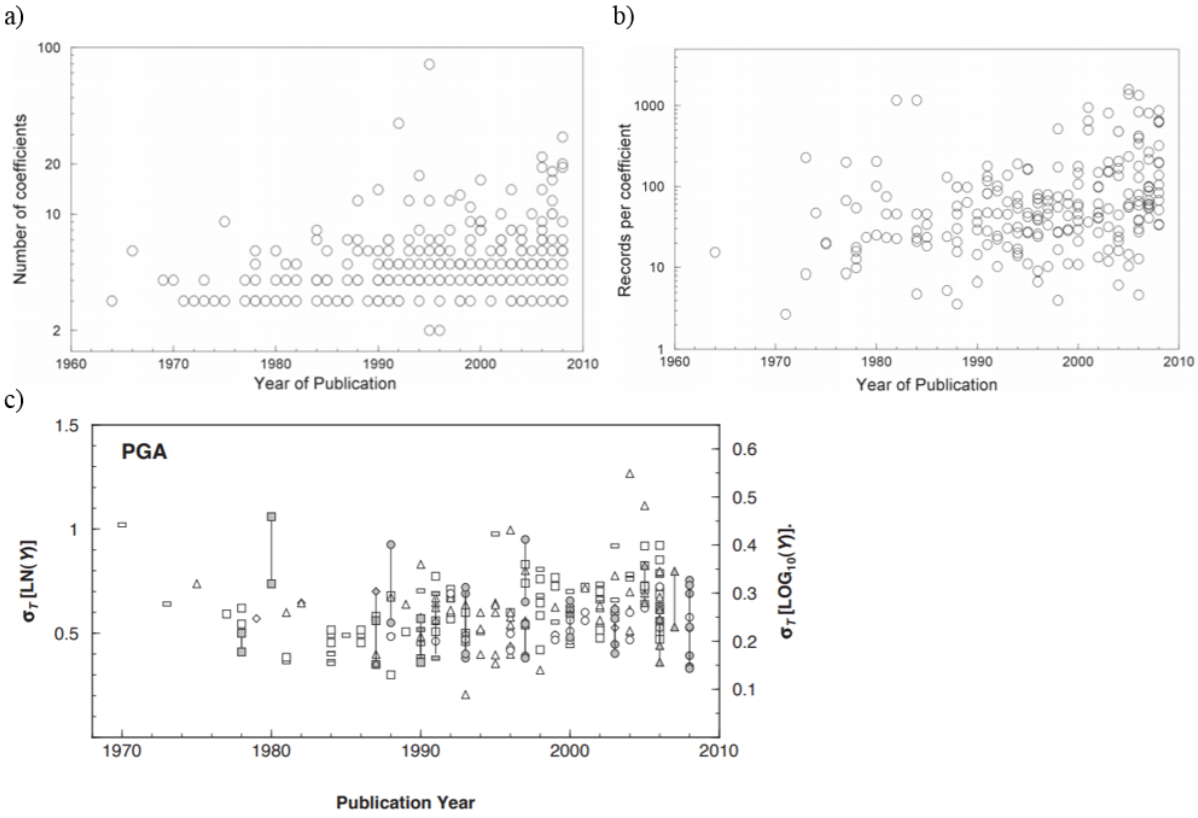


Figure 1.2: Evolution temporelle des équations de prédiction du mouvement du sol (GMPE) en fonction: a) du nombre de coefficients dans l'équation ; du nombre de données par coefficients utilisées pour calibrer l'équation et c) de l'écart-type ($\sigma_T$[LN(Y)]) de l'erreur de modélisation. Sources : figures a) et b) : Bommer et al. (2010) ; Figure c) : Strasser et al. (2009).

appliquées aux pertes modélisées. Celles-ci peuvent concerner des assurés (franchise, limite de couverture, exclusion de garantie), des assureurs partenaires (coassurance), ou des réassureurs (couverture de réassurance). Également, elles peuvent porter sur un bâtiment en particulier ou un groupe de bâtiments au sein d'une même police d'assurance qui partagent une caractéristique commune (par exemple être situé dans le même pays). Appliquer l'ensemble de ces conditions financières en respectant l'ordre de priorité défini contractuellement (par exemple, l'assurance ne peut pas demander aux réassureurs d'être remboursé pour la perte supportée par la coassurance), est toute la difficulté de cette étape.

Les choix de modélisation faits à chacune de ces étapes ont une forte incidence sur les estimations de pertes produites par différents modèles, comme l'illustre la Figure 1.3. Elle montre que pour une période de retour de 100 ans (soit une probabilité de survenance de 1% par an) la perte pour l'ensemble du portefeuille analysé peut varier entre €120m. et €380m., soit

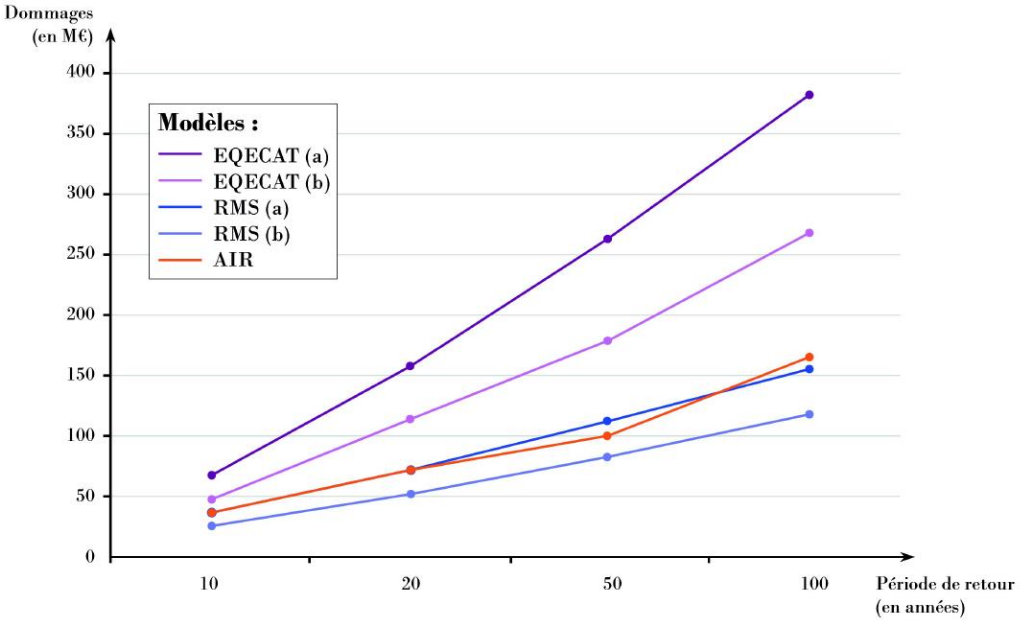


Figure 1.3: Illustration de la distribution de pertes pour un même portefeuille d'assurance selon trois logiciels différents. Source : Bourguignon (2014). EQECAT (CoreLogic depuis 2013), RMS et AIR (nom complet : AIR Worldwide) sont les trois principales entreprises sur le marché de la modélisation stochastique de pertes liées à des catastrophes naturelles, pour les assurances.

un écart supérieur à un facteur 3. Cette variabilité d'un modèle à un autre est d'autant plus incompréhensible pour les compagnies d'assurance qu'elle reste très importante entre deux versions successives d'un modèle fourni par une même entreprise de modélisation (Fig. 1.3 *EQECAT (a)* et *EQECAT(b)*).

Dans ce contexte, les entreprises d'assurance et de réassurance ont développé leur propre modèle stochastique de pertes, afin de maîtriser les différentes hypothèses de modélisation, et donc la distribution de pertes (Fig. 1.3). En outre, les compagnies d'assurances et de réassurance bénéficient de base de données détaillées (Fig. 1.4) sur les bâtiments exposés et les pertes à la suite de séismes passés auxquelles n'ont pas accès les entreprises de modélisation.

Ces données sont très utiles pour améliorer les étapes 3 et 4 dans la chaine d'un modèle de pertes stochastiques (Fig. 1.1). En effet, elles permettent de développer de nouveaux modèles adaptés à ce besoin de modélisation (beaucoup de bâtiments répartis sur un vaste territoire), avec une meilleure connaissance à la fois de chaque bâtiment assuré et du montant de la perte correspondant, à la suite d'un événement passé.

Au-delà du développement de nouveaux modèles de pertes stochastiques, les sociétés d'assurance et de réassurance investissent également sur le développement de nouvelles polices

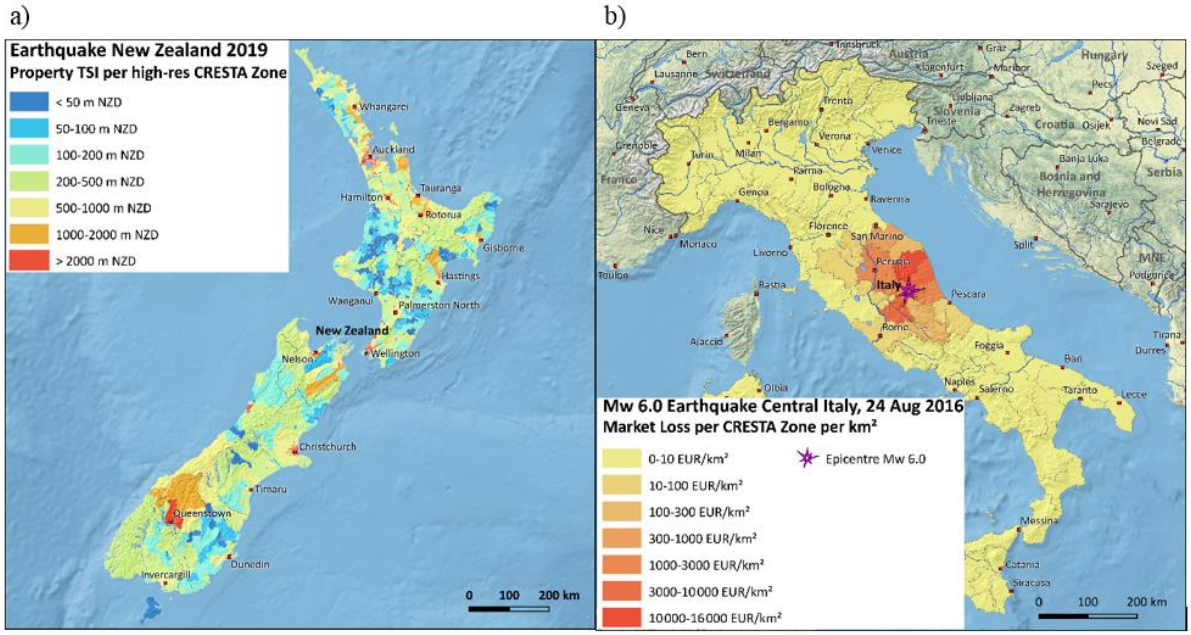


Figure 1.4: Illustration des données : d'exposition (a) et de pertes (b) collectées auprès de différentes compagnies d'assurance par l'organisme PERILS. Les zones high-res CRESTA correspondent au code postal. Source : PERILS (https://www.perils.org/) et Cresta (https://www.cresta.org/ ).

d'assurance pour étendre la couverture assurantielle contre les catastrophes naturelles. À la suite des catastrophes de grandes ampleurs qu'ont connu les Etats-Unis au cours des années 1990 (1992 Ouragan Andrew : $26.5bn ; 1994 Séisme de Northridge : $30bn), le marché de l'assurance et de la réassurance n'avait plus les ressources financières pour porter seul de tels risques (Polacek 2018). Afin de lever de nouveaux capitaux, des obligations catastrophes (ou Cat-Bonds) ont été émises. Ces obligations financières prévoient que l'émetteur du Cat-Bond (généralement une compagnie d'assurance ou de réassurance) ainsi que des investisseurs placent de l'argent dans un fonds de placement très sécurisé pendant une période définie. Si durant cette période une catastrophe survient telle que décrite dans les conditions du contrat (par exemple un séisme avec un épicentre dans une zone donnée et une magnitude supérieure à un seuil donné), alors l'argent du fonds est utilisé par l'émetteur pour compenser les pertes subies. Au terme du contrat, l'argent restant sur le fonds est redistribué entre les investisseurs (mais pas à l'émetteur). Dans le cas où aucune catastrophe n'est survenue, cela représente un bénéfice puisque l'émetteur a également placé de l'argent dans le fonds. La Figure 1.5 représente le montant des fonds correspondant à l'ensemble des Cat-Bonds émis depuis 1997.

En 2019, les Cat-Bonds représentent un montant total de $41bn pour couvrir des pertes associées à différentes catastrophes, alors qu'il n'était que de $786m. en 1997. Cette

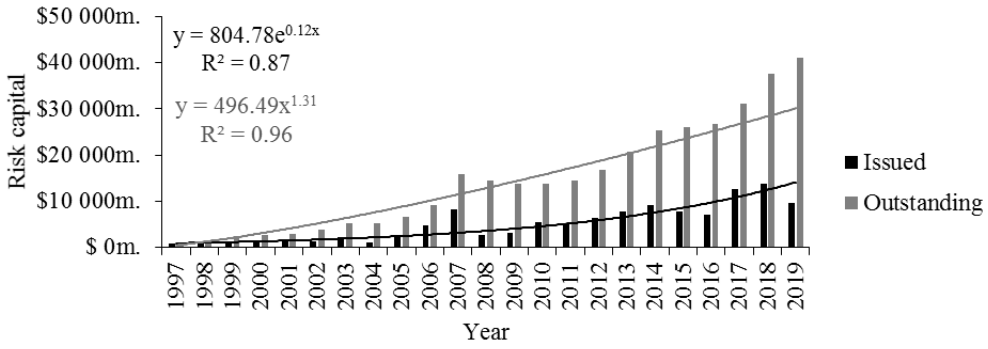


Figure 1.5: Evolution des montants financiers correspondant aux obligations catastrophes (Cat-Bond) depuis 1997. L'histogramme « Issued » correspond au montant émis durant l'année, alors que l'histogramme « Outstanding » correspond au montant des Cat-Bonds en vigueur durant l'année. Les lignes représentent les courbes de tendances empiriques entre 1997 et 2019. Source : after Artemis (www.artemis.bm/dashboard/catastrophe-bonds-ils-issued-and-outstanding-by-year/).

augmentation est visible tant sur le montant des fonds émis chaque année (Fig. 1.5, « Issued ») que sur le montant des fonds en vigueur (Fig. 1.5, « Outstanding ») et démontre la réussite de ce nouveau mécanisme. Au-delà des compagnies d'assurance et de réassurance, des pays (comme le Mexique ; Artemis 2017) et des organismes internationaux (comme la Banque Mondiale ; World Bank 2019) émettent également des Cat-Bonds pour se couvrir. A ce titre, l'Etat mexicain a reçu $150m. à la suite du séisme de magnitude Mw8.1 survenu le 7 septembre 2017 au sud-ouest du pays.

Récemment, le principe des Cat-Bonds a été adapté pour créer une nouvelle police d'assurance appelée l'assurance paramétrique. Le principe est d'indemniser le détenteur de la police si un type de catastrophe tel que décrit au contrat survient. Le montant de l'indemnité est également défini dans le contrat d'assurance paramétrique et ne dépend pas de la perte réelle subie par le détenteur de la police à la suite de la catastrophe en question. Le principal avantage de ce nouveau type de police d'assurance est la simplification de la procédure de règlement des sinistres comme illustré en Figure 1.6.

Cette simplification permet aux compagnies d'assurances à la fois de limiter leur frais et d'avoir une meilleure estimation des pertes possibles à la suite d'une catastrophe car les étapes 3, 4 et 5 de la modélisation (Fig. 1.1) sont déterminées au contrat. Il en résulte un montant de primes d'assurance réduit, faisant l'attrait de ce type d'assurance.

Malgré ces efforts contribuant à une meilleure couverture assurantielle après une catastrophe, et donc un impact économique moindre, elles ne permettent pas de diminuer en amont la

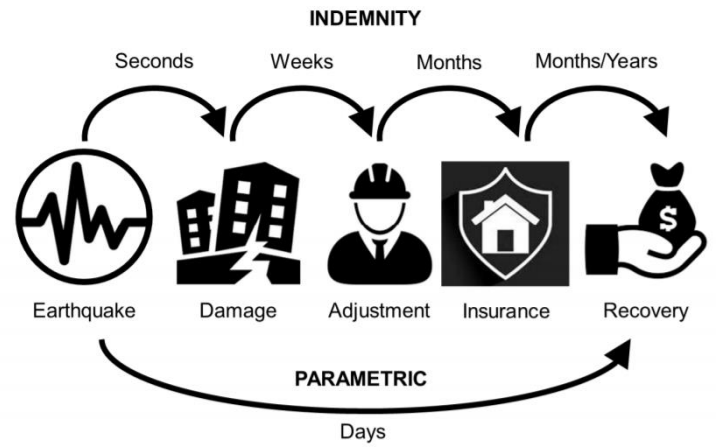


Figure 1.6: Représentation schématique du processus d'indemnisation des assurés dans le cadre d'une assurance classique (Indemnity) et d'une assurance paramétrique (Parametric). Source : Franco et al. 2018.

vulnérabilité des sociétés face à ce risque. C'est pour cela que l'industrie de l'assurance est de plus en plus proactive dans la mise en place de mesures de prévention comme le renforcement de maisons assurées les plus vulnérables (Earthquake Brace & Bolt, www.earthquakebracebolt.com/), la mise en place de table-vibrantes mobiles (Canadian Underwriter 2016) pour sensibiliser les gens à l'effet d'un séisme ou encore la publication de nouvelles recommandations pour reconstruire des logements plus sûrs après une catastrophe (UN-Habitat et AXA 2019).

## 1.2. Plan de la thèse

Cette thèse s'inscrit dans cet effort d'améliorer la connaissance du risque sismique et de développer de nouvelles solutions d'assurance. Elle se découpe en quatre parties pour couvrir les différents axes de développement présentés précédemment.

Le chapitre 2 retrace tout d'abord l'évolution du système d'assurance contre les tremblements de terre en Californie de ses débuts, à la suite du séisme de San Francisco en 1906, jusqu'à nos jours. Cela permet de mettre en perspective le système d'assurance actuel avec les séismes et les événements économiques et politiques qui ont pu l'affecter par le passé. Ensuite, il est comparé aux systèmes assurantiels actuels en France, en Inde et en Indonésie. Des différences importantes sont relevées à la fois liées à l'exposition au risque sismique et au niveau de développement économique du pays. Pour les pays développés, cette analyse met en lumière

les forces et les faiblesses de chaque système : en France, le système assurantiel couvre l'ensemble des personnes mais n'absorbe qu'une faible part des pertes en cas de séismes majeurs. En effet, l'Etat prévoit un large remboursement des compagnies d'assurance via sa compagnie de réassurance la Caisse Centrale de Réassurance (CCR). Pour la Californie, le système assurantiel n'arrive pas à couvrir tout le monde, avec seulement 15% de personnes assurées. Néanmoins, les réserves financières permettent de faire face aux pertes les plus extrêmes.

Le chapitre 3 analyse d'une part les raisons pour lesquelles peu de personnes sont assurées en Californie et, d'autre part, la capacité de l'Etat Français à faire face aux coûts engendrés par un séisme très destructeur. Pour comprendre le manque d'attrait des assurances tremblement de terre auprès des Californiens, une étude économique du montant de la prime d'assurance est menée du point de vue du souscripteur. L'objectif est d'estimer le montant que ces personnes sont prêtes à payer compte tenu de leur perception du risque. Cette analyse met en évidence que la plupart d'entre elles ne sont pas assurées contre le risque sismique à cause d'un montant de primes trop cher et non par sous-estimation du risque.

Dans le système français (dit régime CAT-NAT), l'Etat décide des communes pouvant bénéficier ou non d'une indemnité d'assurance après une catastrophe. L'étude menée dans le cadre de cette thèse montre que cette décision est influencée par la capacité financière de l'Etat : en cas d'événement trop coûteux, l'Etat réduit le nombre de communes qui peuvent bénéficier d'une indemnité d'assurance (comme observé lors de la vague de sécheresse en 2003). Sur la base de ce constat, un événement sismique produisant une sinistralité importante dans une seule commune d'importance économique majeure empêcherait l'Etat Français de segmenter les pertes par commune et donc l'obligerait à assumer un coût financier très lourd.

La principale limite des systèmes assurantiels Français et Californien ayant été analysée, le chapitre 3 se termine sur le développement d'une échelle de maturité. Cet outil permet d'évaluer l'évolution d'un marché (ici celui de l'assurance tremblement de terre) selon différents critères prédéfinis. En l'appliquant aux systèmes d'assurance tremblement de terre en France et en Californie, il ressort que les deux pourraient être améliorés en développant trois axes : une meilleure modélisation du risque sismique, un nouveau modèle d'assurance proposant des primes correspondant aux attentes des clients et la prise compte de mesures de prévention dans le mécanisme assurantiel.

Le chapitre 4 regroupe deux études contribuant à améliorer la modélisation du risque sismique. Dans la mesure où plusieurs nouveaux modèles ont déjà été développés récemment (notamment

par l'association Global Earthquake Model, www.globalquakemodel.org/), les travaux ont consisté à mettre en place des méthodes de comparaison des modèles stochastique de pertes avec des données de référence. La première porte sur une méthode de comparaison entre des empreintes de mouvements de sol (par exemple des empreintes ShakeMap ; Fig. 1.1 étape 2) et une carte probabiliste d'aléa sismique (carte PSHA). Le processus de modélisation stochastique comporte différentes étapes (Fig. 1.1) qui font toutes l'objet d'hypothèses. Cette méthode permet une validation intermédiaire dans le processus (après les étapes 1 et 2) par la comparaison avec la référence que représentent les cartes PSHA. En effet, celles-ci font l'objet de beaucoup d'études scientifiques (par exemple le projet scientifique UCERF-3 en Californie ; Field et al. 2013) et sont notamment utilisées dans l'application des normes parasismiques pour les bâtiments.

La deuxième étude menée porte sur le développement d'une méthode pour comparer les différentes relations dommage-coût existantes (c'est-à-dire entre le niveau d'endommagement d'un bâtiment et le coût de réparation associé) en les appliquant aux données issues de différents séismes historiques. Ces tests permettent de mettre en évidence un éventuel biais dans les estimations de coûts de réparation et permet de calculer l'écart-type de l'erreur de modélisation.

Le chapitre 5 est dédié au développement d'un nouveau modèle d'assurance répondant au double enjeu d'un montant de primes plus faible et de la mise en œuvre de solutions parasismiques. Pour cela, les primes d'assurance collectées sont allouées à chaque bâtiment et alimente un capital qui est placé sur les marchés financiers pour produire des intérêts financiers. Lorsqu'un séisme survient, cet argent sert à payer la réparation ou reconstruction du bâtiment au lieu de verser une indemnité. En cas d'absence de séisme destructeur durant un laps de temps suffisamment long, l'argent est utilisé pour financer des travaux de renforcement parasismique. La diminution du capital que cela représente est compensée par une meilleure résistance du bâtiment au séisme, et donc un coût moyen de reconstruction après un séisme plus faible. Enfin, ce nouveau modèle assurantiel prévoit une prise en charge partielle de la prime d'assurance par les entreprises en bâtiment pour bénéficier du marché de la réparation/reconstruction et du renforcement parasismique. Ainsi, ce nouveau modèle assurantiel répond à la fois au besoin d'organiser le renforcement parasismique des bâtiments tout en proposant un montant de primes inférieur aux assurés.

Enfin, le chapitre 6 synthétise les principaux résultats obtenus et les limites identifiées à la suite de ce travail de thèse. Les différentes perspectives qu'il ouvre, tant sur le plan scientifique qu'économique, sont également abordées.

# CHAPTER 2: IN-DEPTH REVIEW OF EARTHQUAKE INSURANCE SOLUTIONS

## 2.1. Introduction

The International Disaster Database (CRED), shows that the number of damaging earthquakes (i.e. more than 100 people affected) and the consecutive economic loss are increasing since 1960. Analysing the consequences of natural disasters occurred since 1970s at the worldwide scale, Ghesquiere and Mahul (2010) have identified three different phases in post-disaster management: the *Relief* (1-3 months), the *Recovery* (3-9 months) and the *Reconstruction* (>9 months). They have also quantified the financial amount required, as illustrated in Figure 2.1 which highlights the time scale of the post-disaster requirements.

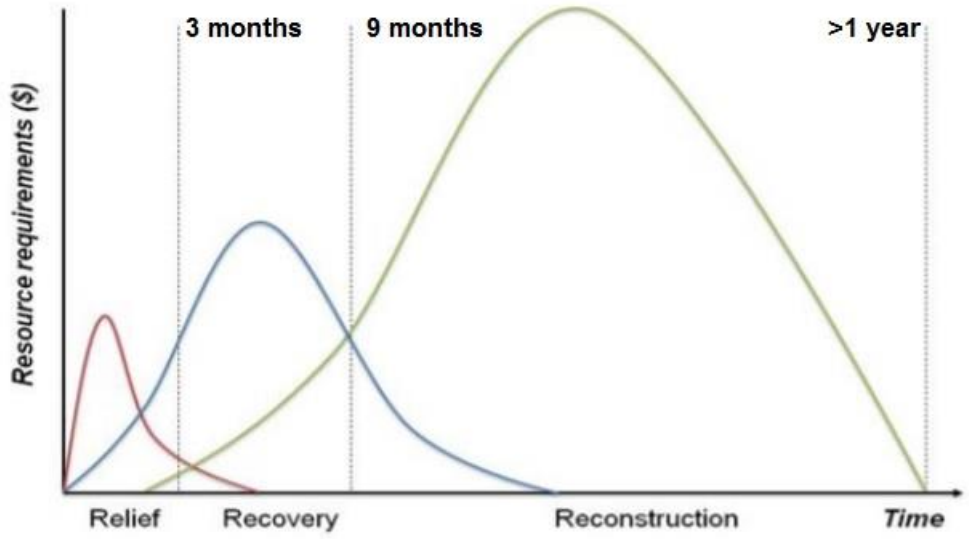


Figure 2.1: Funding requirements during each post-disaster stage. Source: Ghesquiere and Mahul (2010).

Ghesquiere and Mahul (2010) listed 11 financial sources, sorted in three categories: donations, public debt and insurance. Each is characterized by a disbursement period, a quantity of funds available, and the issuance period (either before or after the disaster occurrence). Figure 2.2 shows that insurance solutions (parametric insurance, alternative risk transfer and traditional insurance), donor support and budget contingencies can cover the second and the third months post disaster period (Ghesquiere and Mahul 2010), corresponding to the late *Relief* phase and the beginning of the *Recovery* phase (Fig. 2.1).

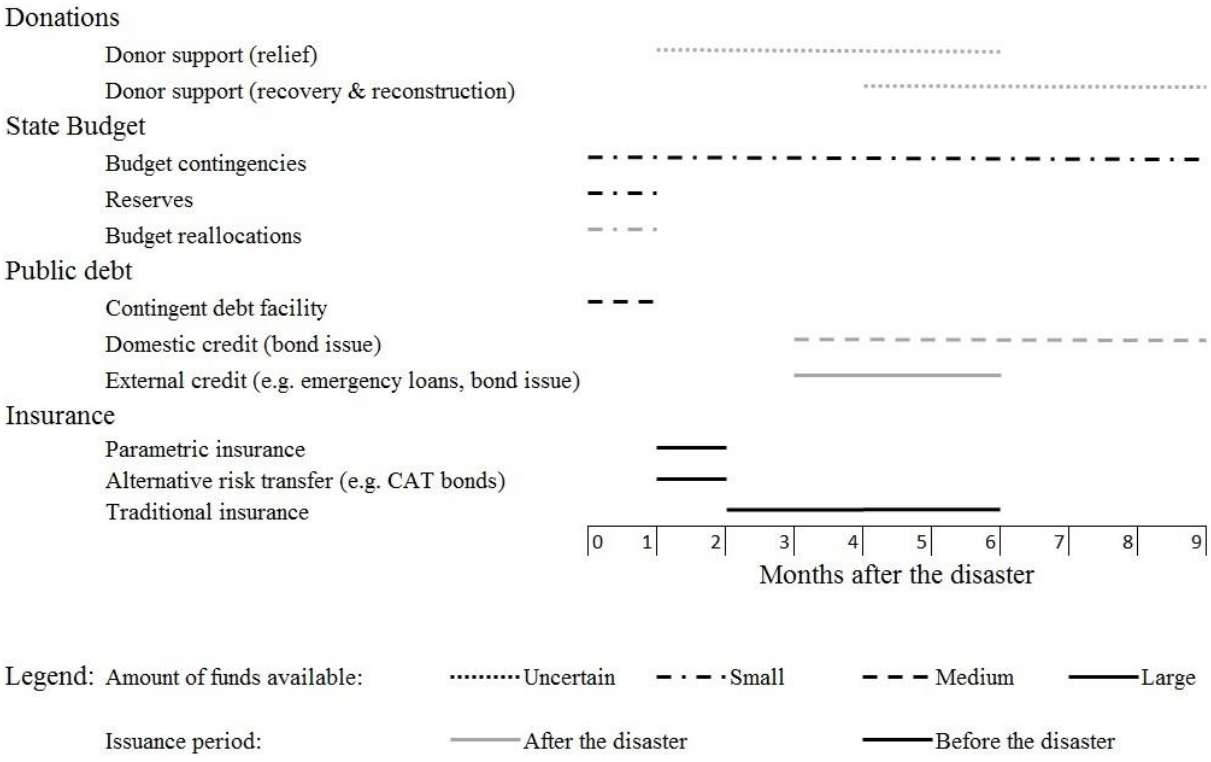


Figure 2.2: Disbursement period, quantity of funds available and issuance period for several post-disaster financing instruments. Source: after Ghesquiere and Mahul (2010).

The financial amount that donor support and budget contingencies is estimated by Ghesquiere and Mahul (2010) at an *Uncertain* and *Small* quantity, respectively. Furthermore, these two kinds of financial sources are determined after the disaster and, consequently the amount available is known only after the disaster. At the opposite, insurance can provide a *Large* funding capacity, depending on the insurance market size. About claim amount and payment pattern, they are agreed at the insurance policy issuance and therefore, known before the disaster. Between the 4$^{th}$ and the 6$^{th}$ month after a disaster, insurance and external credit provide both a *Large* financial assistance (Fig. 2.2). However, funds from external credits are allocated to affected people by public grants, the amount dedicated to each affected people depends on public policies set after the event and does not necessarily meet the affected people's needs. At

the opposite, since insurance policy can be underwritten by households, this financial assistance can be directly allocated to affected people accordingly to each insurance policy.

According to Ghesquiere and Mahul (2010), insurance is a key financial instrument for financing post-disaster needs during the late *Relief* and the *Recovery* phases ($2^{nd}$ – $6^{th}$ months following the disaster) as illustrated in Figures 2.1 and 2.2.

Current earthquake insurance solutions are significantly different from one country to another depending on several variables like the country's wealth or the experience of natural disasters. In this study, four different areas are considered, representing typical combinations of country's wealth and hazard level: France (developed country with a low seismic hazard), India (developing country with a low seismic hazard outside Himalaya), Indonesia (developing country with a high seismic hazard) and California (developed country with a high seismic hazard). Recent earthquakes affecting these countries depict well the wide range of insured loss as reported by the Global Facility for Disaster Reduction and Recovery (Dani 2012): [0%; 10%] for the 2006 Yogyakarta (Indonesia) and the 2001 Gujarat (India) earthquakes and [30%; 40%] for the 1994 Northridge (USA) earthquake. In France, no severe earthquake has occurred since 1982, the creation of the CAT-NAT insurance plan covering earthquake risk, among other perils. Nevertheless, in France, earthquake and windstorm insurance covers are both compulsory in housing insurance policy. So, the share of insured loss can be estimated from the 1999 Lothar and Martin windstorms at [80%; 90%]. While the very low rate of insured loss in India and Indonesia is consistent with a Medium Human Development Index, the share at [30%; 40%] for California compared to [80%; 90%] for France is more surprising. Indeed, California is more exposed to earthquake risk than France, but seems to have a less protective earthquake insurance system.

In California earthquake insurance has existed since the early 1900s. A lot of large events have occurred over the $20^{th}$ century, including the 1994 Northridge, the 1989 Loma Prieta, the 1933 Long Beach, the 1971 San Fernando and the 1925 Santa Barbara earthquakes. These damaging events (Alquist et al. 2009) have forced the insurance scheme to react. In the same time, risk awareness arose, thanks to an active scientific field. California earthquakes are also constantly monitored by the USGS and their consequences are calculated (e.g. PAGER alerts). From the economic side, the California Department of Insurance (CDI) provides an open access to data about earthquake insurance market. For all of these reasons, the California earthquake insurance constitutes an excellent case study.

This chapter reviews the current earthquake insurance models and highlights their strengths and weaknesses. In the first part, the California insurance scheme, for which the most data is available, is analysed. Next, it is compared to the earthquake insurance solutions in India, Indonesia and France from an economic perspective.

## 2.2. Earthquake insurance market in California

### *2.2.1. Historical background*

Earthquake insurance in California started in the aftermath of the 1906 San Francisco earthquake but was initially unpopular (Buffinton 1961; Meltsner 1978; Goltz 1985; Muir-Wood 2016a). Indeed, most of loss related to this event was due to consecutive fires and, therefore, damage was already covered by the fire insurance cover (Goltz 1985; Yeats 2004; Gioncu and Mazzolani 2011). At the opposite, loss caused by the 1925 Santa Barbara earthquake was due to ground shaking, and therefore not insured (Goltz 1985; Alquist et al. 2009). This event boosted drastically the demand for earthquake insurance, as illustrated in Figure 2.3 by the total amount of premium collected by insurance companies.

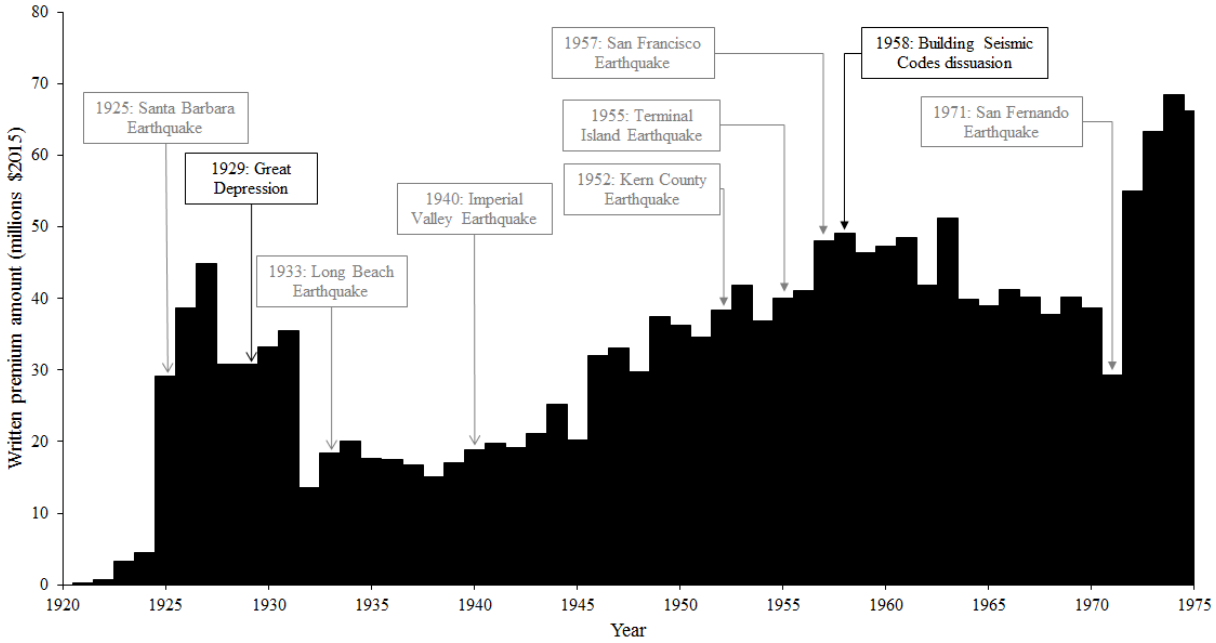


Figure 2.3: Total premium written in earthquake insurance policy in California until 1975. Source: after Goltz 1985.

After the 1925 Santa Barbara earthquake, Great Depression started, stopping the appeal. The occurrence of two other damaging earthquakes in 1933 (Long Beach) and 1940 (Imperial Valley) triggered the attractiveness of earthquake insurance cover, until 1957 (Muir-Wood 2016a; Meltsner 1978). Indeed, is observed (Fig. 2.3) a decreasing trend in the premium amount collected between 1957 and 1970. This evolution is surprising considering solid economic US growth during that period (2.5% average annual growth rate of the GDP per capita between 1950 and 1973, against 2% between 1870 and 2007, according to Jones 2016) and the significant earthquakes occurred the six previous years: 1) the 1952 Kern County earthquake (M7.3): the epicentre was located at 40km of Bakersfield and 90km of Santa Barbara, and it caused $2.8bn (USD 2005) (Alquist et al. 2009) damage (i.e. similar to the 1925 Santa Barbara event); 2) the 1955 Terminal island earthquake (M3.5): occurred in Los Angeles and caused $3m (USD 1955) (Vranes and Pielke 2009) despite the very low magnitude; 3) the 1957 San Francisco earthquake (M5.7): the biggest in this area since the 1906 event, despite a very limited damage estimated at $27m in USD 2005 (Alquist et al. 2009). According to Buffinton (1961) and Meltsner (1978), insurance companies did not record significant losses from these events (the global insured loss ratio is below 20%). Furthermore, the earthquake engineers' community and public officials congratulated themselves about the efficiency of the seismic retrofitting codes settled during the 1940's (Geschwind 2001). Except the damage, they even communicated that there was "no cause to fear an earthquake like 1906" (Geschwind 2001), despite objections raised by earthquake researchers led by Charles Richter. As a likely consequence, people ignored the risk and cancelled their earthquake insurance policy.

The 1971 San Fernando earthquake caused a $6.6bn (USD 2005) damage but less than 10% were covered by insurance companies (Meltsner 1978; Alquist et al. 2009). This event stands out from the previous ones because the commercial and industrial sectors were heavily affected (almost equal to the residential losses in Los Angeles City), and a large share (62%) of buildings affected collapsed or was heavily damaged (Meltsner 1978; Alquist et al. 2009). As a consequence, Goltz (1985) mentions that professionals bought earthquake insurance products, boosting the sector at an unprecedented level (Fig. 2.3). The demand for earthquake insurance was even more triggered by the devastating 1983 Coalinga earthquake ($120m. in USD 2005) and the consecutive Assembly Bill AB2865 (McAlister 1984; Fig. 2.4).

This legislative act mandated insurance companies to offer an optional earthquake coverage complementary to the dwelling insurance. Consequently, after the 1994 Northridge earthquake, the consecutive loss for insurance companies reached $11.4bn (USD 1995), i.e. three times

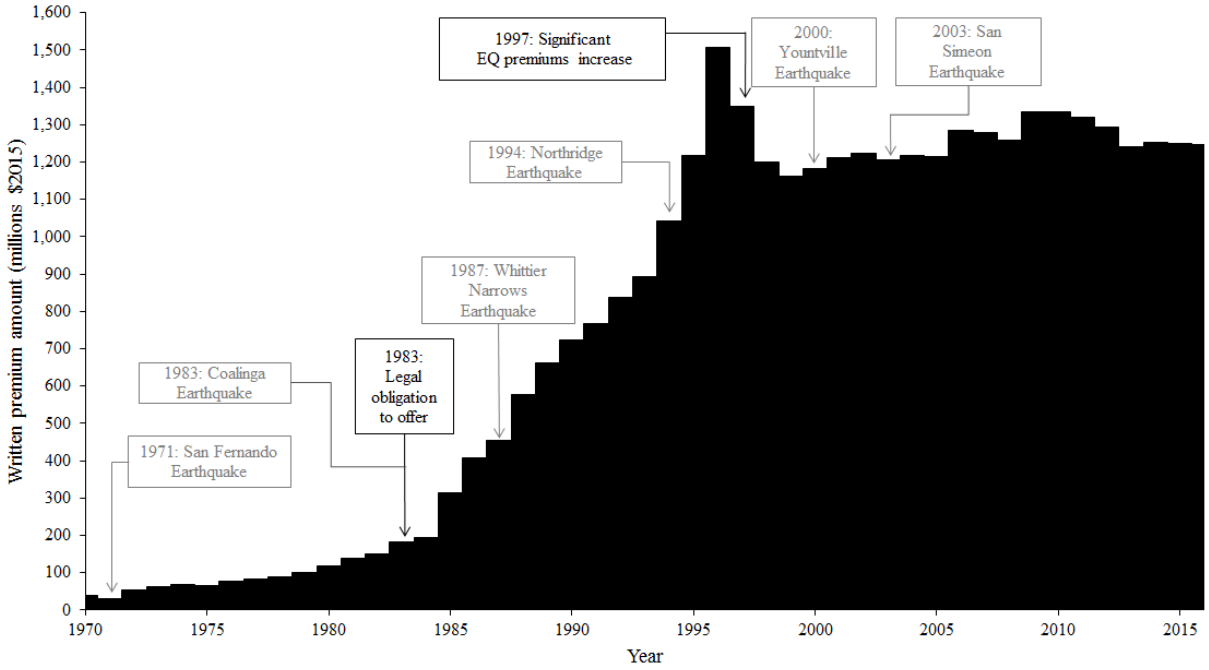


Figure 2.4: Total premium written in earthquake insurance policy in California between 1967 and 2015. Source: after Goltz 1985.

higher than the $3.4bn (USD 1995) earthquake insurance market premiums collected since 1970 (Snyder 1995). Even if no company was declared bankrupt, claims overpassed the maximum loss assessed by the contemporary actuarial models (RMS 2004; Insurance Information Institute 2016). Forced at that time by the Assembly Bill AB2865 (McAlister 1984) to propose an earthquake coverage in residential insurance policies, most of the insurance companies (≈ 90%) decided to restrict or even to stop selling new residential insurance cover in California (California Earthquake Authority 2016a).

The Fair Access to Insurance Requirements (FAIR) is a state-managed insurance syndicate gathering all California insurance companies. Since 1968, it provides in last resort a basic insurance cover to households that insurance companies do not want to cover. Thus, to limit the threat of a shortage in property insurance products, the FAIR plan launched in 1994 a basic earthquake insurance cover (Mulligan 1994). Constrained by the sharp decrease of new insurance policies offer, customers rushed to subscribe the FAIR plan product (Sanchez 1996). This unforeseen popularity generated fears among the authorities about the capacity to face a major earthquake loss. It resulted in a strict limitation of the FAIR plan house insurance subscription on June 1$^{st}$, 1996 to very poor zones and highly exposed to brush fire risk (Sanchez 1996; Reich 1996a; Reich 1996b). The FAIR plan reopened 5 months later while the California

Earthquake Authority (CEA) was created as a response to the earthquake insurance crisis (Reich 1996a; Reich 1996b).

Initiated by law in 1995, the CEA aims at providing an earthquake insurance for households (Consumers Union 1997; Knowles 1997), called the *Mini-policy* because of the low guarantees provided. After the commitment of more than 75% insurance companies to sell it (later referred as CEA insurance company members) and the purchase of the reinsurance cover imposed by such risk, the CEA was officially launched on December 2nd, 1996 (Consumers Union 1997; Knowles 1997). The new insurance conditions of the *Mini-policy* were less attractive than the FAIR plan cover because more expensive and more restrictive as summarized in Table 2.1.

Table 2.1: Main differences between the FAIR plan policy and the *Mini-policy*. Sources: (1): Mulligan 1994; (2): Roth 1997; (3): Garamendi 2003; (4): Kunreuther 2015; (5): California Earthquake Authority 2015a; (6) US Census.

| Conditions | FAIR plan policy[(1)(2)(3)(4)] | *Mini-policy*[(2)(3)(4)(5)] |
|---|---|---|
| Deductibles | 10% | 15% |
| Typical Annual Premium | $487.50 | $576 |
| Typical House Cost[(6)] | $160,000 | |

Consequently, many people were no longer insured against earthquake risk and, despite a significant premium amount increase (Tab. 2.1; Fig. 2.4, *Significant EQ premiums increase*) it resulted in a drop of the total written premium amount (Fig. 2.4). From 31% in 1996, the share of people covered against earthquake falls to 19.5% in 1997 as illustrated in Figure 2.5 (California Department of Insurance database).

After 1997, the number of earthquake insurance policies decreased slightly until 2003 (the year of the San Simeon earthquake) and then has been increasing until now (Fig. 2.5a). However, this increase is slower than for the number of housing insurance policies, resulting in a slight decrease of the ratio between earthquake and housing insurance policies (Fig. 2.5b). Nowadays, the CEA has some competitors representing 25% of the policies and 35% of the premium amount related to the earthquake dwelling insurance market (California Department of Insurance database). The difference between these two values reflects that the CEA protects more low-value houses than its competitors (assuming that all insurance companies use similar pricing models and policies).

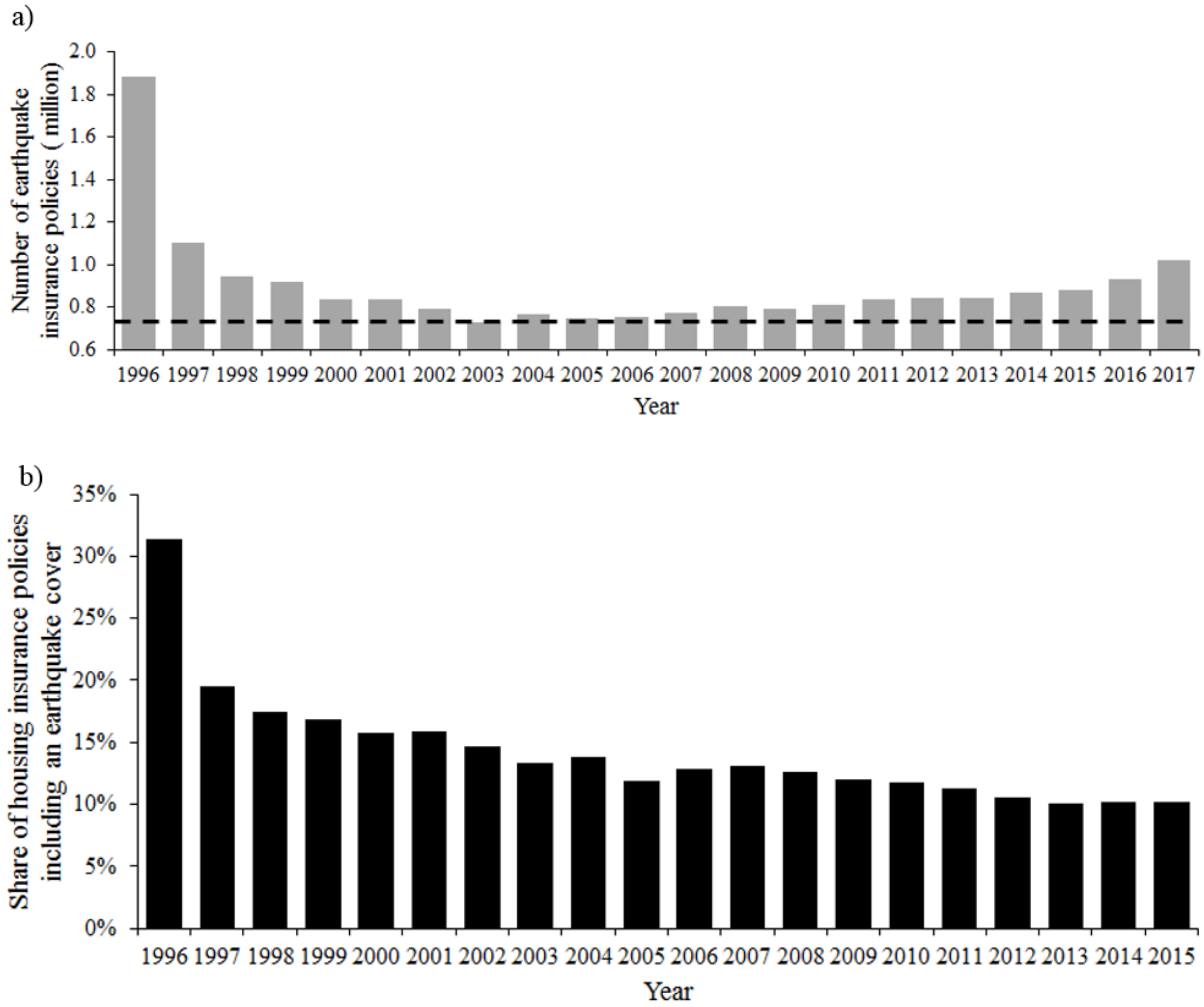


Figure 2.5: CEA Earthquake insurance policy evolution from 1996 to 2015 in terms of: a) number of insurance policies and b) the ratio between the numbers of households covered against earthquake and households with a housing insurance. Source: after California Department of Insurance database.

### *2.2.2. Focus on the California Earthquake Authority*

Until now, the CEA has faced only small losses despite the occurrence of several moderate earthquakes (Fig. 2.6). Indeed, only the 2003 San Simeon and the 2014 Napa earthquakes caused claims above $2m. (USD 2015). The total claim amount paid during the period 1997-2015 is equal to $19m. (USD 2015), which corresponds to only 2‰ of the total premium amount for the same period. Although the period is too short to draw any conclusions on the premium amount adequacy, the issue of the collected premium allocation is raised: does it increase the CEA claim-paying capacity to face more and more devastating earthquakes?

The claim-paying capacity is the maximum amount that an insurance company can pay. This amount is equal to the sum of the company's reserves and the cash-flow that it can benefit from

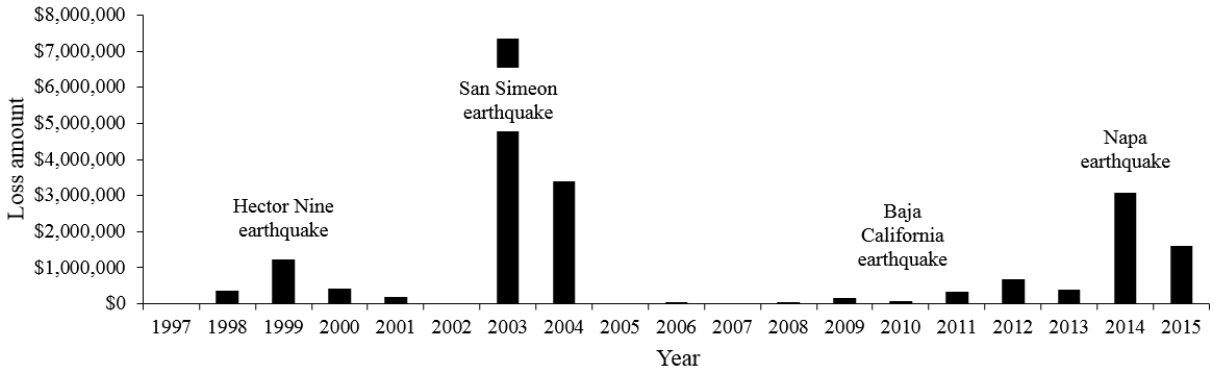


Figure 2.6: Earthquake losses incurred by the CEA (USD 2015). Source: after CEA.

all the risk-transfer mechanisms subscribed. Figure 2.7 shows the CEA's claim-paying capacity between 1997 and 2016.

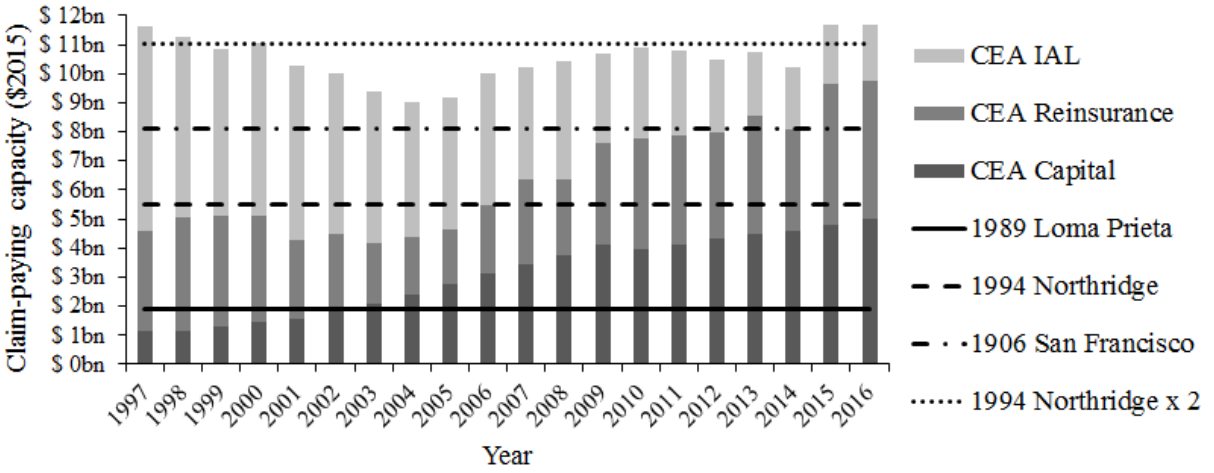


Figure 2.7: CEA's claim-paying capacity according to the source of funds: the CEA's capital, the CEA reinsurance cover, and the Industry Assessment Layer (IAL) corresponding to the funds provided by the CEA's insurance company members. The lines correspond to the loss incurred by the CEA if the 1906 San Francisco, the 1989 Loma Prieta or the 1994 Northridge earthquakes occur today. The '1994 Northridge x2' corresponds to a hypothetical earthquake causing a direct economic loss twice higher than the 1994 Northridge earthquake. Source: after CEA Financial Statements.

According to the California Earthquake Authority (2014), the company has a claim-paying capacity large enough to face the loss of some largest historical earthquakes (1989 Loma Prieta, 1994 Northridge and 1906 San Francisco) if they occur again. The largest event sustainable by the CEA is a two Northridge-size event (Roth 1997), estimated at a 400y return period (California Earthquake Authority 2018a). Figure 2.7 shows also that the CEA's claim-paying capacity is made of its own reserves (dark grey), the reinsurance capacity bought on financial markets (grey) and the Industry Assessment Layer (IAL) which is an additional reinsurance

coverage provided by the CEA insurance company members (light grey). While the capital increases as a consequence of the premium collected and the losses recorded (Fig. 2.6), the IAL is decreasing. It results in a constant claim-paying capacity since 1997 when calculated in $2015. Consequently, Figure 2.7 highlights that part of the premiums collected since 1997 and not used to pay claims (Fig. 2.6) is used to decrease the contribution of the participating insurers in the earthquake coverage. As the IAL is a reinsurance cover free of charge for the CEA (Marshall 2018), this decrease has no impact on the premium amount. However, the excess of premium collected allowed also the CEA to apply several premium discounts since 1997: -11% in 1997, -23% in 2006, -12.5% in 2012 and -10% expected in 2016 (California Earthquake Authority 2015a).

The earthquake premium calculated by the CEA considers several building characteristics, as a proxy of the earthquake vulnerability. For instance, the online CEA premium calculator indicates that the premium amount for a one-story modern house is between 3 and 4 times less expensive than an old one-story house built in earthquake vulnerable materials (for instance unreinforced masonry). In addition to the premium scale, the CEA and the California Governor's Office of Emergency Services launched in September 2013 the prevention plan called *Earthquake Brace+Bolt* (California Department of Insurance 2015). This initiative aims at promoting earthquake retrofit for houses and mobile homes of CEA's clients by financing the work up to $3,000. Table 2.2 draws a global picture of the initiative through different figures.

First, the need for retrofitting in California is huge: among the 13,987,625 housing units in 2015 (US Census), 1,200,000 are particularly at risk and would benefit from this initiative (Lin II 2015; Xia and Lin II 2016). The *Earthquake Brace+Bolt* initiative has been launched cautiously with a budget of $1.8m., with 600 houses retrofitted by the end of year 2015 as objective. Between 2015 and 2017, the funds increased from $1.8m to $6m driving the *Earthquake Brace+Bolt* initiative growth. In 2017, 2,000 houses are targeted to be retrofitted over 140 postal codes mostly in big urban areas (Los Angeles, San Francisco, Eureka and Riverside). Despite the two years-old initiative *Earthquake Brace + Bolt* is expanding quickly, it is still in its infancy. Only 3.5‰ of the highly vulnerable houses have been retrofitted after 3 years of existence. However, the public authorities and the CEA rely on the *Earthquake Brace+Bolt* initiative to increase the public awareness of the risk and to urge households to retrofit their house by themselves (Lin II 2015).

Table 2.2: *Earthquake Brace+Bolt* in figures until 2017. Post Office Boxes are not considered in the number of qualified postal codes. Sources: (1): California Earthquake Authority 2017a; (2): US Census Bureau; (3): California Earthquake Authority 2015b; (4): Lin II 2015; (5): Ousley and Wilkinson 2016; (6): Earthquake Brace+Bolt 2017; (7): Insurance Journal 2017; (8): Xia and Lin II 2016; (9) Earthquake Brace+Bolt 2016; (10) Sands and Brown 2014; (11): O'Mara 2016; (12): Krieger 2017; (13): California Earthquake Authority 2016b; (14): California Department of Insurance 2015.

| Year | 2015 | 2016 | 2017 |
|---|---|---|---|
| Number of houses estimated at risk[4][8] | | 1,200,000 | |
| Number of qualified postal codes[6][9][10] | 26 | 109 | 140 |
| Population living in qualified postal codes | 862,347 | 3,221,973 | 4,865,800 |
| Number of applicant houses[3][4] | > 2000 | 4,427 | - |
| Number of houses expected (goal)[3][11][12] | 600 | 1,600 | 2,000 |
| Number of houses selected[3][14] | 650 | 3,200 | - |
| Number of houses retrofitted[13] | 528 | 1,383 | - |
| Retrofit cost range[1][4][5][6] | | $2,000 - $10,000 | |
| Reimburse up to[6] | | $3,000 | |
| Public funding[5][7] | - | $3m. | $3m. |
| CEA funding[5][7] | $1.8m. | | $3m. |
| Number of postal codes[2] | | 1,707 | |
| Number of houses[2] | | 13,987,625 | |
| Population[2] | | 39,144,818 | |

## 2.3. Main differences with earthquake insurance models in France, India and Indonesia from an economic perspective

In this section, the earthquake insurance models in force in California, France, India and Indonesia are compared based on several economic metrics: the premium amount, the loss allocation between the insured, the insurance companies and public funds and the solvency of insurance companies.

### *2.3.1. The insurance premium*

Comparing the premium rate (equal to the premium amount divided by the insured value of the house) aims at highlighting the affordability of earthquake insurance considering both the insurance development and the seismic hazard level. Figure 2.8 shows the spatialized premium rate for each studied area.

The building characteristics considered for calculating the premium amount (i.e. modern one-

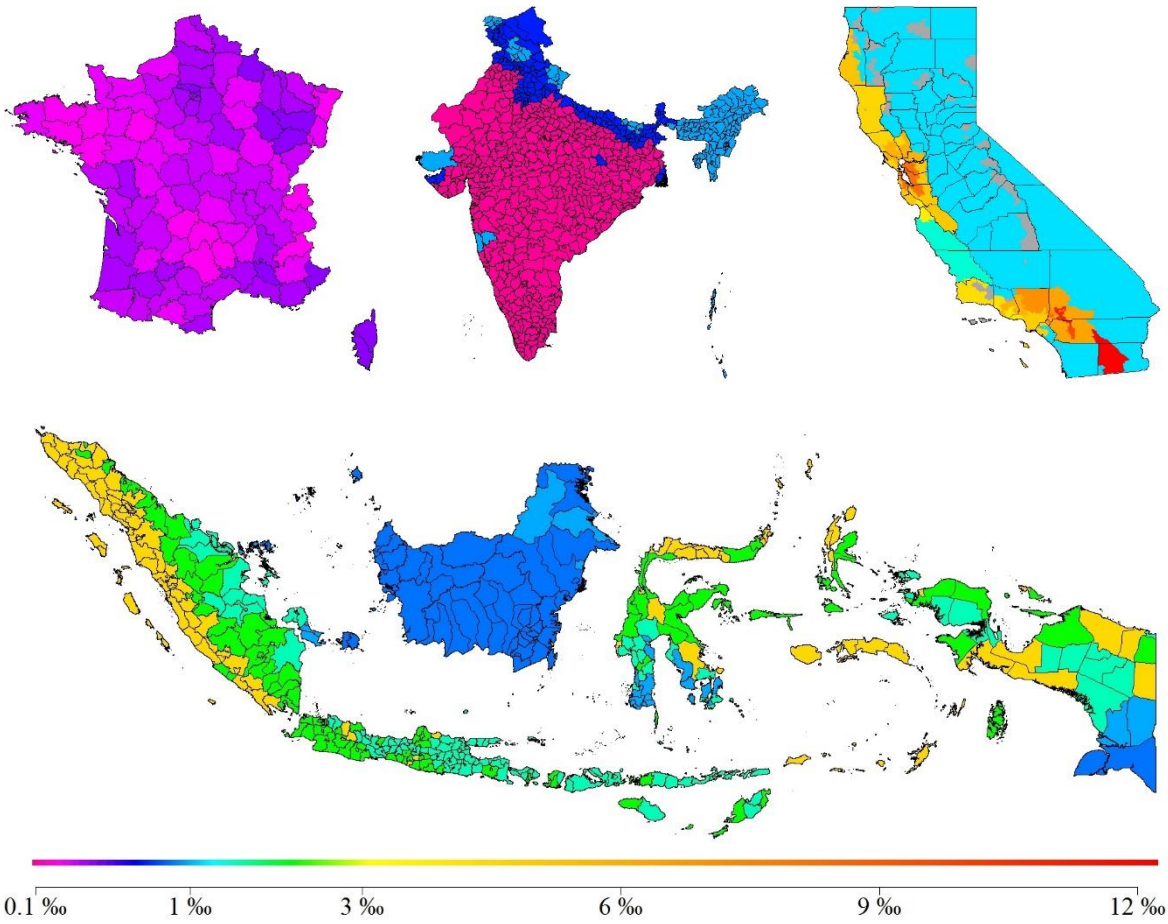


Figure 2.8: Premium rate for a modern one-storey house built in unreinforced masonry for each country studied. Grey areas in California correspond to unoccupied zones like forests and thus premium rate is not available. Sources : after CEA ; Caisse Centrale de Réassurance (2015) ; Les Furets (2016) ; MAIPARK ; Insurance Information Bureau of India (2001).

storey house built in unreinforced masonry) have been chosen because it is assumed to be the most similar from one country to another. Consequently, for a given area, the premium rate illustrated in Figure 2.8 is not representative of the market when the selected conditions are not characterizing the buildings taxonomy.

Figure 2.8 shows first that for each country the premium rate depends on the location. The premium is the lowest in India (shiny pink colour) excluding the Himalayan area, the Gujarat state and the west of Maharashtra state, exposed to induced seismicity after the Koyna dam construction, according to Phadnis (2016). In France, the premium rate appears to be low (below 0.25‰) especially because the premium covers flood and subsidence risks in addition to earthquake risk (Caisse Centrale de Réassurance 2011). In France, this premium rate is established by law (as part of the CAT-NAT plan) and consequently, does not necessarily reflects the risk level. Furthermore, the French State offers under the CAT-NAT plan an

unlimited reinsurance cover. It means that in case of extreme loss, the French State will pay part of insurance claims. Hence, the State budget dedicated to the CAT-NAT plan can be assimilated to an additional premium. Nevertheless, the premium rate is regularly increased (Caisse Centrale de Réassurance 2019a): +64% in 1985 and +33% in 1999. Furthermore, the ongoing revision of the CAT-NAT plan could also include a new premium increase (Bonnefoy 2019). California is the country with the highest premium rate, especially along the San Andreas Fault and in the vicinity of big cities like Los Angeles or San Francisco. It is also the country where the location has the highest impact on the premium amount. Indonesia shows spatial variation in premium rate that can be explained by the different levels of seismic hazard.

To go further in the analysis of the premium amount, Figure 2.9 plots the premium rate against the hazard level extracted from the GSHAP hazard map and corresponding to the return period 475y (Giardini et al. 1999).

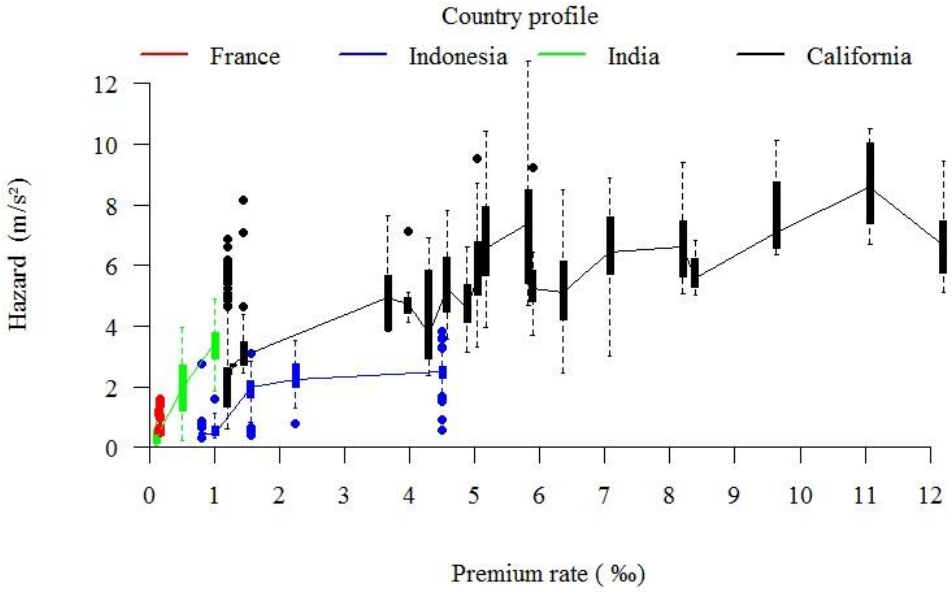


Figure 2.9: Average premium as a function of the hazard level as defined by the GSHAP 475y-PGA hazard map.

When several hazard values refer to the same premium rate, the scatter is represented by a boxplot. This figure highlights the fact that low to moderate seismic countries (France and India excluding Himalaya) have a similar profile. Also, they have a very low premium rate for a given hazard level, when compared to Indonesia or California. Indeed, for a hazard at 2m.s$^{-2}$, the premium rate in India is around 0.5‰ while it reaches 1.6‰ and 1.2‰ in Indonesia and

California, respectively. Last, with a curve lying below all the others, Indonesia is the costliest country in terms of earthquake insurance.

The variability in the hazard for the same premium amount is the most important for California. One explanation could be the difference in geographical resolution between the premium amount and the GSHAP hazard map, as illustrated in Figure 2.10.

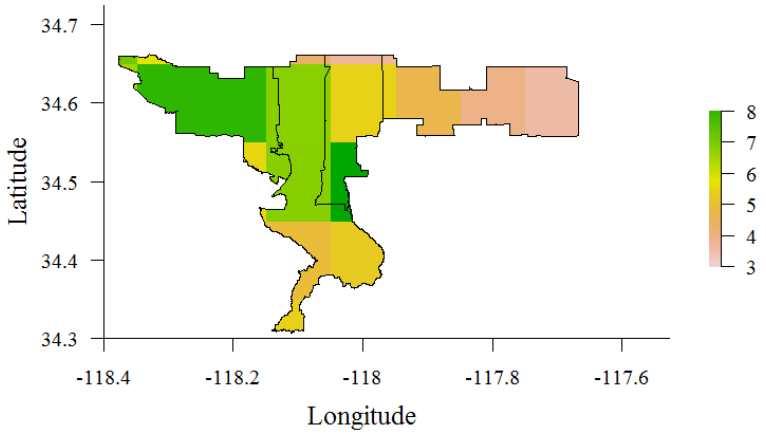


Figure 2.10: Hazard levels from the GSHAP hazard map (in $m.s^{-2}$) for the city of Palmdale, California. For this postcode area, the CEA premium amount is uniform and equal to 7.073‰ for a no-frame house built in 2017 and with one story.

Even if the premium is more location-dependent than for the other studied countries (Fig. 2.8), there is always some mutualisation of the hazard risks within a certain geographical resolution, here the city.

Finally, Figures 2.8, 2.9 and 2.10 show a wide range of premium amount for one area to another that depends on both the hazard level, and the method used to calculate the premium amount.

### *2.3.2. The loss allocation*

After analysing the difference in premium amount, this section aims at assessing the efficiency of the risk transfer mechanism. The theoretical loss share of each insurance scheme stakeholder is compared on the basis of a wide range of direct economic loss. This analysis considers only the insurance and reinsurance conditions currently subscribed even if past natural hazard showed that additional funds can be dedicated to affected people, like in France after the 2016

Seine floods (République Française 2016). Moreover, the loss allocation is performed in order to minimize the loss share for the policyholder. Thus, the following assumptions are made:

- all the damaged buildings are dwellings;
- buildings are destroyed at 100% and contents at 0%;
- underinsurance is neglected, i.e. the building price is equal to the sum insured;
- all the buildings are insured by the CEA with a deductible amount at 5%;
- all insurance companies in France are reinsured by the CCR;
- California households affected receive a $30,000 grant from the Federal Emergency Management Agency (FEMA).

Under these assumptions, the theoretical loss shares between the policyholders, the insurance companies, the CEA/CCR and the public funds can be calculated (Fig. 2.11).

For earthquakes causing low to moderate damage (i.e. up to 7bn loss, Fig. 2.11), the two insurance schemes allocate most of the loss to the insurance market (i.e. insurance company, CEA and CCR). However, for extensive damage (between $7bn and $27bn), the California insurance scheme still manages to allocate more than 50% of loss to the CEA, while the French State is expected to pay more than 85% of the loss. Last, for very extreme earthquake causing a loss above $27bn, whatever the insurance scheme most of the loss is supported by the community (public funds in France and policyholders' own funds in California). Thus, CEA and CCR play a different role: when the first provides a cover for small events, the second protects insured people up to a maximum loss amount, corresponding to the claim-paying capacity. In the USA, the public intervention after a natural disaster is limited to a possible grant up to $30,000 allocated by the FEMA to affected people as part of the *Major Declaration* program (Gustin 2008). Since 2010 the California Earthquake Authority (2015a) asks for a higher participation of the State with a public borrow facility for paying the claims in case of an extreme earthquake. However, in case of a devastating earthquake, the two insurance mechanisms are less efficient, since most of the loss is at the charge of the State and the policyholders in France and California, respectively.

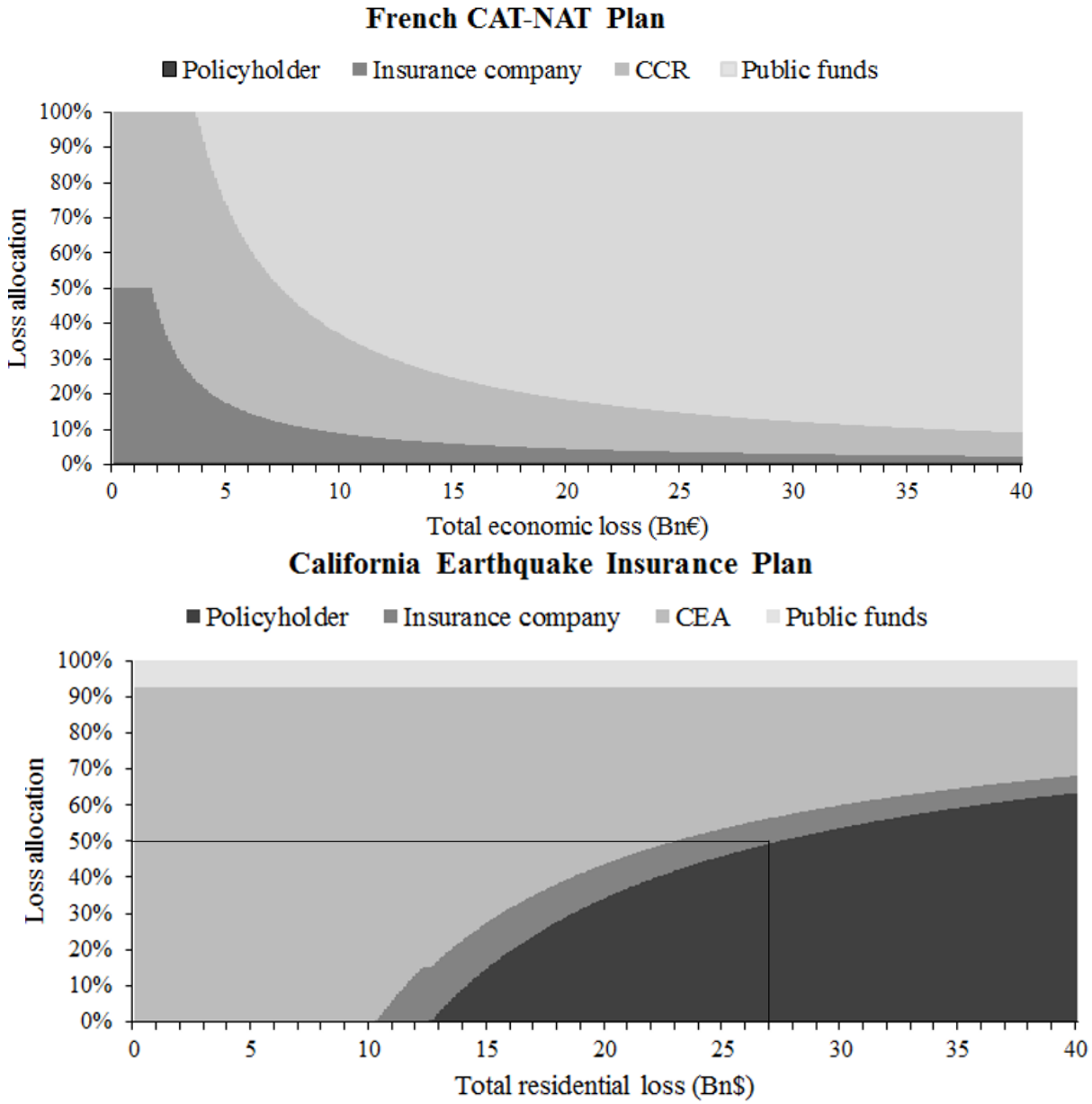


Figure 2.11: Insured loss allocation between stakeholders according to the earthquake insurance scheme currently in force in California and France. For the French CAT-NAT plan the policyholder contribution is too small to be visible.

### *2.3.3. Insurance companies' solvency*

One of the key principles of the insurance theory is the risk mutualisation, which stipulates that for a large portfolio of insured goods (e.g. houses), only a small part can experience a loss at the same time. Consequently, insurance companies can sustain insured losses even with a claim-paying capacity lower than the total sum insured. Then, until the next claim the premium amount collected is used to strengthen the reserves. Insurance companies are interested in a low

claim-paying capacity since the lower the claim-paying capacity, the lower the premium amount. Nevertheless, disasters like earthquakes can affect simultaneously a wide area, and potentially a large part of an insured portfolio. To guarantee that insurance companies have a claim-paying capacity large enough to face such risks, in most countries a minimum level is required by the insurance market authorities. For instance, European insurance companies (i.e. located in a country member of the European Union), are controlled by the European Insurance and Occupational Pensions Authority (EIOPA). One of the most important directives from the EIOPA is *Solvency II* which requires from insurance companies a claim-paying capacity at least equal to the total loss that they could incur, with a probability of exceedance of 0.5% in one year – so-called Solvency Capital Requirement (SCR). To assess this amount, insurance companies can use the framework included in *Solvency II* (called the *Standard Formula*) or developed their own model (called *Internal model*) as long as their supervisor has validated it. Figure 2.12 illustrates the claim-paying capacity for earthquake risk calculated with the *Standard Formula* in each French administrative division.

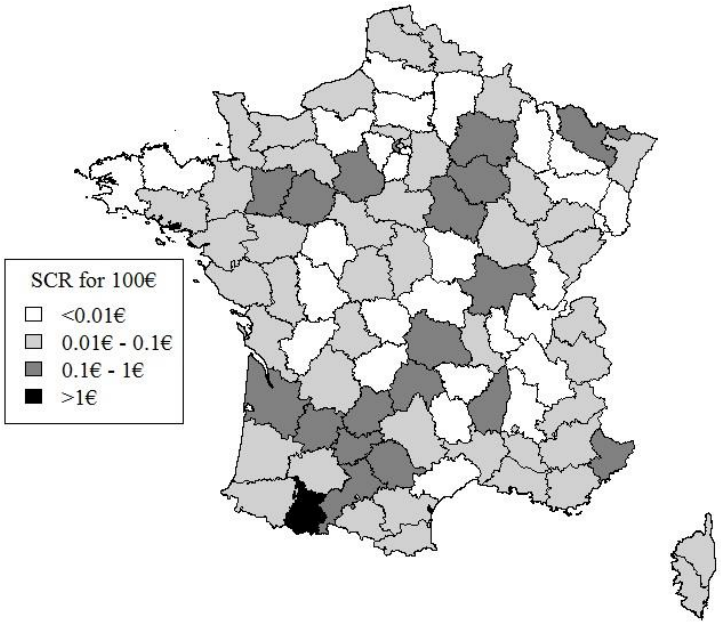


Figure 2.12: Claim-paying capacity required by the EIOPA for earthquake risk, according to the Standard Formula. Source: after EIOPA.

At the country level, the capital requirement associated to the earthquake risk given by the *Standard Formula* is about 0.6% (€0.6 for €100 insured). As a comparison, in 2015 the CEA's claim-paying capacity is able to stand for a 3.5% loss, i.e. almost 60 times more than the EIOPA

solvency requirements for metropolitan France. The reason is twofold: on one hand destructive earthquakes are more likely to occur in California than in metropolitan France and, on the other hand the CEA's claim-paying capacity is designed to sustain a loss with a return period at 400y against 200y in the *Standard Formula*.

Because claim-paying capacity of insurance companies is related to the risk of bankruptcy, it drives their solvency ratio and their financial ratings. For this reason, large insurance companies in Europe tend to have a claim-paying capacity above the threshold of the 200y return period required by *Solvency II*. Table 2.3 shows the ratings for the largest earthquake insurance provider in each country studied (California, France, India and Indonesia).

Table 2.3: Financial rating of some earthquake insurance players as of 2015 according to the following rating agencies: AM Best, Standard & Poor's and Reuters Fitch. The rating description is: AA (Standard & Poor's): very strong capacity to meet its financial commitments; A- (Standard & Poor's): strong capacity to meet its financial commitments but is somewhat more susceptible to the adverse effects of changes in circumstances and economic conditions than insurers in higher-rated categories; A (Reuters Fitch): : high credit quality; BBB+ (Reuters Fitch): good credit quality; A+ (AM Best): superior ability to meet their ongoing insurance obligations; A- (AM Best): excellent ability to meet their ongoing insurance obligations; B++ (AM Best): good ability to meet their ongoing insurance obligations.

| Country | Company | Ratings | | |
|---|---|---|---|---|
| | | Standard & Poor's | Reuters Fitch | AM Best |
| France | CCR | AA | - | A+ |
| | CCR Re | A- | - | - |
| California | CEA | - | A | A |
| India | UIIC | - | - | B++ |
| Indonesia | MAIPARK | - | BBB+ | - |

The CCR and the CEA have an important financial strength. As the CCR benefits from the French state guarantee, its score is the highest, matching the France Sovereign rating. The CCR Re is a subsidiary dedicated to reinsurance operations outside France and without the French state guarantee. Its score (Standard & Poor's A-) is lower or comparable to the CEA's one depending on the rating agency considered (AM Best: A-; Reuters Fitch A). Like for the CEA, the CCR's can face extreme losses, with a claim-paying capacity equal to 1.78 times the 200y return period loss (Cuisse Centrale de Réassurance 2019b). For developing countries, the UIIC (one of the most important insurance company in India) and MAIPARK show a riskier profile, indicating a potential bankruptcy in case of a huge loss.

Aside the solvency regulations applicable to each insurance companies, pool mechanisms are put in place to diversify the risk between insurance companies and consequently reduce the individual risk of bankruptcy. In California, the CEA gathers 24 insurance companies, meaning

that if one of these companies goes to bankruptcy, policyholders are still covered against the earthquake risk by the CEA. In France also the CAT-NAT plan is centralized and the CCR reinsures most of the insurance companies. About Indonesia, non-life insurance companies must be a shareholder of the national reinsurer MAIPARK (KPMG 2016).

In conclusion, this analysis shows that none of the earthquake insurance model reviewed manages to provide both a large cover and sustain extreme losses. This is one of the fundamental reasons of the large protection gap observed for earthquake insurance. Improving earthquake insurance solutions, represents both challenges and opportunities for insurance companies.

## 2.4. Challenges and opportunities in earthquake insurance market development

### *2.4.1. A long-term profitable market with extreme loss*

The 1994 Northridge earthquake damage putted the property insurance market into a crisis which ended by the creation of the CEA. The loss was higher than all the premiums collected and most of insurance companies stopped or restricted sales of new homeowners' policies (Roth 1997; Patton 2014; California Earthquake Authority 2016a). Nevertheless, during most of previous years, the premium amount was collected while no damaging earthquake occurred. Figure 2.13 illustrates the evolution since 1926 of both the premium and the claims amount for the earthquake insurance market in California.

The loss ratio is calculated as the ratio between the claims and the premium amount for a given time step (often one year). A loss ratio below 100% means that the loss amount is lower than the premium amount. Nevertheless, for being sustainable, an insurance solution must have a loss ratio below 100% since part of the premium is necessary to pay the insurance company's overhead costs. In the case of the CEA, the overhead costs represent 17% of the annual premium amount (California Earthquake Authority 2017b) and therefore, the company is cost-effective when the loss ratio is below 83%. Figure 2.13 shows that earthquake insurance in California is profitable over the whole period 1920-2015, despite extreme losses consecutive to the 1994 Northridge, the 1925 Santa Barbara, the 1933 Long Beach, the 1971 San Fernando, or the 1989

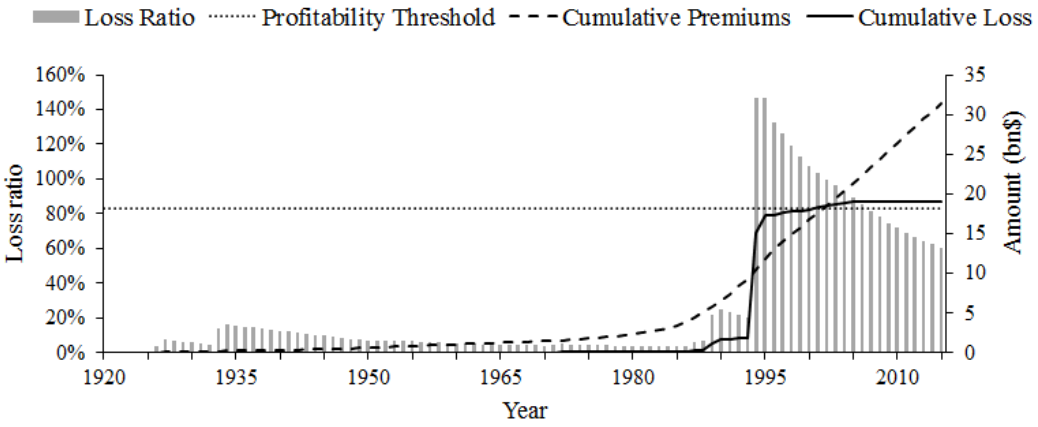


Figure 2.13: Evolution of the premium and the loss amount for the earthquake insurance market in California between 1926 and 2015. Between 1958 and 1969 no loss data is available. The loss ratio is supposed equal to 1% since no damaging earthquake occurred during this period. Source: after Jones et al. 2012; Buffinton 1961; California Department of Insurance database.

Loma Prieta earthquakes. Two earthquakes caused loss above the premium amount collected over the year: the 1989 Loma Prieta earthquake (Yeats 2004; Garamendi 2003) and the 1994 Northridge earthquake (Snyder 1995) and only the latter jeopardized the empirical profitability of the insurance cover (California Earthquake Authority 2016a). Nevertheless, the probable occurrence of extreme events imposes an important need of claim-paying capacity for the insurance companies. Beyond the quantification issue, to raise and hold such a capital is a difficult and costly task.

In conclusion, providing an earthquake cover is more a matter of claim-paying capacity than profitability. Consequently, premium amount is high to capitalize a claim-paying capacity large enough for sustaining extreme losses and to pay the reinsurance premium. The claim-paying capacity also controls the maximum number of earthquake insurance policies (California Earthquake Authority 2018a). Indeed, increasing the earthquake insurance portfolio requires to increase simultaneously the claim-paying capacity. Since raising CEA's capital can take time, increasing the claim-paying capacity means to buy more reinsurance cover which lead to increase the premium amount (California Earthquake Authority 2018a). Thus, the California insurance market is not immune from a new crisis in the case of a sudden increase in earthquake insurance underwriting (10% of California households are insured against earthquake risk in 2015 according to the CDI).

### *2.4.2. A need for being full-covered*

The importance for earthquake insurance policyholders to be fully covered can be perceived through the recent development of the earthquake insurance market in New-Zealand. Following the 2010 and 2011 Canterbury earthquakes, most of insurance companies changed their earthquake residential insurance policy conditions (Sergeant 2016). Initially, the earthquake insurance compensation corresponded to the loss incurred by the policyholder above the deductible amount with no declared insured limit. After these earthquakes, earthquake insurance compensations are capped to a declared amount. Therefore, any additional cost above the declared amount for repairing the insured house is now at the charge of the policyholder. This major insurance policies modification forced the government to publish a report on the forecasted consequences (Sergeant et al. 2015). The main conclusions were: 1) between 40% and 85% of households are exposed to a risk of underinsurance by 10% to 50%; 2) for at least 95% of households no significant insurance shortfall is expected, even after a large earthquake.

However, underinsurance is a real issue in the light of the recent earthquakes. Marquis et al. (2017) show on commercial buildings insured with a declared amount cover in the aftermath of the 2010-2011 Canterbury earthquakes that most of buildings (87%) were underinsured by 12% to 51%. This was the main reason for post-earthquake buildings demolition instead of reconstruction. Similarly, following the 2016 Kaikoura earthquake some homeowners faced rebuilding costs higher than the insurance refund, making the rebuilding process uncertain (MacDonalds 2017; IFSO 2017). From these two developments, New-Zealand government's conclusions in terms of underinsurance level have been corroborated by past earthquakes, but the consequences were underestimated.

In California also, CEA's products are based on a declared amount cover. It means that a claim amount is capped at the declared amount, whatever the repairs cost is above. About the French CAT-NAT plan, there is no direct limit since policies deal with a full replacement cover i.e. the insurance pays for the house rehabilitation whatever the cost.

### *2.4.3. A large untapped market despite new insurance solutions*

Knowing the overall profitability of earthquake insurance, another key element is the potential

size of this market. Figure 2.14 shows the average premium amount for the specific earthquake cover and for the other housing insurance covers (e.g. damage from water damage, theft, etc.).

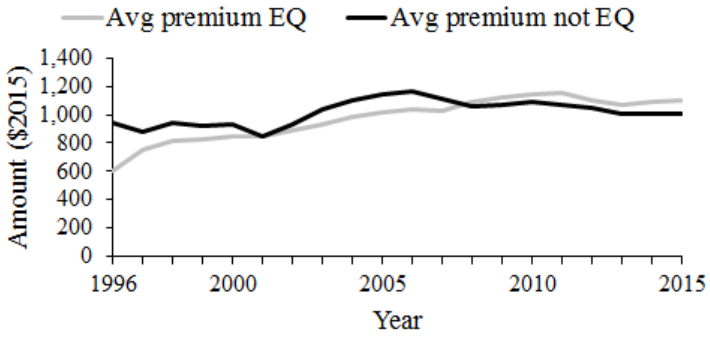


Figure 2.14: Average premium amount for earthquake and household insurance coverage in California (USD 2015). Source: after California Department of Insurance database.

Since 2008, earthquake premium is higher than the housing insurance premium. According to the California Department of Insurance (CDI), in 2015, around 10% of people having a housing insurance coverage are also covered against earthquake risk. To compare the untapped earthquake insurance market in California, we assume that uninsured households have on average the same risk profile than insured people regarding earthquake risk. Considering that 90% of households are not covered against earthquake risk and the average earthquake insurance premium is equal to 1.19 the average housing insurance premium (Fig. 2.14), the untapped earthquake insurance market in California is bigger than the housing insurance market in terms of premium amount ($1.19 \times 0.9 = 1.07$). At a wider scale, most of households are not covered against earthquake risk in many other countries (Fig. 2.15).

This shows that California is not the only rich country prone to earthquake risk to face insurance gap issue (e.g. Italy or Japan). Moreover, Freire et al. (2015) showed that the population in very exposed areas to earthquake risk experienced the fastest growth between 1900 and 2000 (+350%), while the total population grown by +270%; revealing an increasing insurance protection gap. According to a study from the World Bank (Brecht et al. 2013), between 2000 and 2050, the population in big cities (i.e. more than 100,000 inhabitants) exposed to earthquake risk is expected to move approximatively from 350 to 850 million (Birkmann et al. 2016). In conclusion, the untapped earthquake insurance market represents a huge opportunity for insurance companies to develop their business, if well managed.

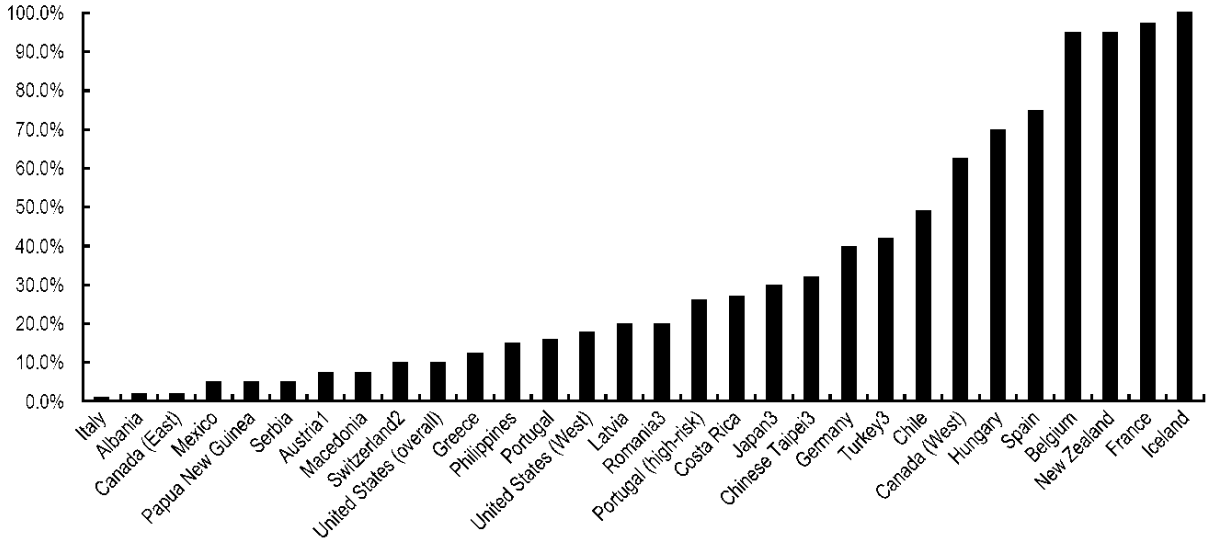


Figure 2.15: Estimated share (in percentage of policies) of households with earthquake insurance coverage. Source: OECD (2018).

## 2.5. Conclusions

The review of earthquake insurance solutions highlights the difficulty for the insurance companies to both offer an earthquake cover affordable and have a large enough claim-paying capacity to face loss consecutive to extreme earthquakes. In France, the premium amount is low, but the insurance scheme benefits from the State guarantee. At the opposite, in California the premium amount is high, but the CEA's claim-paying capacity can sustain a loss twice higher than the 1994 Northridge earthquake. Consequently, depending on the country, the current earthquake insurance scheme focuses either on low premium amount and a loss share in case of extreme events supported by public funds (e.g. in France, Fig. 2.9, 2.11) or on high claim-paying capacity and a loss share in case of extreme events supported by policyholders (e.g. California, Fig. 2.7). Nevertheless, fostering earthquake insurance represents an outstanding challenge for the insurance industry regarding both the need for insured people to be fully covered and the large part of people currently without earthquake insurance. This would definitely contribute to build more resilient cities and improve post-earthquake recovery processes.

# CHAPTER 3: LIMITS OF EARTHQUAKE INSURANCE SOLUTIONS

## 3.1. Introduction

The diversity of earthquake insurance scheme between countries lead us to study them in more depth to identify the main limit. For California, the low rate of insured people is first analysed. This study has been already published in the scientific journal *Natural Hazards and Earth System Sciences* (DOI: 10.5194/nhess-19-1909-2019).

In a second part, the capacity of the French insurance plan against natural disasters (called CAT-NAT) to sustain an extreme loss caused by an earthquake is investigated.

In the last part, the conclusions from the review of current earthquake insurance schemes and the limits identified in the French and California ones are synthetized into key parameters for earthquake insurance market. The result is a maturity scale for earthquake insurance market.

## 3.2. California earthquake insurance unpopularity: the issue is the price, not the risk perception

### *3.2.1. Introduction*

Since 2002, the rate of homeowners insured against earthquake risk in California has never exceeded 16%, according to data provided by the California Department of Insurance (CDI) database. Such a low rate is surprising in a rich area, prone to earthquake risk. Consequently, several studies have already investigated homeowners' behaviour regarding earthquake

insurance in California, in order to identify people who might have an interest in purchasing an earthquake insurance and to understand why they do not so. They have put in light that three main variables have been observed as decisive in purchasing an earthquake insurance: the premium amount, the socio-economic background and the risk perception (Kunreuther et al. 1978; Palm and Hodgson 1992a; Wachtendorf and Sheng 2002).

For the premium amount, both a survey conducted by Meltsner (1978) and the statistics collected from insurance data by Buffinton (1961) and Latourrette et al. (2010) show, as expected, a negative correlation between the premium amount and the insurance adoption. Nevertheless, even uninsured homeowners tend to overestimate the loss they would face in case of a major event and feel vulnerable regardless of their income level (Kunreuther et al. 1978; Palm and Hodgson 1992a). As they are not expecting much from federal aids, they do not know how they will recover (Kunreuther et al. 1978).

Consequently, the decision to purchase an insurance to cover earthquake losses is uncorrelated to the income level (Kunreuther et al. 1978; Wachtendorf and Sheng 2002). Several other socio-economic factors (e.g. duration of residence, neighbours' behaviour or communication strategies of mass media, real estate agencies and insurance companies) have an impact on the risk perception (Meltsner 1978; Palm and Hodgson 1992a; Lin 2013).

Pricing methods used in the real estate market, do not consider seismic risk. Indeed, based on data from the World Housing Encyclopedia, we have shown that building construction price is not correlated to the seismic vulnerability rating (Chapter 4, Section 3). Moreover, earthquake insurance is not mandatory in California for residential mortgage (California Department of Insurance 2019, Information Guides, Earthquake Insurance). Still, lenders for commercial mortgages, are used to require an earthquake insurance only when the probable maximum loss is high (Porter et al. 2004). However, Porter et al. (2004) have also shown that considering earthquake risk for calculating the building's net asset value can have a significant impact in earthquake prone areas like California.

Also, insured people against earthquake risk can receive a compensation lower than the loss incurred because most of earthquake insurance policies in California include a deductibles amount (i.e. at the charge of the policyholder) and are calibrated based on a total reconstruction cost, declared by the policyholder. As reported by Marquis et al. (2017) after the 2010–2011 Canterbury (New Zealand) earthquakes, this amount can be inadequate for the actual repairing costs. Both high deductibles amount (Meltsner 1978; Palm and Hodgson 1992b; Burnett and

Burnett 2009) and underestimated total reconstruction cost (Garratt and Marshall 2003) can make insured people felt unprotected after an earthquake, undermining this kind of insurance.

Since homeowners are aware of the destructive potential of a major earthquake, the risk perception reflects their personal estimate of the occurrence (Kunreuther et al. 1978; Wachtendorf and Sheng 2002). Indeed, most of them disregard this risk because it is seldom, even if destructive earthquake experiences foster insurance underwriting during the following year (Buffinton 1961; Kunreuther et al. 1978; Meltsner 1978; Lin 2015). Consequently, earthquake insurance purchasing behaviour is correlated to personal understanding of seismic risk and is not only related to scientific-based hazard level (Palm and Hodgson 1992a; Palm 1995; Wachtendorf and Sheng 2002).

Limits in earthquake insurance consumption being identified, the next step is to assess the contribution of each factor to the take-up rate. Kunreuther et al. (1978) first proposed a sequential model showing that the individual's purchasing behaviour depends on personal risk perception, premium amount and knowledge of insurance solutions. In the same study (Kunreuther et al. 1978), a numerical model has been also developed, at the same granularity, failing however to reproduce accurately the observed behaviours. According to the authors, the model failed because many surveyed people had a lack of knowledge in existing insurance solutions or were unable to quantify the risk. Models published later (Latourrette et al. 2010; Lin 2013; Lin 2015) assessed the take-up rate by postal code and used demographic variables to capture the disparity in insurance solutions knowledge. Nevertheless because of lack of data, they assumed the premium amount or the risk perception as constant.

The main objective of this study is to introduce a new take-up rate model for homeowners at the scale of California State. Such spatial resolution allows working on most of data available in financial reports, which is numerous enough to use both the premium amount and the risk perception as variables. Contrasting from previous studies, focusing on risk pricing (Yucemen 2005; Petseti and Nektarios 2012; Asprone et al. 2013), this study considers the homeowners' risk perception and behaviour. This shift in point of view approach changes the main issue from: *what should be the price of earthquake insurance considering the risk level?* to: *What is the acceptable price for consumers to purchase an earthquake insurance cover?* Despite results are at the state level, they bring a new framework to model earthquake insurance consumption which allow to quantify the gap between premium amount and homeowners' willingness to pay, depending on the homeowners' risk awareness. Last, this study is also innovative by modelling

separately the contribution of the risk perception and the premium amount to the level of earthquake insurance consumption.

In the first section, data is collected from several sources, processed and summarized in a new database. A take-up rate model is then developed by introducing the two following explanatory variables: the average premium amount and the subjective annual occurrence probability, defined as the risk perceived by homeowners of being affected by a destructive earthquake in one year. The perceived annual probability of occurrence is then studied since 1926, in the next section. Finally, the last section is dedicated to analysing the current low earthquake insurance take-up rate for California homeowners.

### *3.2.2. Data collection and processing*

Developing such a model, even at the State level, faces a first challenge in data collection. Despite California earthquake insurance market has been widely analysed, data volume before the 1990s remains low and extracted from scientific and mass media publications which refer to original data sources that are no longer available. As a consequence, data description is often sparse, incomplete and values can be subject to errors or bias. Consequently, data quality of each data set has to be assessed. Here, it is done on the basis of the support (scientific publication or mass media), the data description (quality of information on the data type and the collecting process) and the number of records. The datasets with the highest quality are used and presented in Table 3.2.1.

This study focuses on the following variables about earthquake insurance policies:

- the total written premium ($W_N$), corresponding to the total amount paid by policyholders to insurance companies during the year $N$;
- the take-up rate ($t_N$), defined as the ratio between the number of policies with an earthquake coverage ($Nb_N$) and those with a fire coverage ($Fi_N$);
- the annual average premium ($P_N$), equal to $W_N$ over $Nb_N$;
- the average premium rate ($p_N$) equal to the ratio between the annual average premium amount $P_N$ and the average value of the good insured (here a house), later referred as the average sum insured ($ASI_N$).

Table 3.2.1: Raw data collected about earthquake insurance. Labels in italic are not extracted from publications but have been inferred by crosschecking with other sources. The data quality scale is: A (good): Scientific publication with methodology explained; B (acceptable): Scientific publication without details on the methodology; C (weak): mass media. CDI: California Department of Insurance database; CPI: Consumer Price Index; Eq: Earthquake; Ho: Homeowners; LA: Los Angeles; LOB: Line of Business; Res: Residential; SF: San Francisco.

| Variable | Metric | LOB | Period | Data quality | Source |
|---|---|---|---|---|---|
| Average premium ($P_N$; $p_N$) | Amount | Ho; Res | 1996-2016 | A | CDI |
| | Rate | Ho | 1972 | A | Kunreuther et al. (1978) |
| | Rate | Ho | 1991 | C | Shiver Jr (1991) |
| | Rate | *Res* | 1926-1930 | A | Freeman (1932) |
| | Rate | Res | 1956 | B | Buffinton (1961) |
| | Amount | Res | 1976 | A | Steinbrugge et al. (1980) |
| | Amount | Res | 1977 | A | Steinbrugge et al. (1980) |
| | Amount | Res | 1978 | A | Steinbrugge et al. (1980) |
| | Amount | Res | 1992 | A | Lagorio et al. (1992) |
| | Annual Variation | Res | 1995 | C | Mulligan (1994) |
| Take-up rate ($t_N$) | Value | Ho | 1972 | A | Kunreuther et al. (1978) |
| | Value | Ho | 1989 | C | Kunreuther (2015) |
| | Value | Ho | 1990 | A | Garamendi et al. (1992) |
| | Value | Ho | 1992 | A | Lagorio et al. (1992) |
| | Value | Ho | 1993 | C | Kunreuther (2015) |
| | Value | Ho | 1994 | A | Roth (1997) |
| | Value | Ho; Res | 1996-2016 | A | CDI |
| | Value | Res | 1926-1930 | A | Freeman (1932) |
| | Value | Res | 1956 | B | Buffinton (1961) |
| | Value | Res | 1971 | B | Roth (1997) |
| | Value | Res | 1976 | B | Kunreuther et al. (1992) |
| | Value | Res | 1978 | A | Steinbrugge et al. (1980) |
| | Annual Variation | Res | 1991 | B | Kunreuther et al. (1992) |
| | Value | Res | 1995 | B | Jones et al. (2012) |
| Total written premium ($W_N$) | *Written amount* | Ho; Res | 1996-2016 | A | CDI |
| | Written amount | Eq | 1992-2016 | A | CDI |
| Total earned premium ($E_N$) | Earned amount | *Eq* | 1921-1929 | A | Freeman (1932) |
| | *Earned amount* | *Eq* | 1930-1969 | B | Meltsner (1978) |
| | Earned amount | *Eq* | 1970-1991 | A | Jones et al. (2012) |
| | Earned amount | Eq | 1992-2016 | A | CDI |
| Number of earthquake policies ($Nb_N$) | Number | Ho | 1990 | A | Garamendi et al. (1992) |
| | Number | Ho | 1994 | A | Roth (1997) |
| Average sum insured ($ASI_N$) | Amount | Ho | 2006-2016 | A | CDI |
| Number of fire policies ($Fi_N$) | Amount | Res | 1996-2016 | A | CDI |
| Socio-economic indicators ($CPI_N$ ; $Pop_N$ ; $RBCI_N$ ) | CPI Urban LA + SF | - | 1921-2016 | A | U.S. Department of Labor |
| | Population census | - | 1921-2016 | A | U.S. Census Bureau |
| | Real Building Cost Index | - | 1921-2015 | A | Shiller (2015) |

All these variables can be calculated for any set of earthquake insurance policies. Insurance companies usually classify their products as follows: the Residential line of business (*Res*) corresponds to insurance policies covering personal goods (e.g. the house, condominium, mobile home, jewellery, furniture). The Homeowners line of business corresponds to the insurance policies included in the Residential line of business but dedicated to homeowners. As

an earthquake insurance cover can be either a guarantee included in a wider policy (e.g. covering also fire or theft risks) or issued in a stand-alone policy, the Earthquake line of business (*Eq*) classifies all insurance policies covering exclusively the earthquake risk. Some of insurance policies within the Earthquake line of business are dedicated to professional clients, and do not belong to the Residential line of business. For clarity, variables hold the acronym of the line of business when they are not related to the Homeowners line of business.

Data for all the variables listed is available only since 1996 (Tab. 3.2.1). In order to expand the historical database, they are also estimated in an indirect way for the following periods: 1926-1930, 1956, 1971-1972, 1976-1978 and 1989-1995, leading to consider additional data (Tab. 3.2.1) and to use linear regressions (Fig. 3.2.1).

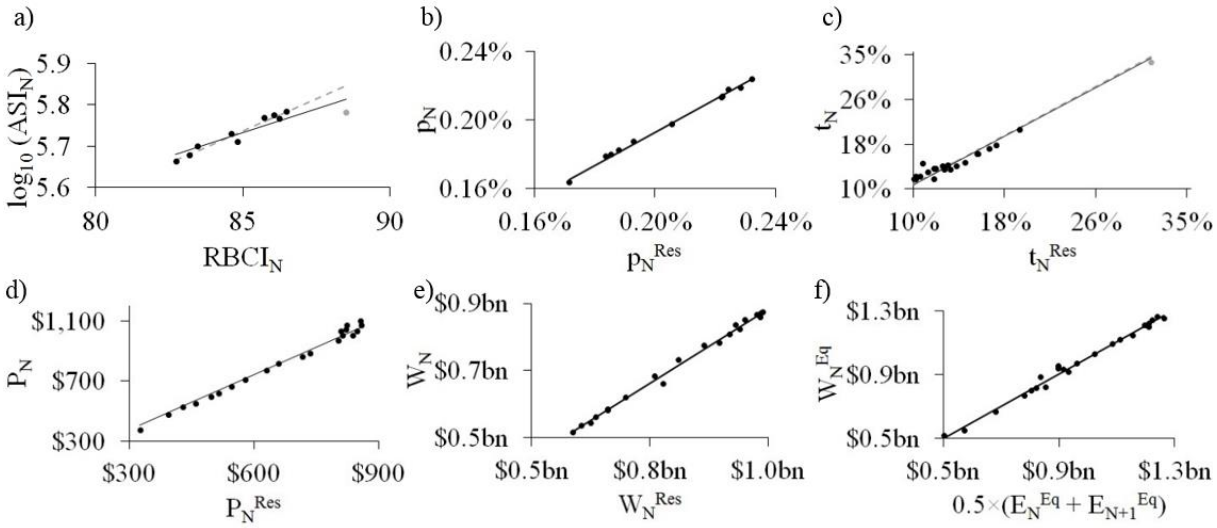


Figure 3.2.1: Fits of the linear regressions for: a) the average sum insured and the Real Building Cost Index, b) the average premium rate between the Residential and the Homeowners lines of business, c) the take-up rate between the Residential and the Homeowners lines of business, d) the average premium amount between the Residential and the Homeowners lines of business, e) the total written premium amount between the Residential and the Homeowners lines of business and f) the written and the earned premium amounts. Grey points on a) and c) represent the extreme values, affecting the linear regression from the solid black line to the dashed grey line, when removed. Financial values are in USD 2015.

By definition of the average premium rate ($p_N$), $P_N$ can be approximated by the product of $p_N$ and the average sum insured ($ASI_N$). The latter is estimated from the Real Building Cost Index ($RBCI_N$), which is an economic index (base: 31/12/1979=100) capturing the evolution of the cost of building construction works (Shiller 2015). The following linear regression has been calibrated on data from Table 3.2.1 between 2006 and 2015:

$$\log_{10}(ASI_N) = 0.0233 \times RBCI_N + 3.7554 \qquad (R^2 = 0.84 \quad \text{Fig. 3.2.1a}) \qquad (3.2.1)$$

where $ASI_N$ is in USD 2015 and $R^2$ is the coefficient of determination. When the average premium rate corresponds to the Residential line of business ($p_N^{Res}$), it can be converted into $p_N$ with the following linear regression built on the CDI database between 2006 and 2016 (Tab. 3.2.1):

$$p_N = 0.96 \times p_N^{Res} \qquad (R^2 = 1 \quad \text{Fig. 3.2.1b}) \qquad (3.2.2)$$

Using again the CDI database between 1996 and 2016 (Tab. 3.2.1), the following linear regressions have also been developed between $P_N$, $t_N$ and $W_N$ and the corresponding metrics for the Residential line of business ($P_N^{Res}$, $t_N^{Res}$ and $W_N^{Res}$):

$$t_N = 1.08 \times t_N^{Res} \qquad (R^2 = 0.95 \quad \text{Fig. 3.2.1c}) \qquad (3.2.3)$$

$$P_N = 1.24 \times P_N^{Res} \qquad (R^2 = 0.99 \quad \text{Fig. 3.2.1d}) \qquad (3.2.4)$$

$$W_N = 0.88 \times W_N^{Res} \qquad (R^2 = 0.99 \quad \text{Fig. 3.2.1e}) \qquad (3.2.5)$$

Before 1996, the total premium amount for earthquake insurance, mentioned in CDI reports, was about the Earthquake line of business, and in terms of total earned premium ($E_N$). While the total written premium ($W_N$) corresponds to the total amount of premium paid by policyholders to insurance companies during the year $N$, $E_N$ is the amount of premium used to cover the risk during the year $N$. To illustrate these two definitions, Figure 3.2.2 takes the example of an insurance policy for which the annual premium is paid every March 1st.

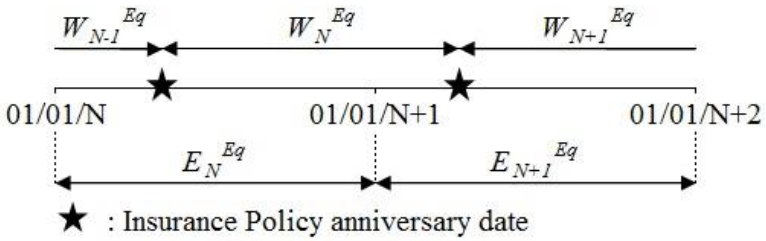


Figure 3.2.2: Illustration of the difference between the earned and the written premium amount.

As the amount received at year $N$ by the insurance company ($W_N$) covers the risk until March 1st, $N+1$, the insurance company can use only 75% of $W_N$ during the year $N$ (9 months over 12). By adding the 25% of $W_{N-1}$, this makes the total earned premium $E_N$, for the year $N$.

To estimate $W_N^{EQ}$ from $E_N^{EQ}$ for the Earthquake line of business, the following relationship has been defined based on data from the CDI database and over the period 1992-2016 (Tab. 3.2.1):

$$W_N^{Eq} = \frac{E_N^{Eq} + E_{N+1}^{Eq}}{2} \qquad (R^2 = 0.99 \quad \text{Fig. 3.2.1f}) \tag{3.2.6}$$

About the difference between $W_N^{EQ}$ and $W_N^{Res}$, despite data (Tab. 3.2.1) shows a significant difference ($W_N^{EQ} - W_N^{Res}$ = \$250m.) since 1996, this study assumes that $W_N^{EQ}$ is equal to $W_N^{Res}$ until 1995:

$$W_N^{Res} \approx \begin{cases} W_N^{Eq} & \text{if } N \leq 1995 \\ W_N^{Eq} - \$249{,}188{,}671 & \text{else} \end{cases} \tag{3.2.7}$$

This strong assumption was used by Garamendi et al. (1992) and was verified for the loss after the 1994 Northridge earthquake reported by Eguchi et al. (1998).

Last, when variables cannot be inferred from other variables, they are estimated based on the annual variation for $P_N^{EQ}$:

$$P_N^{Res} = P_{N-1}^{Res} \times \Delta_{P_{N-1}^{Res}}^{P_N^{Res}} \tag{3.2.8}$$

and the biennial variation for $t_N^{EQ}$:

$$t_N^{Res} = t_{N-2}^{Res} \times \Delta_{t_{N-2}^{Res}}^{t_N^{Res}} \tag{3.2.9}$$

where $\Delta_X^Y$ is equal to the ratio $Y$ over $X$. Furthermore, the variation of the total written premium for the Residential line of business $\left(\Delta_{W_{N-1}^{Res}}^{W_N^{Res}}\right)$ is linked to $\left(\Delta_{P_{N-1}^{Res}}^{P_N^{Res}}\right)$, $\left(\Delta_{t_{N-1}^{Res}}^{t_N^{Res}}\right)$ and $\left(\Delta_{Fi_{N-1}^{Res}}^{Fi_N^{Res}}\right)$as follows:

$$\Delta_{W_{N-1}^{Res}}^{W_N^{Res}} = \frac{W_N^{Res}}{W_{N-1}^{Res}} \tag{3.2.10}$$

$$\Delta_{W_{N-1}^{Res}}^{W_N^{Res}} = \frac{P_N^{Res} \times Nb_N^{Res}}{P_{N-1}^{Res} \times Nb_{N-1}^{Res}}$$

$$\Delta_{W_{N-1}^{Res}}^{W_N^{Res}} = \frac{P_N^{Res} \times Fi_N^{Res} \times t_N^{Res}}{P_{N-1}^{Res} \times Fi_{N-1}^{Res} \times t_{N-1}^{Res}}$$

$$\Delta_{W_{N-1}^{Res}}^{W_N^{Res}} = \Delta_{P_{N-1}^{Res}}^{P_N^{Res}} \times \Delta_{Fi_{N-1}^{Res}}^{Fi_N^{Res}} \times \Delta_{t_{N-1}^{Res}}^{t_N^{Res}}$$

As we have no data regarding the annual variation of the number of fire insurance policy for the residential line of business $\left(\Delta_{Fi_{N-1}^{Res}}^{Fi_N^{Res}}\right)$ before 1996 (Tab. 3.2.1), it is assumed as equal to the variation of the California Population $Pop_N$:

$$\Delta_{Fi_{N-1}^{Res}}^{Fi_N^{Res}} \approx \Delta_{Pop_{N-1}}^{Pop_N} \tag{3.2.11}$$

Figures 3.2.1 and 3.2.3 illustrate the goodness-of-fit of the regressions developed (Eq. 3.2.1 to 3.2.6) and the variations of the population compared to the number of fire insurance policies between 1996 and 2016 (Eq. 3.2.11), respectively.

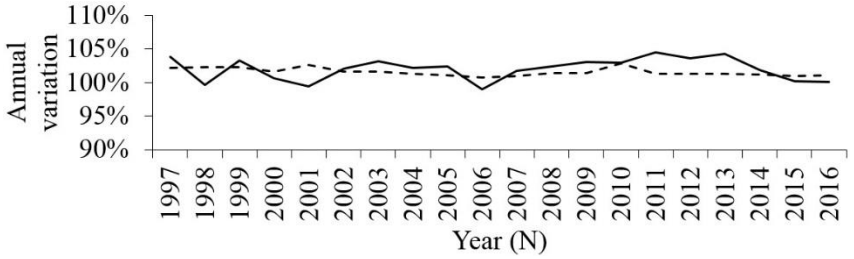


Figure 3.2.3: Comparison between the annual variations of the number of fire insurance policies for the Residential line of business (solid line) and the California population (dashed line).

Finally, values of $P_N$, $t_N$ and $W_N$ collected (Tab. 3.2.1) and estimated in this study (Eq. 3.2.1 to 3.2.11) are aggregated into a new database presented in Table 3.2.2. Financial amounts are converted into USD 2015 using the Consumer Price Index (U.S. Dept. of Labor 2017). The data quality of each variable is also assessed at the weakest data quality used (Tab. 3.2.1), downgraded of as much levels as the number of equations used to assess it (listed in the column Equation Id). For example, the annual average premium $P_{1926}$ has been calculated from the premium rate for the Residential line of business $p_{1926}^{Res}$ (Tab. 3.2.1) and the Equations 3.2.1 and 3.2.4. The associated Data Quality is C (Tab. 3.2.2) because the Data Quality of $p_{1926}^{Res}$ is A (Tab. 3.2.1), downgraded of two levels for the two equations used.

The model developed in the next section uses this new database to estimate the take-up rate for the California homeowners ($t_N$) from the average premium amount ($P_N$) and another variable capturing the relative earthquake risk awareness.

Table 3.2.2: The California Homeowners Earthquake Insurance database developed for this study. Data quality scale is: A (good): all data from scientific publications with methodology explained; (B) acceptable: at least one data from a scientific publication without details on the methodology or one processing has been applied; (C) weak: data is uncertain. Financial amounts are in USD 2015. The total written premium is given in million USD. Column names are Q: Data Quality; E: Equation Id: 3.2.X. Abbreviations are: $E_1$ = {3.2.3; 3.2.6; 3.2.7; 3.2.10}; $E_2$ = {3.2.5; 3.2.6; 3.2.7}.

| $N$ | $t_N$ | $Q$ | $E$ | $P_N$ | $Q$ | $E$ | $W_N$ | $Q$ | $E$ | $N$ | $W_N$ | $Q$ | $E$ | $N$ | $W_N$ | $Q$ | $E$ |
|---|---|---|---|---|---|---|---|---|---|---|---|---|---|---|---|---|---|
| 1926 | 5% | B | 3 | 612 | C | 1; 4 | 3 | C | $E_2$ | 1931 | 1 | C | $E_2$ | 1973 | 12 | C | $E_2$ |
| 1927 | 4% | B | 3 | 809 | C | 1; 4 | 2 | C | $E_2$ | 1932 | 1 | C | $E_2$ | 1974 | 13 | C | $E_2$ |
| 1928 | 6% | B | 3 | 441 | C | 1; 4 | 2 | C | $E_2$ | 1933 | 1 | C | $E_2$ | 1975 | 15 | C | $E_2$ |
| 1929 | 7% | B | 3 | 339 | C | 1; 4 | 2 | C | $E_2$ | 1934 | 1 | C | $E_2$ | 1979 | 33 | C | $E_2$ |
| 1930 | 8% | B | 3 | 287 | C | 1; 4 | 2 | C | $E_2$ | 1935 | 1 | C | $E_2$ | 1980 | 44 | C | $E_2$ |
| 1956 | 3% | C | 3 | 1101 | C | 1; 4 | 5 | C | $E_2$ | 1936 | 1 | C | $E_2$ | 1981 | 54 | C | $E_2$ |
| 1971 | 8% | C | 3 | 285 | C | 1; 4; $E_1$ | 7 | C | $E_2$ | 1937 | 1 | C | $E_2$ | 1982 | 65 | C | $E_2$ |
| 1972 | 1% | A | - | 2228 | B | 1 | 10 | C | $E_2$ | 1938 | 1 | C | $E_2$ | 1983 | 76 | C | $E_2$ |
| 1976 | 3% | C | 3 | 670 | B | 4 | 18 | C | $E_2$ | 1939 | 1 | C | $E_2$ | 1984 | 108 | C | $E_2$ |
| 1977 | 6% | C | $E_1$ | 624 | B | 4 | 21 | C | $E_2$ | 1940 | 1 | C | $E_2$ | 1985 | 158 | C | $E_2$ |
| 1978 | 8% | B | 3 | 576 | B | 4 | 26 | C | $E_2$ | 1941 | 1 | C | $E_2$ | 1986 | 195 | C | $E_2$ |
| 1989 | 22% | C | - | 586 | C | 4; 10; $E_2$ | 360 | C | $E_2$ | 1942 | 1 | C | $E_2$ | 1987 | 244 | C | $E_2$ |
| 1990 | 25% | A | - | 551 | C | $E_2$ | 405 | C | $E_2$ | 1943 | 2 | C | $E_2$ | 1988 | 307 | C | $E_2$ |
| 1991 | 24% | C | 3;9 | 506 | C | 1 | 480 | C | $E_2$ | 1944 | 2 | C | $E_2$ | | | | |
| 1992 | 100% | A | - | 77 | B | 4 | 519 | C | 5;7 | 1945 | 2 | C | $E_2$ | | | | |
| 1993 | 37% | C | - | 348 | C | 4; 5; $E_1$ | 550 | C | 5;7 | 1946 | 3 | C | $E_2$ | | | | |
| 1994 | 31% | A | - | 511 | C | 5; 7 | 668 | C | 5;7 | 1947 | 3 | C | $E_2$ | | | | |
| 1995 | 22% | C | 3 | 842 | C | 4; 8; $E_2$ | 883 | C | 5;7 | 1948 | 3 | C | $E_2$ | | | | |
| 1996 | 33% | A | - | 606 | A | - | 778 | A | - | 1949 | 3 | C | $E_2$ | | | | |
| 1997 | 21% | A | - | 753 | A | - | 606 | A | - | 1950 | 3 | C | $E_2$ | | | | |
| 1998 | 18% | A | - | 810 | A | - | 589 | A | - | 1951 | 4 | C | $E_2$ | | | | |
| 1999 | 18% | A | - | 821 | A | - | 626 | A | - | 1952 | 4 | C | $E_2$ | | | | |
| 2000 | 17% | A | - | 850 | A | - | 637 | A | - | 1953 | 4 | C | $E_2$ | | | | |
| 2001 | 16% | A | - | 851 | A | - | 661 | A | - | 1954 | 4 | C | $E_2$ | | | | |
| 2002 | 15% | A | - | 888 | A | - | 661 | A | - | 1955 | 4 | C | $E_2$ | | | | |
| 2003 | 14% | A | - | 931 | A | - | 661 | A | - | 1957 | 5 | C | $E_2$ | | | | |
| 2004 | 14% | A | - | 990 | A | - | 761 | A | - | 1958 | 5 | C | $E_2$ | | | | |
| 2005 | 12% | A | - | 1020 | A | - | 699 | A | - | 1959 | 5 | C | $E_2$ | | | | |
| 2006 | 14% | A | - | 1035 | A | - | 810 | A | - | 1960 | 6 | C | $E_2$ | | | | |
| 2007 | 14% | A | - | 1025 | A | - | 865 | A | - | 1961 | 5 | C | $E_2$ | | | | |
| 2008 | 14% | A | - | 1092 | A | - | 931 | A | - | 1962 | 6 | C | $E_2$ | | | | |
| 2009 | 14% | A | - | 1128 | A | - | 952 | A | - | 1963 | 6 | C | $E_2$ | | | | |
| 2010 | 14% | A | - | 1148 | A | - | 978 | A | - | 1964 | 5 | C | $E_2$ | | | | |
| 2011 | 13% | A | - | 1157 | A | - | 989 | A | - | 1965 | 5 | C | $E_2$ | | | | |
| 2012 | 12% | A | - | 1101 | A | - | 920 | A | - | 1966 | 5 | C | $E_2$ | | | | |
| 2013 | 12% | A | - | 1073 | A | - | 897 | A | - | 1967 | 5 | C | $E_2$ | | | | |
| 2014 | 12% | A | - | 1092 | A | - | 940 | A | - | 1968 | 6 | C | $E_2$ | | | | |
| 2015 | 12% | A | - | 1103 | A | - | 984 | A | - | 1969 | 6 | C | $E_2$ | | | | |
| 2016 | 15% | A | - | 980 | A | - | 986 | A | - | 1970 | 5 | C | $E_2$ | | | | |

### *3.2.3. Model development for the period 1997-2016*

In order not to presume a linear trend between the consumers' behaviour and explanatory variables (e.g. the average premium amount), this study refers to the Expected Utility theory (Von Neumann and Morgenstern 1944) instead of statistical linear models. The Expected Utility theory is a classical framework in Economic science to model the economical choices

of a consumer, depending on several variables like the wealth or the risk aversion (Appendix A). Here the application field is the California homeowners instead of a single consumer. Within this framework, homeowners are assumed rational and taking decisions in order to maximize their utility. Furthermore, their relative risk aversion is considered constant whatever the wealth because the decision to purchase or not an earthquake insurance is independent from the income level (Kunreuther et al. 1978; Wachtendorf and Sheng 2002). One of the most used utility functions ($U$) is (Holt and Laury 2002):

$$U\big(g_N(t_N)\big) = \frac{g_N(t_N)^{1-\beta}}{1-\beta} \tag{3.2.12}$$

where $g_N$ and $\beta$ are the wealth function at year $N$ and the risk profile controlling the risk aversion level (the larger $\beta$, the higher the aversion), respectively.

Then, the average household's capital $K$ is assumed in this study equal to the average sum insured ($ASI_{2015}$) since the earthquake insurance consumption is uncorrelated to the wealth (Kunreuther et al. 1978; Wachtendorf and Sheng 2002) and equal to $604,124 (USD 2015). Consequently, the wealth of uninsured homeowners is $g_N = K$, if no damaging earthquake occurs. Regarding the loss estimation, homeowners are mostly concerned by destructive earthquakes, defined as earthquakes which can potentially damage their home, and tend to overestimate the impact (Buffinton 1961; Kunreuther et al. 1978; Meltsner 1978; Lin 2015). Furthermore, according to Kunreuther et al. (1978), insured people believe that they are fully covered in case of loss. Therefore, we assume that only uninsured homeowners expect to incur a loss equal to $K$ after a damaging earthquake. This leads us to model that uninsured homeowners expect a wealth at $g_N = 0$ after a damaging earthquake. About insured homeowners, we assume that they expect to have a constant wealth at $g_N = K - P_N$, since they believe to be fully covered in case of losses induced by an earthquake. Table 3.2.3 summarizes these three wealth levels, based on the occurrence of a devastating earthquake and the insurance cover.

Table 3.2.3: The three different wealth levels of a homeowner, considered in this study, according on the occurrence of a damaging earthquake and the insurance cover. The quantities $t_N$ and $1 - t_N$ represent the share of homeowners insured and not insured, respectively.

| Occurrence of a damaging earthquake | Insured ($t_N$) | Not insured ($1 - t_N$) |
|---|---|---|
| Yes | $K - P_N$ | 0 |
| No | $K - P_N$ | $K$ |

Finally, considering the share of insured homeowners ($t_N$) and the results in Table 3.2.3, $g_N$ can be written for all homeowners:

$$g_N(t_N) = K - t_N \times P_N - K \times (1 - t_N) \times \mathrm{B_{EQ}}(r_N) \tag{3.2.13}$$

where $\mathrm{B_{EQ}}(r_N)$ is a random variable following the Bernoulli distribution (i.e. equal to 1 if a damaging earthquake occurs during the year $N$ and 0 otherwise). The parameter $r_N$, called the subjective annual occurrence probability, controls the homeowners' risk perception through the perceived probability of being affected by a destructive earthquake during the year $N$ (Kunreuther et al. 1978; Wachtendorf and Sheng 2002). As homeowners want to maximize their utility, $t_N$ is solution of:

$$t_N^{Estimated} = \underset{0 \le t_N \le 1}{\operatorname{argmax}} \, \mathbb{E}\left(U\left(g_N(t_N)\right)\right) \tag{3.2.14}$$

where argmax stands for the argument of the maxima function (i.e. which returns the value of $t_N$ which maximizes the quantity $\mathbb{E}(\mathrm{U}(g_N(t_N)))$ and $\mathbb{E}(\mathrm{U}(g_N(t_N)))$ is the expected value of $\mathrm{U}(g_N(t_N))$ which depends from the random variable $\mathrm{B_{EQ}}(r_N)$ (Eq. 3.2.13). Assuming that homeowners are risk averse (i.e. $\beta > 0$) and noticing that $P_N / K$ is very small compared to 1, $t_N^{Estimated}$ is shown (Appendix B) to be equal to:

$$t_N^{Estimated} = \min\left(\left(\frac{r_N}{1 - r_N} \times \frac{K}{P_N}\right)^{\frac{1}{\beta}}; 100\%\right) \tag{3.2.15}$$

As a first step, the model is calibrated with data on the period 1997-2016 corresponding to the whole activity period of the California Earthquake Authority (CEA) providing high quality data (Tab. 3.2.2). Created on December 1996, this is a non-profit, state managed, organization, selling residential earthquake policies (Marshall 2017). The stability of the insurance activity and the lack of devastating earthquake lead us to model parameters $\beta$ and $r_N$, capturing the homeowners' risk perception, by constant variables. They are estimated at $r_{\{1997;\ldots;2016\}} = 0.027\%$ and $\beta = 0.93$, using the Least Squared method with the Generalized Reduced Gradient algorithm. The model (Eq. 3.2.15) fits the observed data with a $R^2 = 0.79$ (Fig. 3.2.4).

Furthermore, the values of the two parameters are meaningful: homeowners are modelled "very risk averse" ($\beta = 0.93$), which is consistent with a high severity risk like an earthquake (Holt and Laury 2002). $r_N$ is also somehow consistent with the value that can be calculated from a hazard analysis, as presented later.

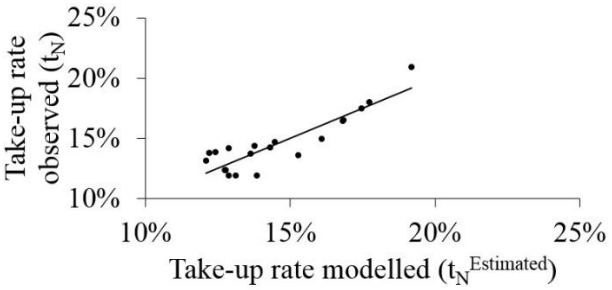


Figure 3.2.4: Fit between the take-up rates modelled and observed for the period 1997-2016.

The model calibration between 1997 and 2016 is not appropriate for other periods corresponding to different seismic activity and insurance economic context. The next section investigates how the homeowners' risk perception has changed since 1926 in order to adapt the model to any period.

### *3.2.4. Evolution of the homeowners' risk perception since 1926*

The homeowners' risk perception is controlled by both the risk materiality (what kind of earthquakes are expected to occur?) and the risk tolerance (how much homeowners are ready to lose?). The associated parameters in the model are $r_N$ and $\beta$, respectively. As we cannot differentiate the one from the other, $\beta$ is assumed constant in this study and all the variations of the homeowner's risk perception are passed on to $r_N$.

According to the model and the relationships developed (Eq. 3.2.3, 3.2.4, 3.2.5, 3.2.10, 3.2.11 and 3.2.15), the variations of the total written premium amount per capita ($W_N$ / $Pop_N$) depend on the variation of the average premium amount ($P_N$) and the subjective annual occurrence probability ($r_N$):

$$\frac{W_N/Pop_N}{W_{N-1}/Pop_{N-1}} = \frac{\Delta_{W_{N-1}^{Res}}^{W_N^{Res}}}{\Delta_{Pop_{N-1}}^{Pop_N}} \tag{3.2.16}$$

$$\frac{W_N/Pop_N}{W_{N-1}/Pop_{N-1}} = \Delta_{P_{N-1}}^{P_N} \times \Delta_{t_{N-1}}^{t_N}$$

$$\frac{W_N/Pop_N}{W_{N-1}/Pop_{N-1}} = \Delta_{P_{N-1}}^{P_N} \times \frac{\min\left(\left(\frac{r_N}{1-r_N} \times \frac{K}{P_N}\right)^{\frac{1}{\beta}}; 100\%\right)}{\min\left(\left(\frac{r_{N-1}}{1-r_{N-1}} \times \frac{K}{P_{N-1}}\right)^{\frac{1}{\beta}}; 100\%\right)}$$

Under the assumption that $t_N^{Estimated}$ has never reached 100% in the past and with $\beta$ = 0.93, Equation 3.2.16 can be simplified as follows:

$$\frac{W_N/Pop_N}{W_{N-1}/Pop_{N-1}} = \Delta_{P_{N-1}}^{P_N} \times \frac{\left(\frac{r_N}{1-r_N} \times \frac{K}{P_N}\right)^{\frac{1}{\beta}}}{\left(\frac{r_{N-1}}{1-r_{N-1}} \times \frac{K}{P_{N-1}}\right)^{\frac{1}{\beta}}} \tag{3.2.17}$$

$$\frac{W_N/Pop_N}{W_{N-1}/Pop_{N-1}} = \left(\frac{P_N}{P_{N-1}}\right)^{-0.07} \times \left(\frac{r_N \times (1-r_{N-1})}{r_{N-1} \times (1-r_N)}\right)^{1.07}$$

The contribution of $P_N$ / $P_{N-1}$ is clearly marginal, leading to consider the regression, built on the variations of $W_N$ / $Pop_N$ and $r_N$ between 1997 and 2016 (Tab. 3.2.2):

$$\frac{r_N}{r_{N-1}} - 1 = 0.92 \times \left(\frac{W_N/Pop_N}{W_{N-1}/Pop_{N-1}} - 1\right) \qquad (R^2 = 1) \tag{3.2.18}$$

Equations 3.2.16 and 3.2.18 are used on the period 1997-2016 and the goodness-of-fit is illustrated in Figures 3.2.5a, b.

Considering that understanding the details of those variations is out of reach given the scarcity of data, this study focuses only on those above 15.5% in absolute value, qualified hereafter as significant variations ($V_N$). Other variations are neglected, and we assume they cancel each other out. Table 3.2.4 lists all of them, together with the most significant event occurred the same year, for the earthquake insurance industry.

Despite these events (Tab. 3.2.4) could have led insurance companies to restrict or enlarge the number of earthquake insurance policies (Born and Klimaszewski-Blettner 2013), contributing in this way to $V_N$, this study focuses only on the homeowners' risk perception variations. Then, the subjective annual occurrence probability ($r_N$) is estimated according to the following time series for $N \in [1926; 2016]$:

$$\begin{cases} r_{2016} = 0.027\% \\ r_N = \dfrac{r_{N+1}}{1+V_{N+1}} \quad \forall\, N \in [1926; 2015] \end{cases} \tag{3.2.19}$$

The time series of $r_N$ is represented in Figure 3.2.6 and illustrates that some earthquakes (indicated by dots) have increased $r_N$ during the year as already published (Buffinton 1961; Kunreuther et al. 1978; Meltsner 1978; Lin 2015) but, more surprisingly, some others had no apparent impact, like the 1952 Kern County and the 1989 Loma Prieta earthquakes.

The first one damaged over 400 unreinforced masonry buildings (Jones et al. 2012) but none of the buildings designed under the latest seismic codes (Geschwind 2001).

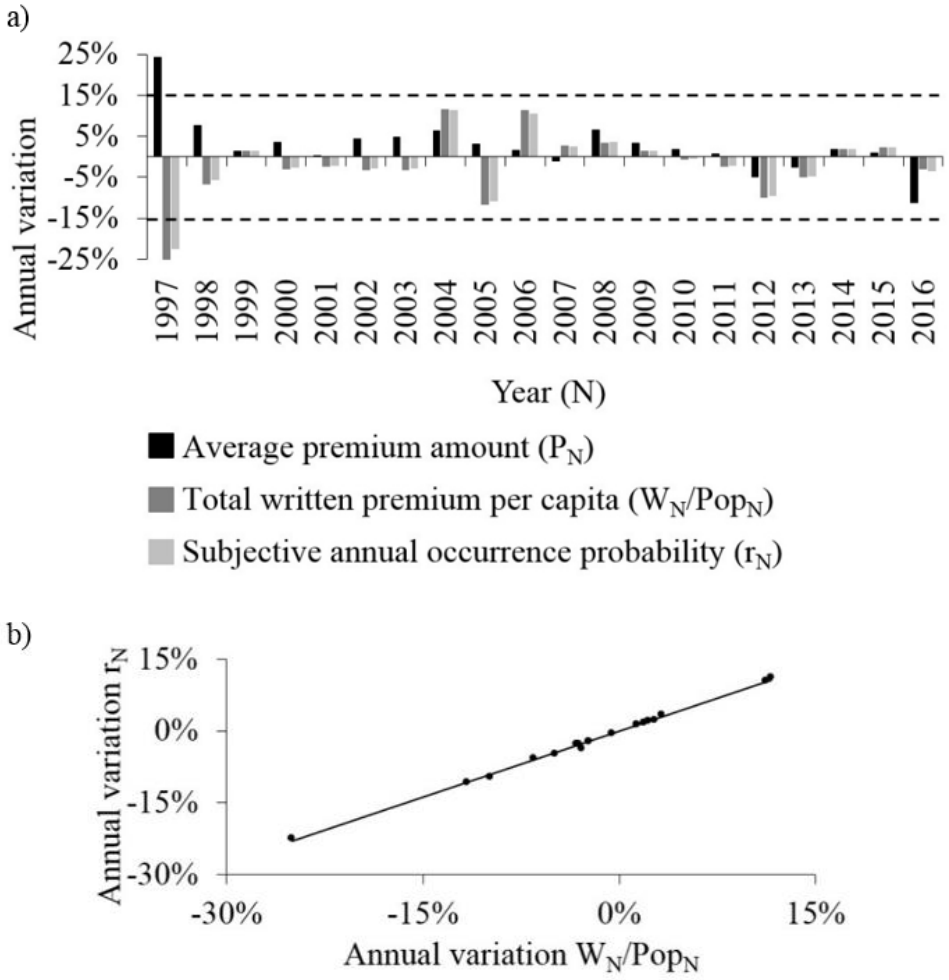


Figure 3.2.5: a) Variations of the average premium amount, the total written premium per capita and the subjective annual occurrence probability between 1997 and 2016. Variations are calculated compared to the previous year. Dashed lines represent the thresholds for a significant variation. b) Fit between the variation of the total written premium per capita and the subjective annual occurrence probability.

Table 3.2.4: Events expected to have significantly modified the homeowners' risk perception through the subjective annual occurrence probability. $V_N$ represents the variation compared to the previous year, with the sign '+' for an increase and '-' for a decrease.

| Category | Period | Major event occurred | Variation ($V_N$) |
|---|---|---|---|
| Earthquake | 1933 | Long Beach earthquake | +22% |
| | 1971-1972 | San Fernando earthquake | +65% |
| | 1979 | Imperial Valley and Coyote Lake earthquakes | +15% |
| | 1984-1988 | High seismic activity | +109% |
| | 1994-1995 | Northridge earthquake | +49% |
| Socio-economic | 1928 | Discredit of a major earthquake in Southern California | -20% |
| | 1931-1932 | Great Depression | -50% |
| | 1946 | Post World War II economic expansion | +22% |
| | 1984-1985 | Earthquake coverage mandatory offer law | +30% |
| | 1997 | Restricted mandatory earthquake coverage | -23% |

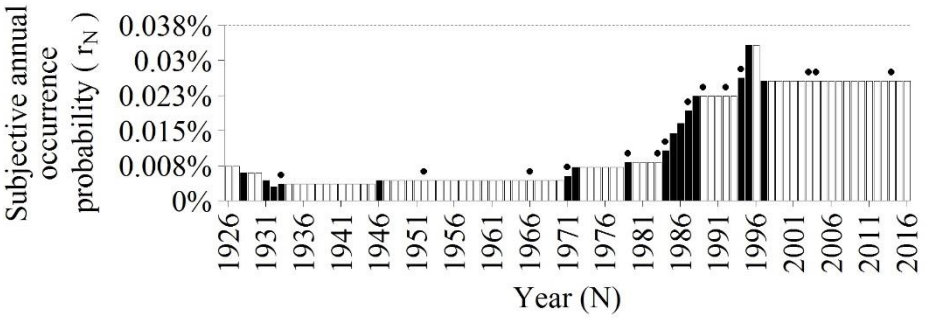


Figure 3.2.6: Estimated subjective annual occurrence probability between 1927 and 2016 for a California homeowner to be affected by a devastating earthquake. Black bars represent the significant evolutions and dots indicate the occurrence of the following big earthquakes in California: 1933 Long Beach, 1952 Kern County, 1966 Parkfield, 1971 San Fernando, 1979 Coyote Lake, 1979 Imperial Valley and Coyote Lake, 1983 Coalinga, 1984 Morgan Hill, 1987 Whittier Narrows, 1989 Loma Prieta, 1992 Big Bear and Landers, 1994 Northridge, 2003 San Simeon, 2004 Parkfield and 2014 Napa. The grey line shows the average annual occurrence probability calculated between 1952 and 2018 using ShakeMap footprints (USGS) and the Global Human Settlement Population Grid (European Commission).

Consequently, structural engineers claimed that new buildings were earthquake-proof and that no additional prevention measures were needed (Geschwind 2001). This message received a great echo among the population despite the warnings of some earthquake researchers like Charles Richter (Geschwind 2001).

Regarding the second one, most of homeowners were only partially refunded, due to large deductibles, and decided to cancel their earthquake insurance policy (Meltsner 1978; Palm and Hodgson 1992b; Burnett and Burnett 2009). Moreover, the 1989 Loma Prieta earthquake struck just after a high seismic activity period during which $r_N$ has increased significantly. Indeed, the number of earthquakes occurring during the preceding 5 years with a moment magnitude greater than M5 reached the highest peak since 1855 between 1984 and 1998, as illustrated in Figure 3.2.7.

The sequence includes in particular the 1983 Coalinga and the 1987 Whittier Narrows earthquakes. This specific temporal burst in seismic activity may have participated in homeowners' rising risk awareness (Tab. 3.2.4).

Some major socio-economic events also had an impact on $r_N$ (Tab. 3.2.4), at the light of the 1929 Great Depression and the Post World War II economic expansion. Insurance regulation acts also have an impact. During the period 1984-1985, the California Senate Assembly voted the Assembly Bill AB2865 (McAlister 1984) which required insurance companies to offer earthquake coverage. A second bill in 1995, named AB1366 (Knowles 1995), amended the

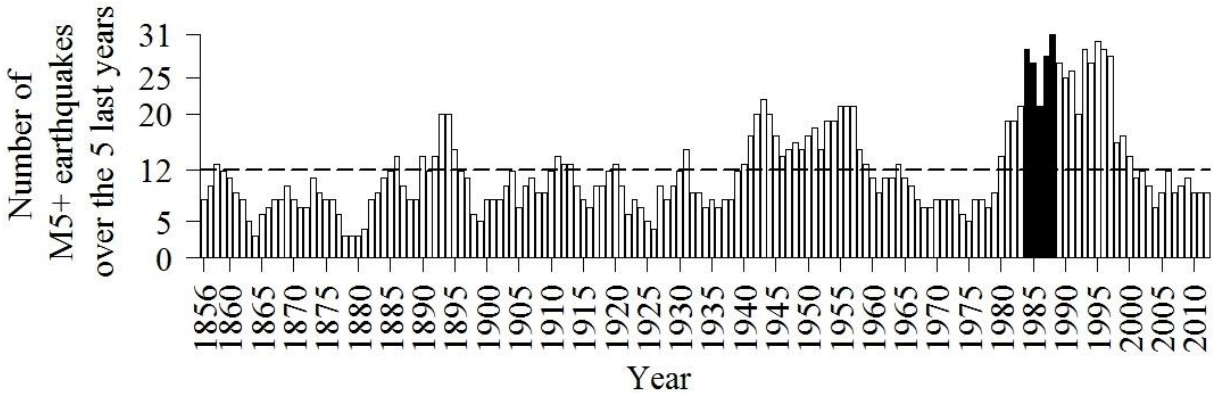


Figure 3.2.7: Number of earthquakes with a moment magnitude M5+ occurring during the 5 previous years. For year *N*, the sum is calculated from $N - 5$ to $N - 1$. Earthquakes occurring the same day count as one. Black bars correspond to the peak of seismicity observed between 1984 and 1988. The dotted line represents the average value from 1855 to 2012. The historical earthquake database used is taken from the UCERF3 database (Felzer 2013).

Insurance Code Section 10089 to restrict the extent of the mandatory cover and addressed the insurance crisis caused by the 1994 Northridge earthquake. The new "mini-policy", met a limited success mainly because the price was more expensive for a lower guarantee (Reich 1996c). Furthermore, the creation of the CEA was at the opposite of the trend in insurance market privatization and people assimilated it to an insurance industry bailout (Reich 1996c). The combined impact on $r_N$ of the two Assembly Bills is null as $(1 + 30\%) \times (1 - 23\%) = 1$ (Tab. 3.2.4). It means that the efforts to promote earthquake insurance among the population by a first Assembly Bill was cancelled 20 years later by the other. Last, the discredit of a mistaken prediction can lead to a decrease of $r_N$, as it happened in 1928 about the occurrence of a major earthquake in Southern California Geschwind 1997; Yeats 2001).

$r_N$ is then compared to a scientific-based earthquake annual occurrence probability to assess the level of the homeowners' risk perception. This requires assessing the annual probability for a homeowner to be affected by a destructive earthquake. For that, the ShakeMap footprints, released by the U.S. Geological Survey (USGS), are used. A ShakeMap footprint gives, for a historical earthquake, the modelled ground motions for several metrics, including the macroseismic intensity on the Modified Mercalli Intensity scale (MMI). In California, a total of 564 ShakeMap footprints are available on the USGS website for the period 1952-2018 and the magnitude range Mw3-Mw7.3. According to the MMI scale, heavy damage can be observed for an intensity above or equal to VIII. Among the 564 historical earthquakes, the ShakeMap footprints report that only 21 have caused such a high intensity and are labelled as destructive

earthquakes. For each of the 21 ShakeMap footprints, the area corresponding to an intensity above or equal to VIII was reported and the population living inside was estimated using the Global Settlement Population Grid from the European Commission (Tab. 3.2.5).

Table 3.2.5: Earthquakes occurred in California since 1952 with a maximum macroseismic intensity on the Modified Mercalli Scale (MMI) modelled by the ShakeMap program (U.S. Geological Survey) above or equal to VIII. The columns Area and Number of people affected give the size and the estimated population of the area affected above or equal to VIII, respectively. The population has been assessed using the Global Human Settlement Population Grid (European Commission).

| Epicentre area | Year | Magnitude | Area (km²) | Number of people affected |
|---|---|---|---|---|
| Parkfield | 1966 | 6.1 | 22 | 4 |
| Borrego Mountain | 1968 | 6.6 | 352 | 1 |
| San Fernando | 1971 | 6.7 | 147 | 55,991 |
| Imperial Valley | 1979 | 6.5 | 385 | 19,280 |
| Coyote Lake | 1979 | 5.8 | 21 | 17 |
| Eureka | 1980 | 7.3 | 4 | 20 |
| Coalinga | 1983 | 6.3 | 151 | 2,043 |
| Chalfant Valley | 1986 | 6.2 | 70 | 278 |
| Elmore Ranch | 1987 | 6 | 97 | 7 |
| Superstition Hills | 1987 | 6.5 | 199 | 1 |
| Loma Prieta | 1989 | 6.9 | 458 | 15,801 |
| Petrolia | 1992 | 7.2 | 46 | 120 |
| Joshua Tree | 1992 | 6.2 | 57 | 1 |
| Big Bear | 1992 | 6.5 | 47 | 9,756 |
| Landers | 1992 | 7.3 | 1,093 | 20,863 |
| Northridge | 1994 | 6.6 | 537 | 630,602 |
| Hector Mine | 1999 | 7.1 | 271 | 24 |
| San Simeon | 2003 | 6.6 | 5 | 10 |
| Parkfield | 2004 | 6 | 5 | < 1 |
| El Mayor – Cucapah | 2010 | 7.2 | 28 | 46 |
| South Napa | 2014 | 6 | 30 | 412 |

Finally, for each year since 1952, the annual rate of people was calculated by dividing the number of people having experienced an intensity above or equal to VIII by the total population of California according to the Global Human Settlement Population Grid (European Commission). The arithmetic means of the annual rates during the period 1952-2018 is equal to $r^{Hist} = 0.038\%$. In this study, we consider $r^{Hist}$ as the true average probability for a California homeowner to be affected by a destructive earthquake. Therefore, the risk has always been underestimated by California homeowners because $AWR_N$ was lower than $r^{Hist}$ since 1926 (Fig. 3.2.6). The severity underestimation is quantified through the earthquake risk awareness ratio ($AWR_N$) defined as:

$$AWR_N = \frac{r_N}{r^{Hist}} = 2632 \times r_N \quad (3.2.20)$$

$AWR_N$ being estimated since 1926, the take-up rate model is generalized in the next section and used to understand the current low take-up rate.

### *3.2.5. Understanding the current low take-up rate*

Introducing the earthquake risk awareness ratio ($AWR_N$), we redefine the take-up rate model (Eq. 3.2.15) as follows:

$$t_N^{Estimated} = \min\left(\left(\frac{AWR_N}{2632 - AWR_N} \times \frac{K}{P_N}\right)^{1.07}; 100\%\right) \quad (3.2.21)$$

From the estimated values of $AWR_N$ (Eq. 3.2.19 and 3.2.20) and $P_N$ (Tab. 3.2.2), Figure 3.2.8 shows the fit between $t_N^{Estimated}$ (Eq. 3.2.21) and $t_N$ (Tab. 3.2.2).

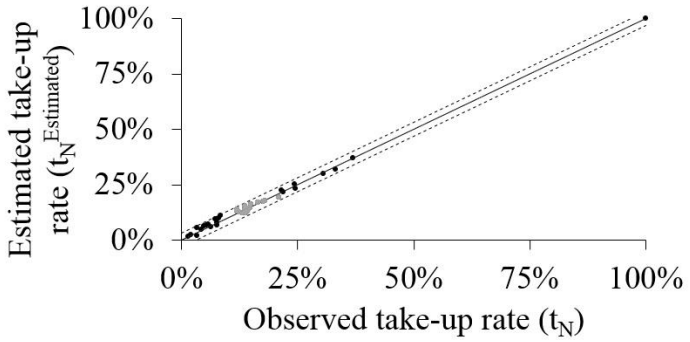


Figure 3.2.8: Comparison between the take-up rates observed and estimated using the model developed in this study. Grey points correspond to the period 1997-2016 which was used to calibrate the model. Dashed lines represent a buffer of ±0.03.

The goodness-of-fit is $R^2 = 0.99$ and the modelling error is below ±3%, as represented by the dashed lines. The record at 100% corresponds to the 1992 California Residential Earthquake Recovery program (CRER), which was a mandatory public earthquake insurance, including a cover amount for households up to $15,000 (USD 1992), at a very low premium amount (Lagorio et al. 1992).

Figure 3.2.9 illustrates the sensitivity of $t_N^{Estimated}$ to the average premium $P_N$ and the earthquake risk awareness ratio $AWR_N$ (Eq 3.2.21).

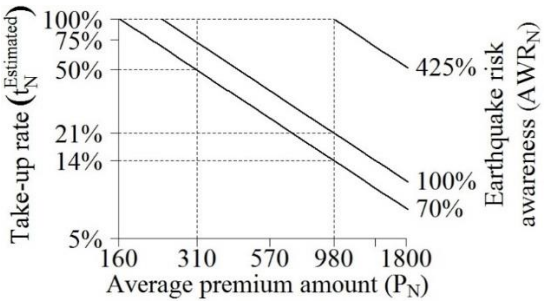


Figure 3.2.9: Relationship between the average premium amount, the take-up rate and the earthquake risk awareness. Financial values are in USD 2015.

The lines $AWR_N$ = 70%, $AWR_N$ = 100% and $AWR_N$ =425% stand for the current situation, the true risk level and the target value of $AWR_N$ for $t_N^{Estimated}$=100%, at the current price at $980 (USD 2015), respectively. According to the first one ($AWR_N$ = 70%), half of homeowners ($t_N^{Estimated}$ = 50%) are not willing to pay an average premium amount exceeding $P_N$=$310 (USD 2015) per year, for an insurance cover. This would represent a 68% decrease in the price of earthquake insurance coverage.

On the opposite, the relatively low earthquake risk awareness ($AWR_N$ =70%), contributes only marginally to the current low take-up rate ($t_N^{Estimated}$ = 14%). In fact, even with the true level of risk ($AWR_N$ =100%), only $t_N^{Estimated}$ = 21% of homeowners are expected to subscribe an insurance. This result is consistent with previous findings by Shenhar et al. (2015) who observed in Israel that the earthquake insurance take-up rate did not significantly increase after a large prevention campaign.

To reach a 100% take-up rate with the current premium amount, according to the model, the earthquake risk awareness ratio has to reach 425%, which is very unlikely. Indeed, the UCERF3 assesses the annual probability of occurrence, in California, of an earthquake with a magnitude above M6.7 at 15% (Field et al. 2013). Under the assumption that the probability for a homeowner to experience a damaging earthquake is proportional to the occurrence of such an earthquake, reaching that awareness ratio would mean that homeowners consider this probability to reach the level of 425% × 15% = 64%. In other words, only the belief that a destructive earthquake is imminent (i.e. a probability of occurrence somewhere in California during the year, for a 1994 Northridge-like earthquake, above 64%) can bring all homeowners to subscribe an earthquake insurance at the current price.

### *3.2.6. Conclusions*

The model developed in the present study shows that the low earthquake insurance take-up rate, observed until 2016 for the Homeowners line of business in California, is due foremost to high premiums. Indeed, it assesses that no homeowners would prefer to stay uninsured against earthquake risk if the annual average premium would decrease from $980 (as observed in 2016) to $160 (USD 2015) or lower. Moreover, Kovacevic and Pflug (2011) have shown that a minimum capital is required to benefit from an earthquake insurance cover, otherwise the cost of the premium would drive to the ruin faster than holding the risk. They have also found that the lower the insurance premium the lower this minimum capital. Consequently, the results of Kovacevic and Pflug (2011) suggest that some uninsured people can be well aware of the earthquake risk but just cannot afford an earthquake insurance at the current price. This corroborates the result of the present study, because bringing such people to buy an earthquake insurance is foremost a matter of price, not of insufficient risk perception.

Nevertheless, as the current average premium amount corresponds to the annualized risk assessment, insurance companies would not have enough reserves to pay future claims following earthquakes if they collect on average only $160 per policy (California Earthquake Authority 2017b). Hence, the current insurance mechanism cannot meet the homeowners' demand and being sustainable, as it was the case for the 1992 CRER program (Kunreuther et al. 1998).

After this initiative, earthquake insurance has never been again mandatory in California. Because compulsory insurance is not only hard to implement, but also has an unpredictable impact (Chen and Chen 2013), new insurance solutions have emerged to increase the earthquake insurance market, like the parametric insurance. This insurance product stands out from traditional insurance policies by paying a fixed amount when the underlying metrics (e.g. the magnitude and the epicentre location) exceed a threshold, whatever the loss incurred by the policyholder. This new insurance claim process reduces significantly the loss uncertainty, the operating expenses and so the premium rate. In California, parametric insurance is offered to cover homeowners against earthquake risk since 2016 (Jergler 2017).

Nevertheless, risk awareness remains important in earthquake insurance consumption, and insurance companies also encourage local policies led by public authorities to improve prevention (Thevenin et al. 2018).

This study supports these initiatives by demonstrating that a new earthquake insurance scheme is necessary to meet the premium expected by homeowners. However, it shows also that the lower the premium amount, the more the earthquake risk awareness contributes in insurance consumption (Fig. 3.2.9). Finally, only a global effort involving all stakeholders may fill the adoption gap in earthquake insurance coverage. This includes also the financial stakeholders, involved in the mortgage loans business. A recent study (Laux et al. 2016) have put in light that most of banks do not require an earthquake insurance from their mortgage loan clients, preferring instead to hold the risk and to increase the interest rate by +0.2% (in 2013). These additional bank fees are, on average, as expensive as the premium rate for the Residential earthquake insurance (0.185% in 2013 according to the CDI). Nevertheless, such a market practice puts an estimated $50bn – $100bn loss risk on the U.S. mortgage system (Fuller and Kang 2018). Consequently, expanding earthquake insurance cover, for homeowners, is also a challenge for the banking industry. In this respect, requiring an earthquake insurance for mortgage loans would strongly enhance the insurances' and public initiatives.

## 3.3. Assessing the performance of the French "CAT-NAT" insurance plan

### *3.3.1. Introduction*

Since July 1982, several kinds of natural catastrophes (e.g. earthquake, flood, subsidence or avalanche) are covered in France by an insurance compensation scheme called "CAT-NAT". It is based on a unique public-private partnership whereby roles and responsibilities are split between insurance market and public authorities. The rationale behind this CAT-NAT compensation scheme is that in case of an extreme natural event, impacted people must benefit from a national solidarity, i.e. public funds must be allocated to help them to recover.

The two main phases in insurance are the underwriting process and the claim process. Regarding the underwriting process, the CAT-NAT cover is mandatory for any property insurance policy (e.g. housing insurance, car insurance). Furthermore, the additional premium amount corresponding to the CAT-NAT cover is determined by the public authorities and is given as a percentage of the total premium for the underlying policy. For example, in housing

insurance, the additional premium amount for the CAT-NAT cover accounts for 12% of the total premium amount. According to its principle of national solidarity, this rate is uniform across all the French territory and, therefore, does not match the risk level.

Regarding the claim process, Figure 3.3.1 shows the different steps from the occurrence of the event to the insurance compensation.

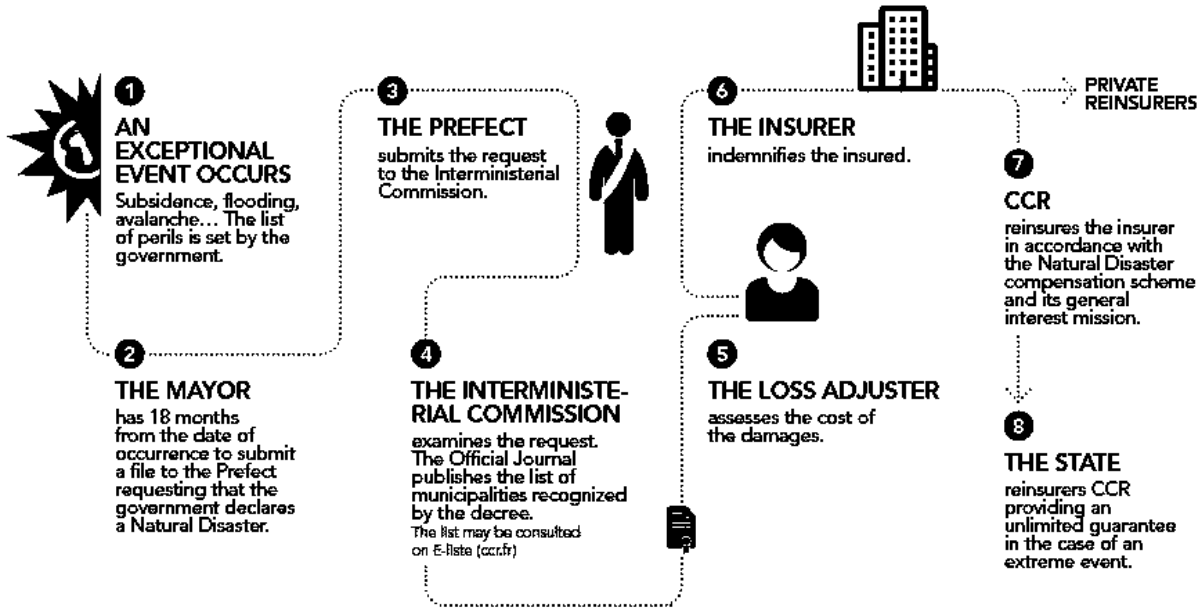


Figure 3.3.1: Scheme of the French CAT-NAT compensation scheme. Source : Caisse Centrale de Réassurance (2015).

It shows that local public authorities (steps 2 and 3) firstly make the request to declare the municipality in CAT-NAT situation. All the requests are studied at State level (step 4) which decides which municipalities can benefit from the CAT-NAT compensation scheme. Impacted people living in a municipality declared in CAT-NAT situation can then claim for an insurance indemnity and get a compensation corresponding to the loss incurred (steps 5 and 6). Impacted people living in municipalities that are not declared in CAT-NAT situation cannot ask for any CAT-NAT compensation. Lastly (steps 7 and 8), as the premium amount is set by law, the French State shares with the insurance company the extreme losses through the public reinsurance company called the Caisse Centrale de Réassurance, (CCR). The guarantee offered by the French State is unlimited (or in practice limited to the French State financial strength), meaning that from the insurance company perspective, the insured loss that can occur following a CAT-NAT event cannot exceed a given threshold (usually corresponding to twice the total

premium amount collected during the year). Above that threshold, the State will take the entire liability to its charge.

The CAT-NAT compensation scheme makes France one of the countries where the insurance against natural catastrophes is the most efficient in the sense that the share of uninsured loss is the lowest. Figure 3.3.2 shows the rank of several countries considering both the share of uninsured loss and the average annual loss caused by natural catastrophes.

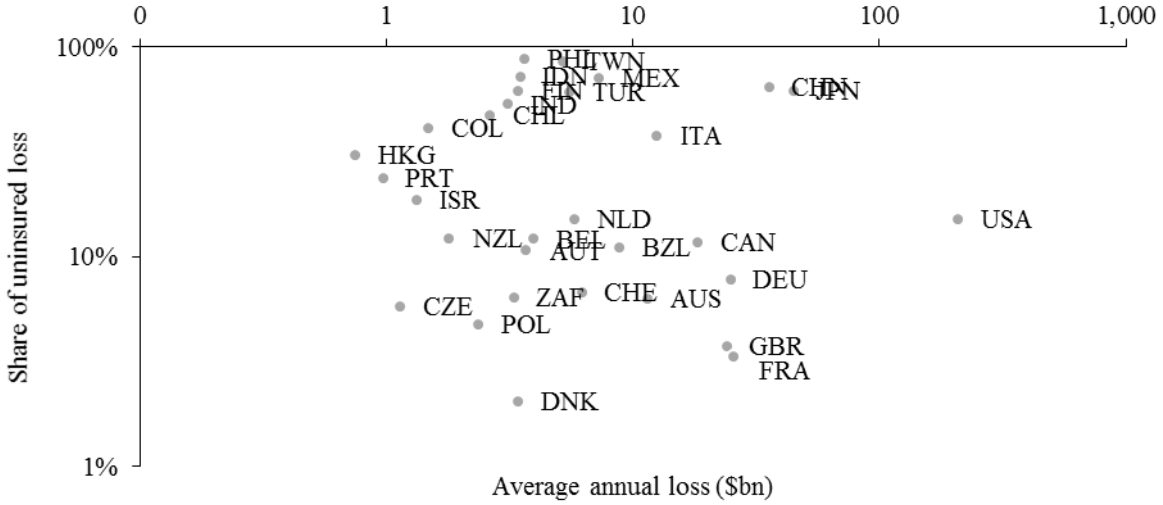


Figure 3.3.2: Country profile regarding the share of uninsured loss (modelled) and the annual average loss consecutive to natural catastrophes (modelled), released by Swiss RE (Holzheu and Turner 2018).

Figure 3.3.2 shows that France is one of the countries with the lowest modelled uninsured loss following a natural catastrophe (including CAT-NAT events). Only Denmark is performing better but is also less exposed to natural catastrophes, characterized by a lower average annual loss.

This finding is corroborated by the performance of the CAT-NAT compensation plan since its creation, 37 years ago, including major events such as the 2003 heatwave. Nevertheless, the CAT-NAT compensation plan has not experienced any major earthquake event like the 1909 Lambesc earthquake (M6.2), the latest major earthquake in France with injuries and significant economic losses. The first part of this study is dedicated to review past CAT-NAT declarations (extracted from the GASPAR database) until 2014 that relate to earthquakes occurred in metropolitan France. Next, the case of the 2003 heatwave is examined as it is the costliest event that the CAT-NAT compensation plan has faced so far. Based on data collected, a new model

is proposed to assess the probability for a municipality to be declared in CAT-NAT situation based on the macroseismic intensity observed and the population. Lastly, this model is applied to the scenarios of the 1909 Lambesc earthquake and a hypothetical major event close to Nice.

### *3.3.2. Review of past CAT-NAT declarations following an earthquake*

Between July 1982 and April 2014, 22 earthquakes occurred in metropolitan France leading the French government to declare 630 municipalities in CAT-NAT situation. They are illustrated in Figure 3.3.3.

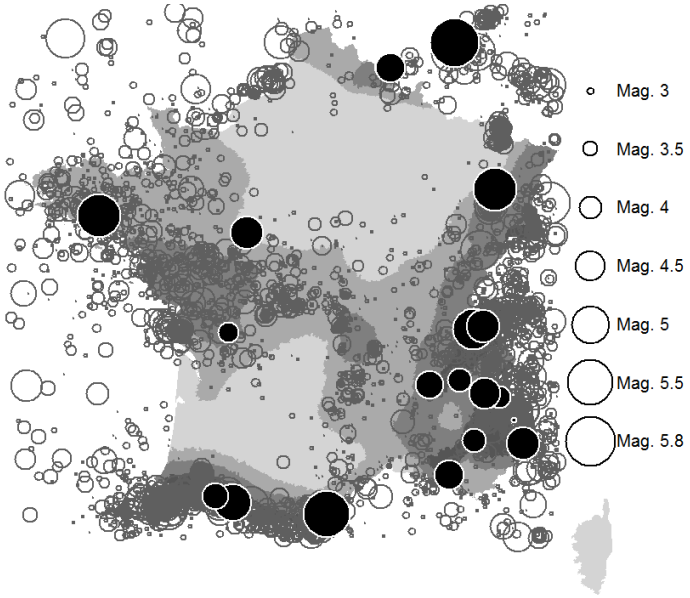


Figure 3.3.3. Illustration of the past seismicity in metropolitan France between July 1982 and end of 2013. The black points represent those associated to at least one CAT-NAT declaration. The underlying map shows the official seismic hazard levels (grey zones). Source : www.planseisme.fr/Zonage-sismique-de-la-France.html; RéNass catalog: https://renass.unistra.fr/; database of CAT-NAT declarations: www.data.gouv.fr/fr/datasets/arretes-de-catastrophe-naturelle-en-france-metropolitaine-2/.

The SisFrance database (Scotti et al. 2004) contains the observed macroseismic intensity on the MSK scale for 11,434 municipalities in metropolitan France, following 21 different earthquakes between 1982 and 2003. This database is used rather than official reports from the Bureau Central Sismologique Français (in charge of assessing the macroseismic intensity after any

major earthquake occurring in France) because data is compiled into a single table and, therefore easily accessible.

Even if the SisFrance does not contain data after 2007, there was no CAT-NAT declarations related to earthquake risk in metropolitan France from 2004 to April 2014 (date of the 2014 Barcelonnette M4.8 earthquake). Indeed, the 2006 Argelès-Gazost earthquake (M4.9) has not been subject to a CAT-NAT declaration, despite a macroseismic intensity observed at VI at the epicentre, according to the SisFrance database. Therefore, the dataset of the analysis of the CAT-NAT declarations until April 2014 is the same as in the previous period until 2003. Lastly, for 2,169 out of 11,434 records in the SisFrance database, intensity values are not meaningful (either empty or equal to 0). Consequently, this study relies on a dataset of 9,265 municipalities with macroseismic intensities ranging from II to VII.

Figure 3.3.3 shows that earthquakes associated to CAT-NAT declaration have very different profiles, ranging from low to moderate magnitudes, located not only in the most seismic areas (Pyrenees and Alps) but also in lower seismic areas (Central, West and North of France). Furthermore, there is no clear correlation between the seismic activity (represented by the seismic hazard zones) and the number of earthquakes producing a CAT-NAT declaration. In addition, Figure 3.3.3 shows also that some relative major earthquakes have not produced any CAT-NAT declaration, like the 2004 Besançon (117,000 inhabitants) earthquake (M5.1).

The macroseismic intensities extracted from the SisFrance database for the 630 municipalities declared in CAT-NAT situation are shown in Figure 3.3.4. This figure puts in light that as much as 21% of past CAT-NAT declarations in metropolitan France between 1982 and 2014 have been made for municipalities where earthquake events had limited impact. Indeed, according to the MSK macroseismic scale, there is no damage to building for grades IV or below. For instance, after the 1988 Laval earthquake (M4), the municipality La Rouaudière have been declared in CAT-NAT situation, while the observed macroseismic intensity was III (MSK scale) and the distance to the epicentre about 50km.

This analysis highlights that decisions to declare a municipality in CAT-NAT situation were not only based on the sole macroseismic intensity level. In the next section, the CAT-NAT procedure following the 2003 heatwave is shown as an example.

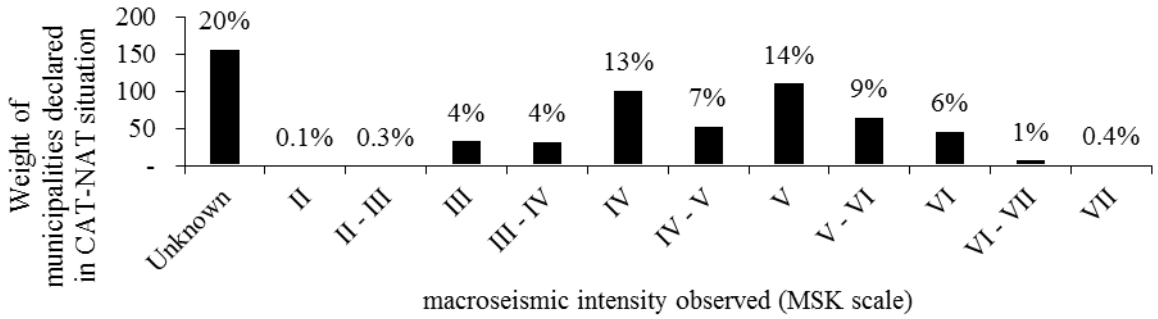


Figure 3.3.4: Distribution of the observed macroseismic intensities reported in the SisFrance database for municipalities in metropolitan France declared in CAT-NAT situation until 2014. The unknown category corresponds to of CAT-NAT declarations for which the intensity in the SisFrance either equal to 0 (i.e. not felt by people living in the municipality) or empty (i.e. no data has been collected).

### *3.3.3. The CAT-NAT procedure following the 2003 heatwave*

The costliest event covered by the CAT-NAT plan was the 2003 heatwave (Fédération Française de l'Assurance 2017) with a total direct economic loss estimated at €1bn (Frécon and Keller 2009). While causing 14,802 deaths, the cost only reached €12m for the French National Health Insurance (Caisse Centrale de Réassurance 2019c). Indeed, most of damage was caused by the subsidence effect, i.e. the downward settling of the ground's surface.

A report from the French Senate provides further insights on how the event has been covered by the CAT-NAT compensation scheme (Frécon and Keller 2009), summarized hereafter. Until 2003, the physical index used to declare a municipality in CAT-NAT situation due to subsidence was based on water deficit in the soil. However, the 2003 heatwave was characterized by a sudden severe heatwave inducing subsidence, instead of soil water deficit. It resulted that among the 8,022 municipalities experiencing damage and requiring to be declared in CAT-NAT situation, only 200 had a water deficit high enough to be declared in CAT-NAT situation. Again, according to the French Senate report, the CCR assessed the total loss at €3.5bn and would have required the French State to pay between €0.5bn and €1bn (€2003) for refunding the CCR. In order to provide a claim compensation to most of affected people by subsidence without asking for any State guarantee, the physical index has been modified to consider subsidence due to high temperature and low water deficit, leading to declare 1,750 municipalities in CAT-NAT situation in 2004. In 2005 this index was again modified, bringing additional 2,691 municipalities into the CAT-NAT compensation plan. Finally, in 2006, 2,370 municipalities received an exceptional grant as a contribution to the damage following the 2003

heatwave. The Figure 3.3.5 illustrates the breakdown of the CAT-NAT cover for the 8,022 municipalities which have been affected by the 2003 heatwave.

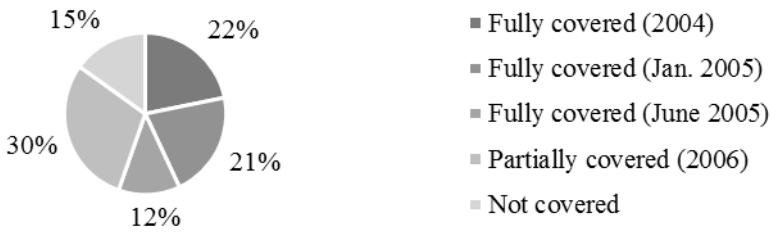


Figure 3.3.5: Breakdown of the CAT-NAT declaration among the 8,022 municipalities affected by the 2003 heatwave. Source: after Frécon and Keller 2009.

Eventually, the 2003 heatwave costed €1bn (€2009) to the CAT-NAT compensation scheme and the French State did not need to refund the CCR (Frécon and Keller 2009).

### *3.3.4. An empirical model for the declaration of municipalities in CAT-NAT situation*

In order to study the impact by a major earthquake on the CAT-NAT compensation plan, this section introduces a new model quantifying the probability for a municipality to be declared in CAT-NAT situation after an earthquake. To build a model for CAT-NAT declarations, the 630 CAT-NAT declarations observed in metropolitan France between 1982 and 2013 for earthquake events are matched with the 9,265 observed macroseismic intensities from the SisFrance database. For 159 CAT-NAT declarations, no associated data are in the SisFrance database. However, since this database is not exhaustive, no information can be inferred. Consequently, this empirical model is based on 9,265 macroseismic intensity values, among which 471 have led to a CAT-NAT declaration. The ratio of CAT-NAT declaration by macroseismic intensity level is illustrated in Figure 3.3.6.

Figure 3.3.6 shows that the rate is very low up to an intensity of IV and then sharply increases to reach 100% at an intensity level of VII. Furthermore, the discontinuity between the levels V and V-VI suggests that most of municipalities are damaged at an intensity V-VI or higher, which is consistent with the definition of the macroseismic scale.

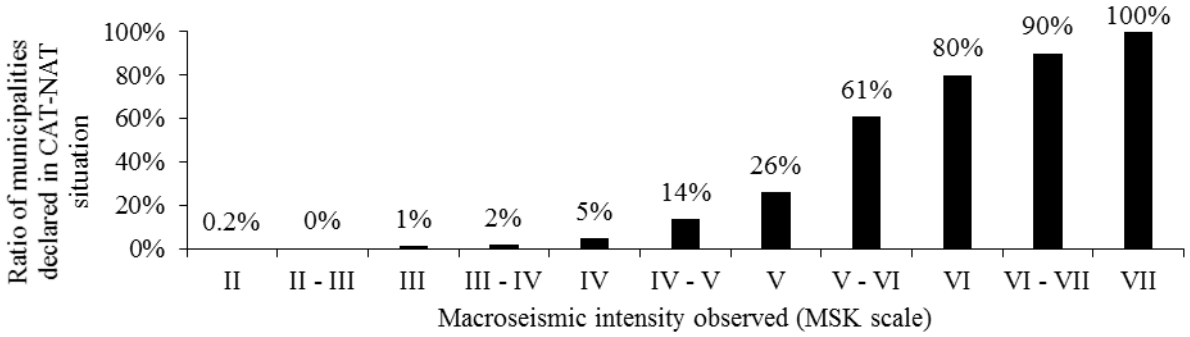


Figure 3.3.6: Ratio of municipalities in metropolitan France declared in CAT-NAT situation between July 1982 and end of 2003 according to the observed macroseismic intensity reported in the SisFrance database. Sources: after SisFrance database (Scotti et al. 2004); GASPAR database.

About the level of exposure, the population density is used as proxy. Extracting the population for each municipality in the SisFrance database from the national census performed by the French National Institute of Statistics and Economic Studies (INSEE) is difficult because some municipalities have existed only on a short period of time. Moreover, before 2006, the national census was not done annually. Consequently, the population for each municipality has been assessed in this study as the average between the national census of 1982, 1990, 1999, 2006, 2007 and 2008, when available. For some municipalities like Le Cannet or Digne, only the population in 2008 and 1982 are available, respectively. Finally, the population of a municipality at the time of the earthquake having produced the macroseismic intensity in the SisFrance database is supposed equal to the average value calculated.

Figure 3.3.7 illustrates the distribution of the population for the municipalities in the SisFrance database associated to a CAT-NAT declaration or not.

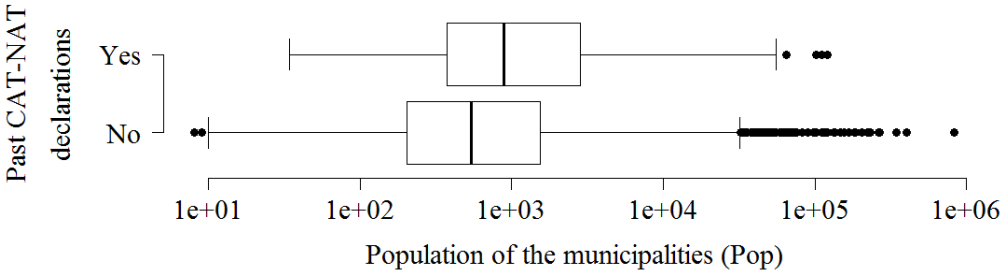


Figure 3.3.7: Distribution of the population in municipalities in metropolitan France affected by a past earthquake according to the SisFrance database for those benefiting from a CAT-NAT declaration and not. Black points represent outliers. Source: INSEE; GASPAR database; SisFrance database.

Figure 3.3.7 highlights that CAT-NAT declaration usually happens in municipalities with higher population than those not declared in CAT-NAT situation. In other words, the more populated a municipality is, the higher is the chance to observe damage and to be compensated for a given macroseismic intensity.

A Logit regression model is then calibrated on the database, made of 9,265 hazard intensities linked to 471 CAT-NAT declarations. The two explanatory variables used are the decimal logarithm of the population $\log_{10}(Pop)$ and the macroseismic intensity *MSK*. Fitting the Logit regression model to the data confirms that these two explanatory variables are meaningful (according to the statistical z-test: z=28.13 and z=9.17 for the variables *MSK* and $\log_{10}(Pop)$, respectively) and leads to the following equation:

$$\ln\left(\frac{\mathbb{P}\left(CN\middle|(Pop,MSK)\right)}{1-\mathbb{P}\left(CN\middle|(Pop,MSK)\right)}\right) = 0.75 \times \log_{10}(Pop) + 2 \times MSK - 13.14 \qquad (3.3.1)$$

where $\mathbb{P}\left(CN\middle|(Pop,MSK)\right)$ is the conditional probability for a municipality to be declared in CAT-NAT situation, given its population and the intensity level. When Equation 3.3.1 is back-tested on the same database, it predicts correctly 96% of observations (i.e. $\mathbb{P}\left(\mathrm{CN}\middle|(\mathrm{Pop,MSK})\right) \leq 50\%$ and no CAT-NAT declaration or the opposite).

### *3.3.5. Modelling the performance of the French CAT-NAT plan in case of extreme earthquakes*

Using Equation 3.3.1, the CAT-NAT compensation scheme is analysed for two examples of extreme earthquakes occurring in metropolitan France: the 1909 Lambesc earthquake and a hypothetical major earthquake close to Nice. These two events mostly differ by the exposure density within the area surrounding the epicentre: low for Lambesc and high for Nice.

Since 1998, the official macroseismic intensity scale is no longer the MSK but the EMS98. However, according to Musson et al. (2009), the EMS-98 and the MSK macroseismic scale are equivalent for grades below or equal to XI. Therefore, the two scales are used interchangeably in the two following case studies.

#### The 1909 Lambesc earthquake

The 1909 Lambesc earthquake was the last major earthquake that occurred in metropolitan France, causing 46 deaths (Barroux et al. 2003). Riedel (2015) modelled the potential

consequences if this earthquake occurred again in a present exposure situation. Estimated direct economic losses arrived at €5.1bn. They resulted from observed macroseismic intensities from the SisFrance database as well as new exposure, vulnerability, and loss assessment models that were appropriate for the metropolitan France context (Riedel et al. 2015).

Based on this loss scenario the CAT-NAT declaration for each affected municipality can be modelled based on Equation 3.3.1. To convert the probability to be in CAT-NAT situation $\mathbb{P}\big(CN\big|(Pop, MSK)\big)$ into a bimodal decision ("CAT-NAT" or "No CAT-NAT") a threshold can be used. Using the Bayes classifier methodology, a municipality is assumed to be declared in CAT-NAT situation when $\mathbb{P}\big(CN\big|(Pop, MSK)\big) \geq 50\%$. Figure 3.3.8 shows the distribution of the total direct economic loss based on 1 million simulations of the CAT-NAT declaration model (Eq. 3.3.1).

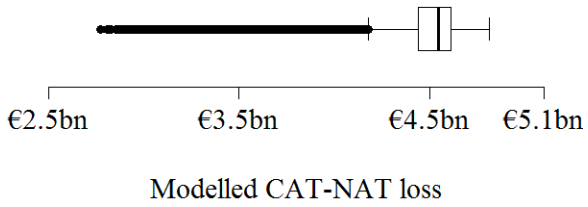


Figure 3.3.8: Distribution of the total direct economic loss paid by the CAT-NAT compensation scheme after a replica of the 1909 Lambesc earthquake based on 1 million simulation of the CAT-NAT declaration model developed in this study. The underlying loss scenario produces €5.1bn of total direct economic losses (Riedel et al. 2015).

Currently, the CAT-NAT compensation plan can face a €4.5bn (€2019) loss without requiring any State guarantee according to its 2018 Financial Statements (Caisse Centrale de Réassurance 2019c). Consequently, in case of a replica of the 1909 Lambesc earthquake, the CAT-NAT declaration procedure (Fig. 3.3.1) can either produce a direct economic loss below the claim-paying capacity of the CAT-NAT compensation plan or above (Fig. 3.3.8), and in this last case, involve the State Guarantee.

**The case of an extreme earthquake in the vicinity of Nice**

The European RISK-UE project (Mouroux et al. 2004) suggested to represent the risk of a major earthquake close to Nice using a M6.3 earthquake with an epicentre located at 30km of Nice. It is the same as from the 2001 Nice earthquake (M4.6), but with a higher magnitude comparable to the 1887 Ligurian earthquake. The modelled macroseismic intensity ranges from VI-VII to VIII (Mouroux et al. 2004) and the population of Nice in 2015 is estimated at 342,522

inhabitants. Despite no CAT-NAT declaration was made for the 2001 earthquake, the Nice modelled scenario would lead the town to be conducted in CAT-NAT situation with a 99.5% probability, according to the model developed in this study (Eq. 3.3.1).

For the municipality of Nice only, the total direct economic loss was assessed at €7bn (Mouroux et al. 2004). According to the INSEE, the GDP of France has increased by +20% between 2004 and 2019. Therefore, we assume in this study that the loss amount assessed at €7bn (€2004) in 2004 is equivalent to €8.4bn (€2019) in 2019. As the CAT-NAT compensation plan can face €4.5bn without requiring the State guarantee, if the considered earthquake occurs today and the municipality of Nice is declared in CAT-NAT situation, the French State will have to refund the CCR by €3.9bn (€2018). This amount is four times more important than the cost of all the affected municipalities by 2003 heatwave being declared in CAT-NAT situation. Despite a €3.9bn loss is low compared to the French State expenses (€330bn in 2018), this amount for paying the claims needs to be raised within the 3 months after the CAT-NAT declaration. Therefore, one can question the capacity for the French State to sustain a major earthquake event as currently defined in the CAT-NAT compensation plan.

Last, the RISK-UE project (Mouroux et al. 2004) investigated an even worse earthquake scenario, characterized by the same epicentre location but a magnitude at M6.8. The associated total direct economic loss for the municipality of Nice was €13bn (€2004). With the same approach, this would result in a loss for the French State about €11.1bn (€2019).

### *3.3.6. Conclusions*

Since 1982, the CAT-NAT compensation plan has provided an efficient cover against several natural catastrophes, including earthquakes. Even if the CAT-NAT compensation plan experienced some costly events like the 2003 heatwave, with a total direct economic loss at €3.5bn (€2003), it has never experienced any extreme catastrophe like a major earthquake close to Nice, or a replica of the 1909 Lambesc event.

One of the main strengths of the CAT-NAT compensation scheme lies in the determination of areas that can benefit from the insurance plan, which permits to adapt the loss to its claim-paying capacity, as it was done for the 2003 heatwave. However, at the light of an extreme earthquake close to Nice, this study shows that the CAT-NAT compensation plan could not

mitigate alone the economic consequences of the event to fit its claim-paying capacity, letting the French State to pay a very large claim amount.

The current reform project of the CAT-NAT compensation scheme includes a threshold (EMS-98 intensity of VI) for deciding whether a municipality can benefit from the CAT-NAT cover after an earthquake (Frécon and Keller 2009). Even if this modification would restrict the use of the CAT-NAT compensation to major catastrophes only, it will not prevent the French State from supporting most of the loss in case of an extreme event seriously affecting a large municipality like Nice.

According to this study, it also seems unlikely that following an extreme earthquake the French State would pay the entire loss owing to the CAT-NAT compensation scheme. Indeed, after having paid €263m in 1999, the French State decided to not declare all the municipalities affected by the 2003 heatwave to avoid paying €1bn (Frécon and Keller 2009). Based on these conclusions, the next reform shall consider the State claim-paying capacity to better define the role of the French State. Risk transfer solutions may also be investigated, like reinsurance, financial vehicles such as insurance-linked securities, or co-insurance and other pooling mechanisms (potentially pan-European), as it is already in force under the California Earthquake Authority, a public funded but privately managed earthquake insurance provider in California.

## 3.4. A maturity scale for earthquake insurance development based on the California experience

### *3.4.1. Introduction*

Since 1970, the number of earthquakes having an economic or a human impact is increasing according to the EM-DAT database. The reasons are twofold: the population is increasing in high seismic risk areas and a decreasing quality of physical structures (Spence et al. 2011). To help people recover from such disasters, insurance is one of the essential socio-economic tools (Noy et al. 2017). Therefore, we have collected from the EM-DAT and the Swiss Re Institute databases the insurance losses and the total direct economic losses for 100 earthquakes that occurred between 1985 and 2016 and over 31 countries. The annual average insured loss share

has been calculated as the ratio between the sum of insurance losses and the sum of the total (economic) damage for each year. This variable captures the efficiency of an insurance model whatever the disaster magnitude. Indeed, the higher the insured loss share, the more insurance companies cover the damage caused by earthquakes. Therefore, it allows to compare insurance models from one country to another even if they are exposed to different earthquake risk levels. Figure 3.4.1 shows that, at the worldwide scale, the historical average of the annual average insured loss share is 15% since 1985 with no noticeable trend, meaning that insurance protection has increased as fast as the total direct economic losses caused by earthquakes.

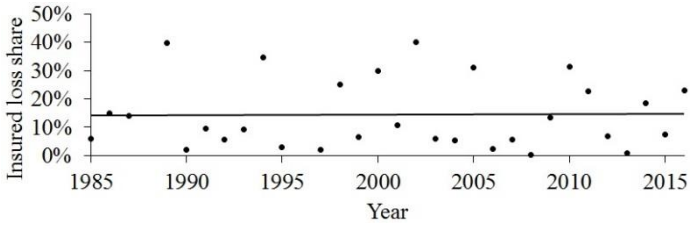


Figure 3.4.1: Annual average insured loss share caused by earthquakes between 1985 and 2016. Sources: EM-DAT and Swiss Re Institute.

Consequently, insurance protection at the worldwide scale has not been extended to new population groups since 1985 and the increase of the insured loss is related to the exposure amount. From the same dataset, the average insured loss share by country for the period 1985-2016 has been also calculated as the sum of insurance losses between 1985 and 2016 divided by the sum of total direct economic losses between 1985 and 2016. Figure 3.4.2 shows the result for the 31 countries and highlights a large heterogeneity in earthquake insurance efficiency since some countries have a high average insured loss share (e.g. New Zealand and Mexico), while some others have not (e.g. Japan, Italy and Turkey).

The average insured loss share does not depend on the earthquake risk level as countries prone to earthquake risk like New Zealand (NZL) and Japan (JPN) have a high and a low average insured loss share, respectively.

Furthermore, the difference in average insured loss share cannot be explained only by the GDP per capita (Fig. 3.4.2). Indeed, insurance solutions in New Zealand, and Mexico are more effective than those existing in Japan and Turkey respectively, despite a comparable GDP per capita. As a consequence, the flat trend of the annual average insured loss share (Fig. 3.4.1)

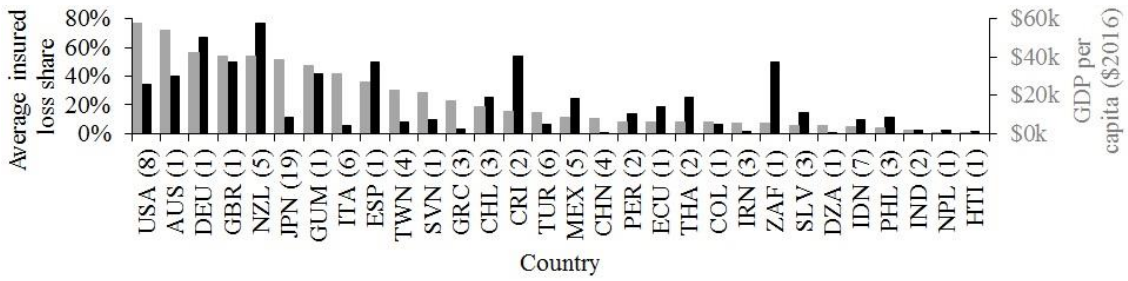


Figure 3.4.2: Average insured loss share between 1985 and 2016 (black bars) and GDP per capita in 2016 (grey bars) for 31 countries labelled with the corresponding ISO 3166-1 alpha-3 code (https://unstats.un.org/unsd/tradekb/knowledgebase/country-code). The number of earthquakes affecting each country between 1985 and 2016, according to the EM-DAT and the Swiss Re Institute databases, is given in parentheses. Sources: EM-DAT, Swiss Re Institute and UNDATA.

means that since 1985 a lot of countries with a low average insured loss share have not managed to adopt better insurance solutions already used in countries with a comparable GDP per capita and a high insured loss share.

In this context, this paper introduces a new maturity scale for earthquake insurance. A maturity scale is a common tool in insurance industry to identify the actions that could help the business to grow sustainably. A maturity scale is divided in several levels where each of them is representative of a typical business development stage. To characterize each level, a set of qualitative indicators is used: each level corresponds to a unique combination of modalities for the set of qualitative indicators (Fig. 3.4.3).

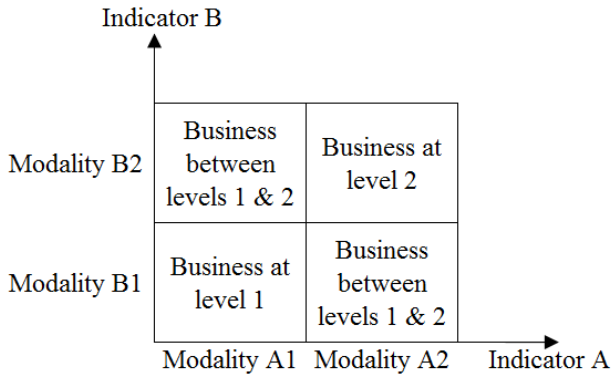


Figure 3.4.3: Illustration of a maturity scale with two levels characterized by two qualitative indicators A and B.

Most of maturity scales are built empirically, either by analysing past evolutions of the market considered or by comparing the market characteristics between different areas.

In this study, we analyse the evolution of the earthquake insurance market in California since 1906 to develop a maturity scale for the earthquake insurance industry. The levels considered for this maturity scale are the following: *Emerging*, *Standard*, *Advanced* and *Sustainable*. Furthermore, the qualitative indicators used to characterize these levels are : the level of risk monitoring, i.e. the level of knowledge of probable future losses, the premium affordability, the market demand, the investment in prevention measures and the solvency level of insurance companies.

This paper is first dedicated to present each level at the light of the history of earthquake insurance in California. In the last section, the maturity scale is introduced and the way to use it for developing earthquake insurance is proposed.

### *3.4.2. Level "Emerging": the birth of the earthquake insurance (California 1906 - 1925)*

First earthquake insurance policies were issued in 1916 as a separate policy covering damage induced by ground-shaking (Goltz et al. 1985). Nevertheless, most of damage from the 1906 San Francisco earthquake was caused by fires and covered by the fire insurance. Consequently, earthquake insurance was in its infancy until the 1925 Santa Barbara earthquake.

**Risk monitoring**

Despite the 1906 San Francisco and the 1925 Santa Barbara earthquakes, insurance companies considered that the occurrence of another strong earthquake was unlikely until 1927 (Geschwind 1997). Therefore, the premium amount collected was treated as pure profit and was not reserved for paying future claims (Geschwind 1997).

**Premium affordability**

During the period 1906-1925, the insurance premium was low, at an average rate of 4 cents per $100 coverage (Goltz et al. 1985). By comparison, Gilbert (1909) assessed that based on historical damage caused by earthquakes between 1800 and 1908 and the buildings value at that time, the corresponding average insurance premium should have been 72 cents per $100 coverage, without including the overhead costs. In conclusion, the level *Emerging* is characterized by under-priced insurance premium, which is in line with the lack of risk monitoring and awareness.

**Market demand**

Since 80% of the losses from the 1906 San Francisco earthquake were due to following fires, they were covered by the standard fire insurances (Goltz et al. 1985). Consequently, people did not buy an earthquake insurance, considering the damage caused by ground shaking as insignificant (Goltz et al. 1985).

**Investment in prevention measures**

Even if officials and mass media downplayed the consequences of the 1906 San Francisco earthquake (Natural Hazards Observer 2006), a basic building code (based on a 1.4kPa wind force) was however required during reconstruction works in the city in order to protect buildings against both earthquake and wind effects (Popov 1994). Furthermore, some technical reports (Natural Hazards Observer 2006) and scientific papers (Gilbert 1909) were published highlighting the importance of prevention measures.

**Solvency level of insurance companies**

Even if many insurance companies went bankrupt after the 1906 San Francisco earthquake (Insurance Information Institute 2018), insurance companies' solvency regarding earthquake risk was not considered until the 1925 Santa Barbara earthquake (Geschwind 1997; Eren and Lus 2014) for which the total insured loss exceeded the total premium amount collected to cover earthquake risk between 1921 and 1924 (Freeman 1932).

### *3.4.3. Level "Standard": An empirical insurance model (California 1926 – 1994)*

The 1925 Santa Barbara earthquake has exacerbated the need to manage earthquake risk in California, fostering academic research on the destructiveness of a major earthquake (Geschwind 1997), highlighting the need for earthquake mitigation plans (Natural Hazards Observer 2006), and boosting earthquake insurance market (Goltz et al. 1985). Despite the model successfully faced major earthquakes like the 1933 Long Beach, the 1971 San Fernando and the 1989 Loma Prieta earthquakes, it did not sustain the extreme losses caused by the 1994 Northridge earthquake, pushing the insurance sector into an unprecedented crisis (Pomeroy 2010) characterized by a massive drop of housing insurance offer. Indeed, as insurance companies are forced to offer an earthquake coverage aside a housing insurance policy since

1984 (McAlister 1984), they preferred to stop writing new business rather than to be more exposed to earthquake risk (Marshall 2017).

**Risk monitoring**

Until the 1994 Northridge earthquake, insurance companies have underestimated the loss they could face (Monning et al. 2014). Indeed, the insured losses after this event was 7 time higher than the estimates from actuarial models for this kind of earthquake (Osteraas and Gupta 2008). Even if the 1994 Northridge earthquake was caused by an unknown seismic fault at that time (Grossi et al. 2008), the underestimate in economic loss models at that time was mostly due to inadequate buildings vulnerability and repair cost models (Osteraas and Gupta 2008). After this event, insurance companies did not longer rely on actuarial models based on historical experience, using instead stochastic models aiming at reproducing physical properties of ground motion and seismic building response (Grossi et al. 2008).

**Premium affordability**

In the late 20s, insurance companies understood that damaging earthquakes in California are frequent and the buildings stock at that time highly vulnerable (Geschwind 1997). Consequently, they sharply increased the insurance premium (Freeman 1932; Geschwind 1997), from an average of $0.04 in 1925 (Goltz et al. 1985) to $1.79 in 1927 (Freeman 1932) for a $100 coverage. However, because, on one hand, insurance companies were unable to price the risk accurately (Dong 2002; Muir-Wood 2016b), and on the other hand the market was very competitive (Muir-Wood 2016b), the premium was pulled down at 20 cents per $100 coverage in the early 70s (Kunreuther et al. 1978) and stayed at the same level until 1994 (Mulligan 1994).

**Market demand**

The 1925 Santa Barbara earthquake produced a surge of earthquake insurance demand (Goltz et al. 1985), which has been amplified by an aggressive selling strategy from insurance companies (Geschwind 1997). Later, the 1971 San Fernando earthquake boosted also the market demand, as well as the 1985 Assembly Bill AB2865 (McAlister 1984) which imposed to insurance companies to offer an earthquake cover aside the residential fire insurance. At the beginning of 1994, 31% of people had an earthquake insurance (source: California Department of Insurance database).

**Investment in prevention measures**

The first earthquake mitigation program was set in the aftermath of the 1933 Long Beach earthquakes under the Riley Act and the Field Act (Natural Hazards Observer 2006). Since then, after each significant earthquake new mitigation plans have been put in place by the authorities (Wiley et al. 2000). Furthermore, seismic design codes have been initiated after the 1933 Long Beach earthquake but culminated only in the early 50s (Popov 1994).

**Solvency level of insurance companies**

Despite no insurance company went bankrupt after the 1994 Northridge earthquake, one was near the insolvency (Monning et al. 2014) and 3 insurance companies have been fines $3.5bn in 2000 for having restricted claims payments for an amount adjudged at $262.6m. (Ellis 2000). Furthermore, rating agencies have downgraded many insurance companies forcing them to reduce their exposure to earthquake risk (Monning et al. 2014) and pushing the sector into a crisis (Pomeroy 2010).

### *3.4.4. Level "Advanced": an insurance model designed to face extreme events (California 1995 - Today)*

The insurance crisis following the 1994 Northridge earthquake ended by the creation of the California Earthquake Authority (CEA) in December 1996, a private-funded and state-managed insurance company dedicated to earthquake cover for residential properties (Pomeroy 2010).

**Risk monitoring**

Earthquake risk is monitored with very complex stochastic models, at the state-of-the-art of earthquake-related sciences (Grossi et al. 2008), including very extreme losses as the USGS *ShakeOut* scenario (Jones et al. 2008) and the Jaiswal et al. (2017) study providing return period losses up to 2,500y. Insurance pricing, capital and risk management directly derive from these stochastic seismic models combined with comprehensive building vulnerability assessment through vulnerability models.

**Premium affordability**

CEA's insurance premium amounts are based on stochastic seismic models to assess damage that can causes any kind of earthquakes, in order to collect enough money to sustain an extreme

earthquake (California Earthquake Authority 2018b) or a series of consecutive severe earthquakes in a short timeframe. Although premiums are risk-based, they do not match the consumers' point of view. For example, consumer activists considered that the large premium increase after the 1994 Northridge earthquake was about increasing the profitability of insurance companies and not pricing the risk (Reich 1996c; Jaffee and Russell 1997).

**Market demand**

Most of Californians do not buy earthquake insurance because on one hand they do not think that an earthquake could impact them and on the other hand, for low income people especially, the current premium amount is not affordable (Dixon 2014). As a consequence, the share of insured people decreased from 37% in 1993 to 31% in 1994 and 13-14% since 2003 (source: California Department of Insurance database).

**Investment in prevention measures**

After the conviction of 3 insurance companies for having restricted claims payment after the 1994 Northridge earthquake, the California Insurance Commissioner required them to finance for $10m. a research and education foundation instead of paying the fines for a total amount of $3.6bn (Ellis 2000).

**Solvency level of insurance companies**

The CEA is designed to sustain an earthquake with a return period up to 400y (California Earthquake Authority 2017c), i.e. more severe than the 1994 Northridge earthquake, the 1906 San Francisco earthquake, and the USGS *ShakeOut* Scenario (Pomeroy 2010). However, in case of a very extreme earthquake exceeding the CEA's claim-paying capacity, insurance policies contain a clause of pro-rata payments, meaning that affected policyholders would be partially refunded.

#### *3.4.5. Level "Sustainable": current initiatives for a sustainable insurance model (unreached level)*

Against the current low level of people covered, two kinds of innovative solutions are developed by the insurance industry to bring more and more people to get access to earthquake insurance. On one hand, insurance policies are redesigned for offering a lower, more attractive

rate. On the other hand, prevention measures are fostered to decrease the expected loss following an earthquake and so the premium amount.

**Risk monitoring**

Earthquakes do not occur randomly in time, but according to a time-dependent process. This is considered in some recent risk assessment studies (e.g. UCERF3; Field et al. 2014, Field et al. 2015) which have released both a time dependent (short term) and a time independent (long term) model. These two time scales are relevant for the insurance industry because while the premium amount is calibrated on a long-term view, the minimum solvency capital is reassessing each year and, consequently, consider only extreme losses that could occur over the following year. For this reason, time dependent model can be very valuable to better estimate the minimum solvency capital. Indeed, since the occurrence probability of devastating earthquakes over the next year is better captured by a time-dependent than a time-independent process, the minimum solvency capital assessment would benefit from a time-dependent model.

**Premium affordability**

Several innovative insurance solutions are currently developed to offer lower prices, like Jumpstart Recovery, a parametric insurance which pays out to the insured a predefined compensation amount as soon as a given type of earthquake occurs (Jergler 2017). Market response regarding this new insurance offer is still unclear since this company started offering insurance cover since October 2018 (Rogers 2019; Lloyds 2019). Nevertheless, its financial strength is strong, being guaranteed by the Lloyds, the world's specialist insurance market (Lloyds 2019). Meanwhile the CEA decreased on average their tariff by 10% in 2016 for being more attractive (California Earthquake Authority 2016c).

**Market demand**

Following the 10% decrease adopted by the CEA in 2016, the rate of people insured against earthquakes by the CEA has never grown so fast since 1996: +0.6% in 2016 and +0.8% in 2017. Meanwhile, the California State promotes earthquake insurance through aggressive advertising campaigns (Fuller 2018). Also, the occurrence of severe earthquakes outside California may have raised risk awareness of Californian people, supporting insurance demand.

**Investment in prevention measures**

The CEA and the California Governor’s Office of Emergency Services jointly launched the Earthquake, Brace & Bolt initiative which aims at promoting simple seismic retrofitting work

with both a $3,000 grant for paying part of the work, and a premium discount between 5% and 20% depending to the building vulnerability (California Earthquake Authority 2018c).

**Solvency level of insurance companies**

Today, the California Earthquake Authority (2018d) is able to sustain a 400y return period earthquake loss (i.e. the probability for the CEA to run for bankruptcy after an earthquake is estimated at 1/400 = 0.25%), corresponding to an amount of $15.3bn in 2017 (California Earthquake Authority 2017c). In case of higher loss, CEA's insurance policies stipulate that the CEA will only provide a compensation amount, in proportion to its financial capacity compared to the total loss incurred by the CEA. In conclusion, the solvency level of the CEA can have an impact on the compensation amount and therefore limits the efficiency of this insurance scheme.

Nevertheless, in other countries like in France, the solvency level of insurance companies can be dissociated from the insurance compensation amount. Indeed, the so-called *CAT-NAT* insurance regime covering earthquake risk since 1982 includes the unlimited French State guarantee in case of extreme losses (Caisse Centrale de Réassurance 2015). Benefiting from this financial guarantee, the compensation amount that affected people will receive is no longer threatened by the occurrence of an earthquake in France and its overseas territories.

### *3.4.6. The maturity scale for earthquake insurance*

The characteristics collected for each qualitative indicator, at each level of the maturity scale, can be summarized as proposed in Table 3.4.1. Furthermore, Figure 3.4.4 presents the synthetic view of the maturity scale based on the previous observations on the California earthquake insurance market.

When using this maturity scale, the first step is to determine the grade of each qualitative indicator. Considering the case of the French CAT-NAT plan (Caisse Centrale de Réassurance 2015), the *Risk monitoring* is *Controlled* because stochastic models capturing physical behaviours of both seismic waves and buildings response are available and used by insurance companies but none of them include both short-term and long-term views. The *Premium Affordability* and the *Market demand* indicators are *Commercial-based* and *High*, respectively because in the CAT-NAT plan (Caisse Centrale de Réassurance 2015), the premium amount is

Table 3.4.1. Detailed description of the state of each indicator for each level of the earthquake maturity scale developed in this study.

| Indicator | Emerging | Standard | Advanced | Sustainable |
|---|---|---|---|---|
| Risk monitoring | **Not material**: A destructive earthquake is not expected to occur again. | **Experienced**: Recent events showed the destructive power of an earthquake. | **Controlled**: The risk is monitored, and extreme events are modelled. | **Anticipated**: The risk is monitored both at short term and long-term view. |
| Premium affordability | **Very low**: The risk being ignored; the premium is low and considered as a profit. | **Commercial-based:** The premium amount reflects the market and does not consider the risk level. | **Risk-based**: The premium is calculated based on the risk in order to guarantee the solvency of the insurance company. | **Economic-based**: The premium depends on both the risk and the consumers' expectations. |
| Market demand | **Low**: People do not feel the need to be protected against the risk. | **High**: Following the last earthquakes, insurance need is spreading over the population. | **Low**: High premiums lead to a trade-off between the risk and the cost. Only few people prefer to be insured, especially if no earthquake has occurred recently. | **High**: Most people purchase an earthquake insurance encouraged by a significant premium amount decrease and a better risk awareness. |
| Prevention measures | **Emerging**: Only academic researches work on prevention measures. Applications are very few and on a very simple basis. | **Institutional**: Prevention measures are managed by the authorities and considered as a public mission. | **Risk holders**: Prevention measures are supported both by the officials and the insurance companies. | **Economical**: Prevention is funded by the market and is recognized as the only long-term efficient risk reduction process. |
| Solvency level of insurance companies | **Low**: The solvency of insurance companies is questionable because the earthquake risk is not monitored. | **Medium**: Insurance companies are subject to solvency regulations. | **High**: Insurance companies' reserves are designed to face a very extreme loss. | **Secured**: Additional mechanisms are used to support insurance companies if their reserves are exceeded. |

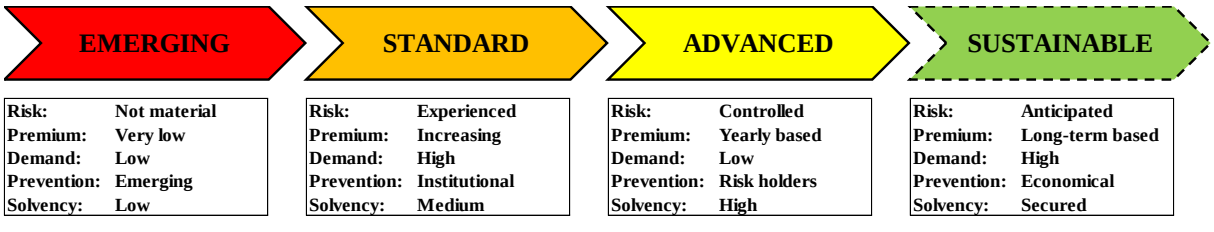


Figure 3.4.4. Summary of the earthquake maturity scale developed in this study.

assessed by the authorities at an amount affordable for most of housing insurance policyholders. The *Prevention measures* indicator is *Institutional* since the CAT-NAT plan (Caisse Centrale de Réassurance 2015) assigns the responsibility of prevention measures to a dedicated public institute called the *Fonds de prévention des risques naturels*. Last, the *Solvency level of insurance companies* indicator is *Secured* since the CAT-NAT plan (Caisse Centrale de Réassurance 2015) indicates that insurance companies are refunded by public funds for loss in excess of twice the premium amount collected. Consequently, insurance companies benefit from an additional mechanism if the loss exceeds the reserves. Finally, the earthquake insurance scheme in France is ranked at the level *Standard* because, the *Solvency level of insurance companies* is at level *Sustainable*, the indicator the *Risk monitoring* indicator is at level *Advanced* and the three others at level *Standard*.

Next, this maturity scale (Tab. 3.4.1 and Fig. 3.4.4) can be used to identify measures and draw an action plan to move from one level to the next one. First, for creating an earthquake insurance market (i.e. moving from *Emerging* to *Standard* levels) the optimal time is in the aftermath of a damaging earthquake. Furthermore, insurance industry should be focused on selling earthquake insurance at the market price, without targeting a high solvency capital or investing in prevention plans. The challenge of moving from the *Emerging* to the *Standard* level is to meet the people's need about being covered if a similar earthquake that they just experienced happen again. From the authorities' side, funds must be allocated to prevention plan to support this economic trend toward a better protection against risk.

The next level (*Advanced*) is about making insurance companies financially strong enough to sustain extreme losses. For this purpose, premium amount must be increased and assessed based on scientific models. Insurance companies also invest on prevention plans in order to decrease the risk and therefore the probability of extreme losses.

Last, the level *Sustainable* aims at reconciling the market demand with insurance companies' solvency. To do so, long-term insurance mechanisms need to be developed because damaging earthquakes are seldom. They also need to leverage on prevention plans as it is the one of the most efficient solution for reducing the vulnerability of buildings. Nevertheless, long-term insurance policies require to guarantee that insurance companies will be able to face extreme loss both at short- and long-term view. About the solvency of insurance companies, a State guarantee for the insurance companies at the light of the one included in France in the CAT-NAT plan (Caisse Centrale de Réassurance 2015) can be a solution.

Table 3.4.1 and Figure 3.4.4 show also that such a maturity scale can drive counter-intuitive decision as decreasing the market demand between the *Standard* and the *Advanced* levels. Indeed, this maturity scale allow to understand that such a decrease is a consequence of the premium increase, from a commercial-based to a risk-based assessment. Nevertheless, this change in premium amount is also related to a decrease of insurance companies' insolvency risk. Overall, the *Advanced* level is an improvement compared to the *Standard* level because an insurance protection for few people provided by financially robust insurance companies is preferred to one covering more people but potentially running for bankruptcy in case of a devastating earthquake.

### *3.4.7. Conclusions*

In the previous sections of this work we have shown the limits of the current earthquake insurance mechanism in California, France, India or Indonesia. To identify the next steps to improve the earthquake insurance mechanism in any of these countries, a maturity scale has been developed. According to several qualitative indicators, an earthquake insurance scheme can be ranked and consequently associated to a level of this maturity scale. Next, the qualitative indicators point the targets to meet to reach the upper level.

In conclusion, this maturity scale can be used to rank the current level of earthquake insurance solutions to cover this risk and drive the further development for improvement. This tool can also warn countries that they are actually downgrading, if they jump from a rating to a lower one, which could happen over time due to passivity or complacency towards this rare risk.

When using this maturity scale to the current earthquake insurance mechanism in California (ranked at the level *Advanced*) it shows that a *Sustainable* level requires to develop a new insurance model, and to improve loss models for a better risk monitoring.

As this maturity scale has been developed only based on the California earthquake insurance market history, using this maturity scale to other countries at past or present times would definitely contribute to assess its added-value for driving earthquake insurance business and to identify new qualitative indicators to improve it.

## 3.5. Summary

The maturity scale tells us that several improvements must be made to move toward a *Sustainable* earthquake insurance model, including on the fields of the risk modelling, the premium affordability and the development of prevention measures. In the next chapter two works are presented, as part of the effort to release better risk models. About the two other topics (premium and prevention measures), a new earthquake insurance model is introduced in Chapter 4, dedicated to lower the premium amount and finance seismic retrofitting works.

# CHAPTER 4: IMPROVING THE RISK MODELLING

## 4.1. Introduction

This chapter is dedicated to present the studies made during the thesis to contribute to improve earthquake risk modelling. The large scientific production, released in the recent years, on new probabilistic hazard and loss models lead us to focus on developing methods to compare them or to test them against historical data.

The first part of this chapter presents a method to test probabilistic seismic hazard assessment (PSHA) maps against a large set of ShakeMap footprints (Allen et al. 2009) on Indonesia. This study has been already published in the scientific journal *Seismological Research Letters* (DOI: 10.1785/0220190171).

The second part is dedicated to build an economic model for testing damage-cost relationships which gives the replacement or repair cost ratio for each damage grade on the EMS-98 or the HAZUS-99 scale. The model uses the number of buildings damaged, destroyed and the total direct economic loss estimated for 297 past earthquakes.

## 4.2. Comparing probabilistic seismic hazard maps with ShakeMap footprints for Indonesia

### *4.2.1. Introduction*

Probabilistic seismic hazard assessment (PSHA) maps are used to assess seismic hazard levels for earthquake engineering, prevention plans, and insurance risk management. A PSHA map represents the level of seismic ground motion that can be observed at each site with a probability

of exceedance *p* and the corresponding return period *RP*. The ground motion parameter used is usually peak ground acceleration (PGA) at rock sites and official PSHA maps are generally calibrated for an exposure time *T*=50y and a probability of exceedance *p*=10%, which corresponds to a return period of *RP*=475y.

Over the last decade, several authors have compared PSHA maps with macroseismic or instrumental intensities, for example in Japan (Miyazawa and Mori, 2009; Fujiwara et al., 2009) and France (Rey et al. 2018), or with ground motion observations in Italy (Albarello and D'Amico, 2008), New-Zealand (Stirling and Gerstenberger, 2010), France (Tasan et al. 2014) and Turkey (Tasan et al. 2014). The purpose for testing PSHA maps is to identify their strengths and weaknesses, then to conclude which one is the most reliable for a given area and how the maps can be improved (Albarello and Peruzza 2017).

However, limits and questions remain regarding the relevance of such testing because of the different time scales between the return period of interest for PSHA maps and the length of the observation period available. In most places, the number of earthquakes producing a ground motion intensity above the PSHA reference acceleration is not statistically meaningful (Iervolino 2013). To compensate for the lack of seismic records, several studies (Allen et al. 2009, Miyazawa and Mori 2009, Tasan et al. 2014, Rey et al. 2018) have already proposed to extrapolate the observation period by estimating the ground motion produced by older earthquakes or by considering the ergodicity assumption to extend the period of observation by summing the observation periods of several sites.

This study compares three PSHA maps for Indonesia from the Global Seismic Hazard Assessment Program (GSHAP; Giardini et al. 1999), the 2015 Global Assessment Report (GAR2015; CIMNE and INGENIAR 2015) and the Standar Nasional Indonesia (SNI2017; Irsyam et al. 2017), the latest official PSHA map released for Indonesia. There is not enough accelerometer data to test the PSHA maps, because of the small number of seismological stations and the short operational period of the actual network. Figure 4.2.1 shows the number of operational seismic stations in Indonesia for each year (black bars) and the length of the observation period of stations still open in 2018 (grey line).

We can observe that only 25 stations were operational in the period 2006-2018, which is not enough to test the PSHA maps for Indonesia. The literature suggests three different methods to extend the length of the observation period: 1) to use PGA estimates from ShakeMap footprints (Allen et al. 2009); 2) to estimate PGA values using a Ground Motion Prediction Equation (GMPE) on past earthquakes (Tasan et al. 2014); 3) to use a Ground Motion Intensity

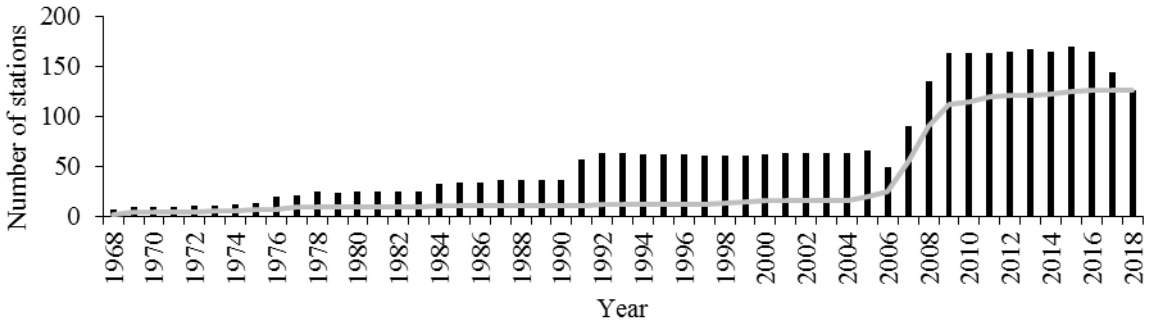


Figure 4.2.1: Number of operational seismic stations in Indonesia listed by the International Seismological Centre. The grey line corresponds to the number of stations still open in 2018.

Conversion Equation to convert historical macroseismic intensity into PGA values (Rey et al. 2018).

The first method was applied by Allen et al. (2009) to compare the PSHA map produced by the Global Seismic Hazard Assessment Program (GSHAP, Giardini et al. 1999) with the maximum PGA assessed by ShakeMap footprints for past earthquakes. The observation period used was 1973 to 2007 (i.e. $T$=35y). The methodology consisted in counting the number of gridded spatial points where the maximum PGA from the ShakeMap footprints exceeded the reference acceleration given by the PSHA map. The results gave a ratio of 7.3% considering all gridded points and 3.8% considering only the gridded points where the PSHA map gave a reference acceleration above 0.8m/s$^2$. Allen et al. (2009) concluded that ShakeMap footprints could be used effectively to test the PSHA map produced by the GSHAP (Giardini et al. 1999), since $p$=7% for $T$=35y is equivalent to $p$=10% for $T$=50y. However, Allen et al. (2009) also observed that the PSHA map was conservative for the most seismic areas (with a ratio at 3.8%) and they suggested that this could be due to a lack of observations for large inland earthquakes.

Similar to Allen et al. (2009), our study uses ShakeMap footprints to test PSHA maps considering the PGA values computed within an independent framework and models used are published and open-source. The novelty of this study is to use 50 years of ShakeMap footprints, from May 1968 to May 2018 in Indonesia. Furthermore, our study introduces a new methodology to consider the uncertainty of ShakeMap PGA estimates. It consists in comparing the distribution of the number of independent maximum ground motion estimates above a threshold calibrated according to the PSHA map tested for one location. Here is explored a new process to extract a set of independent PGA values from ShakeMap footprints and verified that the estimate from the ShakeMap footprint can be reasonably assumed to represent the maximum historical PGA at that site over the historical period.

The first section describes the ShakeMap footprints, the selection process and the range of uncertainty when estimating the maximum historical PGA. The new methodology for testing PSHA maps is presented in the second section. Finally, the procedure is applied to three PSHA maps released by the GSHAP, the GAR and the latest national seismic hazard map (SNI2017).

### *4.2.2. Dataset*

The USGS ShakeMap program provides estimated hazard footprints after an actual earthquake or based on a fictive scenario, characterized by seismic sources parameters, and supported by field records or reports when available. In ShakeMap, the PGA is calculated based on several GMPEs. A GMPE can be split into different components, as labelled by Graizer and Kalkan (2016):

$$\ln(PGA) = \ln(G_1) + \ln(G_2) + \ln(G_3) + \ln(G_4) + \ln(G_5) + \sigma_{\ln(PGA)} \quad (4.2.1)$$

where $G_1$ is the scaling function for magnitude and style of faulting, $G_2$ captures the path-scaling, $G_3$ accounts for the regional inelastic attenuation, $G_4$ is the site amplification and $G_5$ represents the basing scaling function and $\sigma_{\ln(PGA)}$ is a centred Gaussian distribution capturing the total variability.

Although ShakeMap footprints are mainly issued for loss estimation purposes (Wald et al. 2009), they are also widely used in other fields, such as seismic hazard assessment, designing financial products or emergency management and response projects (Wald et al. 2005).

A total of 959 ShakeMap footprints were released between May 1968 and May 2018 for earthquakes occurring in Indonesia with a magnitude of M4.5 or more. In this study, we looked at PGA estimates from ShakeMap footprints corresponding to the maximum value in each grid cell corresponding to rock soil, during the period May 1968 – May 2018. The first step for extracting such data from the ShakeMap footprint catalogue is to assess the maximum PGA value at each cell grid from the 959 ShakeMap footprints. Despite the uncertainty of PGA estimates in ShakeMap footprints ($\sigma_{\ln(PGA)}$ in Eq. 4.2.1), the comparison is only based on the median PGA values (when $\sigma_{\ln(PGA)}$=0). As the 959 ShakeMap footprints were not computed on the same spatial grid (different size, different resolution), we defined a new spatial grid *G* with a resolution 0.01° × 0.01°. For each ShakeMap footprint, the median PGA value is extracted for each grid point of the ShakeMap footprint. If a grid point in *G* is not a point on

the ShakeMap footprint grid, the median PGA value is assumed to be the same as that of the closest grid point. It was found that only 310 of the 959 footprints contribute to the maximum historical PGA, as illustrated on Figure 4.2.2.

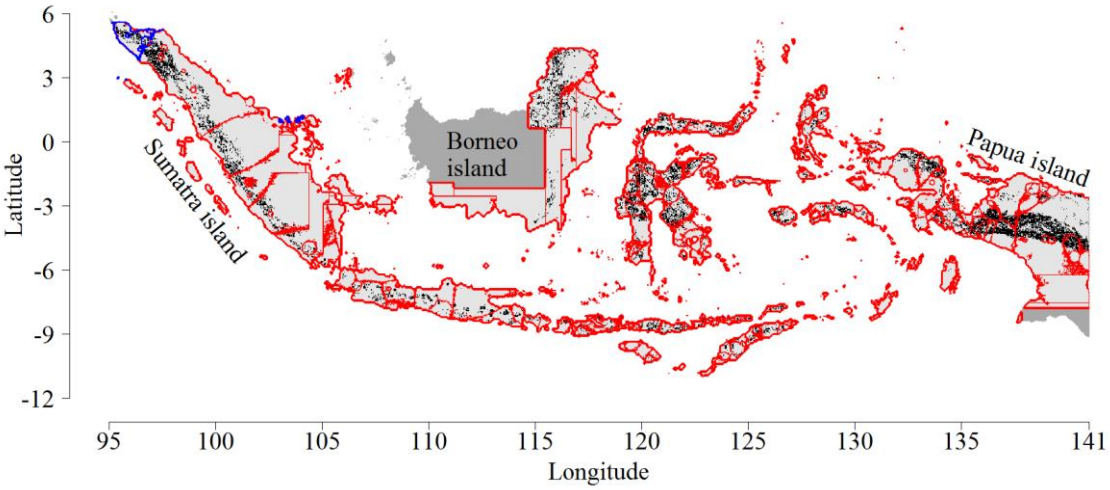


Figure 4.2.2: Contours of the 310 ShakeMap footprints contributing to the maximum estimated historical median PGA since June 1968. The blue contour represents the area where the maximum historical PGA was caused by the 2004 Andaman earthquake (Mw9). The black points represent rock sites according to the USGS Global slope-based Vs30 database (Allen and Wald, 2007).

This shows that the 310 ShakeMap footprints cover most of Indonesia (except for the south of Papua Island and the northwest of Borneo Island, in dark grey on Fig. 4.2.2).

The second step was to filter the rock sites. Considering the USGS Global slope-based Vs30 database and assuming that a rock site verifies $Vs30 \geq 760 m.s^{-1}$, the 310 ShakeMap footprints (Fig. 4.2.2) cover 177,674 rock sites. The distribution of rock sites among the ShakeMap footprints is given in Table 4.2.1.

Table 4.2.1: Distribution of ShakeMap footprints by number of points with the maximum PGA estimates at rock sites.

| Rock sites per ShakeMap footprint | 0 | 1 | 2-10 | 11-50 | 51-100 | 101-1000 | >1000 |
|---|---|---|---|---|---|---|---|
| Number of ShakeMap footprints | 78 | 13 | 28 | 44 | 18 | 86 | 43 |

Seventy-eight ShakeMap footprints do not include rock sites, therefore the total number of ShakeMap footprints contributing to the maximum PGA observed decreases from 310 to 232. Considering the set of relevant ShakeMap footprints for this study, the process to provide

ShakeMap was analysed to assess possible weaknesses in the PGA estimates. Firstly, 232 ShakeMap footprints were processed after 2013, i.e. produced by the latest version of the ShakeMap model. Furthermore, the seismic source parameters (epicentre coordinates, magnitude and depth) inputted into the ShakeMap program are different from the values in the ANSS catalogue (USGS) for 169 ShakeMap footprints; for some of them, the difference is significant (Tab. 4.2.2).

Table 4.2.2: Maximum differences between the epicentre location, magnitude and depth for the earthquakes considered in this study as given by the ANSS catalogue and the ShakeMap footprints. Positives values capture when the features from the ANSS catalogue is greater than those extracted from ShakeMap footprints. Acronym: Avg: average.

| Major change | Epicentral distance | Magnitude increase | Magnitude decrease | Depth increase | Depth decrease |
|---|---|---|---|---|---|
| Value | 31.6km | +1.4 | -1.1 | +46.5km | -43.6km |
| Date of event | 13/02/2001 | 08/08/2007 | 23/02/1969 | 23/02/1969 | 24/02/1982 |
| Avg occurrence year | 1993 | 1985 | 1993 | 1991 | 1991 |

These variations are large enough to have a significant impact on the PGA estimates. As expected, the earthquakes concerned by these differences are mostly old (Tab. 4.2.2), and therefore, lack seismic records. Recently produced ShakeMap footprints are assumed to use better quality seismic source parameters than those in the ANSS catalogue. Consequently, the PGA estimates from ShakeMap footprints benefit from the up-to-date information implement into the process, considering source parameters or ground motion prediction.

Furthermore, the ShakeMap program relies mostly on two GMPEs for Indonesia: the Zhao et al. (2006) and the Chiou and Youngs (2008) for the subduction and the shallow crustal region, respectively, having very different attenuation profiles, as illustrated in Figures 4.2.3a, b.

For both GMPEs the standard deviation of the Gaussian distribution ($\sigma_{\ln(PGA)}$ in Eq. 4.2.1) is close to 0.7, which represents significant uncertainty in PGA estimates (Fig. 4.2.3c). Indeed, for a median PGA estimate of 0.3g, the probability that the PGA experienced is above 1g is still about 5%, while mode (i.e. the value most frequently observed) is equal to 0.18g. To reduce this uncertainty, the ShakeMap programme uses field data, such as station records or reports from the web application DYFI (Did You Feel It?), a questionnaire that collects information from people who felt an earthquake. This can provide a record, or a good estimate of the ground motion felt at the site. This input makes a valuable contribution to decreasing uncertainty, as illustrated in Figure 4.2.3d.

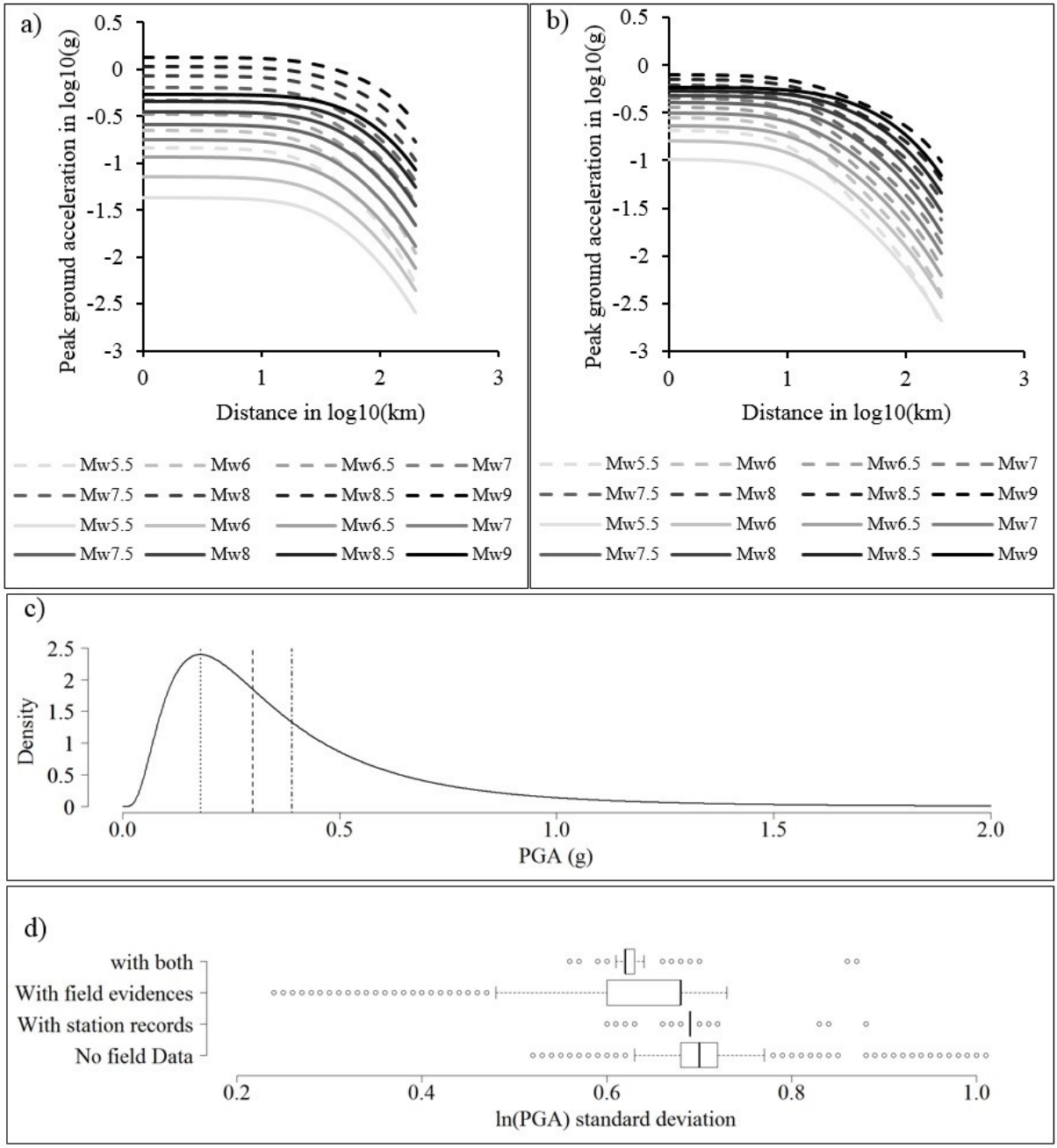


Figure 4.2.3: Characteristics of the two main GMPEs used in ShakeMap footprints for Indonesia, according to magnitude and distance to epicentre for a focal depth equal to 30km (a) and 10km (b). (c): distribution of the PGA uncertainty for median equal to 0.3g and standard deviation equal to 0.72, corresponding to the Zhao et al. (2006). Vertical lines represent the mode value 0.18g (value the most frequently observed), the median value 0.3g (corresponding to the deterministic part of the GMPE), and the mean value 0.39g. (d): distribution of the standard deviation at grid cell resolution for the 232 ShakeMap footprints selected for this study. Distributions are differentiated according to the data (seismic records or field reports) used for ShakeMap.

However, data archives are not available for most of the ShakeMap footprints, as shown in Table 4.2.3, because at the time of the earthquake, the DYFI application was not available and the seismic station network was limited (Fig. 4.2.1).

Table 4.2.3: Number of ShakeMap footprints considered in this study built using DYFI information and/or seismic station records.

| Period | No field data | Using seismic recordings | Using felt reports (DYFI) | Using seismic recordings and felt reports | Total |
|---|---|---|---|---|---|
| Before 2012 | 194 | 0 | 7 | 0 | 201 |
| After 2012 | 6 | 9 | 5 | 11 | 31 |
| Total | 200 | 9 | 12 | 11 | 232 |

Here, we assume that ShakeMap methodology (Wald et al. 2005) provides the most relevant spatial distributed ground motion model. Consequently, the PGA estimates and the associated uncertainty from the ShakeMap footprints are assumed to correspond to the spatially distributed PGA produced by earthquakes contained in the ShakeMap catalogue.

Finally, the representativeness of the set of 232 ShakeMap footprints for maximum PGA at each rock site for the period May 1968 – May 2018 needs to be verified before testing the PSHA maps. This implies to verify if any earthquakes occurred during the observation period, but not modelled by a ShakeMap footprint, could have produced a higher PGA at any of the rock sites considered. This analysis is performed according to the flowchart presented in Figure 4.2.4.

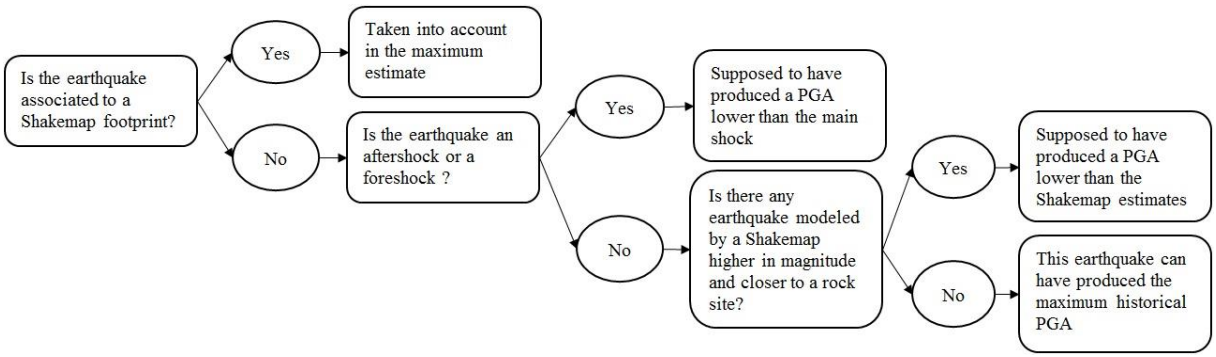


Figure 4.2.4: Flowchart for testing the completeness of the ShakeMap catalogue of earthquakes producing the maximum PGA at rock sites.

The reference catalogue considered is the ANSS Comprehensive Earthquake Catalogue (USGS) which contains 37,077 earthquakes occurring in Indonesia between May 1968 and May 2018, and with a magnitude of at least M4.5. ShakeMap footprints were obtained for 959 earthquakes, therefore another 36,118 earthquakes remain to be analysed using the flowchart (Fig. 4.2.4).

Aftershocks and foreshocks are assumed to have produced lower PGA than the associated main shock, because they occur in the same area and usually at a lower magnitude (Båth 1965). We used the Gardner and Knopoff (1974) algorithm to identify aftershocks and foreshocks, as presented by Petersen et al. (2007) in their study for a PSHA map of Western Indonesia. The algorithm classified 24,622 as foreshocks and aftershocks among the 36,118 previous earthquakes with no ShakeMap footprints. Next, the 24,622 aftershocks and foreshocks are removed from the reference catalogue. Consequently, it remains 11,496 (36,118–24,622=11,496) past earthquakes in the reference catalogue not modelled by a ShakeMap footprint and assumed main shock according to the Gardner and Knopoff (1974) algorithm. Among the set of 11,496 main shock earthquakes not modelled by a ShakeMap footprint, 2,689 are the largest events occurring at one or more rock sites. Therefore, according to Figure 4.2.4, these events could have produced the maximum historical PGA at some of the surrounding rock sites.

To analyse which of the 2,689 could have produced the maximum historical PGA, their characteristics are compared with those of the 232 earthquakes associated with ShakeMap footprints. All of these 232 events had a magnitude of at least M5.4 and 221 out of 232 had a depth lower than 100km. Among the 2,689 earthquakes investigated, only 353 had a magnitude of at least M5.4 and a depth of at the most 100km.

Among the 177,674 rock sites, 160,197 have a maximum PGA estimated from the 232 ShakeMap footprints above 0.01g. Considering this sub-dataset, 95% of them are less than 30km, 150km, 150km and 290km distant from the hypocenter of the earthquake associated to the maximum PGA for magnitude equal to M5, M6, M7 and M8, respectively. As expected, the larger the magnitude, the larger the affected area. When applying the same constraint to the hypocentral distance of the 353 earthquakes verifying the previous conditions, 92 do not meet this condition, i.e. the hypocentre is further from any rock site than the thresholds.

Finally, we calculate that 261 (353–92=261) previous earthquakes not modelled by a ShakeMap footprint could have produced the maximum historical PGA at certain rock sites. They verify the following conditions: 1) neither an aftershock, nor a foreshock; 2) the closest event to a rock site at such a high magnitude; 3) magnitude above M5.4 and depth below 100km; 4) small hypocentral distance. A total of 58,889 rock sites are suspected to be affected by such earthquakes (i.e. not modelled by a ShakeMap) which represents 33% of the rock soil database (Fig. 4.2.5).

In Figure 4.2.5, rock sites are spread over the whole of Indonesia, although the density is higher

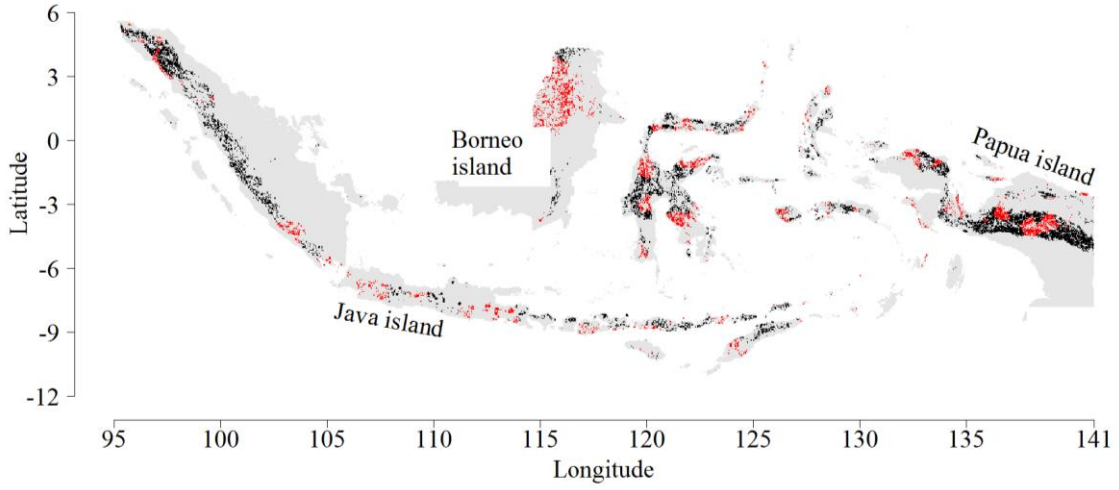


Figure 4.2.5: Illustration of the rock sites withdrawn from the study (red points) because of the possibility of underestimating the maximum historical PGA over the last 50 years using the ShakeMap footprint catalogue.

in Borneo Island. This observation is consistent with a low seismicity level area and no major earthquakes occurred during the observation period. Similarly, the small number of rock sites for which the maximum PGA produced by an earthquake not modelled by a ShakeMap in Sumatra Island is consistent with the high level of seismic activity observed there during the last 50 years.

In order to test PSHA maps only on rock sites for which the maximum historical PGA can be reasonably supposed to have been captured by a ShakeMap footprint, these 58,889 questionable rock sites were withdrawn from the study. This reduces the number of ShakeMap footprints contributing to the maximum historical PGA from 232 to 198, covering a total of 118,785 rock sites (177,674–58,889=118,785).

The next section presents the method developed for comparing PSHA maps with an independent set of maximum historical PGA values.

### *4.2.3. The testing method*

We propose hereafter to test a PSHA map based on the number of rock sites where at least one previous earthquake produced a PGA higher than the threshold given by the tested PSHA map for this site. Usually, for a period of 50 years, the probability of exceedance expected for a PSHA map is 10%. Earthquake occurrence is assumed to follow a Poisson Stationary Process

(i.e. the occurrence of one earthquake is independent from another), which means that over a period of 50 years, at any given site, the probability for experiencing at least one PGA higher than the threshold defined for the site is equal to 10%. Thus, a large set of observations covering 50 years for each site analysed would be necessary to test a PSHA map. The Central Limit Theorem could then be used to test the 10% probability of exceedance statistically.

In this study, only one 50-year set of observations is available for each of the 118,785 rock sites. The observation period is too small for site by site testing of the PSHA map, therefore all the sites must be analysed assuming that the probability of the maximum historical PGA ($PGA_i^{50}$) exceeding the PSHA threshold ($PSHA_i$) during the period May 1968 - May2018 at site $i$ is site and time independent (i.e. follows an ergodic process) and equal to a constant $b$:

$$\forall\, i : \mathbb{P}\left(PGA_i^{50} \geq PSHA_i\right) = b \tag{4.2.2}$$

We define the maximum historical PGA ($PGA_i^{50}$) as the median PGA taken from the ShakeMap footprint ($SM_i$), adjusted by an error term ($\zeta$) :

$$PGA_i^{50} = SM_i \times e^{\zeta} \tag{4.2.3}$$

where $\zeta$ is the sampling of a Gaussian distribution with zero mean and a standard deviation given by the ShakeMap footprint for the rock site $i$ (Fig. 4.2.3c, d).

For each rock site $i$, the random variable $B_i$ is introduced to Equation 4.2.2. It is equal to 1 when $PGA_i^{50} \geq PSHA_i$ and to 0 otherwise. Hence, the variables $B_i$ are distributed according to a Bernoulli probability distribution with parameter $b$. Furthermore, they are independent, identically distributed, and follow an ergodic process. For a subset of sites $N$, the sum of $B_{i \in N}$, called $S_N$, follows a Binomial probability distribution with parameters $b$ and $N$, according to the Binomial distribution definition:

$$\mathbb{P}(S_N \geq k) = \mathbb{P}\left(\sum_{i \in N}\left[PGA_i^{50} \geq PSHA_i\right] \geq k\right) = \binom{\#N}{k} b^k (1-b)^{\#N-k} \tag{4.2.4}$$

where $\#N$ corresponds to the number of sites in the subset $N$.

To identify a set of rock sites $N$ for which the random variables $B_i$ are independent, we must identify the sites $i$ for which the random variable $PGA_i^{50}$ is realised independently of the other sites. Using the Law of Total Probability (Tijms 2003), the distribution of $PGA_i^{50}$ can be written as the probability of occurrence of the earthquake ($\mathbb{P}(O_i)$) producing the maximum historical PGA and the probability of the earthquake $O_i$ producing such a PGA:

$$\mathbb{P}\left(\mathrm{PGA}_i^{50} \geq x\right) = \mathbb{P}\left(\mathrm{PGA}_i^{50} \geq x \middle| O_i\right) \times \mathbb{P}(O_i) \quad (4.2.5)$$

Equation 4.2.5 shows that for two rock sites, *i* and *j*, $\mathrm{PGA}_i^{50}$ and $\mathrm{PGA}_j^{50}$ are not independent if $O_i$ and $O_j$ are not independent. In a first case, we consider that $O_i$ and $O_i$ refer to the occurrence of the same earthquake. This means that the maximum historical PGA for rock sites *i* and *j* come from the same ShakeMap footprint (Fig. 4.2.3). In this case, the distributions of $\mathrm{PGA}_i^{50}$ and $\mathrm{PGA}_j^{50}$ are not independent because $\mathbb{P}(O_i) = \mathbb{P}\left(O_j\right)$. Consequently, the subset *N* cannot contain two rock sites for which the maximum historical PGA was extracted from the same ShakeMap footprint.

If $O_\mathrm{i}$ and $O_\mathrm{j}$ refer to the occurrence of two different earthquakes, they are independent if, and only if, they are two main shocks (i.e. not a foreshock or an aftershock), since the occurrence process of main shocks is assumed to follow a Poisson Stationary Process. Thus, assumption is verified by comparing the empirical distribution of the occurrence time of the 198 earthquakes with a ShakeMap footprints to a theoretical Poisson distribution with an annual frequency equal to 198/(12×50)=0.33. The result of the Kolmogorov-Smirnov test (equal to 0.09) is slightly above the usual threshold (equal to 0.05) for considering the sample following the theoretical distribution. This weak adequacy can be explained by some hysteresis effects and time-dependency in the earthquake occurrence process in Indonesia over the last 50 years (Papadimitriou and Papazachos 1994).

Finally, the occurrence process of the 198 earthquakes associated with the ShakeMap footprints can be assimilated to a Poisson stationary process, meaning that $O_i$ and $O_j$ are independent.

Variables $\left(\mathrm{PGA}_i^{50} \geq x \middle| O_i\right)$ and $\left(\mathrm{PGA}_j^{50} \geq x \middle| O_j\right)$ are independent if sites *i* and *j* and earthquake occurrences $O_\mathrm{i}$ and $O_\mathrm{j}$ are different. Finally, the subset *N* for which the random variables $\mathrm{B}_i$ are independent comprises 198 rock sites, with each one corresponding to a different ShakeMap footprint contributing to the maximum historical PGA. Since there is no condition determining the point of each ShakeMap footprint, subset *N* is made of one point sampled from each ShakeMap footprint (Tab. 4.2.1). Figure 4.2.6 gives one illustration of a possible *N* subset.

If the dataset of past earthquakes, represented by ShakeMap footprints, cannot be considered as a Poisson Stationary Process, this test cannot be performed. Indeed, if the probabilistic distribution of the arrival time is not memoryless (e.g. in the case of a renewal process), the ergodicity assumption is not verified and, therefore $\mathrm{S}_N$ is not distributed according to a Binomial distribution (Eq. 4.2.4).

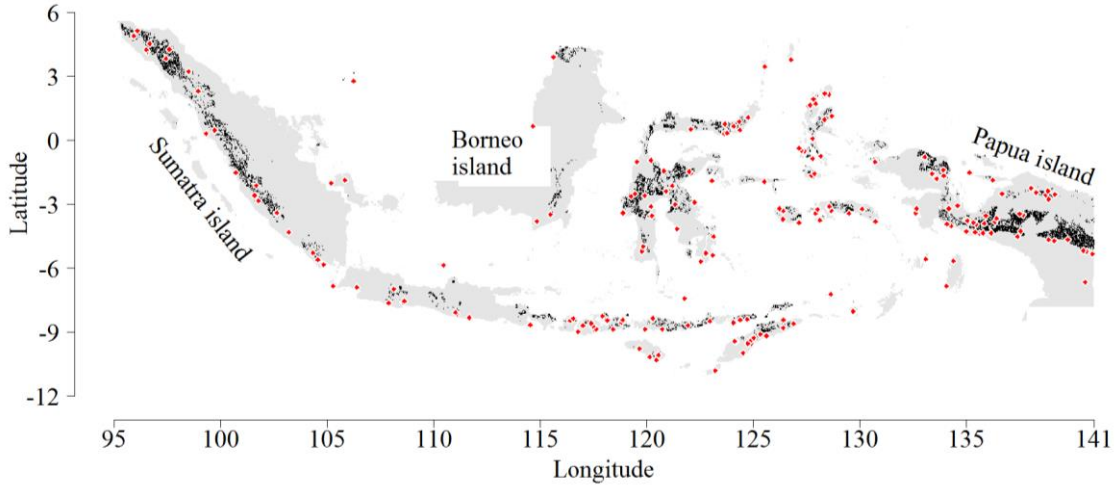


Figure 4.2.6: Illustration of a set of 198 points selected for testing PSHA maps (red dots). Each point is associated with a different ShakeMap and a single rock site.

The implementation of this methodology can be divided into four steps: 1) sampling the rock sites in $N$ (Fig. 4.2.6); 2) assessing the value of $PGA_i^{50}$ for each rock site $i$ in $N$ by sampling the error term as given by the ShakeMap footprint (Eq. 4.2.3); 3) comparing with the PSHA map threshold at each rock site $i$ (Eq. 4.2.2); 4) summing the number of sites for which the sampling of the maximum historical PGA exceeds the PSHA map threshold (Eq. 4.2.4). This procedure is summarized in Figure 4.2.7.

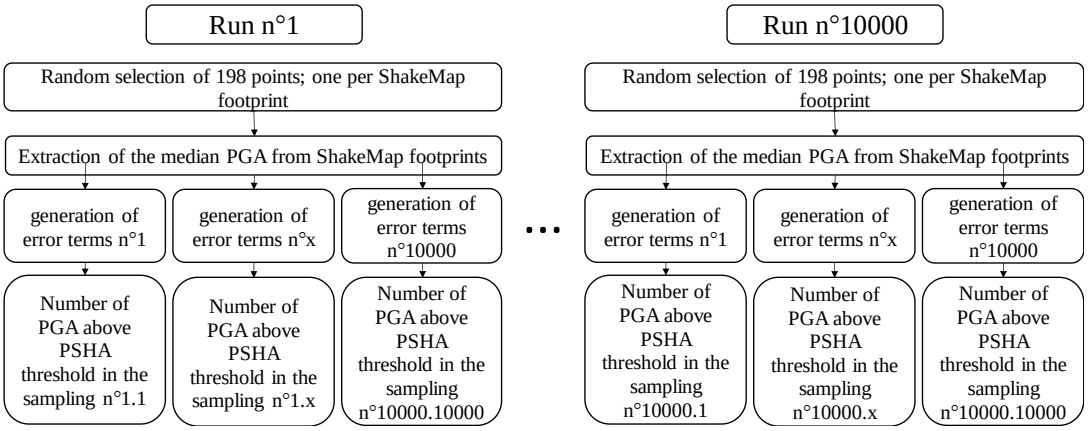


Figure 4.2.7: Procedure for sampling a stochastic set of points on which PSHA maps are tested in the case of 10,000 rock site samples and 10,000 PGA error samples for each rock site sample.

If a PSHA map indicates that the probability of exceedance is equal to 10% over 50 years, then $b$ is expected to equal 10% (Eq. 4.2.2). Finally, the empirical distribution of $S_N$ is compared with the theoretical Binomial distribution with parameter $b$=10%.

In the next section, we apply this method to the following three PSHA maps: GAR2015, SNI2017 and GSHAP.

### *4.2.4. Testing PSHA maps for Indonesia*

Several PSHA maps have been published for Indonesia since 1999, including GAR2015 (CIMNE and INGENIAR 2015), GSHAP (Giardini et al. 1999) and SNI2017 (Standar Nasional Indonesia, Irsyam et al. 2017), which are represented in Figure 4.2.8.

These three maps differ foremost about the scope covered: the GAR2015 is at the worldwide scale and includes all the main natural catastrophes (earthquake, tropical cyclone, floods, tsunami and volcanic eruptions); the GSHAP is also at the worldwide scale but dedicated to the seismic risk; the SNI2017 is about the seismic risk only in Indonesia. Furthermore, they use different set of GMPEs: the GAR2015 is made of 4 different GMPEs released before 2008 (CIMNE and INGENIAR 2015) against 10 for the SNI2017 PSHA map, including 4 released in 2014.

Although they all deal with PGA at rock sites for a period $T$ = 50y and a probability of exceedance $p$ = 10%, the reference accelerations can differ significantly, by up to 1g (Fig. 4.2.9). Figure 4.2.9 shows that the GAR2015 map thresholds (CIMNE and INGENIAR 2015) differ most from the GSHAP map thresholds, with lower values: for example, in the Jakarta area, the difference is about -0.2g. At the opposite, the hazard level given by the SNI2017 map (Irsyam et al. 2017) is very high in North Papua, with a value up to 1g above the threshold given by the GSHAP map. SNI2017 differs also from the GSHAP map with higher PGA values along the west coast of Sumatra Island and throughout Sulawesi Island.

These differences can be explained by different modelling approaches, as illustrated by the GMPEs used to model the PGA footprints of subduction earthquakes: GSHAP (Petersen et al. 2004) uses the Fukushima and Tanaka (1990) GMPE, GAR2015 (CIMNE and INGENIAR 2015) on the Zhao et al. (2006) GMPE and SNI2017 (Irsyam et al. 2017) on GMPEs from Youngs et al. (1997), Atkinson and Boore (2003) and Zhao et al. (2006).

To determine which PSHA map is most representative of the seismic activity over the last 50 years for the part of Indonesia covered by the 198 ShakeMap footprints (Fig. 4.2.2), the method developed in this study is applied. This involves calculating the number of runs required to

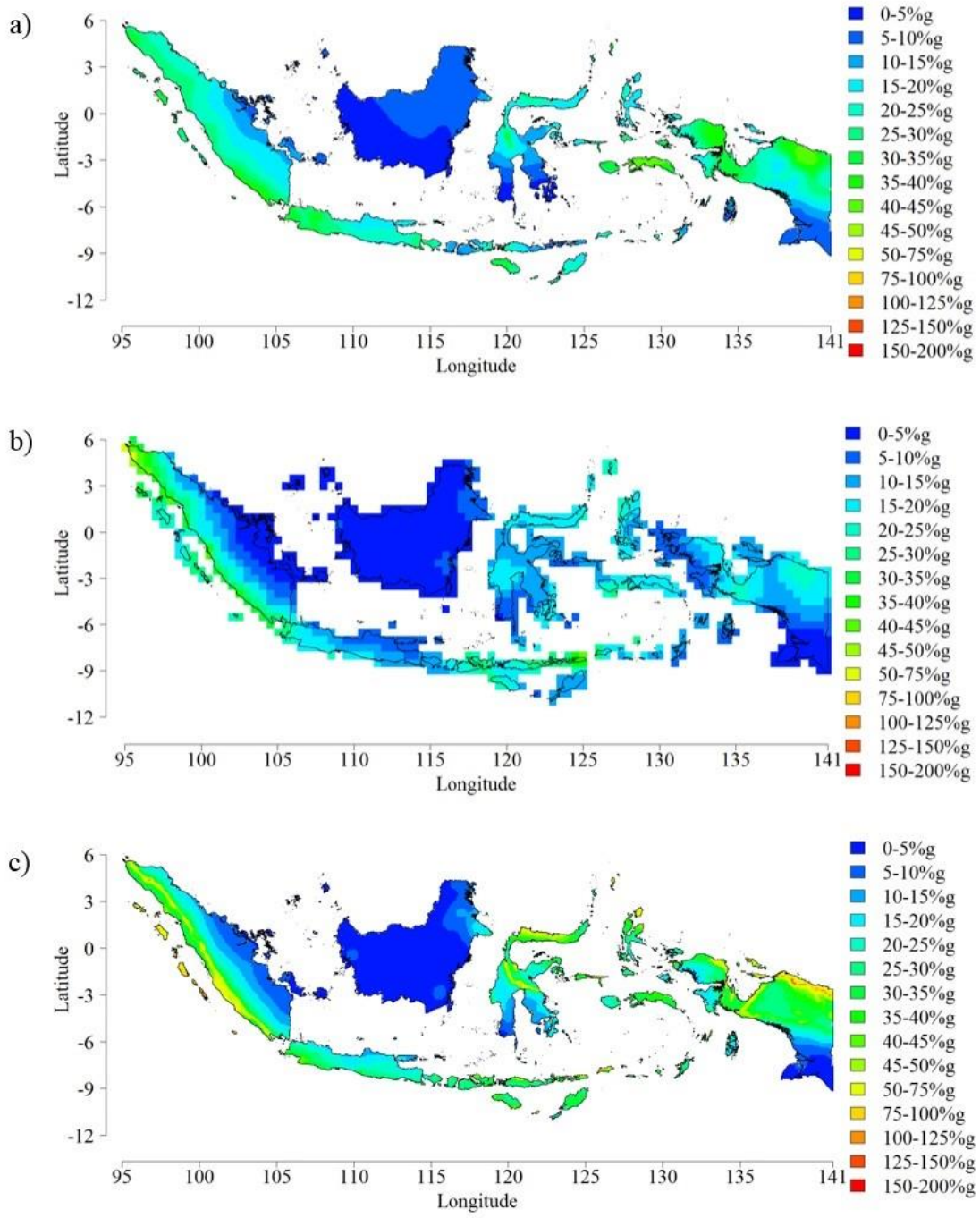


Figure 4.2.8: PSHA maps considering PGA for rock sites, a period T=50y and a probability of exceedance p=10%. a) GSHAP (Giardini et al. 1999); b) GAR2015 (CIMNE and INGENIAR 2015); c) SNI2017 (Irsyam et al. 2017).

achieve convergence of the distribution of $S_N$, as illustrated in Figure 4.2.10a, c, e.

Figure 4.2.10 shows that for the three PSHA maps, convergence is reached with a total of 100 million runs, with sampling of 10,000 rock sites and then sampling the PGA error term 10,000 times. Figure 4.2.10 shows also that the empirical distribution ($S_N$) overlaps the theoretical

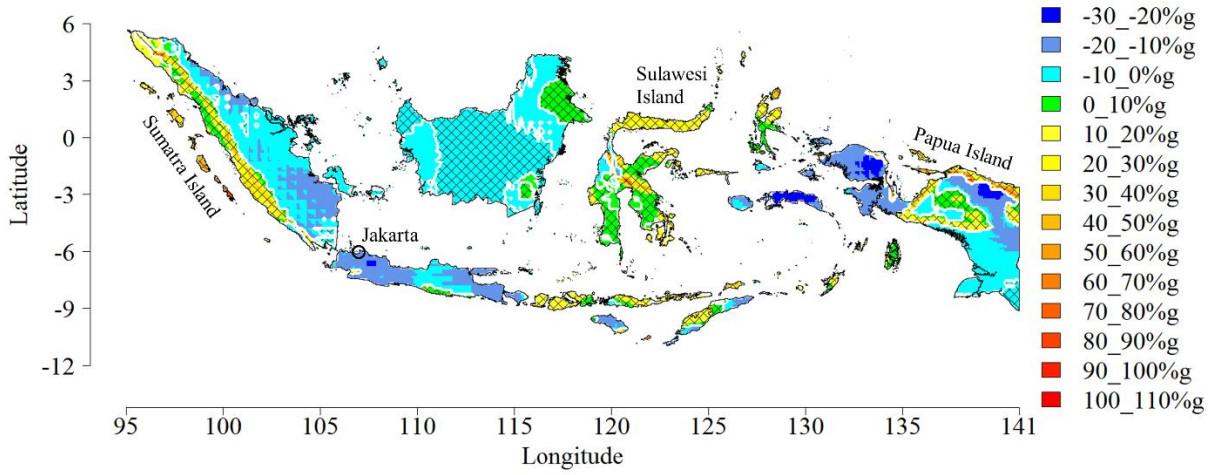


Figure 4.2.9: Maximum absolute differences of the GAR2015 and the SNI2017 PSHA maps compared with the GSHAP PSHA map. Positive (+) and negative (-) signs indicate a value above or below the GSHAP map threshold, respectively. The gridded areas represent locations where the maximum absolute difference is obtained with the SNI2017 map.

distribution, which, statistically speaking, means that the number of exceedances modelled by the PSHA map is close to the value that can be estimated from the ShakeMap footprints of past earthquakes over the last 50 years. However, there is a significant difference between the empirical and the theoretical distributions for the GAR2015 (Fig. 4.2.10b) and GSHAP (Fig. 4.2.10c) PSHA maps, and lesser for the SNI2017 PSHA map.

The test method is applied again, considering only the western part of Indonesia (limited by longitude 120°: mainly Sumatra, Java, Borneo, Bali and Lombok islands). This is because most of the economic activity and urban areas in Indonesia are located in the western part of the country. The number of footprints containing at least one rock site with the maximum historical PGA decreases from 198 to 68. The results are presented in Figure 4.2.11.

Thus, for western Indonesia, the three PSHA maps give thresholds corresponding to a probability of exceedance of 10%, which fits the data from previous seismic events from the past 50 years, captured by the 68 ShakeMap footprints.

Even if the same testing method and the same dataset for characterizing historical seismicity (ShakeMap footprint catalogue over the last 50 years) are used, results on Western Indonesia are significantly different from those on Indonesia. Furthermore, the testing method is not suitable for differentiating areas where the past seismicity fits or not a PSHA map since testing points are aggregated into a single probabilistic distribution (Eq. 4.2.4). We conclude that results from this testing method are meaningful only at the scale of the analysis and cannot be

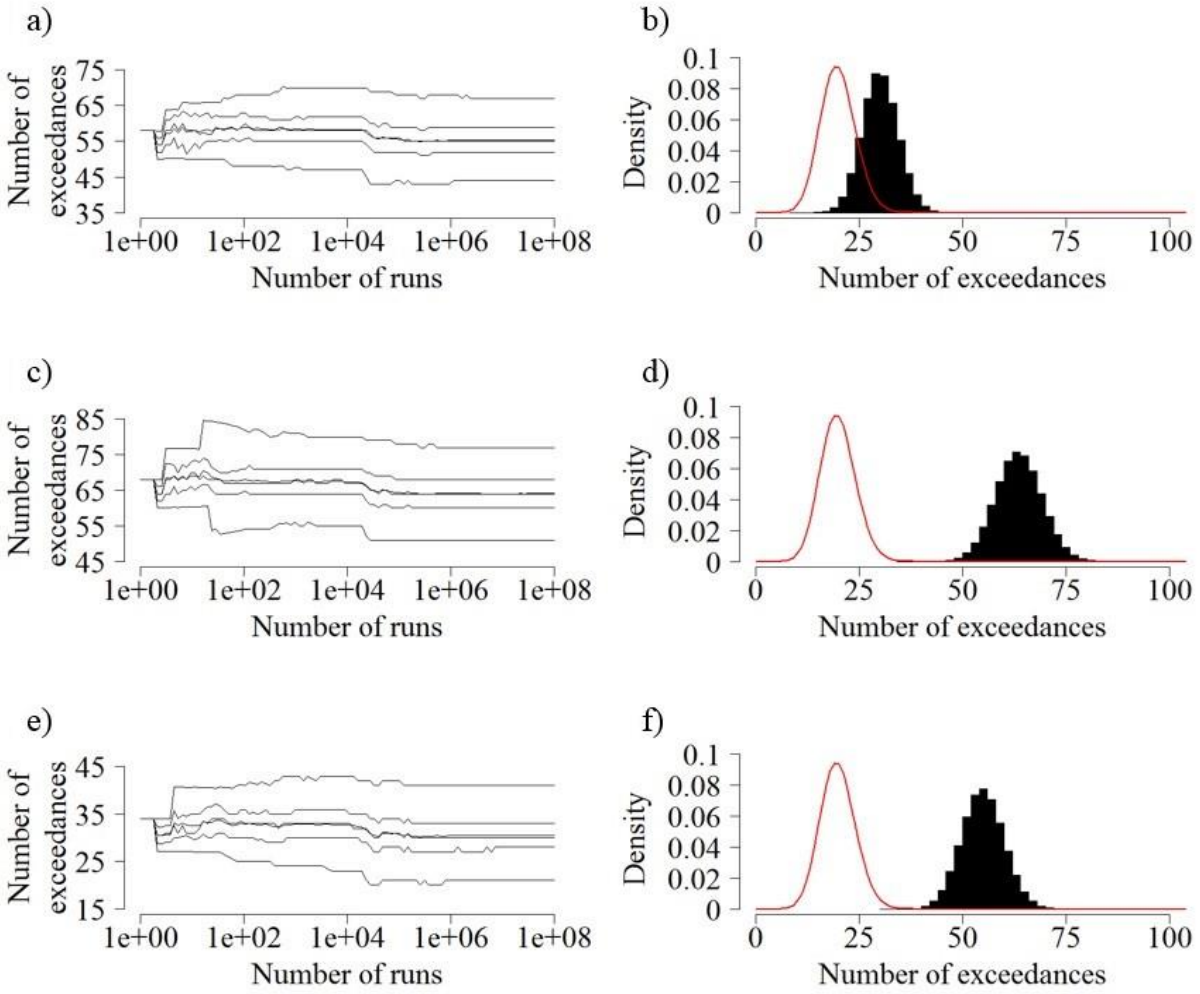


Figure 4.2.10: The sub-figures a), c) and e) show the convergence of the quantiles (5%, 25%, 50%, 75%, and 95%) and the mean of the empirical Binomial distribution according to the number of runs (left). The sub-figures b), d) and f) illustrate the distribution of the number of points exceeding hazard map thresholds for the empirical (black bars) and the theoretical (red line) distributions for the whole Indonesia. Figures on the first line, second line and third line correspond to the seismic hazard map tested SNI2017, the GAR2015 and the GSHAP, respectively.

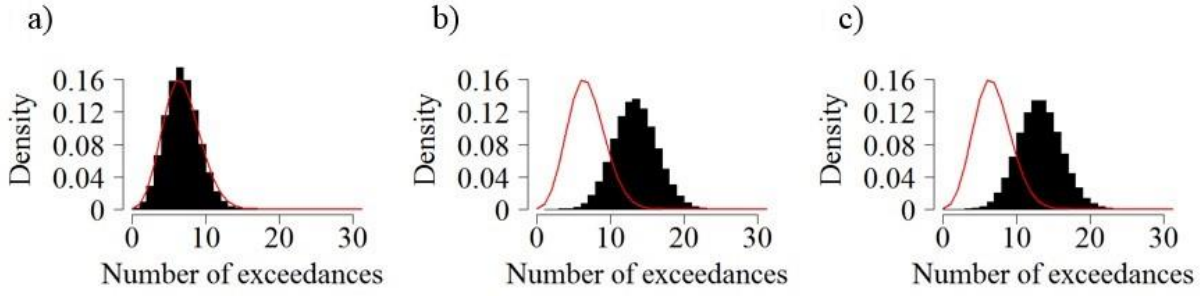


Figure 4.2.11: Comparison of the empirical (black bars) and the theoretical (red line) distributions of the number of points exceeding: a) the SNI2017, b) the GAR2015 and c) the GSHAP hazard map thresholds for Western Indonesia.

extrapolated at a wider or a finer scale. To illustrate it, the tests performed in this study indicate that the GSHAP map is comparable to the past seismicity, represented by the catalogue of ShakeMap over the last 50 years, for Western Indonesia but not for the whole Indonesia.

### *4.2.5. Conclusions*

USGS ShakeMap footprints of earthquakes occurring in Indonesia between May 1968 and May 2018 can be used to assess the maximum historical PGA at 118,785 rock sites, and, consequently, to test PSHA maps. Although PSHA map and ShakeMap footprint are both modelling outputs, the variety and the complexity of underlying assumptions prevent analytical comparisons. For this reason, this study introduces a statistically-based PSHA map testing method using ShakeMap footprints. Nevertheless, assumptions regarding PSHA models and the testing catalogue must be verified before. First, ShakeMap footprint is assumed to correctly describe the ground motion produced by the past earthquake considered. Earthquake occurrence is also supposed to be distributed according to a Poisson occurrence process (i.e. earthquakes in the testing catalogue are main shocks and can be assumed to occur independently). This assumption specifically implies to neglect any renewal process.

The results show that PSHA maps can be tested to differentiate them by comparison with previous ground motion intensities observed using ShakeMap footprints. Indeed, the SNI2017 PSHA map fits past seismicity for the set of rock sites spread over the whole of Indonesia, but the GSHAP and GAR2015 PSHA maps do not. The better fit when testing the SNI2017 PSHA map can be explained on one hand by the state-of-the-art improvement, especially regarding GMPEs, between 1999 (release date of the GSHAP PSHA map) and 2017 (release date of the SNI2017 PSHA map) and on the other hand, by capitalizing on previous works done by Petersen et al. on West Indonesia (2004; 2007). As the number of PSHA maps for the same areas increases, testing methodologies can help to decide which is preferred for a purpose.

Nevertheless, this testing method relies on ShakeMap footprints and consequently depends on their accuracy. So, improving ShakeMap footprint modelling framework can also contribute to improve this PSHA maps testing method. Last, PSHA maps testing results can be dependent on both the observation period considered and the spatial extent. Studying this dependence would definitely help to improve PSHA map testing methods.

## 4.3. Assessing the performance of existing repair-cost relationships for buildings

### *4.3.1. Introduction*

Forecasting earthquake losses is decisive for many applications, including cost-benefit analysis (Riedel and Guéguen 2018), insurance cover or insurance policy design (Werland and Pitts 1997), earthquake mitigation plans and emergency preparedness (Harvey et al. 2010, Federal Emergency Management Agency 2017). Daniell (2009) has listed 28 different models released for estimating earthquake losses. These models differ especially on the computational resources needed, the spatial extent and resolution of models' outputs and the underlying exposure model (Lang 2012; Daniell and Wenzel 2014). For example, exposure models require using seismic vulnerability assessing method that can be at the resolution of a building (e.g. Irwansyah and Hartati 2014) or an administrative area (e.g. Moudi et al. 2019), based on field observations (e.g. Bevington et al. 2012), online survey (Silva et al. 2018), literature and public statistics (e.g. Aulady and Fujimi 2019) or machine learning tools (e.g. Riedel et al. 2015).

Once exposure model defined, economic losses can be calculated according to different models. While some are based on the GDP (e.g. Dunbar et al. 2003), others are calibrated upon post-disaster funding after past events (e.g. Bal et al. 2008) or again using economic data about the cost of repair or reconstruction works (e.g. Federal Emergency Management Agency 2010). Loss models also consider the earthquake effect on the exposure through several variables as the magnitude and focal depth (Choi et al. 2019) or more usually hazard level metrics as the peak ground acceleration or the macroseismic intensity (Calvi et al. 2006).

Uncertainty remains the main drawback of existing loss models. As an example, after the 2015 Nepal earthquake the immediate assessment, for the direct economic loss to be below USD $100m, moved from more than 60% to less than 10% between the PAGER alerts version 1 and 6 (Bialik 2015). Models based on building damage are more accurate than those derived from economic variables (Guettiche et al. 2018). Therefore, making loss models more accurate requires to work on the relationship between building damage state and the repair-cost. Many damage-cost relationships have already been released for different building types and different regions (Meroni et al. 2017; Riedel and Guéguen 2018; Fang et al. 2011; Bal et al. 2008; Roca

et al. 2006; Kappos et al. 2006; Di Pasquale et al. 2005; Tyagunov et al. 2004; Milutinovic and Trendafiloski 2003; Federal Emergency Management Agency 2010; Blong 2003; Timchenko 2002 and Di Pasquale et al. 2001). This study proposes to test existing damage-cost relationships for buildings using data from historical earthquakes consequences. To optimize the residual distribution and to avoid any bias related to additional losses (i.e. contents, business interruption…), only building damage is considered.

In the first section, a database of earthquake losses named Earthquake Damage Database is built. Next, the damage-cost relationships are defined, and the associated parameters assessed. Last, the distributions of building loss estimate residuals are calculated and compared, using the Earthquake Damage Database.

### *4.3.2. The Earthquake Damage Database*

In this study, a new database (called the Earthquake Damage Database) about the economic consequences of past earthquakes is defined. The variables of interest are the hazard related parameters (i.e. the epicentre location, the date of occurrence, the magnitude and the hazard footprint), and loss-related parameters (original source of the damage and loss estimates, the estimated number of buildings damaged, buildings destroyed, total direct economic loss and housing sector loss).

All the hazard-related parameters contained in the Earthquake Damage Database have been collected from the ShakeMap USGS database, an open-source database provided by the USGS. The estimated footprints of the ground shaking (in several metrics as the Peak Ground Acceleration PGA, Peak ground Velocity PGV or macroseismic intensity MMI) are given for historical earthquake (Wald et al. 2005). Although other sources are available in open-source for some countries, the ShakeMap database is the largest homogeneous worldwide database. Therefore, it was possible to collect a ShakeMap footprint for almost all the past earthquakes for which economic consequences estimates were available.

Loss-related parameters have been extracted from existing international databases presented in Table 4.3.1. Most of records in the Earthquake Damage Database are extracted from the DESINVENTAR database, provided by the United Nations Office for Disaster Risk Reduction (UNDRR). It contains a large set of detailed data about the consequences of past man-made and natural disasters for several countries, mainly located in the Americas continent. The CATDAT

Table 4.3.1. Databases and sources used to build the Earthquake Damage Database. The number of earthquakes in the Earthquake Damage Database extracted from each database and source is given in the column Nb. Sources: (1): Wald et al. 2005, https://earthquake.usgs.gov/data/shakemap/; (2): Sendai Framework for Disaster Reduction, United Nations Office for Disaster Risk Reduction - www.desinventar.net/DesInventar/results.jsp; (3): Daniell et al. 2011; (4) Ruffle et al. 2012; (5): Significant Earthquake Database. National Geophysical Data Center / World Data Service – www.ngdc.noaa.gov/nndc/struts/form?t=101650&s=1&d=1; (6): https://earthquake-report.com/; (7): World Bank, Global Facility for Disaster Reduction and Recovery www.gfdrr.org. (8): UN Office for the Coordination of Humanitarian Affairs, ReliefWeb, http://reliefweb.int/; (9): Center for Disaster Management and Risk Reduction Technology www.cedim.kit.edu.

| Source | Nb | Source | Nb |
|---|---|---|---|
| ShakeMap(1) | 297 | USGS (1987) | 2 |
| DESINVENTAR(2) | 191 | CEDIM(9) | 1 |
| CATDAT(3) | 58 | Kazantzidou-Firtinidou et al. (2015) | 1 |
| GEM(4) | 54 | Saatcioglu et al. (2001) | 1 |
| NGDC(5) | 37 | Sinadinovski and McCue (2013) | 1 |
| Earthquake-Report(6) | 3 | Astaneh-Asl (1994) | 1 |
| World Bank(7) | 3 | Erdik (2000) | 1 |
| OCHA(8) | 2 | | |

database contains the consequences of damaging earthquakes and secondary effects, occurred all around the world. Despite the CATDAT database includes data for past earthquakes occurred since 1900, only datasets corresponding to the years 2010, 2011 and 2012 are open-source. The Global Earthquake Model (GEM) provides an open-source database about consequences of 71 past earthquakes, called the Earthquake Consequences Database. Contrary to the previous ones, GEM data has been collected from different sources and aggregated. The NGDC database is provided by the National Oceanic and Atmospheric Administration (NOAA) and contains data about damaging earthquakes occurred all around the world since 2150 B.C. It contains 6,152 past events, but only 37 are included in our Earthquake Damage Database by lack of data about the number of buildings damaged or destroyed. Finally, 10 other sources have been browsed to complete the Earthquake Damage Database providing 16 additional datasets. They are either real-time reports during the post-disaster phase of a damaging earthquake (Earthquake-Report, World Bank, OCHA, USGS and CEDIM) or part of scientific peer-reviewed studies focused on a particular event (Astaneh-Asl, 1994; Erdik, 2000; Saatcioglu et al., 2001; Sinadinovski and McCue, 2013).

Only few information is available about the accuracy and the methodology for collecting the data populated in these databases, with consequences on their relevancy. For example, the NGDC and the World Bank reported a total direct economic loss at $10bn and $3.5bn, respectively, for the 2015 Nepal earthquake (Mw7.8). Consequently, to determine whether or

not a data is reliable enough to be included in our Earthquake Damage Database, the method used for assessing loss-related and hazard-related data was considered, depending on whether it is based on a stochastic approach or on field data. First, we assume the stochastic approach as the reference, since data providers are either scientists (e.g. CAT-DAT) or well-known institutions (e.g. USGS, NOAA, World Bank). Nevertheless, several state-of-the-art models coexist, and they rely on different assumptions and inputs. For instance, differences in the total direct economic loss caused by an earthquake calculated with the PAGER (Jaiswal and Wald 2011), the HAZUS (Federal Emergency Management Agency 2010) or the RISK-UE (Milutinovic and Trendafiloski 2003) models, can be observed. Therefore, when two databases provide two different estimates (e.g. for the number of buildings destroyed after the 2015 Nepal earthquake Mw7.8), it is not possible to know if this gap is related to a different modelling framework, a different understanding of the event or the both.

About field observations, this issue remains since differences can also be observed, due to the area covered during the field-investigation or the methodology used for collecting data.

In this study any data from the databases listed in Table 4.3.1 is considered to be meaningful and consistent with all other data from the same database since the modelling framework is assumed to be the same. However, between two different databases, data is considered not comparable as the modelling framework can be different. Consequently, the number of buildings damaged, number of building destroyed and total direct economic loss come from the same database for each dataset in Earthquake Damage Database (Tab. 4.3.2).

Table 4.3.2. Extract of the Earthquake Damage Database for the 2015 Nepal earthquake (Mw7.8). Financial values are given in USD 2015 and NA stands for a missing value. References: (1): Significant Earthquake Database. National Geophysical Data Center / World Data Service – www.ngdc.noaa.gov/nndc/struts/form?t=101650&s=1&d=1; (2): World Bank, Global Facility for Disaster Reduction and Recovery www.gfdrr.org.

| Source | ShakeMap Id | Number of buildings damaged | Number of buildings destroyed | Total direct economic loss (million $) | Housing sector loss (million $) |
|---|---|---|---|---|---|
| NGDC(1) | us20002926 | 269,107 | 299,588 | 10,000 | *NA* |
| World Bank(2) | us20002926 | 256,697 | 498,852 | 3,504 | 2,830 |

Only the housing sector loss variable is allowed to be missing since it available only for 21 past

earthquakes (Tab. 4.3.2). When several databases provide all the economic consequence variables (except the housing sector loss) for a past earthquake, it results in two datasets in the Earthquake Damage Database (Tab. 4.3.2).

Finally, the Earthquake Damage Database is made of 356 datasets and covers 297 different historical earthquakes. The epicentre location, the occurrence year and the magnitude of these 297 past events are illustrated in Figure 4.3.1.

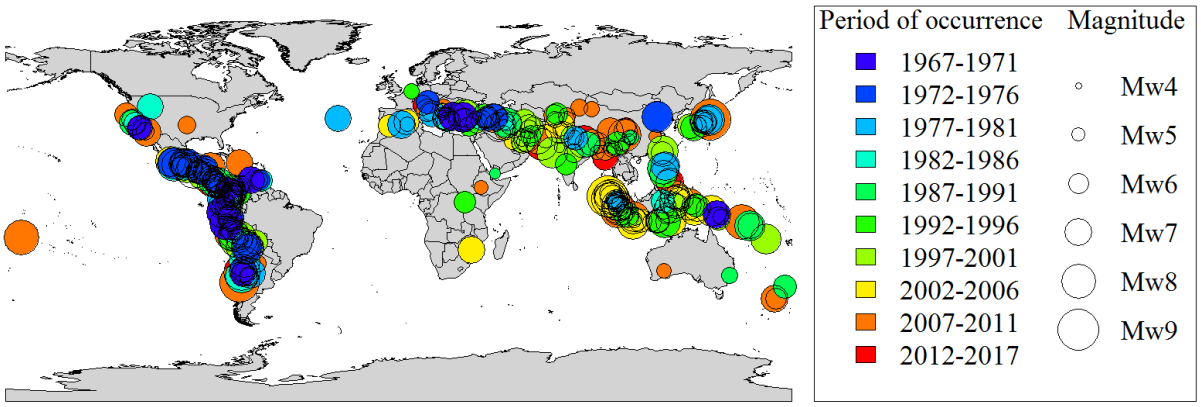


Figure 4.3.1. Map of the past earthquakes included in the Earthquake Damage Database (Tab. 4.3.1). Dots are located at the epicentre, the circle size and the colour scheme represent the magnitude and the period of occurrence, respectively.

All the past events in the Earthquake Damage Database occurred between 1966 and 2015. As this study was undertaken in 2016, the upper bound corresponds to the last year of full seismicity record. Figure 4.3.1 highlights that most of the 297 historical earthquakes are located on the most seismically active areas (the "Ring of Fire" along the Pacific Ocean border and the south border of the Eurasian tectonic plate). Nevertheless, several intraplate earthquakes are also covered, e.g. in Western and Central Europe. Without rational explanation, we also observe (Fig. 4.3.1) that the oldest earthquakes (i.e. between 1966 and 1980) are mostly located in the Central and South America or around the Mediterranean Sea. At the opposite, earliest events (i.e., after 1986) are in Asia and South-Western Pacific (i.e. after 1986).

A large range of magnitude is covered, from Mw4.4 up to Mw9 for the 2004 Indian Ocean and the 2011 Tohoku earthquakes. Figure 4.3.2 shows the distribution of the magnitude both on a histogram and a Gutenberg-Richter plot.

Most of events in the Earthquake Damage Database are magnitude 6 to 7 (Fig. 4.3.2.a). For lower magnitude, most of earthquakes caused small to insignificant damage and therefore, are

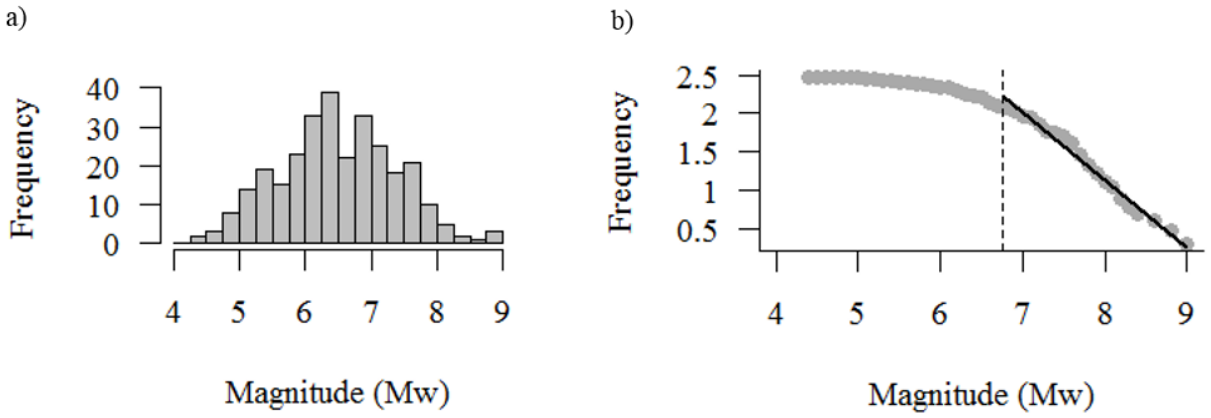


Figure 4.3.2: Empirical distribution (a) and Gutenberg-Richter plot (b) of the moment magnitude (Mw) of past earthquakes included in the Earthquake Damage Database. The y-axis represents the frequency on the full period range (from 1967 to 2015) by magnitude and cumulated above a magnitude threshold, on Figure a) and b), respectively. On Figure b), solid line represents the linear regression using method of least squares for magnitude above Mw6.75 (shown by the dotted line). The corresponding slope coefficient (i.e. the b-value) is equal to 0.88.

not in the database, let us suppose an incomplete database. At the opposite, for magnitude above Mw7, almost all historical earthquakes have been considered, as illustrated by the linear regression in the Gutenberg-Richter plot (Fig. 4.3.2b).

The distribution of the total direct economic loss is also investigated. Economic loss data are given in USD at the year of the earthquake. Therefore, the total direct economic losses at year *t* are actualised at the same date *s* (i.e. 2008), using Neumayer and Barthel (2011) approach as follows:

$$Normalized\ Damage_t^s = Damage_t \times \frac{GDP\ Deflator_s}{GDP\ Deflator_t} \times \frac{Pop_s}{Pop_t} \times \frac{Wealth\ per\ capita_s}{Wealth\ per\ capita_t} \qquad (4.3.1)$$

with $Pop_s$ and $Wealth\ per\ capita_s$ the population and the wealth per capita at year *s* and $Pop_t$ and $Wealth\ per\ capita_t$ the same at year *t*. The $GDP\ Deflator_t$ is the economic metric capturing the level of prices and defined as follows:

$$GDP\ Deflator_t = \frac{Nominal\ GDP_t}{Real\ GDP_t} \qquad (4.3.2)$$

where the $Nominal\ GDP_t$ corresponds to the GDP at year *t* calculated in USD at year *t*. The $Real\ GDP_t$ is also the GDP at year *t* but calculated in USD at a reference year (usually 2010). In this study, we approximate the *Wealth per capita* at any year *t* by the real GDP per capita at year *t* ($GDP_t\ per\ capita$), as already done in previous studies reported by Neumayer and Barthel (2011). Moreover, Lange et al. (2018) found a high correlation between the Wealth per capita

and the real GDP per capita, leading us to expect a marginal impact of this approximation. Finally, the normalized damage (*Normalized Damage*$_t^s$) from the year *t* (occurrence of the earthquake) to *s* (reference year) is given by (Eq. 4.3.1 and 4.3.2):

$$Normalized\ Damage_t^s = Damage_t \times \frac{\frac{Nominal\ GDP_s}{Real\ GDP_s}}{\frac{Nominal\ GDP_t}{Real\ GDP_t}} \times \frac{Pop_s}{Pop_t} \times \frac{Real\ GDP_s\ per\ capita}{Real\ GDP_t\ per\ capita} \quad (4.3.3)$$

$$= Damage_t \times \frac{\frac{Nominal\ GDP_s}{Real\ GDP_s}}{\frac{Nominal\ GDP_t}{Real\ GDP_t}} \times \frac{Real\ GDP_s}{Real\ GDP_t}$$

$$Normalized\ Damage_t^s = Damage_t \times \frac{Nominal\ GDP_s}{Nominal\ GDP_t}$$

Where $Damage_t$ corresponds to the total direct economic loss recorded at the time of the event. The total direct economic loss in the Earthquake Damage Database has been normalized at year *s*=2008 according to Equation 4.3.3 and using nominal GDP database provided by the World Bank. The distribution of the normalized total direct economic loss is shown on Figure 4.3.3.

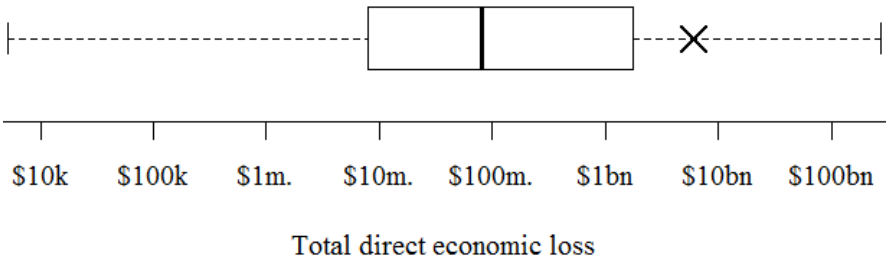


Figure 4.3.3: Distribution of the normalized total direct economic loss (USD 2008) for the 297 past earthquakes in the Earthquake Damage Database. The thick vertical black line represents the median while the box the first and the third quartiles. The dotted lines show the extent of the distribution beyond the first and the third quartiles, up to the maximum and minimum values of the distribution. The cross shows the mean value of the distribution. The scale of the x-axis is in decimal logarithm.

The normalized total direct economic loss varies from $5k up to $274bn. The upper value is obtained for 2011 Tohoku earthquake (Mw9), the costliest earthquake that occurred (OECD 2018). The lower ($5k) corresponds to the 2010 Bangladesh earthquake (Mw5.1) occurred on September 30$^{th}$. Furthermore, the distribution of the normalized total direct economic loss is wide, with 25% of data below $8m. and another 25% above $1.73bn (Fig. 4.3.3), with the variance $\sigma^2$ equal to $6.68\times10^{20}$. Figure 4.3.3 shows that the median is around $100m. and the mean of the distribution (called *m*) is equal to $6.12bn. That means that few very costly

earthquakes contribute significantly to the mean value. Indeed, three past earthquakes have a normalized total direct economic loss up to more than $100bn in the Earthquake Damage Database: the 2011 Tohoku (Mw9; $173-274bn in 2008 USD), the 1976 Tangshan (Mw7.6; $209bn in 2008 USD) and the 2008 Sichuan (Mw7.9; $86-141bn in 2008 USD). These three past earthquakes are associated to five records with a normalized total direct economic loss above $100bn.

To characterise the variability in the normalized total direct economic loss corresponding either to the information contained in different databases for a given earthquake, or between two different earthquakes, the variance $\sigma^2$ is split as follows (Weiss et al. 2006):

$$\sigma^2 = \underbrace{\frac{1}{n}\sum_{i=1}^{k} n_i \sigma_i^2}_{\text{intra-event variance } (\sigma_a^2)} + \underbrace{\frac{1}{n}\sum_{i=1}^{k} n_i (m_i - m)^2}_{\text{inter-event variance } (\sigma_e^2)} \quad (4.3.4)$$

where $n$ = 356 is the number of records and $k$ = 297 is the number of past earthquakes in the Earthquake Damage Database. The variables $\sigma_i^2$ and $m_i$ are the variance and the mean of the normalized total direct economic loss for the past earthquake $i$ (when only one database is available, the variance $\sigma_i^2$ is equal to 0). The left-hand side term is called the intra-event variance ($\sigma_a^2$) and captures the variance between databases, while the right-hand side term is the inter-event variance ($\sigma_e^2$) and is related to the variance between historical earthquakes. $\sigma_a^2$ and $\sigma_e^2$ are equal to $3.1\times10^{19}$ and $6.4\times10^{20}$, respectively (Eq. 4.3.4). Thus, the variance between databases represents only 4.6% ($\sigma_a^2$ / $\sigma^2$=4.6%) of the total variance of the normalized total direct economic loss, i.e. the differences between databases for a given earthquake is marginal compared to the variability between earthquakes.

To analyse further the distribution of the normalized total direct economic loss, Figure 4.3.4 shows the histogram of the distribution. Figure 4.3.4 shows that the distribution is bimodal with two peaks at $42m. (Fig. 4.3.4, tag 1) and $2.52bn (Fig. 4.3.4, tag 2). The first mode (Fig. 4.3.4a; grey histogram) includes the 227 records of earthquakes with a magnitude lower than Mw7.5 and occurred in a country with a GDP per capita in 2008 lower than $10k. The second mode (Fig. 4.3.4a; light-grey histogram) is the complement (129 records) and includes only data earthquakes either with a magnitude above 7.5 or occurred in a high-income country (GDP per capita in 2008 above $10k). These two sub-distributions (Fig. 4.3.4) show that the normalized total direct economic loss is significantly lower for moderate (magnitude lower or equal to Mw7.5) than for large (magnitude above to Mw7.5) earthquakes in low-income countries. However, this difference is not material for high-income countries. Last, for large

earthquakes there is no significant difference in the normalized total direct economic loss

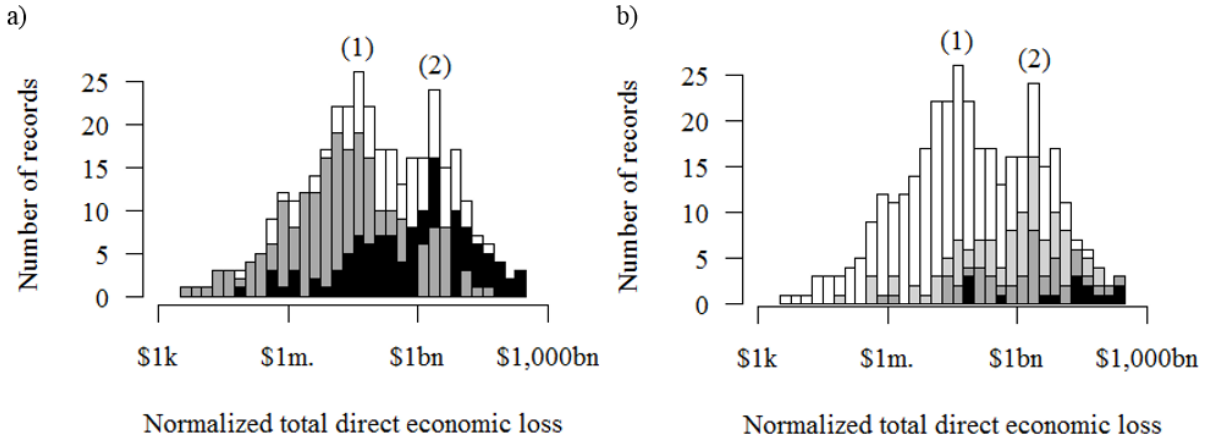


Figure 4.3.4: Histogram (white bars) of the normalized total direct economic loss (in USD 2008) extracted from the Earthquake Damage Database. In figure a) the distribution is split as follows: earthquakes with a magnitude Mag ≤ Mw7.5 and occurred in a country with a GDP per capita in 2008 lower or equal to GDPcap ≤ $10k (grey), and the complementary set (black). The latter is split again in Figure b): earthquakes with Mag ≤ Mw7.5 and GDPcap > $10k (light grey), earthquakes with mag > Mw7.5 and GDPcap<=$10k (dark grey) and earthquakes with mag > Mw7.5 and GDPcap > $10k (black). The scale of the x-axis is in decimal logarithm and the y-axis shows the number of records. Tags 1 and 2 shows the two modes of the distributions and is discussed in the text.

between low-income and high-income countries (Fig. 4.3.4.b).

In the next section a buildings loss model is proposed to test existing damage-cost relationships using data in the Earthquake Damage Database.

### *4.3.3. Using the Earthquake Damage Database to test existing damage-cost relationships*

The total damage cost of a single building *i* after an earthquake ($CBD(i)$), is estimated according to the framework HAZUS-MH MR5 defined by the Federal Emergency Management Agency (Federal Emergency Management Agency 2010), as follows:

$$CBD(i) = BRC(i) \times \left( \sum_{ds=1}^{5} [PMBTSTR_{ds}(i) \times RCS_{ds}(i)] + \sum_{ds=1}^{5} [PONSA_{ds}(i) \times RCA_{ds}(i)] + \sum_{ds=1}^{5} [PONSD_{ds}(i) \times RCD_{ds}(i)] \right) \quad (4.3.5)$$

where $BRC(i)$ is the replacement cost for the building $i$. The variables $RCS_{ds}(i)$, $RCA_{ds}(i)$ and $RCD_{ds}(i)$ correspond to the structural, acceleration-sensitive non-structural and the drift-sensitive non-structural repair and replacement ratios for the building $i$ at damage state $ds$, respectively. $PMBTSTR_{ds}(i)$, $PONSA_{ds}(i)$ and $PONSD_{ds}(i)$ are the probabilities for the building $i$ to be in damage state $ds$, for the structural, the acceleration-sensitive non-structural and the drift-sensitive non-structural components, respectively.

Data in the Earthquake Damage Database are not detailed enough to distinguish damage components. Consequently, we simplified Equation 4.3.5 by aggregating these three components into only one:

$$CBD(i) = BRC(i) \times \sum_{ds=1}^{5} P_{ds}(i) \times RC_{ds}(i) \tag{4.3.6}$$

where $P_{ds}(i)$ and $RC_{ds}(i)$ are the probability for the building $i$ to be in damage state $ds$ and the damage-cost ratio for damage $ds$. Calculating $CBD(i)$ (Eq. 4.3.6) for each building $i$ in the area affected by a past earthquake gives the total buildings loss $L_B$:

$$L_B = \sum_{i=1}^{N} \left[ BRC(i) \times \sum_{ds=1}^{5} P_{ds}(i) \times RC_{ds}(i) \right] \tag{4.3.7}$$

where $N$ is the number of buildings in the affected area. Noticing that the number ($N_{ds}$) of buildings in damage state $ds$ is given by:

$$N_{ds} = \sum_{i=1}^{N} P_{ds}(i) \tag{4.3.8}$$

Equation 4.3.7 can be rewritten as follows to highlight the contribution of $N_{ds}$:

$$L_B = \sum_{ds=1}^{5} \left[ \sum_{i=1}^{N} BRC(i) \times RC_{ds}(i) \times N_{ds} \times \left( \frac{P_{ds}(i)}{\sum_{i=1}^{N} P_{ds}(i)} \right) \right] \tag{4.3.9}$$

In this study, damage $ds$ is measured on the EMS-98 damage scale (Grünthal et al. 1998) summarized in Table 4.3.3.

To link the EMS-98 damage scale to data in the Earthquake Damage Database, we consider the buildings damaged in grades $ds = \{2;3\}$ and the buildings destroyed in grades $ds = \{4;5\}$. The variables used in Equation 4.3.9 are assessed using the process described in the next section.

**The building loss ($L_B$)**

The buildings loss ($L_B$) is not available in the Earthquake Damage Database. The authors have

Table 4.3.3: Summarized description of the EMS-98 damage scale. Source: Grünthal et al. 1998.

| Grade (*ds*) | Description |
|---|---|
| 1 | Negligible to slight damage (no structural damage, slight non-structural damage) |
| 2 | Moderate damage (slight structural damage, moderate non-structural damage) |
| 3 | Substantial to heavy damage (moderate structural damage, heavy non-structural damage) |
| 4 | Very heavy damage (heavy structural damage, very heavy non-structural damage) |
| 5 | Destruction (very heavy structural damage) |

calculated on AXA's internal data, that housing buildings represent 82% of the World building stock. Furthermore, the house corresponds in average to 85% of the total homeowner's wealth. This leads us to assume first that the number of non-housing building damaged after an earthquake is low compared to the total number of buildings damaged. We conclude from the AXA's study that the buildings losses for the housing sector is most of the total of the housing loss ($L_H$). Based on these two assumptions, we consider that the total buildings loss ($L_B$) is equal to the housing loss ($L_H$).

The linear regression between the housing loss ($L_H$) and the total direct economic loss ($L_D$) has been fitted to the historical earthquakes (21) contained in the Earthquake Damage Database for which $L_D$ and $L_H$ are available (Fig. 4.3.5), as follows:

$$L_H = 0.3395 \times L_D \qquad (R^2 = 0.7 \quad \text{Fig. 4.3.5}) \qquad (4.3.10)$$

where $R^2$ is the coefficient of determination..

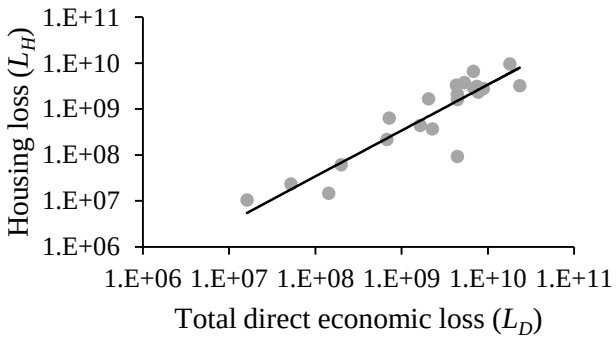


Figure 4.3.5: Linear regression between the total direct economic loss and the housing loss for 21 historical earthquakes contained in the Earthquake Damage Database. The solid black line represents the linear regression with a coefficient of determination $R^2$ equal to 0.7. Financial values are given in USD 2008.

From Equation 4.3.10, the housing loss modelling error ($\epsilon_1$) represented in Figure 4.3.6 is calculated as follows:

$$\epsilon_1 = \log_{10}(L_H) - \log_{10}(0.3395 \times L_D) \quad (4.3.11)$$

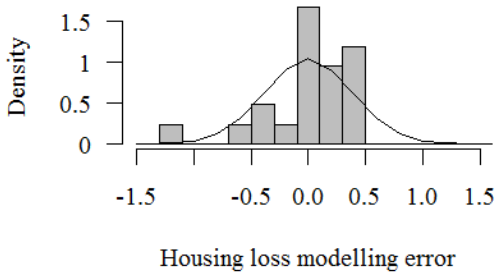


Figure 4.3.6. Empirical distribution of the housing loss modelling error ($\epsilon_1$) calculated according to Equation 4.3.10. The solid black line represents the probability density of a Gaussian distribution with a zero mean and the same variance than $\epsilon_1$.

Figure 4.3.6 shows that the distribution of $\epsilon_1$ is centred on zero, with variance equal to 0.15 and a shape similar to the Gaussian distribution. The adequacy between $\epsilon_1$ and a Gaussian distribution with a zero mean and the same variance as $\epsilon_1$ has been confirmed by a Kolmogorov-Smirnov test (Daniel 1990), with a p-value at 0.29 (usually, a test is passed for a p-value above 0.05).

**The number of buildings per damage grade $N_{ds}$**

The next variable in Equation 4.3.9 to assess is the number ($N_{ds}$) of buildings in each grade *ds*. Based on data after damaging earthquakes in Europe, Lagomarsino and Giovinazzi (2006) showed that the probability for a building *i* to be in damage state *ds* is:

$$\mathbb{P}_i(ds) = \binom{5}{ds} \times \left(\frac{\mu_D}{5}\right)^{ds} \times \left(1 - \frac{\mu_D}{5}\right)^{5-ds} \quad (4.3.12)$$

where $\mathbb{P}_i$ is the probability mass function associated to the building *i*, $\binom{5}{ds}$ the binomial coefficient and $\mu_D$ the mean damage value. Assuming no correlation between the damage of two different buildings, the number ($N_{ds}$) of buildings damaged at grade *ds* after an earthquake is equal to;

$$N_{ds} = \mathbb{P}_i(ds) \times N \quad (4.3.13)$$

Therefore, the number of buildings damaged ($N_{ds=\{2;3\}}$) and destroyed ($N_{ds=\{4;5\}}$) are solution of the following equation system:

$$\begin{cases} N_{ds=\{2;3\}} = N \times \left( \binom{5}{2} \times \left(\frac{\mu_D}{5}\right)^2 \times \left(1 - \frac{\mu_D}{5}\right)^3 + \binom{5}{3} \times \left(\frac{\mu_D}{5}\right)^3 \times \left(1 - \frac{\mu_D}{5}\right)^2 \right) \\ N_{ds=\{4;5\}} = N \times \left( \binom{5}{4} \times \left(\frac{\mu_D}{5}\right)^4 \times \left(1 - \frac{\mu_D}{5}\right)^1 + \binom{5}{5} \times \left(\frac{\mu_D}{5}\right)^5 \times \left(1 - \frac{\mu_D}{5}\right)^0 \right) \end{cases} \quad (4.3.14)$$

Thus, $\mu_D$ is solution of the following equation:

$$\frac{N_{ds=\{4;5\}}}{N_{ds=\{2;3\}}} = \frac{5 \times \left(\frac{\mu_D}{5}\right)^4 \times \left(1 - \frac{\mu_D}{5}\right) + \left(\frac{\mu_D}{5}\right)^5}{10 \times \left(\frac{\mu_D}{5}\right)^2 \times \left(1 - \frac{\mu_D}{5}\right)^3 + 10 \times \left(\frac{\mu_D}{5}\right)^3 \times \left(1 - \frac{\mu_D}{5}\right)^2} \quad (4.3.15)$$

After simplification, $\mu_D$ is solution of the following three-degree equation:

$$4 \times \left(\frac{\mu_D}{5}\right)^3 + \left(\frac{\mu_D}{5}\right)^2 \left(10 \times \frac{N_{ds=\{4;5\}}}{N_{ds=\{2;3\}}} - 5\right) - \left(\frac{\mu_D}{5}\right)\left(20 \times \frac{N_{ds=\{4;5\}}}{N_{ds=\{2;3\}}}\right) + 10\frac{N_{ds=\{4;5\}}}{N_{ds=\{2;3\}}} = 0 \quad (4.3.16)$$

The root of Equation 4.3.16 lying between 0 and 5 is selected because the mean damage value $\mu_D$ is defined between 0 and 5 (Lagomarsino and Giovinazzi 2006). This solution is called $\mu_D^{\text{overall}}$ and represents the mean damage value on the whole exposed area.

Using $\mu_D^{\text{overall}}$ instead of $\mu_D$ in Equations 4.3.12 and 4.3.13, $N_{ds}$ is assessed for each damage state *ds*. Furthermore, one can verify that $N_{ds=\{4;5\}} = N_{ds=4} + N_{ds=5}$ and $N_{ds=\{2;3\}} = N_{ds=2} + N_{ds=3}$. The variable $\mu_D^{\text{overall}}$ allows also to calculate the number of buildings in the affected area ($N$) by changing $\mu_D$ by $\mu_D^{\text{overall}}$ in Equation 4.3.14. However, since for a building *i* the probability to be in a damage state *ds* and the replacement cost depend on its location, the $N$ buildings in the exposed area need to be localised. For that, the World Housing Encyclopedia (Brzev et al. 2004) is used, which contains the number of occupants during the day and the night for 71 typical residential buildings in 44 different countries. Based on this data, we calculate an average number of occupants per building in rural ($O_r$) and urban ($O_u$) areas equal to 1.3 and 26.5, respectively, assuming that the day and the night have the same time duration. These figures allow to approximate the buildings density $D_B$ from the population density ($D_{Pop}$) as follows:

$$D_B = \begin{cases} D_{Pop} \,/\, 1.3 & \text{in rural area} \\ D_{Pop} \,/\, 26.5 & \text{in urban area} \end{cases} \quad (4.3.17)$$

The number $N$ of buildings in the affected area is then equal to the buildings' density multiplied by the exposed area affected in rural and urban areas.

The two last variables to assess for implementing Equation 4.3.9 are, for a given building *i*, the replacement cost ($BRC(i)$) and the probability ($P_{ds}(i)$) to be damaged state *ds*. For that, a global

model calibrated upon open source data is presented in the next section.

**A model for estimating the replacement cost of a building ($RC_{ds}$)**

Equation 4.3.9 requires the replacement cost of every building damaged in each grade ds. As no open source world census exists on damaged buildings replacement cost, we develop hereafter a model to assess it. The World Housing Encyclopedia (WHE) contains data on 162 representative residential buildings in several countries, including:

1. the building replacement cost in USD 2008;
2. the country (44 modalities);
3. the land-use (2 modalities: rural and urban);
4. the structure type (10 modalities: steel (S); reinforced concrete (RC) ; stone (St) ; precast-concrete (PC) ; unreinforced masonry (UM); confined masonry (CM); wood (W); reinforced masonry (RM); mud (M) and adobe(A));
5. the EMS-98 (Grünthal 1998) seismic vulnerability class: (5 modalities: A-B; B-C; C-D; D-E; E-F).

In the WHE database, the building replacement cost is missing for 38 out of 162 records. Consequently, only 124 data can be used in this study. The high number of modalities (44 countries × 10 structure type × 5 vulnerability class × 2 land use = 4,400) compared to the number of observations (124) does not allow to build a linear model between the replacement cost and the buildings' characteristics, because of overfitting issue (Harrell 2015).

The variable with the highest number of modalities is the country. According to Egert and Mihaljek (2007), the housing price is strongly correlated to the GDP per capita. Thus, the GDP per capita (called GDPcap($i$) and extracted from the World Bank database: https://data.worldbank.org/indicator) is used for defining the replacement cost (BRC($i$)) for each building $i$. The following linear regression has been fitted on the 124 data in the WHE database:

$$\log_{10}(BRC(i)) = 1.24 \times \log_{10}(\text{GDPcap}(i)) + 0.4 + res \quad (R^2 = 0.37 \quad \text{Fig. 4.3.7}) \qquad (4.3.18)$$

where *res* is the residuals and correspond to the replacement cost effect which is not captured by the GDP per capita. Equation 4.3.18 is illustrated in Figure 4.3.7.

The next variable in the WHE database with a large number of modalities is the structure type. The statistical method of Agglomerative Hierarchical Clustering (Rokach and Maimon 2005)

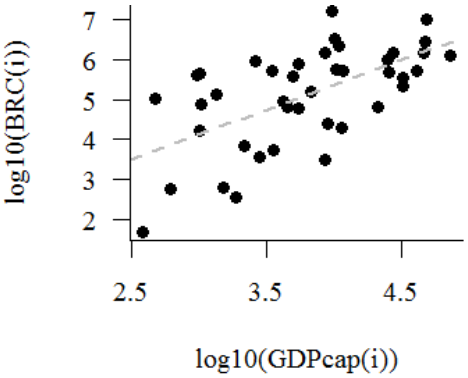


Figure 4.3.7. Linear regression between the decimal logarithms of the 2008 real GDP per capita and the building's replacement cost. The dotted grey line shows the linear trend. Financial values are in USD 2008. Source: WHE and World Bank databases.

is used on the residuals (Eq. 4.3.18; *res*) to remove the contribution of the GDP per capita on the building replacement costs. The Agglomerative Hierarchical Clustering method consists in clustering into a single group several modalities which are similar. To measure how different a modality is to another, a dissimilarity distance is necessary. In this study, the Euclidean distance is used and applied to the average residuals of the replacement cost (Eq. 4.3.18; *res*) in each modality. Figure 4.3.8 illustrates the clustering process.

Figure 4.3.8 shows that the two modalities to be first clustered are Wood (W) and Reinforced

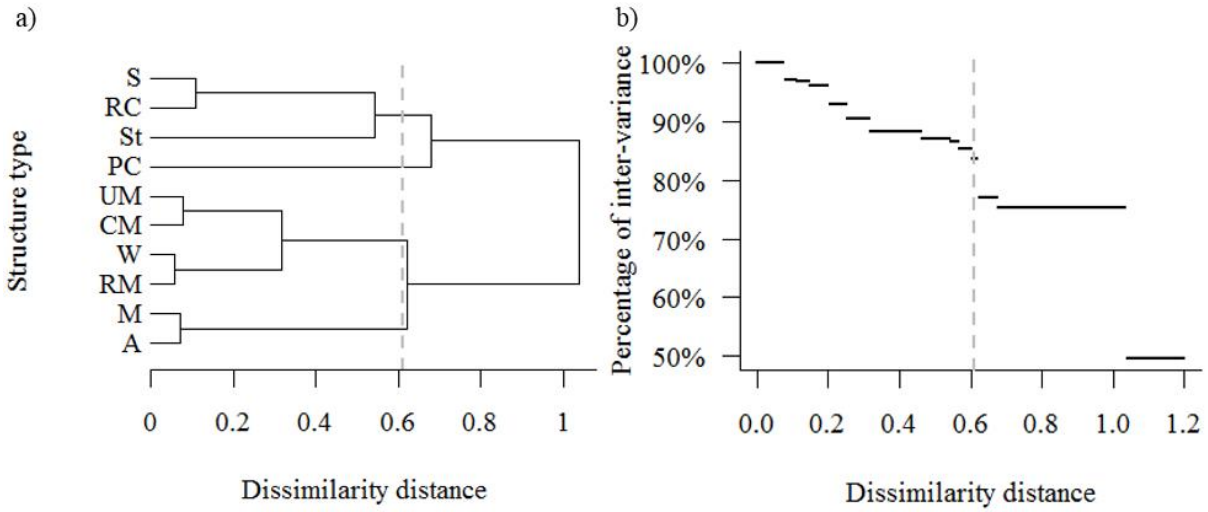


Figure 4.3.8. Classification of the structure type modalities using the Agglomerative Hierarchical Clustering method. The dissimilarity distance used is the Eucledean distance between centroids and applied to the residuals term (*res*) of Equation 4.3.18. Figure a) shows the clustering process according to the dissimilarity distance. Figure b) shows the weight of the inter-variance into the total variance according to the dissimilarity distance. Each drop in the figure b) corresponds to a clustering stage in figure a). Acronyms are : S : steel ; RC : reinforced concrete ; St : stone ; PC : precast-concrete ; UM : unreinforced masonry ; CM : confined masonry ; W : wood ; RM : reinforced masonry ; M : mud and A : adobe.

Masonry (RM) because the dissimilarity distance is the lowest (Fig. 4.3.8a). The second clustering concerns the modalities Unreinforced Masonry (UM) and Confined Masonry (CM). At the end, all the modalities are clustered into only one class, with a dissimilarity around 1 (Fig. 4.3.8a). To determine the dissimilarity distance at which to stops the clustering process, Figure 4.3.8b shows the variation of the percentage of inter-event variance in the total variance with the dissimilarity distance. The lower this percentage, the more information lost by clustering the modalities. We decide to stop the clustering process at a dissimilarity distance equal to 0.61 because it corresponds to the level just before a large drop in the percentage of the inter-event variance (Fig. 4.3.8b). Furthermore, the four groups obtained in Figure 4.3.8a (*GRC* made of Reinforced Concrete, Stone and Steel, *GPC* made only of Precast-Concrete, *GM* made of Unreinforced Masonry, Confined Masonry, Wood and Reinforced Masonry and *GA* made of Adobe and Mud) capture most of the total variance (Fig. 4.3.8b; percentage of inter-event variance equal to 84%).

Finally, the number of modalities decreases from 4,400 to 40 (4 structure type groups, 5 vulnerability classes and 2 land-use types) by replacing the variables country by the GDP per capita and by considering four clusters for the structure type (Fig. 4.3.8). This number of modalities is small enough compared to the number of observations (124) allowing to calibrate a linear model without overfitting (Harrell 2015), as follows.

$$\log_{10}\big(BRC(i)\big) = c_1 + c_2 \log_{10}\big(GDP_{cap}(i)\big) + c_3\delta_{GPC}(i) + c_4\delta_{GRC}(i) + c_5\delta_{GM}(i) + c_6\delta_{Urban}(i) + c_7\delta_{A-B}(i) + c_8\delta_{B-C}(i) + c_9\delta_{C-D}(i) + c_{10}\delta_{D-E}(i) \quad (4.3.19)$$

where $\delta_{GPC}$, $\delta_{GRC}$, $\delta_{GM}$, $\delta_{Urban}$, $\delta_{A\text{-}B}$, $\delta_{B\text{-}C}$, $\delta_{C\text{-}D}$ and $\delta_{D\text{-}E}$ are the Dirac functions (i.e. 1 when the condition is verified, otherwise 0) if the structure type of the building *i* is in the group *GPC*, *GRC*, *GM*, if the building *i* is located in an urban area and if the EMS-98 vulnerability class of the building *i* is A-B, B-C, C-D and D-E, respectively. Explanatory variables in a linear model must be independent. For this reason, there is no Dirac function associated to the modality land use rural, i.e. if $\delta_{Urban}$=1 then $\delta_{Rural}$ =0. Alike, there is no Dirac function for the modalities structure type group *GA* and vulnerability class E-F.

The coefficients $c_1$, $c_2$, $c_3$, $c_4$, $c_5$, $c_6$, $c_7$, $c_8$, $c_9$, and $c_{10}$ are fitted using the QR decomposition method (Stoer and Bulirsch 2002). The results are presented in Table 4.3.4.

Table 4.3.4 shows that variables $c_1$, $c_7$, $c_8$, $c_9$, $c_{10}$ and $c_{11}$ are not meaningful because probability is above 0.05 (represented in the table by a significance factor empty). In this model based on the WHE database, the EMS-98 vulnerability class is not a variable controlling the replacement

Table 4.3.4. Estimate and significance of the explanatory variables in linear model of the decimal logarithm of the building replacement cost (Eq. 4.3.19). Coefficients are determined by the least square method. The Estimate and Standard error columns give the value and the uncertainty of each parameter (Eq. 4.3.19). The lower the probability ℙ(>|t|), the higher the significance.

| Variable | Symbol | Estimate | Standard error | t value | ℙ( >\|t\| ) | Significance |
|---|---|---|---|---|---|---|
| Intercept | $c_1$ | 0.45777 | 0.49301 | 0.929 | 0.355106 | |
| GDP per capita | $c_2$ | 0.86158 | 0.10984 | 7.844 | 2.57E-12 | *** |
| Urban land use | $c_3$ | 0.58131 | 0.15554 | 3.737 | 0.000292 | *** |
| structure type group *GRC* | $c_4$ | 1.55678 | 0.2312 | 6.734 | 7.04E-10 | *** |
| structure type group *GPC* | $c_5$ | 0.73426 | 0.19794 | 3.71 | 0.000322 | *** |
| structure type group *GM* | $c_6$ | 1.86313 | 0.33864 | 5.502 | 2.34E-07 | *** |
| Vulnerability class A-B | $c_7$ | -0.1423 | 0.26412 | -0.539 | 0.591108 | |
| Vulnerability class B-C | $c_8$ | -0.11232 | 0.28146 | -0.399 | 0.690588 | |
| Vulnerability class C-D | $c_9$ | -0.07146 | 0.28758 | -0.248 | 0.80421 | |
| Vulnerability class D-E | $c_{10}$ | 0.16393 | 0.29401 | 0.558 | 0.578234 | |

cost of a building. By applying the same method but after removing these coefficients, we get finally the following equation:

$$\log_{10}\big(BRC(i)\big) = 0.95\log_{10}\big(GDP_{cap}(i)\big) + 2.02\delta_{GPC}(i) + 1.62\delta_{GRC}(i) + 0.78\delta_{GM}(i) + 0.6\delta_{Urban}(i) \quad (4.3.20)$$

From Equation 4.3.20, the building replacement cost modelling error ($\epsilon_2$) is calculated as follows:

$$\epsilon_2 = \Big( 0.95\log_{10}\Big(GDP_{cap}(i)\Big) + 2.02\delta_{GPC}(i) + 1.62\delta_{GRC}(i) + 0.78\delta_{GM}(i) + 0.6\delta_{Urban}(i)\Big) - \log_{10}\big(BRC(i)\big) \quad (4.3.21)$$

Figure 4.3.9 shows the distribution of $\epsilon_2$ and the fit with the Gaussian distribution at mean zero and the variance of $\epsilon_2$, equal to 0.43. It illustrates a good fit which can be corroborated by the Kolmogorov-Smirnov test (Daniel 1990), giving a p-value at 0.96.

The replacement cost for any building *i* being assessed (Eq. 4.3.20), the next section is dedicated to calculate the probability for each building *i* to have been damaged at a state *ds* after a past earthquake.

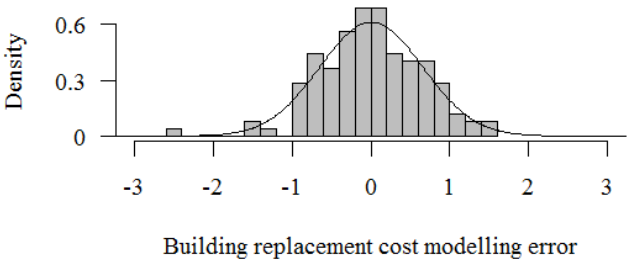


Figure 4.3.9. Empirical distribution of the building replacement cost modelling error ($\epsilon_2$) calculated according to Equation 4.3.21. The solid black line represents the probability density of a Gaussian distribution with a zero mean and the same variance than $\epsilon_2$.

**The probability for a building to be damaged by a past earthquake**

The last variable to assess before using the proposed model (Eq. 4.3.9) for testing damage-cost ratios ($RC_{ds}(i)$) is the ratio of probabilities $\frac{P_{ds}(i)}{\sum_{i=1}^{N} P_{ds}(i)}$. The probability $P_{ds}(i)$ for a building $i$ to be damaged at state $ds$ is calculated. We use again the building damage model released by Lagomarsino and Giovinazzi (2006) and presented in Equation 4.3.12. According to Lagomarsino and Giovinazzi (2006), the mean damage for a single building $i$ (called $\mu_D{}^B$) is given by:

$$\mu_D^B = 2.5 \times \left(1 + \tanh\left(\frac{I + 6.25 \times V - 13.1}{2.3}\right)\right) \quad (4.3.22)$$

where $I$ is the EMS-98 macroseismic intensity and $V$ the seismic vulnerability index. The macroseismic intensity is available in the Earthquake Damage Database but on the MMI scale (ShakeMap footprints; Wald et al. 2005). Therefore, we assume in this study that the macroseismic scales MMI and EMS-98 are equivalent, according to Musson et al. (2009).

The vulnerability index $V$ depends on the EMS-98 vulnerability class (Lagomarsino and Giovinazzi 2006) as illustrated in Figure 4.3.10. It shows that each EMS-98 vulnerability class corresponds to a range of vulnerability index with a confidence level represented by the membership function. The value of the vulnerability index considered in this study, for each EMS-98 vulnerability class is the central value (e.g. for the EMS-98 vulnerability class D, $V$=0.42). Furthermore, in the EMS-98 (Grünthal 1998), main structure types are associated to vulnerability classes (Tab. 4.3.5).

A structure type can be associated to different vulnerability classes with a qualitative probability: “most likely”, “probable” and “less probable” (Tab. 4.3.5). These qualitative probabilities are associated to the weights 1, 0.6 and 0.2, respectively, as proposed by Barbat et

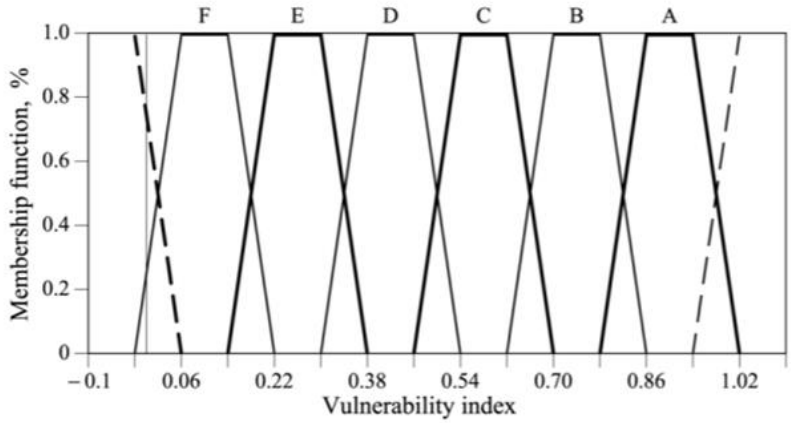


Figure 4.3.10. Membership function between the vulnerability index (Eq. 4.3.22) and the EMS-98 structure type. Source: Lagomarsino and Giovinazzi 2006.

Table 4.3.5: Vulnerability classes by structure type as defined in the EMS-98 macroseismic scale. Source Grünthal 1998.

| Type of Structure | | Vulnerability Class A | B | C | D | E | F |
|---|---|---|---|---|---|---|---|
| MASONRY | rubble stone, fieldstone | ○ | | | | | |
| | adobe (earth brick) | ○ | | | | | |
| | simple stone | | ○ | | | | |
| | massive stone | | | ○ | | | |
| | unreinforced, with manufactured stone units | | ○ | | | | |
| | unreinforced, with RC floors | | | ○ | | | |
| | reinforced or confined | | | | ○ | | |
| REINFORCED CONCRETE (RC) | frame without earthquake-resistant design (ERD) | | | ○ | | | |
| | frame with moderate level of ERD | | | | ○ | | |
| | frame with high level of ERD | | | | | ○ | |
| | walls without ERD | | | ○ | | | |
| | walls with moderate level of ERD | | | | ○ | | |
| | walls with high level of ERD | | | | | ○ | |
| STEEL | steel structures | | | | | ○ | |
| WOOD | timber structures | | | | ○ | | |

○ most likely vulnerability class; — probable range;
····· range of less probable, exceptional cases

al. (2006). Table 4.3.6 shows for each structure type defined in the EMS-98 (Tab. 4.3.5) the corresponding weight and how it is connected to the structure types in the WHE database and used to estimate the replacement cost (Eq. 4.3.20).

Table 4.3.6: Vulnerability classes by structure type as defined in the EMS-98 macroseismic scale and the WHE database with a weight of 1 for "most likely"; 0.6 for "probable" and 0.2 for "less probable". The line *average* corresponds to the average weight calculated by vulnerability class for the EMS-98 structure types associated to the same WHE structure type. Missing values are associated to 0 for the mean calculation. Sources: after WHE (Brzev et al. 2004); Grünthal (1998) and Barbat et al. (2006).

| WHE structure type | EMS-98 structure type | Vulnerability class | | | | | |
|---|---|---|---|---|---|---|---|
| | | A | B | C | D | E | F |
| A and M | adobe (earth brick) | 1 | 0.6 | | | | |
| St | rubble stone; field stone | 1 | | | | | |
| | simple stone | 0.2 | 1 | | | | |
| | massive stone | | 0.6 | 1 | 0.2 | | |
| | *Average* | *0.4* | *0.5* | *0.3* | *0.1* | | |
| UM | unreinforced, with manufactured stone units | 0.2 | 1.0 | 0.2 | | | |
| | unreinforced with RC floors | | 0.6 | 1.0 | 0.2 | | |
| | *Average* | *0.1* | *0.8* | *0.6* | *0.1* | | |
| CM and RM | reinforced or confined | | | 0.2 | 1 | 0.6 | |
| RC and PC | frame without ERD | 0.2 | 0.6 | 1 | 0.2 | | |
| | frame with moderate level of ERD | | 0.2 | 0.6 | 1 | 0.6 | |
| | frame with high level of ERD | | | 0.2 | 0.6 | 1 | 0.6 |
| | walls without ERD | | 0.2 | 1 | 0.6 | | |
| | walls with moderate level of ERD | | | 0.2 | 1 | 0.6 | |
| | walls with high level of ERD | | | | 0.2 | 1 | 0.6 |
| | *Average* | *0.03* | *0.2* | *0.5* | *0.6* | *0.5* | *0.2* |
| S | steel structures | | | 0.2 | 0.6 | 1 | 0.6 |
| W | timber structures | | 0.2 | 0.6 | 1 | 0.6 | |

According to this classification, weights by vulnerability class have been associated to each structure type in the WHE database. When it is associated to several structure types in the EMS-98, the average weight is considered (Tab. 4.3.6; *Average*). These weights are next normalized in order to get a probability distribution.

Finally, the vulnerability index $V$ depends on the structure type of the building $i$. This data can be different from one location to another, as illustrated in Table 4.3.7 with the building typology matrix used in the PAGER program (Jaiswal and Wald 2008).

Table 4.3.7 highlights that the structure type is dependent on the country and the land-use. To take into account this spatial variability in the structure type, the PAGER building typology matrix is used in this study. For that, the not specified structure type are removed and the others are linked to the structure type in the WHE database corresponding the best to the description, as shown in Table 4.3.7.

All the input for the testing model of damage-cost ratios (Eq. 4.3.9) being assessed, an example of application with the 2015 Nepal earthquake (Mw 7.8) is proposed in the next section, before testing several existing damage-cost ratios on the full Earthquake Damage Database.

Table 4.3.7. Extract of the Global Building Inventory implemented in the PAGER program for the residential buildings in China (CHN), India (IND) and Nepal (NPL). The "Str. Code" column gives the structure type from the WHE database associated to each structure description given by the PAGER. Source: after WHE (Brzev et al. 2004);Jaiswal and Wald (2008).

| Land Use | Str. Code | Description | CHN | IND | NPL |
|---|---|---|---|---|---|
| Rural | W | Wood | 10% | 13% | 0% |
| | W | Wood stud-wall frame with plywood/gypsum board sheathing. | 0% | 0% | 20% |
| | RC | Nonductile reinforced concrete frame with masonry infill walls | 3% | 1% | 0% |
| | A | Adobe blocks (unbaked sundried mud block) walls | 40% | 0% | 43% |
| | A | Adobe block, mud mortar, wood roof and floors | 0% | 37% | 0% |
| | St | Rubble stone (field stone) masonry | 3% | 12% | 0% |
| | St | Rectangular cut stone masonry block with cement mortar | 0% | 0% | 11% |
| | UM | Unreinforced fired brick masonry | 10% | 35% | 0% |
| | UM | Unreinforced brick masonry in mud mortar without timber posts | 35% | 0% | 26% |
| | NA | Not specified (unknown/default) | 0% | 2% | 0% |
| Urban | W | Wood | 5% | 4% | 0% |
| | W | Wood stud-wall frame with plywood/gypsum board sheathing. | 0% | 0% | 9% |
| | RC | Ductile reinforced concrete moment frame with or without infill | 12% | 0% | 0% |
| | RC | Reinforced concrete shear walls | 5% | 0% | 0% |
| | RC | Nonductile reinforced concrete frame with masonry infill walls | 5% | 6% | 2% |
| | A | Adobe blocks (unbaked sundried mud block) walls | 4% | 0% | 20% |
| | A | Adobe block, mud mortar, wood roof and floors | 0% | 11% | 0% |
| | St | Rubble stone (field stone) masonry | 2% | 7% | 0% |
| | St | Rectangular cut stone masonry block with cement mortar | 0% | 0% | 55% |
| | UM | Unreinforced fired brick masonry | 61% | 69% | 0% |
| | UM | Unreinforced brick masonry in mud mortar without timber posts | 5% | 0% | 14% |
| | UM | Concrete block unreinforced masonry with lime or cement mortar | 2% | 0% | 0% |
| | NA | Not specified (unknown/default) | 0% | 3% | 0% |

### *4.3.4. Example: the Nepal Mw7.8 earthquake*

In this section, the model for testing existing damage-cost ratios is first illustrated on the 2015 Nepal earthquake (Mw 7.8). The implementation of the model follows the procedure given here.

**Step 1**: For the 2015 Nepal earthquake (Mw 7.8), the dataset in the Earthquake Damage Database from the World Bank provides the following dataset (Tab. 4.3.2): number of buildings damaged: 256,697; number of buildings destroyed: 498,852; total direct economic loss: $3,504m. (USD 2015) and housing sector loss: $2,830m. (USD 2015).

In addition to data related to this earthquake, several socio-economic variables are also necessary to assess the characteristics of damaged buildings: the GDP per capita in 2008 (World Bank database), the buildings taxonomy (Global Inventory Database, Jaiswal and Wald 2008: https://github.com/walshb1/gRIMM/find/UR2018), the country boundaries (CRESTA: www.cresta.org) and the density population at 1km² grid (European Commission, Global Human Settlement database: https://ghsl.jrc.ec.europa.eu).

The land-use on a 1km² grid is also necessary to assess both the structure type (Tab. 4.3.7) and the replacement cost (Eq. 4.3.20) of a building *i*. The Global Human Settlement database (European Commission: https://ghsl.jrc.ec.europa.eu) provides the built-up area normalized density (between 0 and 1) on a 1km² grid. The two grids from the Global Human Settlement database allow calculating the population living in each built-up area normalized density. Furthermore, the number of people by country living in a rural and an urban area is provided by the United Nations (https://population.un.org/wup/Download/). Therefore, we calculate for each country the built-up normalized density threshold $t_{bu}$ in order to have the population living in urban area (from the United Nations) equal to the population living in a built-up area normalized density above the threshold $t_{bu}$. Figure 4.3.11 illustrates how the urban and rural areas are defined for the Nepal.

This threshold allows to define rural and urban areas with a built-up area density lower and higher than $t_{bu}$, respectively (Fig. 4.3.11c).

**Step 2**: We calculate $\mu_D^{\text{overall}}$ which controls the distribution of the number of buildings damaged at each state *ds* is solution of (Eq. 4.3.16) as follows:

$$4 \times \left(\frac{\mu_D^{\text{overall}}}{5}\right)^3 + \left(\frac{\mu_D^{\text{overall}}}{5}\right)^2 \times \left(10 \times \frac{498{,}852}{256{,}697} - 5\right) - \left(\frac{\mu_D^{\text{overall}}}{5}\right) \times \left(20 \times \frac{498{,}852}{256{,}697}\right) + 10 \times \frac{498{,}852}{256{,}697} = 0 \quad (4.3.23)$$

The three roots for this equation are: $\mu_D$ = -27.6; $\mu_D$ = 3.79 and $\mu_D$ = 5.79. As only the first one lies between 0 and 5, we get that $\mu_D^{\text{overall}}$ = 3.79. Next, the number of buildings in the affected area (*N*) can be calculated (Eq. 4.3.14) as:

$$N = \frac{256{,}697}{\binom{5}{2} \times \left(\frac{3.79}{5}\right)^2 \times \left(1 - \frac{3.79}{5}\right)^3 + \binom{5}{3} \times \left(\frac{3.79}{5}\right)^3 \times \left(1 - \frac{3.79}{5}\right)^2} = 766{,}022 \quad (4.3.24)$$

Knowing *N*, the number of buildings damaged at each damage state can be calculated (Eq. 4.3.12) as:

$$N_{1 \le ds \le 5} = 766{,}022 \times \binom{5}{ds} \times \left(\frac{3.79}{5}\right)^{ds} \times \left(1 - \frac{3.79}{5}\right)^{5-ds} \quad (4.3.25)$$

The results are: $N_1$ = 9,847; $N_2$ = 61,933; $N_3$ = 194,764; $N_4$ = 306,242 and $N_5$ = 192,610. These results are consistent with data in the Earthquake Damage Database: $N_{2+3}$ = 256,697 and $N_{4+5}$ = 498,852.

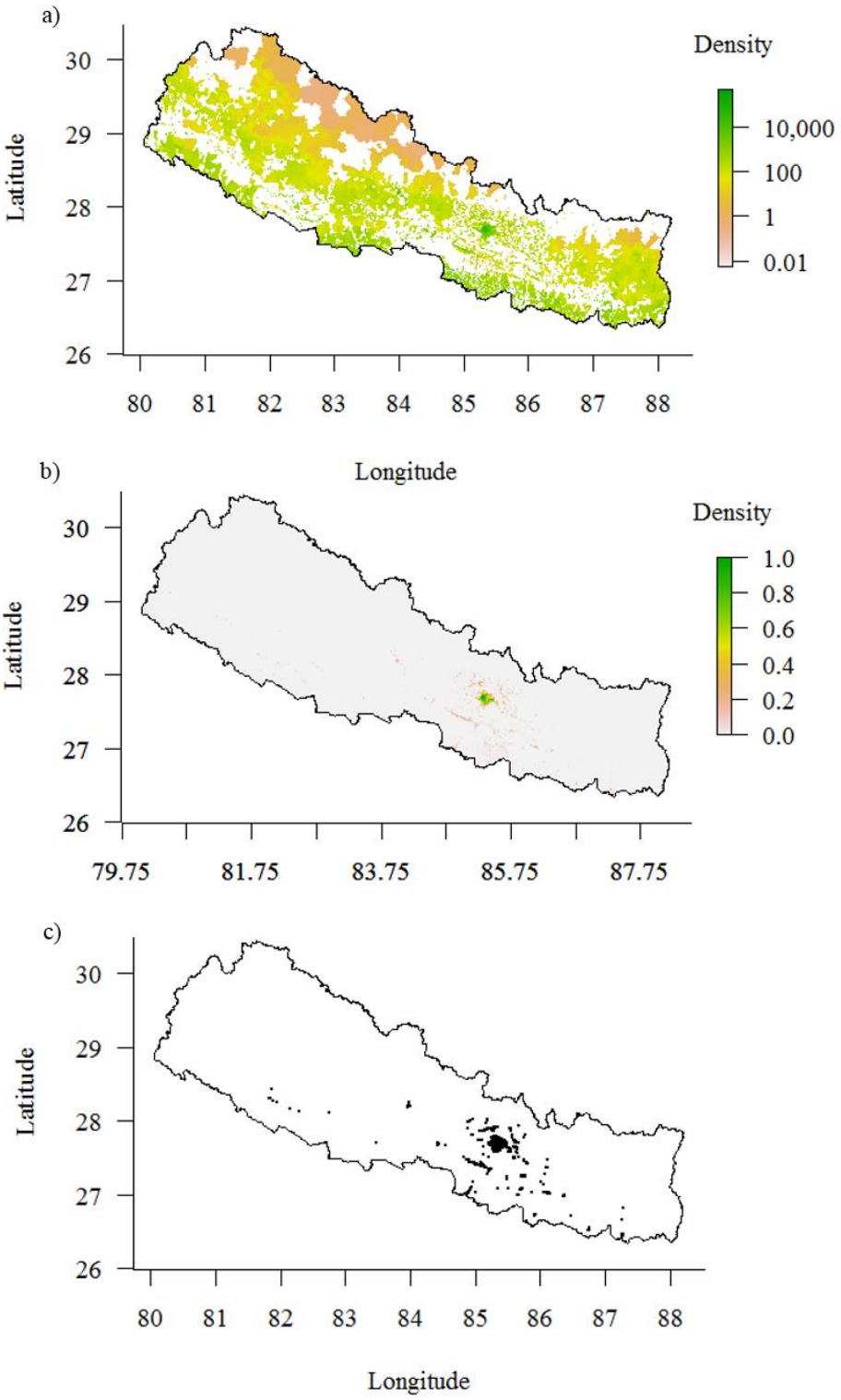


Figure 4.3.11. Illustration of: a) the 2014 population density according the Global Human Settlement; b) the 2015 built-up normalized density according to the Global Human Settlement and c) land-use as defined in this study for the Nepal. In figure c), urban and rural areas are represented in black and white, respectively. The United Nations reports that in 2014, 18.2% of the population lives in an urban area. The threshold ($t_{bu}$) of built-up normalized density to define urban and rural areas has been calculated at $t_{bu}$ = 0.13 (b), in order to get 18.2% of the density population (a) in urban areas (c). Sources: after European Commission (Global Human Settlement database; https://ghsl.jrc.ec.europa.eu); United Nations (https://population.un.org/wup/Download/) and CRESTA (www.cresta.org).

**Step 3**: According to Equation 4.3.10, a total direct economic loss $L_D$ = \$3,504m for Nepal earthquake corresponds in average to a housing sector loss $L_H$ equal to $L_H = 0.3395 \times L_D$ = \$1,190m. Despite the Earthquake Damage Database contains a different value (\$2,830m.), the estimate calculated from Equation 4.3.10 (here, $L_D$ = \$1,190m.) is always used for having the same procedure for all the past earthquakes in the Earthquake Damage Database (only 21 datasets out of 356 have a data for the housing sector loss). As the buildings loss is supposed equal to the housing sector loss, we get: $L_B$ = \$1,190m.

**Step 4**: The characteristics of buildings in the affected area are estimated. The affected area is defined as extent of the ShakeMap footprint. Using the density of population and the land-use, the density of buildings on a 1km² grid can be calculated (Eq. 4.3.17). For example, at grid point (85.32°, 27.71°; coordinates of Kathmandu), the land-use is urban, and the density of population is equal to 40,452. This gives a density of buildings equal to 40,452/26.5 = 1,526 (Eq. 4.3.17).

Next, the Global Building Inventory (Jaiswal and Wald 2008) indicates that 2%×1,526=31 are in reinforced concrete; 9%×1,526=137 are in wood; 14%×1,526=214 are in unreinforced masonry; 20%×1,526=305 are in adobe and 55%×1,526=839 are in stone (Tab. 4.3.7). The EMS-98 vulnerability class is then inferred from the structure type (Tab. 4.3.6). The distribution of vulnerability class is given in Table 4.3.8.

Table 4.3.8: Estimation of the number of buildings at the grid point (85.32°, 27.71°; coordinates of Kathmandu) according to the structure type taxonomy used in this study and the EMS-98 vulnerability class.

| Structure type | EMS-98 vulnerability class | | | | | |
|---|---|---|---|---|---|---|
| | A | B | C | D | E | F |
| W | | 11 | 34 | 57 | 34 | |
| RC | | 3 | 8 | 9 | 8 | 3 |
| A | 191 | 114 | | | | |
| St | 258 | 323 | 194 | 65 | | |
| UM | 13 | 107 | 80 | 13 | | |

Table 4.3.8 shows that most of buildings in the centre of Kathmandu (grid point: 85.32°, 27.71°) are made of stone and have an EMS-98 vulnerability class B (corresponding to $V$ = 0.74).

**Step 5**: The probability $P_{ds}$(i) for each building $i$ to be damaged is calculated according to Equations 4.3.12 and 4.3.22 at each grid point, according to the macroseismic intensity from the ShakeMap footprint in the Earthquake Damage Database and the vulnerability index

assessed at Step 4. Figure 4.3.12 illustrates the hazard footprint and the probabilities ($P_1(i)$ and $P_5(i)$) for a building $i$ with a vulnerability index equal to 0.74 (corresponding to an EMS-98 vulnerability class B) to be in damage state $ds$=1 and $ds$=5.

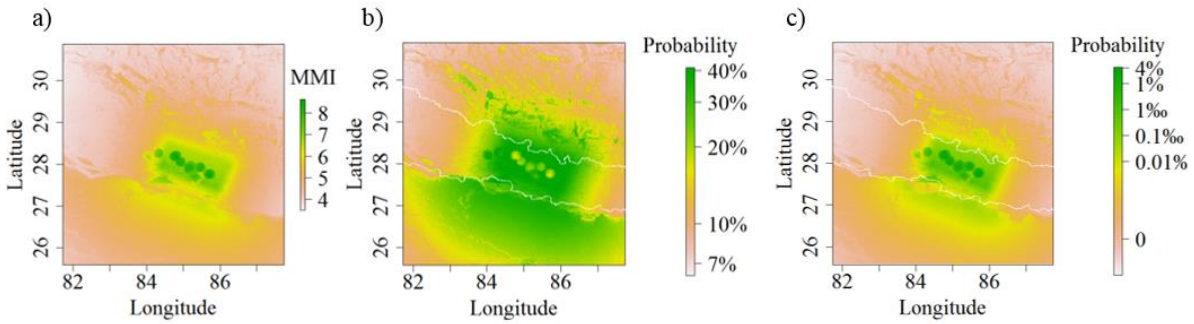


Figure 4.3.12: Footprints of: a) the hazard (ShakeMap); b) the probability for a building in the EMS-98 vulnerability class B to be damaged at grade $ds$=1 and c) the probability for a building in the EMS-98 vulnerability class B to be damaged at grade $ds$=5.

Figure 4.3.12 shows that while the probability for a building in the EMS-98 class B to be damage at state $ds$=1 ($P_1(i)$) is high over a large area (Fig. 4.3.12b), for the damage state $ds$=5 ($P_5(i)$), it is localized in the epicentre area (Fig. 4.3.12a, c). Furthermore, where the probability $P_5(i)$ is the highest (Fig. 4.3.12b circles in the epicentre area), the probability $P_1(i)$ shows a significant decrease because the macroseismic intensity (Fig. 4.3.12a) is too high for do not observing severe damage for this building's vulnerability class.

**Step 6**: The last step is about calculating the replacement cost $BRC(i)$ for each building $i$. Equation 4.3.20 can be used with the characteristics of the buildings as determined in Step 4 and the groups of structure types defined in Figure 4.3.8. For example, the replacement cost for a building $i$ made in stone (i.e. in the structure type group *GM*) in Kathmandu (land use urban) is:

$$\log_{10}\big(BRC(i)\big) = 0.95\log_{10}(\$477) + 2.02 \times 0 + 1.62 \times 0 + 0.78 \times 1 + 0.6 \times 1 \qquad (4.3.26)$$

$$BRC(i) = 10^{3.924} = \$8{,}398 \text{ (USD 2008)}$$

### *4.3.5. Testing some existing damage-cost relationships*

The same process is applied to each dataset in the Earthquake Damage Database to test existing

damage-cost ratios. Most of the recent damage-cost ratio rely on the HAZUS-99 (Federal Emergency Management Agency 1999) or EMS-98 (Grünthal et al. 1998) damage scales and are listed in Table 4.3.9.

Table 4.3.9. Literature review of damage-cost relationships. Authors and Source refer to the scientists who developed the relationship and who wrote the paper from which the values are extracted, respectively. The cost ratios indicated correspond to the central values. When a damage-cost relationship uses the HAZUS-99 damage scale, damage grade is converted into EMS-98 damage grade according to the method proposed by Milutinovic and Trendafiloski (2003), Lagomarsino and Giovinazzi (2006) and Hill and Rossetto (2008b). Acronym: FEMA: Federal Emergency Management Agency.

| Authors | Source (when differs from the authors) | Studied area | EMS-98 Damage Grade | | | | |
|---|---|---|---|---|---|---|---|
| | | | D1 | D2 | D3 | D4 | D5 |
| Meroni et al. (2017) | | Italy | 5% | 20% | 45% | 100% | 100% |
| Riedel (2015) | | France | 3% | 14% | 34% | 65% | 90% |
| Fang et al. (2011) | Wei et al. (2016) | China | 15% | 40% | 70% | 100% | 100% |
| Eleftheriadou and Karabinis (2008) | | Greece | 0.5% | 15% | 65% | 100% | 100% |
| Bal et al. (2008) | | Turkey | 16% | 33% | 100% | 100% | 100% |
| Roca et al. (2006) | Hill and Rossetto (2008a) | Spain | 1% | 20% | 40% | 80% | 100% |
| Kappos et al. (2006) | | Greece | 1% | 9% | 29% | 63% | 77% |
| Di Pasquale et al. (2005) | Hill and Rossetto (2008a) | Italy | 1% | 10% | 35% | 75% | 100% |
| Tyagunov et al. (2004) | | Germany | 0.5% | 10% | 40% | 80% | 100% |
| Milutinovic and Trendafiloski (2003) | | Europe | 3% | 15% | 50% | 100% | 100% |
| FEMA (2010) | | USA | 2% | 10% | 41% | 100% | 100% |
| Blong (2003) | Hill and Rossetto (2008a) | Australia | 2% | 10% | 40% | 75% | 100% |
| Timchenko (2002) | Hill and Rossetto (2008a) | Georgia | 2% | 10% | 30% | 80% | 100% |
| Di Pasquale et al. (2001) | Riedel (2015) | Italy | 4% | 22% | 41% | 78% | 81% |

The HAZUS-99 damage scale is made of 4 grades (Slight, Moderate, Extensive and Complete). The conversion table proposed by Milutinovic and Trendafiloski (2003), Lagomarsino and Giovinazzi (2006) or Hill and Rossetto (2008b) between the two damage scales consists in associating the grades Negligible, Moderate, Substantial in the EMS-98 (Tab. 4.3.3) to the grades Slight, Moderate and Extensive in the HAZUS-99. The grade Complete in the HAZUS-99 is associated to the grade Very heavy and Destruction in the EMS-98 scale (Tab. 4.3.3). This conversion is used in Table 4.3.9 for the relationships provided by Fang et al. (2011), Eleftheriadou and Karabinis (2008), Bal et al. (2008), Milutinovic and Trendafiloski (2003) and the Federal Emergency Management Agency (2003).

Some relationships give an interval of ratios instead of a single value (e.g. Milutinovic and Trendafiloski 2003). In such a case, the central values are considered in Table 4.3.9. Moreover, when a relationship depends on building characteristics, values are aggregated as proposed by the corresponding source. Finally, ratios proposed by Bal et al. (2008) for damage grades D3, D4 and D5 are above 100% because they include additional costs like the debris removal. When they are removed, the cost ratios proposed by Bal et al. (2008) for the damage grades D3, D4, and D5 are 100%.

Although the damage-cost relationships in the literature have been calibrated over a specific area, they are assumed in this study to be consistent for any country. This strong assumption is often used because of the lack of relationships where earthquake economic losses are limited, i.e. in low seismicity or developing countries (Riedel and Guéguen 2018).

For each damage-cost relationship (Tab. 4.3.9), the buildings loss $L_B$ is calculated for each of the 356 datasets in the Earthquake Damage Database. The log difference ($\epsilon_3$) with the estimated housing sector loss (Eq. 4.3.9) is:

$$\epsilon_3 = Log_{10}\left(\sum_{ds=1}^{5}\left[\sum_{i=1}^{N} BRC(i) \times RC_{ds}(i) \times N_{ds} \times \left(\frac{P_{ds}(i)}{\sum_{i=1}^{N} P_{ds}(i)}\right)\right]\right) - Log_{10}(L_H) \qquad (4.3.27)$$

Under the assumption made in this study that the buildings loss is equal to the housing sector loss, $\epsilon_3$, called the modelling error, represents the performance of a damage-cost relationship to reproduce the buildings loss of historical earthquakes. Figure 4.3.13 represents the mean against the standard deviation of the modelling error $\epsilon_3$, calculated for the 356 past earthquakes in the Earthquake Damage Database (Tab. 4.3.9).

Figure 4.3.13 shows a positive trend between the mean and the standard deviation, i.e. the larger the modelled buildings loss (Eq. 4.3.27), the more dispersed is the modelling error. Furthermore, the modelling error $\epsilon_3$ has a similar mean and a standard deviation for most of the relationships (between -0.15 and 0.05 for the mean and 0.795 and 0.82 for the standard deviation). Three relationships show a different distribution of $\epsilon_3$: Kappos et al. (2006), Fang et al. (2011) and Bal et al. (2008). This result is consistent with the ratios indicated in Table 4.3.9: for Kappos et al. (2006) they are below 77% while for Fang et al. (2011) and Bal et al. (2008) they are always above or equal to 15%.

When the mean of $\epsilon_3$ is not equal to zero, it means that the damage-cost relationship is biased. For instance, a mean at -0.1 corresponds to an average underestimate of buildings loss by a factor of -20% (Eq. 4.3.27). Nevertheless, it is difficult to draw any conclusion on the tested

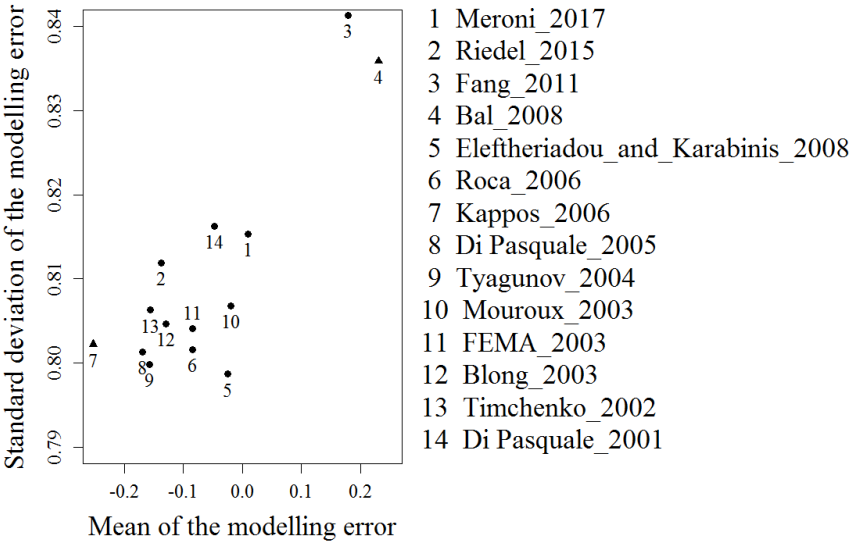


Figure 4.3.13. Mean and standard deviation of the modelling error $\epsilon 3$ (Eq. 4.3.27) for several damage-cost relationships. Dots and triangles correspond to a mean of the modelling error not significantly (i.e. p-value above 0.05) and significantly (i.e. p-value below 0.05) different from zero, respectively, according to the Student's t test when all the uncertainties in the test are considered (Eq. 4.3.28).

relationships from Figure 4.3.13 because several variables have been estimated for implementing the model and can have a significant impact on the modelling error $\epsilon_3$. The two main source of approximation are represented by the housing loss modelling error ($\epsilon_1$) and the building replacement cost modelling error ($\epsilon_2$). They can be considered to calculate $\epsilon_4$ as follows:

$$\epsilon_4 = Log_{10}\left(\sum_{ds=1}^{5}\left[\sum_{i=1}^{N} BRC(i) \times RC_{ds}(i) \times N_{ds} \times \left(\frac{P_{ds}(i)}{\sum_{i=1}^{N} P_{ds}(i)}\right)\right]\right) - Log_{10}(L_H) - (\epsilon_1 + \epsilon_2) \quad (4.3.28)$$

Assuming that $\epsilon_1$ and $\epsilon_2$ follow a Gaussian distribution (Fig. 4.3.6 and 4.3.9), the Student's *t*-test (Hazewinkel 1988) can be performed to test if the mean of the distribution of $\epsilon_4$ (Eq. 4.3.28), is significantly different to zero. The test indicates that the modelling error is significantly different from zero only for the relationships provided by Fang et al. 2011 and Bal et al. 2008 (Fig. 4.3.13). It means that, knowing the number ($N_{ds}$) of buildings damaged at each damage grade (*ds*) and the building replacement cost (*BRC*(*i*)), the relationships proposed by Fang et al. 2011 and Bal et al. 2008 underestimates and overestimate the building loss, on average (Eq. 4.3.28; Fig. 4.3.13). Consequently, this test shows that these relationships are not suitable for risk assessment studies at the scale of the affected area by an earthquake.

### *4.3.6. Conclusions*

Estimating the loss subsequent to an earthquake, either a fictive scenario or a historical event, is a work subject to a lot of uncertainties. Several studies have been released, relying on different loss models. In most of current loss models like HAZUS (Federal Emergency Management Agency 2010), RISK-UE (Milutinovic and Trendafiloski 2003) or PAGER (Jaiswal and Wald 2011), the loss is calculated upon the damage grade for a representative set of buildings. This framework requires to use damage-cost ratios, which have been already proposed in several studies with very different replacement cost ratios. Consequently, improving them requires first to better understand why they differ one from another.

In this perspective, this work is a first step to develop a framework to test existing damage-cost relationships. It relies on both socio-economic variables and observations from past earthquakes, aggregated in a database called the Earthquake Damage Database. From the number of damaged and destroyed buildings, it models the number of buildings damaged at each damage grade at each location. Furthermore, a building replacement cost has also been developed to calculate the building loss considering a damage-cost relationship and to compare it with the total direct economic loss.

The lack of economic data and the uncertainty around the consequences of past earthquakes lead us to make assumptions which have a direct impact on the accuracy of the testing method. Nevertheless, it allows already to identify that the relationships released by Fang et al. (2011) and Bal et al. (2008) are biased. Therefore, one can expect inaccurate loss estimates when they are used at the scale of the whole affected area. For the other relationships tested, the large uncertainty does not allow to conclude on the accuracy. Thus, further developments on frameworks to test damage-cost relationships would be necessary to better identify the strengths and weaknesses of each of them.

## 4.4. Summary

The increase number of equations and probabilistic models on seismic hazard assessment and loss modelling needs to be compared to identify their strengths and weaknesses and finally figure out the best way to combine them and how to improve them with further scientific

studies. Nevertheless, it would be wrong to summarize earthquake insurance market limits to the lack of risk knowledge. For this reason, a new insurance model meeting the needs of clients and fostering prevention measures is introduced in the next chapter.

# CHAPTER 5: A NEW INSURANCE MODEL

## 5.1. Abstract

For several seismic-prone countries, current earthquake insurance solutions cover only a small part of the economic loss. Innovative insurance products like parametric insurance are emerging for which the compensation is calculated upon a trigger instead of a claim amount, covering more people but with drawbacks due to probable difference between the insurance compensation and the actual loss. In this paper, new insurance model is proposed, covering earthquake risk for residential houses. Its main characteristics are: (1) the compensation is to rebuild the insured house, instead of paying a financial amount; (2) the model leverages both on long-term financial investment and seismic retrofitting of the insured buildings to make the premium amount affordable; and (3) joint participation of the public authorities and the homebuilder companies in this insurance model are expected since the first ones are the key player in risk prevention plans and the second ones are the beneficiary of this new market (incentivizing repairs/reconstruction and retrofitting works). In this chapter, the model is tested with several case studies in California, where only 15% of homeowners are currently covered against the earthquake risk. Results show that in most cases the price (i.e. premium amount and retrofitting costs) for this earthquake insurance model is lower than the premium amount considering the traditional earthquake insurance. For the optimal deductible amount, the decrease can even be three times lower than for classical model, by assuming a contribution from both the public authorities and the homebuilder companies. Such a decrease could raise the rate of California homeowners insured against earthquake risk from 15% up to 50%.

## 5.2. Introduction

In 2016, Joaquim Levy, Chief Finance Officer at World Bank, alerted on the need to reduce the gap between the total economic loss and the total insured loss caused by natural disasters (Thevenin et al. 2018). This metric, called the "nat-cat" protection gap, is usually calculated as the ratio between the total insured losses and the total economic losses. Actually, natural disasters are more and more devastating in terms of economic impact and the share of uninsured loss remains very large. For example, considering the three most devastating natural disasters (i.e., flood, windstorm and earthquake), the "nat-cat" protection gap since 2000 mostly concerns the earthquake risk, which has also the lowest evolution between 2000 and 2016 (OECD, 2018). At the opposite of the windstorm hazard is the most covered by the insurance sector (OECD, 2018). One reason is that windstorm insurance can be compulsory (e.g. in Florida) or required for mortgage (e.g. in Texas), while earthquake insurance is paradoxically optional in many seismic prone areas such as California, Japan or Italy.

This observation is corroborated by Holzheu and Turner (2018) who modelled the average annual loss insured and uninsured for several countries and natural disasters. Their results showed that most of the uninsured loss after a natural disaster is due to earthquake hazard, concerning developing countries but also developed countries (Thevenin 2017; OECD, 2018). These two results conclude that countries with large uninsured earthquake modelled losses correspond to those with a low number of households covered against earthquakes. Interestingly, earthquake protection gap cannot be explained only by the country wealth, neither by the hazard level itself. For example, more than 90% of households in Iceland and New-Zealand are insured while both countries are prone to earthquake hazard. At the opposite, in France a moderate seismic prone country, more than 90% of people are covered against earthquake hazard because this insurance is mandatory, and the premium amount is low: only 12% of the housing insurance premium amount (i.e. around €40) for covering several natural disasters including earthquake, flood and subsidence. In California, the model developed in the Chapter 3, Section 2, showed the direct link between the low rate of homeowners covered against earthquake risk and the high insurance premium amount. According to the model developed in the Chapter 3, Section 2, the premium amount should be divided by three for encouraging most of California homeowners to buy earthquake insurance. Currently, it costs on average as much as traditional housing insurance (California Department of Insurance

database), i.e. the premium amount is twice when earthquake insurance cover is integrated to the traditional housing coverage.

To reduce the earthquake protection gap, insurance companies have launched a new insurance cover called the parametric insurance. It stands out from traditional insurance policy by a lower premium amount and a fixed claims amount triggered upon a physical index (e.g. earthquake magnitude measured at a given location). Despite the rising interest in parametric insurance, penetration rates remain low as this model suffers from a potential post-disaster gap between the insurance compensation and the real loss amount for the policyholder (Clyde & Co LLP 2018), i.e. contributing to the earthquake protection gap. Aside parametric insurance, other solutions are also investigated, with the same objective (Thevenin et al. 2018), in close collaboration with the public authorities and the other private stakeholders. For instance, the California Earthquake Authority (CEA), a non-profit organization, gathering several insurance companies in California and the largest earthquake insurance provider, has recently launched in partnership with the California Governor's Office of Emergency Services the Earthquake Brace & Bolt initiative (www.earthquakebracebolt.com). It provides a grant to retrofit most vulnerable houses, insured by the CEA, in the highly earthquake prone areas. Moreover, homeowners benefit from a premium discount for their CEA earthquake insurance policy since the retrofitted house is more resistant. This initiative is consistent with the development of the earthquake insurance sector, as identified in the maturity scale for the earthquake insurance market (in Chapter 3, Section 4). This maturity scale provides an overall framework to develop the earthquake insurance market in any country. It highlights that, aside prevention efforts, insurance solutions can be improved by anticipating earthquake risk and being more affordable by smoothing premium amount over a long period.

In this paper, a new kind of earthquake insurance is introduced, called “long-term property insurance”. While current earthquake insurance policies have a short expiry date (most often 1 year and usually below 3 years), the policy proposed herein, inspired by life insurance products, stops only after paying the claim caused by the first damaging earthquake. As damaging earthquakes are seldom, the duration of the insurance policy studied is, on average, very long, typically spanning over decades. This long-term property insurance is also innovative by involving homebuilder companies, as they are the main economic player in charge of repairing or reconstructing damaged houses after earthquakes. Finally, this model organizes and provides funds for earthquake retrofitting works as part of the insurance policy. Since earthquake retrofitting works decrease the building vulnerability (and consequently the expected loss after

an earthquake), part of collected premium amount can indeed be dedicated to finance such works.

The first section introduces some key insurance notions, later used in this study to describe this proposed earthquake insurance model. Next, the choice to build it according to life insurance principles instead of property insurance scheme is motivated. In the third part, a probabilistic loss model combining the UCERF3 (Field et al. 2013) and the HAZUS-MH MR5 (Federal Emergency Management Agency 2010) models for California is introduced to then produce premium amount estimates. The fourth section is about the benefit of earthquake retrofitting works for the insurance scheme. Finally, the contribution of homebuilder companies and public authorities to this insurance scheme is investigated.

## 5.3. Example of the CEA insurance model

Most of insurance companies covering earthquake risk cannot alone withstand an extreme loss caused either by a very damaging earthquake or a short sequence of severe earthquakes. Consequently, they buy a reinsurance cover, i.e. they transfer part of the risk they hold to other insurance market players, called reinsurance companies, in exchange for a premium. Thus, in case of an extreme loss, the insurance company will be reimbursed of part of the claims by the reinsurance company. As an example, the CEA (already introduced in Chapter 2, Section 2.2) uses the reinsurance scheme presented in Figure 5.1.

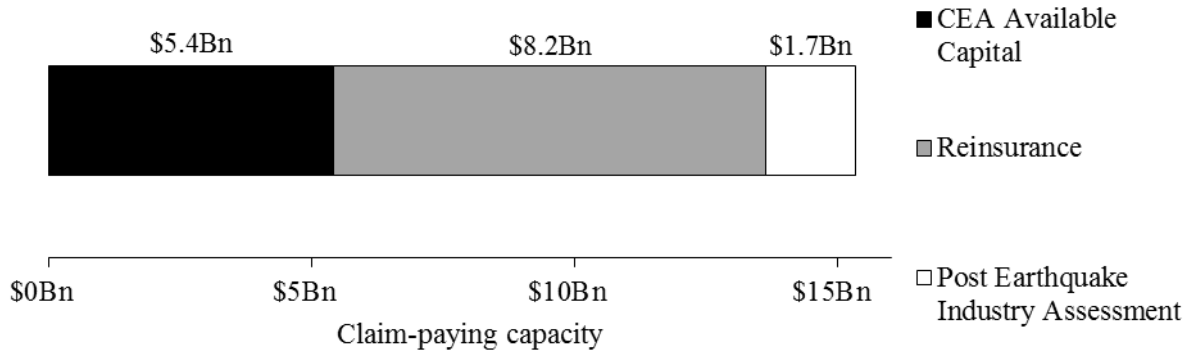


Figure 5.1: Breakdown of the claim-paying capacity of the California Earthquake Authority (CEA) as of September 30th, 2017. Source: after California Earthquake Authority (2017c).

Figure 5.1 shows that if an earthquake causes more than \$5.4bn loss for the CEA, the company will be refunded by reinsurance companies up to \$8.2bn in excess of losses above \$5.4bn. In the case of an earthquake more devastating than the 1906 San Francisco earthquake, the loss for the CEA could exceed \$13.6bn (California Earthquake Authority 2018a), leading the insurance companies member of the CEA to participate to the claims up to \$1.7bn in excess of losses above \$13.6bn (under the layer "Post Earthquake Industry Assessment"). Thus, the Post Earthquake Industry Assessment is similar to a reinsurance cover but provided by the insurance company members of the CEA themselves and free of charge for the CEA (Marshall 2018). The CEA claim-paying capacity (equal to \$15.3bn) corresponds to the maximum amount that the CEA can pay for claims after an earthquake, whatever the loss amount covered by the CEA insurance policies. According to the California Earthquake Authority (2018a) model, it corresponds to a 400y return period event. The loss amount in excess of \$15.3bn will be uninsured and kept by the policyholders, and therefore will contribute also to the earthquake protection gap.

For this reinsurance cover, the CEA pays an annual premium ($P_2^M$) which represents an important share of the annual premium amount collected from the insured ( $P^M$), as illustrated in Figure 5.2.

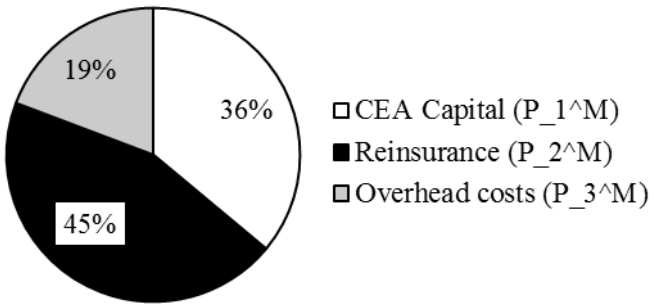


Figure 5.2: Allocation of California Earthquake Authority (CEA) premium amount as of December 31th, 2017. Source: after California Earthquake Authority (2018e).

Aside the cost of the reinsurance cover, $P^M$ includes also a premium amount, called $P_1^M$, for the risk transferred from the policyholder to the insurance company and hold by the insurance company. Last, $P_3^M$ is dedicated to pay the insurance company's overhead costs (e.g. commissions, fees…). $P_1^M$ and $P_2^M$ correspond to the technical or pure premium in the actuarial literature, which is allocated to the claim-paying capacity: while $P_1^M$ contributes to the CEA available capital, $P_2^M$ is used to pay the reinsurance (Fig. 5.1). The Post-Earthquake Industry

Assessment is not associated to a premium amount since it is free of charge for the CEA (Marshall 2018). The premium $P_2^M$ is the largest contribution to $P^M$ (Fig. 5.2) and reflects the \$8.2bn reinsurance cover out of the \$15.3bn claim-paying capacity (Fig. 5.1).

The premium amount dedicated to the risk held by the insurance company ($P_1^M$) is usually calculated based on the average annual loss using comprehensive probabilistic models derived from physical properties of seismic waves and buildings. Indeed, an insurance company needs to collect enough money for paying all the claims, on average. When the risk is transferred to a reinsurance company the latter also requires collecting a premium amount ($P_2^M$) made of the annual average transferred loss in addition to an administrative loading to cover its own expenses.

The insurance company's overhead costs are highly dependent on the business profile. According to the line of business (commercial, residential, industrial…), the insurance company size, the distribution channels used, or the client's profile (single or multi policies holders, the total sum insured…), $P_3^M$ can change drastically. However, the only data available on insurance company's overhead costs for residential earthquake line of business in California is the premium share of 19% (Fig. 5.2). In this study, we assume the insurance company's overhead costs is always equal to 19% of the total premium amount $P^M$, whatever the risk profile.

The difference between the premium amount hold by an insurance company to cover the risk ($P_1^M$) and the total claims amount during the year makes the annual insurance company's technical profit. Since the CEA is a non-profit organisation, no dividends are paid and all the profit is dedicated either to increase the CEA's claim paying-capacity, decrease the reinsurance cover need or drop the premium amount for the following year. This kind of insurance company is not unusual, especially in France, under the label of "*sociétés mutuelles d'assurances*". This herein study refers to this model of insurance company in order to disregard any investors' profitability and risk appetites.

The premium shares corresponding to the reinsurance ($P_2^M$) and the CEA overhead costs ($P_3^M$) are spent each year and therefore, cannot be invested on financial markets. Therefore, only the share of the premium not used to pay claims and retained as capital (Fig. 5.2: $P_1^M = 36\%P^M$) is available for investing on financial markets. However, since the funds are dedicated to pay future insurance claims, they must be very immediately available and only invested in very secure and liquid financial products. For a given currency, one of the most secure financial products to invest in is the long-term treasury bonds of high-rated countries (Mukherji 2011).

For the United States, Figure 5.3 illustrates the evolution of the annual return of the long-term US treasury bonds issued since 2000 by the US Federal Reserve System.


Figure 5.3: Evolution of the US Treasury Real Long-Term rate between 2000 and 2019. The dotted line represents the value 1.3%, corresponding to the rate of return on investments made by CEA in 2017. Source: after U.S. Department of the Treasury (www.treasury.gov/resource-center/data-chart-center/interest-rates/Pages/default.aspx); California Earthquake Authority 2017c.

As illustrated in Figure 5.3, this rate is low (with even negative interest rates during a short period of time) because the risk of insolvency is remote or mitigated by public policies (e.g. the quantitative easing policy launched by the FED to address the 2008-2009 financial crisis). Other investments such as company stocks or debt instruments are more profitable but also more at risk, since most companies are more likely to go bankrupt than the United States. In 2017 the CEA's financial statements (California Earthquake Authority 2017b) reported that 98% of the investments were made in US Treasury bonds and the 2% remaining in company stocks. The resulting rate of return on investment, called $t_I$, reached 1.3%. As illustrated in Figure 5.3, it represents the upper bond of the variation of the US treasury long-term bonds since 2014.

Several insurance policies, including the CEA's earthquake insurance policies, mention that part of the risk is hold by the insured. Insurance terminology calls this risk share the 'deductible amount' and called *F* in our study. The first reason for introducing deductible amount is to align interests between the insurance company and the insured, more precisely to avoid moral hazard: insured people do not want to experience any loss because they would have to pay part of it. Therefore, they are interested in having the best earthquake-resistant house. Moreover, the higher the deductible amount, the less the annual premium amount $P^M$, because a lower risk is retained by the insurance company. In the case of the CEA's insurance policies, deductible amount corresponds to the minimum loss amount to incur after a single earthquake for

benefiting from compensation. When an earthquake causes a loss higher than the deductible amount, the CEA's compensation corresponds only to the loss above the deductible amount (i.e. the deductible amount is always at the charge of the CEA's policyholders). CEA's policyholders can choose a deductible amount ranging from 5% to 25% of the total exposure amount (i.e. the declared value of the insured good). Similarly, the deductible amount considered in this study is always at the charge of the policyholder and is labelled as a percentage of the house price.

## 5.4. A life insurance mechanism to increase affordability

Two main insurance mechanisms exist: the allocation and the mutualisation systems (Haddad 2017). For the allocation system, the share of the annual premium collected and not spent during the year for the overhead costs or the reinsurance cover is allocated to a special fund called the mathematical provisions. This fund is then invested in financial products and the resulting profits are allocated back to each insurance policy. The total amount made of the premium amount and the subsequent profits are used to pay the claim after the first loss. Once it has occurred, the insurance policy is cancelled, meaning that no more premium is paid and there is no longer insurance cover. Currently, this mechanism is mostly used for life or retirement insurances, which are characterized by a long period without a claim, until the dead/retirement of the insured people. The occurrence of the claims is certain: the uncertainty is not *if* the claim will occur but *when* the claim will occur.

At the opposite, for a mutualisation system, the total premium amount collected during a year from all policyholders is used to pay all the claims occurred during the same period. The pure premium is then calculated as the expected loss multiplied by the annual frequency of the risk, under the so-called "collective risk model" (Kaas et al. 2008). Contrary to the allocation insurance mechanism, the financial profits are dedicated to the insurance's capital and therefore, are not considered in the pricing. Furthermore, insurance policies are not automatically cancelled after a claim and, for some risk profiles called attritional (e.g. car or health insurance), a policyholder is covered for potential multiple claims occurring during the same exposed period. The mutualisation mechanism is mostly used in property insurance where the number of claims by year is large (e.g. car insurance or fire insurance) and the total premium amount is calibrated upon the statistical mean of claims amount. The high and predictable frequency of

claims and the size of the portfolio of insured with homogeneous risk factors validate the use of the Law of Large Number and the Central Limit Theorem (Tijms 2003), enabling reasonable pricing and reserving assumptions.

Current earthquake insurance policies are built upon the mutualisation mechanism. However, potentially damaging earthquakes are seldom, even in the most exposed areas. For instance, a large earthquake (M6.7+) in California has a return period of 6 years, according to the UCERF3 model (Field et al. 2013). At the scale of a California homeowner, the average annual probability to be affected by such an earthquake is only at 0.038% (Chapter 3, Section 2.4).

In our study, the allocation system is considered to develop a long-term property insurance, since the average return period of claims is by far more akin to life insurance than car or housing insurance. Over a long period of time, the probability of experiencing one damaging earthquake increase to close 1. Again, the question is *when* and not *if*. Consequently, the premium amount is no longer mutualised but dedicated to each policyholder and capitalized on financial markets until an earthquake damages the insured house above the deductible amount $F$. Then, the insurance policy is cancelled after paying the insurance compensation. Studying an insurance model that considers only one claim is also meaningful for earthquake risk since a single earthquake can destroy the insured building. In such a case, considering other claims would also be meaningless.

This study proposes to calculate the annual premium amount $P$ for houses in California under the allocation insurance scheme. The premium $P$ is calculated hereafter for a normalised \$1 exposure cost because if the deductible amount is a percentage of the exposure amount, the insurance premium amount is usually proportional to the exposure (with respect to other parameters). It means that if a house costs \$400,000, the insurance premium is equal to $400{,}000 \times P$. We consider an insurance company with the same reinsurance structure (Fig. 5.1) and premium allocation (Fig. 5.2) than the CEA. Reinsurance pricing model is also simplified by neglecting the reinsurance companies' overhead costs, any cyclical reinsurance fluctuations, and any reinstatement premium (i.e. an additional premium amount to benefit again from the reinsurance cover after getting a reinsurance compensation). Finally, the Post Earthquake Industry Assessment and the reinsurance cover (Fig. 5.1) are aggregated into a single reinsurance layer corresponding to the premium amount $P_2{}^M$ (Fig. 5.2). A policyholder covered by this insurance policy will receive a compensation only after the first earthquake occurrence (called $EQ$) causing a loss to the insured building (called $L_{EQ}$) above the deductible amount $F$. It means that the average insured loss for each \$1 exposure is equal to:

$$\text{average insured loss} = \mathbb{E}(L_{EQ}) - F \tag{5.1}$$

with $\mathbb{E}(L_{EQ})$ the expected loss caused by *EQ* that corresponds to the arithmetical mean of the distribution of $L_{EQ}$. The average insured loss is lower than $\mathbb{E}(L_{EQ})$ by a factor of *F* since the deductible amount remains at the charge of the policyholder. In the mutualisation system the pure premium ( $P_1^M + P_2^M$) is calculated according to the collective risk model (Kaas et al. 2008) and is equal to the annual average insured loss as follows:

$$P_1^M + P_2^M = \frac{\mathbb{E}(L_{EQ}) - F}{\mathbb{E}(Y_{EQ})} \tag{5.2}$$

with $\mathbb{E}(Y_{EQ})$ the average time in years before the occurrence of the earthquake *EQ*. Thus, the variable $Y_{EQ}$ is called the time before the next damaging earthquake and represents, for a given location, the probabilistic distribution between occurrence time of the first damaging earthquake and the time when the insurance policy is priced.

Within this framework and according to the CEA's premium breakdown (Fig. 5.2), the premium amounts $P_1^M$, $P_2^M$ and $P_3^M$ can be calculated from the pure premium (Fig. 5.2 and Eq. 5.2) as follows:

$$\begin{cases} P_1^M = \dfrac{36\%}{81\%} \times (P_1^M + P_2^M) = \dfrac{36\%}{81\%} \times \dfrac{\mathbb{E}(L_{EQ}) - F}{\mathbb{E}(Y_{EQ})} \\ P_2^M = \dfrac{45\%}{81\%} \times (P_1^M + P_2^M) = \dfrac{45\%}{81\%} \times \dfrac{\mathbb{E}(L_{EQ}) - F}{\mathbb{E}(Y_{EQ})} \\ P_3^M = (P_1^M + P_2^M) \times \dfrac{19\%}{81\%} \end{cases} \tag{5.3}$$

To calculate the annual premium amount $P_1$, defined as the counterpart of $P_1^M$ under the allocation system, we use the Theory of Interest (Slud 2001). It states that a capital of €1 received at year *N* is equivalent to a capital of €$(1+t_I)$ at year *N*+1, where $t_I$ is the rate of return on investment. Recursively, it comes that €1 at year *N* is equivalent to €$(1+ t_I)^i$ at year *N*+*i*. Consequently, the total amount of $P_1$ paid until the occurrence of *EQ* and actualised at the occurrence time of *EQ* (called $P_1^{EQ}$) is given by the following formula:

$$P_1^{EQ} = P_1 \times (1 + t_I)^{Y_{EQ}-1} + P_1 \times (1 + t_I)^{Y_{EQ}-2} + \cdots + P_1 \times (1 + t_I) + P_1 \tag{5.4}$$

The value of $P_1^{EQ}$ is illustrated in Figure 5.4.

For the first year *i*=1, the annual premium $P_1$ is always paid and no financial return has yet been made ($P_1^{EQ} = P_1 \times (1 + t_I)^0 = P_1$). At each year *i*, if the earthquake *EQ* has not occurred, the

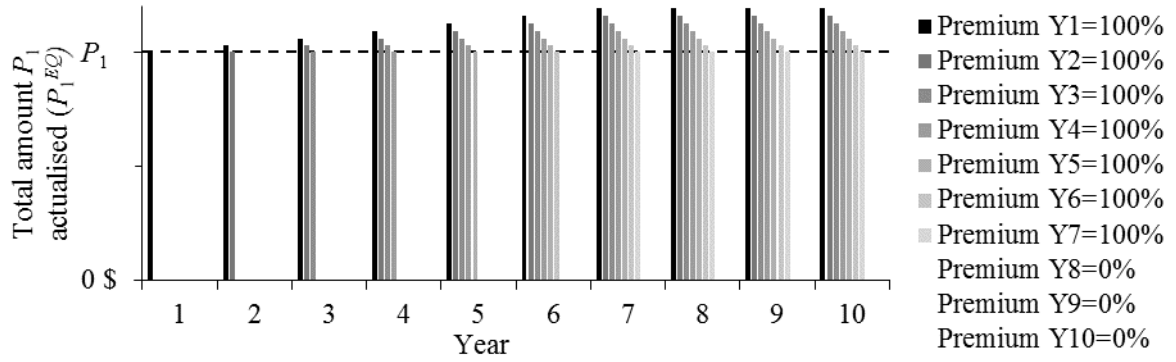


Figure 5.4: Illustration of the total amount of the premium $P_1$ actualised ($P_1^{EQ}$) since earthquake insurance policy issuance according to the Theory of Interest (Slud 2001). The first earthquake causing a claim above the deductible amount is assumed to occur during the 7th year ($Y_{EQ}$ = 7). A total premium amount at 100% corresponds to the amount paid each year by the policyholder. The quantity above the threshold 100% represents the profit made on financial markets.

premium amount for this year is collected and the capital made of the premiums already collected during the previous years and the compounded interests increases by a factor $t_I$. Since $Y_{EQ}$ is a random variable, so does $P_1^{EQ}$. The expected value of $P_1^{EQ}$ $\left(\text{written as } \mathbb{E}\left(P_1^{EQ}\right)\right)$ is by definition equal to:

$$\mathbb{E}\left(P_1^{EQ}\right) = \sum_{i=1}^{+\infty}\left[P_1 \times (1+t_I)^{i-1} \times \mathbb{P}\left(Y_{EQ} \geq i\right)\right] \tag{5.5}$$

where $\mathbb{P}\left(Y_{EQ} \geq i\right)$ is the probability that *EQ* occurs during the year *i* or later. About the loss distribution $L_{EQ}$, is not affected by the insurance mechanism used to calculate the premium amount. Furthermore, the reinsurance cover is the same under the two systems. Consequently, the same total premium amount must be collected until the occurrence of *EQ*, on average, under the two insurance mechanisms. Then, the expected value of $P_1^{EQ}$ must be equal to $P_1^M$ multiplied by the expected time before the occurrence of *EQ* (Eq. 5.3):

$$\mathbb{E}\left(P_1^{EQ}\right) = P_1^M \times \mathbb{E}\left(Y_{EQ}\right) = \left(\mathbb{E}\left(L_{EQ}\right) - F\right) \times \frac{36\%}{81\%} \tag{5.6}$$

Finally, in the allocation system $P_1$ is derived from Equations 5.5 and 5.6, as follows:

$$\sum_{i=1}^{+\infty}\left[P_1 \times (1+t_I)^{i-1} \times \mathbb{P}\left(Y_{EQ} \geq i\right)\right] = \frac{36\%}{81\%} \times \left(\mathbb{E}\left(L_{EQ}\right) - F\right) \tag{5.7}$$

Regarding the premium amount $P_2$ paid by the insurance company to the reinsurance providers, it is equal to the annual average insured loss covered by reinsurance companies, according to the simplified reinsurance pricing model. As $P_2$ is paid each year, it cannot be invested at the

same time on financial markets. This is captured by $t_I = 0$ and similarly to $P_1$ (Eq. 5.7), $P_2$ is given by:

$$\sum_{i=1}^{+\infty}\left[P_2 \times \mathbb{P}\left(Y_{EQ} \geq i\right)\right] = \frac{45\%}{81\%} \times \left(\mathbb{E}\left(L_{EQ}\right) - F\right) \tag{5.8}$$

$P_3$, representing the overhead costs, is supposed equal to 19%$P$ (Fig. 5.2), in the same manner as for the mutualisation system (Eq. 5.3), and expressed as follows:

$$P_3 = \frac{19\%}{81\%}(P_1 + P_2) \tag{5.9}$$

Comparing Equation 5.3 to Equations 5.7, 5.8 and 5.9, the main difference lies between $P_1$ and $P_1^M$. Assuming that $Y_{EQ}$ follows an exponential distribution (common assumption in probabilistic seismic hazard assessment; Gardner and Knopoff 1974), Figure 5.5 illustrates the evolution of the ratio $P_1/P_1^{\mathrm{M}}$ according to $t_{\mathrm{I}}$ and $\mathbb{E}\left(Y_{EQ}\right)$.

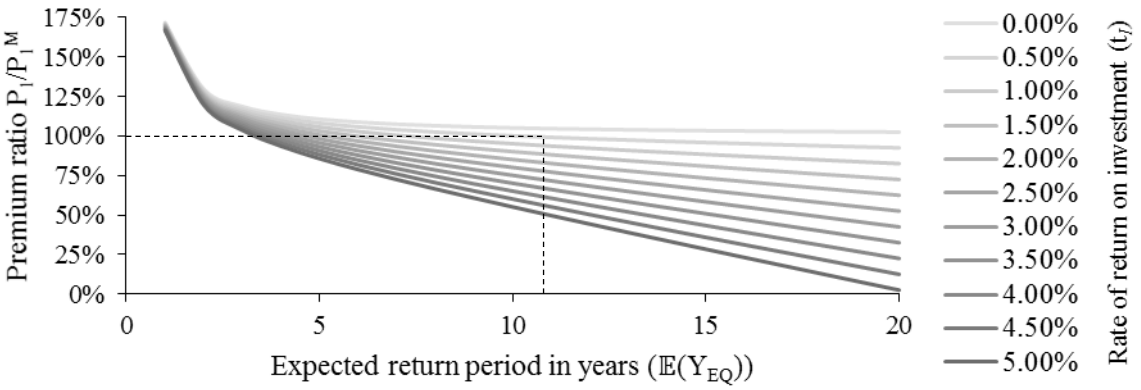


Figure 5.5: Ratio between the annual premium amount calculated under the allocation insurance scheme ($P_1$) and the mutualisation insurance scheme ($P_1^M$), according to the expected return period $\left(\mathbb{E}\left(Y_{EQ}\right)\right)$ of the next earthquake causing a claim. Each curve corresponds to a different rate of return on investment ($t_I$) on the financial markets.

Figure 5.5 highlights that the allocation insurance scheme is the most efficient for long return period risk because the premium amount is capitalized. Moreover, the higher the interest rate, the lower the premium amount compared to $P_1^M$. At the opposite, for the smallest values of $\mathbb{E}\left(Y_{EQ}\right)$, $P_1^M$ is lower than $P_1$ because the premium amount is not used to cover only one claim but all the others occurring the same year.

In the next section, the annual premium amount under the allocation and the mutualisation system are compared for the residential homeowner earthquake insurance in California.

## 5.5. Case studies on cities of San Francisco and Los Angeles

In this study, we consider the Probabilistic Seismic Hazard Assessment (PSHA) estimates given in the UCERF3 time-independent hazard model (Field et al. 2013) for rock sites. The probabilistic loss assessment model HAZUS-MH MR5 released by the Federal Emergency Management Agency (2010) is used to get a loss distribution from the PSHA hazard curves. The inputs for this UCERF3/HAZUS-MH MR5 model are the following:

- A location, corresponding to a city in California;
- A soil profile, characterized by the time-averaged shear-wave velocity to 30 m depth (Wald and Allen 2007);
- An occupancy class describing the building use (house, condominium, mobile home, hotel…);
- A building structure type mentioning the main structural material of the building (e.g. wood, masonry, reinforced concrete…);
- A building seismic design level indicating if the building has been built under a seismic building code and the standards level, if any.

The two locations selected for the case studies are San Francisco and Los Angeles. These two large cities have been chosen because they are representative of two earthquake risk profiles. While both have already experienced at least one devastating earthquake (1906 San Francisco earthquake, 1989 Loma Prieta and 1994 Northridge), less than 10% of people were insured by the CEA in 2009 in San Francisco, against more than 30% in Los Angeles at the same time (Lin 2013).

The hazard input in the HAZUS-MH MR5 is characterized by the spectral displacement which is estimated from the maximum considered earthquake ($MCE_R$) ground motion response acceleration at 0.2 and 1 seconds according to the ASCE 7-10 standards (ASCE 2010). They have been taken from the UCERF3 model outputs at site coordinates 122.40°W; 37.75°N and 118.25°W; 34.05°N for San Francisco and Los Angeles, respectively (Fig. 5.6).

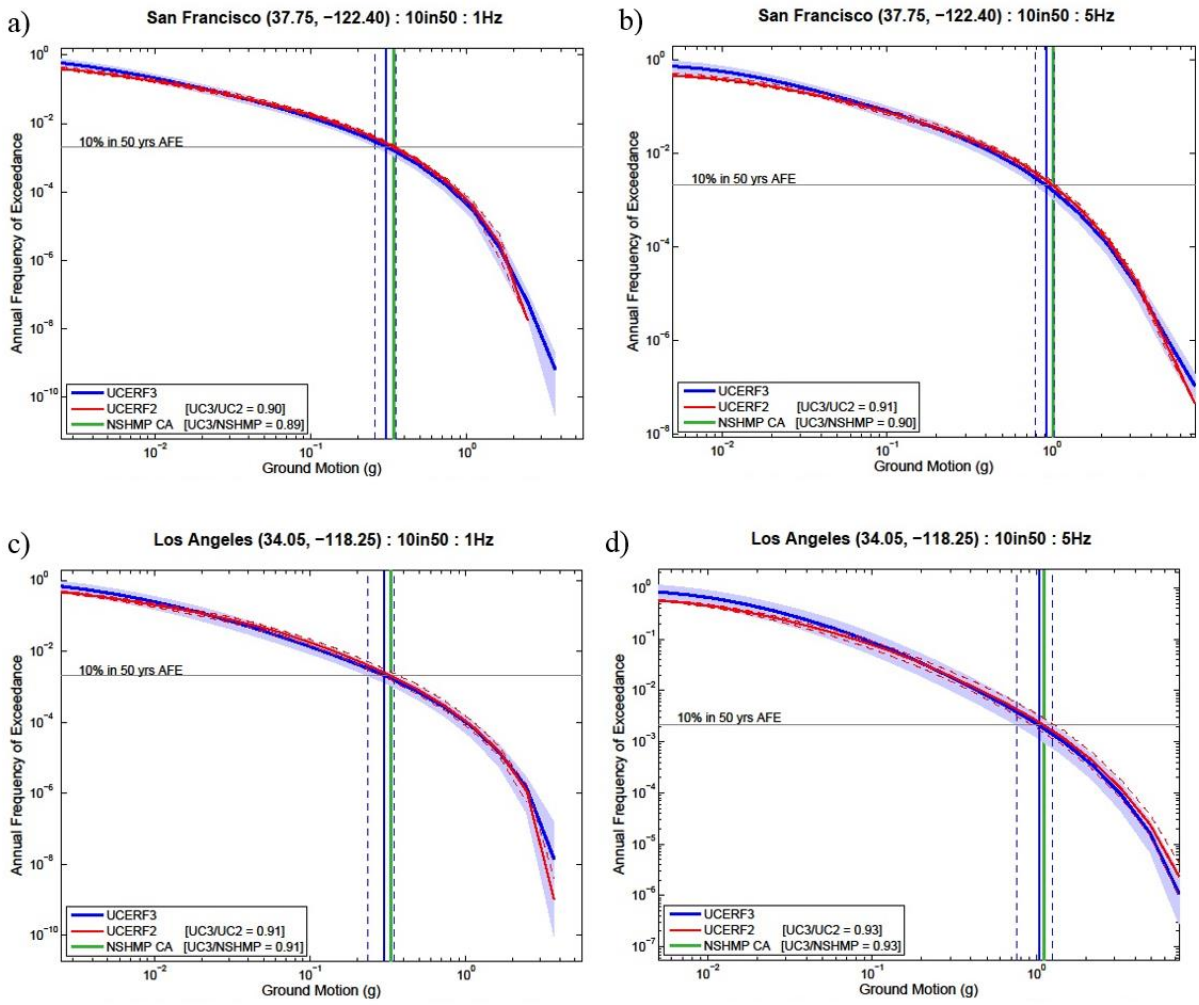


Figure 5.6: Maximum considered earthquake ($MCE_R$) ground motion response acceleration at 0.2 and 1 seconds for San Francisco and Los Angeles estimated from different models. Source: USGS (https://pubs.usgs.gov/of/2013/1165/data/UCERF3_SupplementalFiles/UCERF3.3/Hazard/HazardCurves/Sites/index.html).

For site conditions, we use the Global Slope-Based proxy released by the USGS and illustrated in Figure 5.7 for Los Angeles and San Francisco.

The HAZUS-MH MR5 model relies on the soil classification released by the 1997 NEHRP Provisions. Using this framework, the C and D classes are represented in Figure 5.7 by the green ($360 m.s^{-1} < Vs_{30} < 760 m.s^{-1}$) and the yellow/orange ($180 m.s^{-1} < Vs_{30} < 360 m.s^{-1}$) shades, respectively. Therefore, we assume in this study that the soil category representative of San Francisco and Los Angeles is C and D, respectively.

Because this study focuses on earthquake insurance for homeowners, the occupancy class considered is house (Occupancy code RES1: "single family dwellings" in HAZUS-MH MR5).

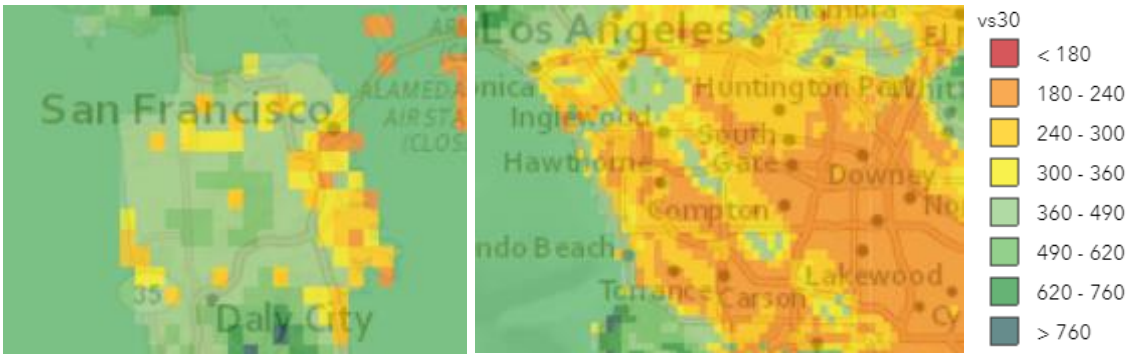


Figure 5.7: Screen shots of the Global Slope-Based proxy for the Vs30 soil profile for San Francisco and Los Angeles areas. Source: USGS (https://earthquake.usgs.gov/data/vs30/).

According to the HAZUS-MH MR5 Technical manual (Federal Emergency Management Agency 2010), 99% of houses in California are wooden light frame building (code W1). This rate is corroborated by the US Census Bureau which reports that more than 99% of houses built after 2009 in Western USA are made in this material. Four building seismic design levels defined in the model HAZUS-MH MR5 (Pre-Code *PC*, Low-Code *LC*, Moderate-Code *MC* and High-Code *HC*) are considered in this study in order to value its impact to the premium amount.

The two main outputs from the UCERF3/HAZUS-MH MR5 model for calculating the premiums $P$ and $P^M$ are the expected loss $L_{EQ}$ and the time before the next damaging earthquake $Y_{EQ}$ (Eq. 5.3, 5.7 and 5.8). Figure 5.8 illustrates the distribution of $L_{EQ}$ and $Y_{EQ}$ for San Francisco and Los Angeles obtained from the UCERF3/HAZUS-MH MR5 model.

In Figure 5.8, Los Angeles is more at risk than San Francisco because on one hand the average loss caused by an earthquake is higher (Fig. 5.8.a) and, on the other hand, the first damaging earthquake is expected to occur sooner (Fig. 5.8.b). The variable $Y_{EQ}$ is distributed following an exponential distribution, according to the UCERF3 time-independent hazard model (Field et al. 2013). In order to validate the UCERF3/HAZUS-MH MR5 model, the premium amounts under the mutualisation scheme ($P^M$) are compared to those offered by the CEA (available at: www.earthquakeauthority.com/California-Earthquake-Insurance-Policies/Earthquake-Insurance-Premium-Calculator). Results are presented in Figure 5.9 for the minimum and the maximum deductibles amount proposed by the CEA and according to the year built.

Figure 5.9 shows that the modelled premium for the Moderate-Code seismic design level fits well the CEA's premium amount before 1970 for San Francisco, while the High-Code seismic

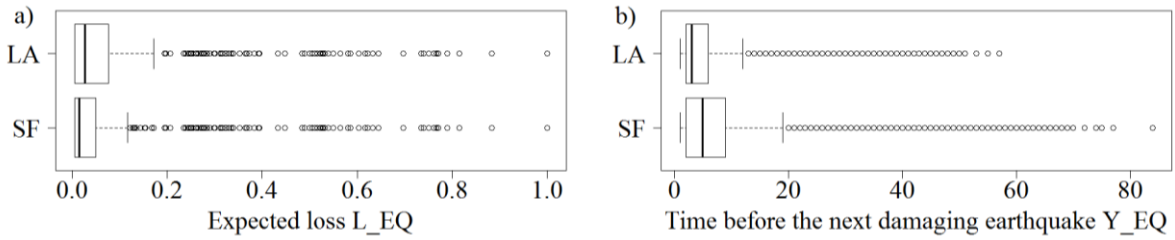


Figure 5.8: Distribution of: a) the expected loss ($L_{EQ}$) and b) the time before the next damaging earthquake ($Y_{EQ}$), as calculated with the UCERF3/HAZUS-MH MR5 model for a Pre-Code seismic design level wooden house located in Los Angeles (LA: 118.25°W; 34.05°N) and San Francisco (SF: 122.40°W; 37.75°N). The deductibles amount is taken equal to 0. The box represents the first and the third quartiles and the thick solid line the second quartile. The length of the right-hand side dotted line is equal to 1.5 times the box length. On the left-hand side, the dotted line is capped by the minimum value of the distribution (equal to 0 for $L_{EQ}$ and 1 for $Y_{EQ}$). Dots show values beyond the end of dotted lines (materialized by the small solid vertical line). Source: after UCERF3.3 Hazard Analysis Sites.

design level fits well the CEA's premium amount after 1970 for Los Angeles. According to HAZUS-MH MR5, wooden houses in California built before and after 1973 have a Moderate-Code and a High-Code seismic design levels, respectively. Consequently, these two fits mean that the UCERF3/HAZUS-MH MR5 is representative of the CEA's pricing for Los Angeles after 1970 and San Francisco before 1970. At the opposite, the same model does not capture well the CEA's pricing for Los Angeles before 1970 and San Francisco after 1970. However, a premium offered by an insurance company is usually adjusted according to other variables not considered in this study, like commercial discount to attract new customers.

In conclusion, the UCERF3/HAZUS-MH MR5 is supposed suitable for calculating earthquake insurance premium in California. Nevertheless, in order to exclude the gap between the CEA's premium amount and the model (Fig. 5.9) from the analyses, $P^M$ is used as the reference instead of the observed CEA's premium amount. This assumption means that the CEA is supposed to have used the UCERF3/HAZUS-MH MR5 model to price their insurance policies. Therefore, the premium reduction allowed by this long-term property earthquake insurance policy is calculated later in this study by the following premium ratio:

$$\text{premium ratio} = \frac{P}{P^M} \tag{5.10}$$

Each premium ratio calculated hereafter is also compared to the thresholds 33% and 16% which are targeted to encourage respectively most of, and all California homeowners to buy an insurance policy, respectively (Chapter 3, Section 2). The variables $\mathbb{E}(Y_{EQ})$ and $\mathbb{P}(Y_{EQ} \geq i)$ being calculated using the UCERF3/HAZUS-MH MR5 model, the premiums $P$ and $P^M$ can be assessed for Los Angeles and San Francisco, as well as the full ranges of seismic design levels

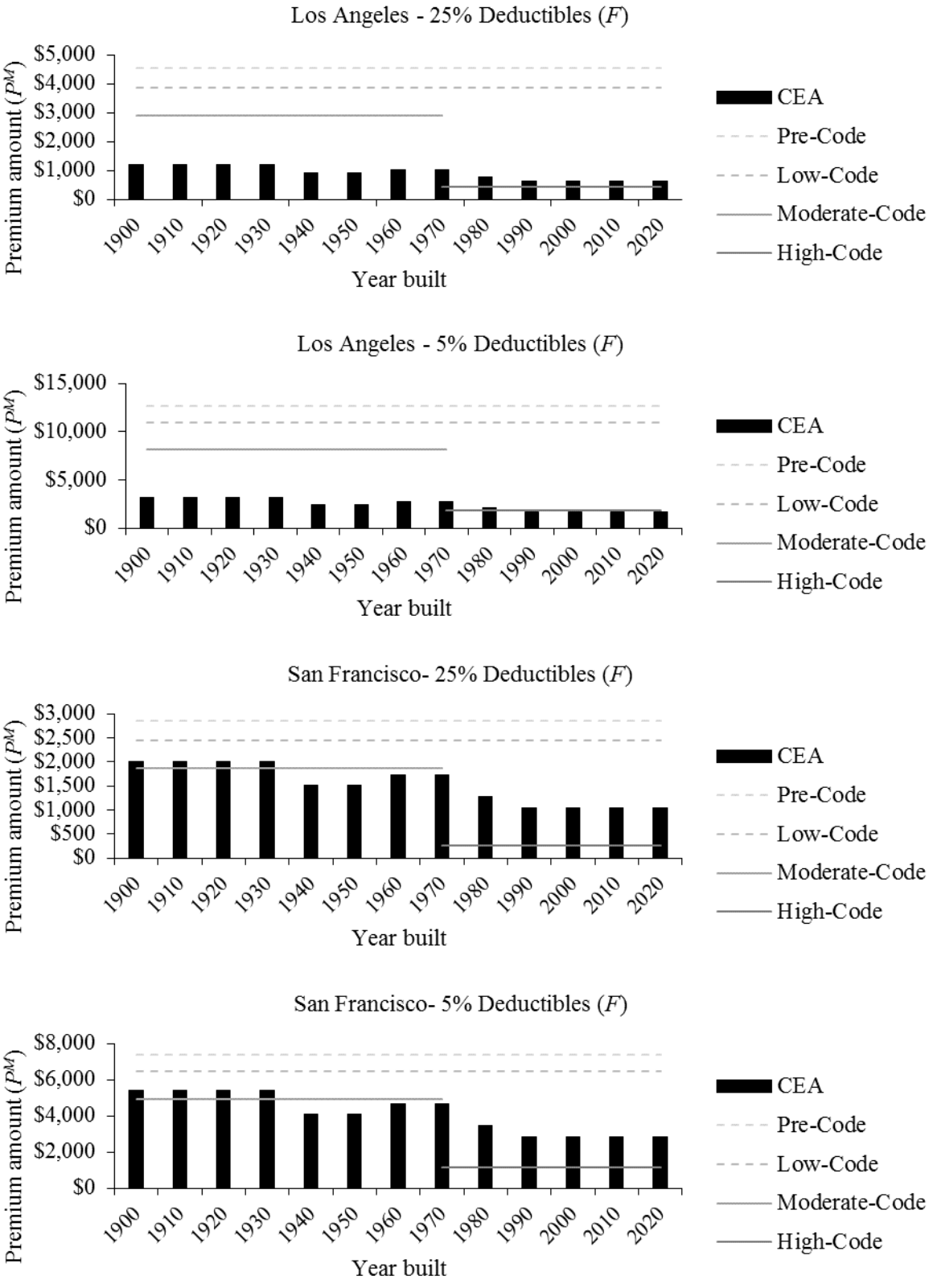


Figure 5.9: Comparison of the annual premium amount modelled under the mutualisation scheme for different seismic design levels (grey continuous and dashed horizontal lines) and offered by the CEA (black bars). Results are presented for a wooden house located in San Francisco (postal code used: 94102) and Los Angeles (postal code used: 90001),

and deductibles amounts (Eq. 5.3, 5.7, 5.8 and 5.9). The results are shown in Figure 5.10 in terms of premium ratio.

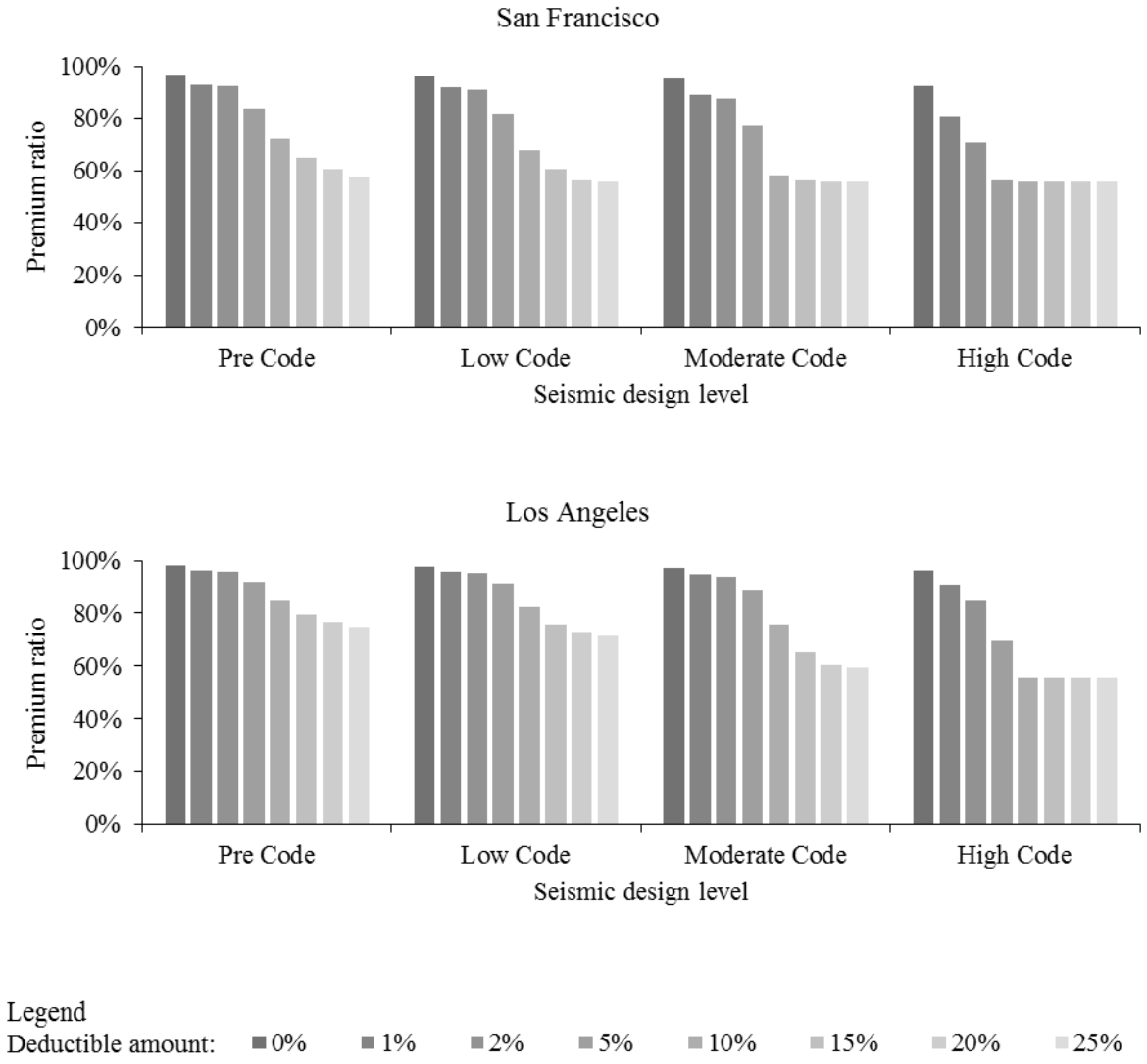


Figure 5.10: Premium ratio between the allocation and the mutualisation insurance scheme ($P/P^M$) for different seismic design levels and deductible amounts in San Francisco and Los Angeles. A premium ratio below 100% means that the premium is lower in the allocation than in the mutualisation insurance scheme.

Figure 5.10 shows that the premium decrease is very limited for a deductible amount below 2%. This can be explained by the high frequency of earthquakes producing very low damage and consequently, making an allocation insurance system inappropriate. For large deductibles amount (above 10% in case of Moderate-Code or High-Code), Figure 5.10 shows that the premium ratio is constant and equal to 55%, because the return period of an earthquake

damaging above 10% is so high that the contribution of $P_1$ into $P$ is marginal. As the premium parts $P_2$ and $P_3$ are similar under the allocation and the mutualisation insurance schemes, it results in a floor at 55% (55% = 45% / 81%).

Even if a premium ratio at 55% means a premium amount almost twice lower than the current one, the decrease is not enough for convincing most of California homeowners to buy an earthquake insurance (Chapter 3, Section 2). Moreover, using the allocation instead of the mutualisation insurance system has no impact on $P_2$ (Eq. 5.3 and 5.8). As it represents the risk transferred from the insurance company to reinsurance companies, only a lower risk can decrease $P_2$ (and consequently $P_1$ according to Eq. 5.7). Therefore, in the next section, a risk reduction plan for buildings is presented, using earthquake retrofitting solutions.

## 5.6. Leveraging on building retrofitting works for a risk reduction

Earthquake retrofitting is one of the solutions to decrease the vulnerability and then, the risk. According to Equations 5.7, 5.8 and 5.9, it consists in reducing $P_1$, $P_2$ and $P_3$. The question is therefore to know if the premium decrease induced by the risk reduction is important enough to pay the retrofitting works. Under the allocation system, the capital made by collected premiums and subsequent financial profits is dedicated to each policyholder. Consequently, the allocation system enables to compare, for each insured house, if the cost of seismic retrofitting works is lower or higher than the premium amount decrease. This approach is not possible under the mutualisation system because there is no personalized and long-term capital management. Indeed, the premium amounts are aggregated to pay the claims over the year and the share not spent in claims is used either to increase the insurance company's capital or to pay dividends. In this section, the premium amount in case of financing retrofitting works (i.e. considering both the cost and the vulnerability decrease) is first calculated and next compared to the premium amount obtained in the previous section (i.e. without financing retrofitting works).

For each seismic design level (*PC*, *LC*, *MC* and *HC*), HAZUS-MH MR5 (Federal Emergency Management Agency 2010) gives a specific vulnerability curve, which can be used to calculate the corresponding distribution of $Y_{EQ}$ and $L_{EQ}$. Then, the premium $P_1$ and $P_2$ (Eq. 5.7 and 5.8) must include the evolution of the vulnerability profile of the insured building. For that, the

variables $T^{LC}$, $T^{MC}$, and $T^{HC}$ are introduced and correspond to the year of retrofitting works from Pre-Code (*PC*) to Low-Code (*LC*), Low-Code (*LC*) to Moderate-Code (*MC*) and Moderate-Code (*MC*) to High-Code (*HC*), respectively. As illustrated in Table 5.1, when the initial seismic design code of a newly insured house (*IC*) is higher than *PC*, the corresponding year of retrofitting is set at 0 (e.g. $T^{LC}$ =0).

Table 5.1: Time in years between the insurance policy issuance and the beginning of the retrofitting works required to reach a given seismic design level, according to the initial seismic design code (*IC*). The time is equal to 0 when the building is already at the seismic design level or above at the time of the insurance policy issuance.

| Initial seismic design code (*IC*) | Time in years before the retrofitting works to reach the level: | | |
|---|---|---|---|
| | Low Code (*LC*) | Moderate Code (*MC*) | High Code (*HC*) |
| Pre Code (*PC*) | $T^{LC}$ | $T^{MC}$ | $T^{HC}$ |
| Low Code (*LC*) | 0 | $T^{MC}$ | $T^{HC}$ |
| Moderate Code (*MC*) | 0 | 0 | $T^{HC}$ |
| High Code (*HC*) | 0 | 0 | 0 |

Furthermore, as the insurance policy stops after the first loss under the allocation system, the insured building is retrofitted only if the first damaging earthquake (*EQ*) has not occurred yet (i.e. $T^{LC} \leq Y_{EQ}$ for *PC* to *LC*; $T^{MC} \leq Y_{EQ}$ for *LC* to *MC*; $T^{HC} \leq Y_{EQ}$ for *MC* to *HC*).

To include the periods $T^{LC}$, $T^{MC}$, and $T^{HC}$ into the expression $\mathbb{P}(Y_{EQ} \geq i)$ in Equations 5.7 and 5.8, the Law of Total Probability is used (Tijms 2003). The new equation for calculating $P_1$ is (detailed in Appendix C):

$$\sum_{i=1}^{+\infty}\left[P_1 \times (1+t_I)^{i-1} \times \mathbb{P}(Y_{EQ} \geq i)\right] \tag{5.11}$$

$$= \sum_{i=1}^{T^{LC}}\left[P_1 \times (1+t_I)^{i-1} \times \mathbb{P}(Y_{EQ} \geq i | Y_{EQ} \leq T^{LC})\right] \times \mathbb{P}(Y_{EQ} \leq T^{LC})$$

$$+ \sum_{i=1}^{T^{MC}}\left[P_1 \times (1+t_I)^{i-1} \times \mathbb{P}(Y_{EQ} \geq i | T^{LC} < Y_{EQ} \leq T^{MC})\right] \times \mathbb{P}(T^{LC} < Y_{EQ} \leq T^{MC})$$

$$+ \sum_{i=1}^{T^{HC}}\left[P_1 \times (1+t_I)^{i-1} \times \mathbb{P}(Y_{EQ} \geq i | T^{MC} < Y_{EQ} \leq T^{HC})\right] \times \mathbb{P}(T^{MC} < Y_{EQ} \leq T^{HC})$$

$$+ \sum_{i=1}^{+\infty}\left[P_1 \times (1+t_I)^{i-1} \times \mathbb{P}(Y_{EQ} \geq i | T^{HC} < Y_{EQ})\right] \times \mathbb{P}(T^{HC} < Y_{EQ})$$

Similarly, the expression of $P_2$ (Eq. 5.8) becomes (replacing $P_1$ by $P_2$ and taking $t_I = 0$ in Eq. 5.11):

$$\sum_{i=1}^{+\infty}\left[P_2 \times \mathbb{P}\left(Y_{EQ} \geq i\right)\right] \tag{5.12}$$

$$\begin{aligned}
&= \sum_{i=1}^{T^{LC}}\left[P_2 \times \mathbb{P}\left(Y_{EQ} \geq i | Y_{EQ} \leq T^{LC}\right)\right] \times \mathbb{P}\left(Y_{EQ} \leq T^{LC}\right) \\
&+ \sum_{i=1}^{T^{MC}}\left[P_2 \times \mathbb{P}\left(Y_{EQ} \geq i | T^{LC} < Y_{EQ} \leq T^{MC}\right)\right] \times \mathbb{P}\left(T^{LC} < Y_{EQ} \leq T^{MC}\right) \\
&+ \sum_{i=1}^{T^{HC}}\left[P_2 \times \mathbb{P}\left(Y_{EQ} \geq i | T^{MC} < Y_{EQ} \leq T^{HC}\right)\right] \times \mathbb{P}\left(T^{MC} < Y_{EQ} \leq T^{HC}\right) \\
&+ \sum_{i=1}^{+\infty}\left[P_2 \times \mathbb{P}\left(Y_{EQ} \geq i | T^{HC} < Y_{EQ}\right)\right] \times \mathbb{P}\left(T^{HC} < Y_{EQ}\right)
\end{aligned}$$

When $Y_{EQ}$ follows an exponential distribution (e.g. in the UCERF3/HAZUS-MH MR5 model), Equations 5.11 and 5.12 can be rewritten without conditional probabilities (as detailed in Appendix D), making numerical applications easier.

Regarding the expression $\mathbb{E}\left(L_{EQ}\right)$ in Equations 5.7 and 5.8, it changes as follows when introducing the variables $T^{LC}$, $T^{MC}$, and $T^{HC}$ (Law of Total Expectation, Tijms, 2003):

$$\begin{aligned}
\mathbb{E}\left(L_{EQ}\right) = \ & \mathbb{E}\left(L_{EQ} | Y_{EQ} \leq T^{LC}\right) \times \mathbb{P}\left(Y_{EQ} \leq T^{LC}\right) \\
&+ \mathbb{E}\left(L_{EQ} | T^{LC} < Y_{EQ} \leq T^{MC}\right) \times \mathbb{P}\left(T^{LC} < Y_{EQ} \leq T^{MC}\right) \\
&+ \mathbb{E}\left(L_{EQ} | T^{MC} < Y_{EQ} \leq T^{HC}\right) \times \mathbb{P}\left(T^{MC} < Y_{EQ} \leq T^{HC}\right) \\
&+ \mathbb{E}\left(L_{EQ} | T^{HC} < Y_{EQ}\right) \times \mathbb{P}\left(T^{HC} < Y_{EQ}\right)
\end{aligned} \tag{5.13}$$

Since the studied earthquake insurance model includes an option to retrofit the insured house, the cost of works $W_{LC}$, $W_{MC}$ and $W_{HC}$, for retrofitting from *PC* to *LC*, *LC* to *MC* and *MC* to *HC*, respectively, have to be also considered when calculating the premium amount. Using the Theory of Interest (Slud 2001), the retrofitting cost from *PC* to *LC* actualised at the occurrence date of *EQ* ($Y_{EQ}$) is:

$$\text{retrofitting cost from } PC \text{ to } LC \text{ actualised} = \sum_{i=T^{LC}}^{+\infty}\left[W_{LC} \times (1+t_I)^{i-T^{LC}} \times \mathbb{P}\left(Y_{EQ} = i\right)\right] \tag{5.14}$$

As the retrofitting works are undertaken only if *EQ* has not occurred before $Y_{EQ}$, the sum in Equation 5.14 starts at I = $T^{LC}$. Furthermore, each year after $T^{LC}$ without *EQ* occurrence increases the value of $W_{LC}$ by a factor of $(1+t_I)$, according to the Theory of Interest (Slud 2001).

To calculate the premiums add-on $P_{LC}$, $P_{MC}$ and $P_{HC}$ corresponding to $W_{LC}$, $W_{MC}$ and $W_{HC}$ respectively, we assume that an insurance company does not need to be reinsured for financing the retrofitting works. Indeed, reinsurance cover is usually dedicated to transfer part of the risk insured, not to insurance company's expenditure. In this study, the insured risk is the loss caused by the first damaging earthquake event ($L_{EQ}$) and benefits from a reinsurance cover (Fig. 5.1). At the opposite, the decision to pay for seismic retrofitting works depends on the prevention strategy of the insurance company. Consequently, this initiative is expected to be funded by the insurance company's cash flow, and any profit or capital loss have to be supported by the insurance company.

In the model developed here, $P_{LC}$, $P_{MC}$ and $P_{HC}$ can be calculated according to the Theory of Interest (Slud 2001), as described in Figure 5.4. Then, according to Equations 5.11 and 5.14, $P_{LC}$, $P_{MC}$ and $P_{HC}$ are given by:

$$\begin{cases} \sum_{i=1}^{+\infty}\left[P_{LC}\times(1+t_I)^{i-1}\times\mathbb{P}\left(Y_{EQ}\geq i\right)\right] = \sum_{i=T^{LC}}^{+\infty}\left[W_{LC}\times(1+t_I)^{i-T^{LC}}\times\mathbb{P}\left(Y_{EQ}=i\right)\right] \\ \sum_{i=1}^{+\infty}\left[P_{MC}\times(1+t_I)^{i-1}\times\mathbb{P}\left(Y_{EQ}\geq i\right)\right] = \sum_{i=T^{MC}}^{+\infty}\left[W_{MC}\times(1+t_I)^{i-T^{MC}}\times\mathbb{P}\left(Y_{EQ}=i\right)\right] \\ \sum_{i=1}^{+\infty}\left[P_{HC}\times(1+t_I)^{i-1}\times\mathbb{P}\left(Y_{EQ}\geq i\right)\right] = \sum_{i=T^{HC}}^{+\infty}\left[W_{HC}\times(1+t_I)^{i-T^{HC}}\times\mathbb{P}\left(Y_{EQ}=i\right)\right] \end{cases} \quad (5.15)$$

Finally, the total annual premium amount including the retrofitting works *P* is given by:

$$P = P_1 + P_2 + P_3 + P_{LC} + P_{MC} + P_{HC} \quad (5.16)$$

where the overheads premium $P_3$ is now calculated from *P* (Eq. 5.9 and Fig. 5.2) as follows:

$$P_3 = \frac{19\%}{81\%}(P_1 + P_2 + P_{LC} + P_{MC} + P_{HC}) \quad (5.17)$$

The value of *P* and, therefore, the benefit for financing retrofitting works within an insurance model is highly dependent from the associated costs $W_{LC}$, $W_{MC}$ and $W_{HC}$ (Eq. 5.15 and 5.16). Unfortunately, the HAZUS-MH MR 5 models does not indicate such costs, and this information was not found in other sources. However, several scientific studies have already published cost-benefit analyses for retrofitting residential buildings (Dan 2018; Riedel 2015; Porter et al. 2006). Furthermore, several construction companies have launched advertising web-campaigns

about retrofitting works for houses in the USA. Table 5.2 summarizes different retrofitting costs mentioned in both scientific papers and advertising campaigns for several countries and building types.

Table 5.2: Retrofitting costs for residential buildings retrieved for scientific studies and advertising campaigns. The symbol * means that the rate has been calculated assuming an average $290,000 price for a wooden house (source: HomeAdvisor). Abbreviations: Ma; Masonry; RC: Reinforced concrete; Str.: Structure type; W1: Wood light frame.

| Media | Authors | Year | Country | Str. | Dwelling | Retrofitting cost |
|---|---|---|---|---|---|---|
| Scientific | Dan | 2018 | GRC | RC | Multi | 5% - 11% |
| | Riedel | 2015 | FRA | RC/Ma | Multi | 5% - 30% |
| | Porter et al. | 2006 | CAL | W1 | Single | 3.6% - 3.8% |
| Advertising | HomeAdvisor | 2019 | CAL | W1 | Single | 0.3%* - 2.1%* |
| | ImproveNet | 2019 | USA | W1 | Single | 1.3%* - 3.4%* |
| | CXC Contracting | 2019 | USA | W1 | Single | 1%* - 2.1%* |
| | Earthquake Safety | 2019 | USA | W1 | Single | 1%* - 3.4%* |

Table 5.2 shows a wide range of retrofitting costs, from below 1%, up to 30%. Despite Riedel (2015) and Dan (2018) reported retrofitting costs for multi-family dwelling buildings built in masonry and reinforced concrete, these values can be considered as an upper bound. Furthermore, Riedel (2015) expected also that the retrofitting cost to reach the next level increases with the seismic design level: for instance, retrofitting a house from *PC* to *LC* is less expensive than from *LC* to *MC*.

In order to investigate the full range of retrofitting costs shown in Table 5.2, four different cases have been considered: 1) $W_{LC}$ = 2.5%, $W_{MC}$ = 2.5%, $W_{HC}$ = 2.5%; 2) $W_{LC}$ = 2.5%, $W_{MC}$ = 5%, $W_{HC}$ = 7.5%; 3) $W_{LC}$ = 10%, $W_{MC}$ = 10%, $W_{HC}$ = 10%; 4) $W_{LC}$ = 10%, $W_{MC}$ = 20%; $W_{HC}$ = 30%. They include both constant and increasing retrofitting cost with the seismic design level, as well as a large range of total retrofitting costs ($W_{LC} + W_{MC} + W_{HC}$), from 7.5% up to 60% . Although data collected by Riedel (2015) shows that the retrofitting costs decrease when two works are done simultaneously (e.g. retrofitting works from Low-Code to High-Code is less expensive than $W_{MC} + W_{HC}$), we assume for simplicity that the retrofitting costs are additive (e.g. retrofitting works from Low-Code to High-Code is equal to $W_{MC} + W_{HC}$).

For a given set of retrofitting costs and an initial seismic design code *IC*, the dates for the retrofitting works $T^{LC}$, $T^{MC}$ and $T^{HC}$ are defined in order to minimize the total premium amount *P*:

$$(T^{LC};T^{MC};T^{HC}) = \begin{cases} \min\limits_{(T^{LC};T^{MC};T^{HC})} P(\text{Eq. 5.11 to 5.17}) & \text{if } IC = PC \\ \left(0; \min\limits_{(T^{MC};T^{HC})} P(\text{Eq. 5.11 to 5.17})\right) & \text{if } IC = LC \\ \left(0;0; \min\limits_{(T^{HC})} P(\text{Eq. 5.11 to 5.17})\right) & \text{if } IC = MC \\ (0;0;0) & \text{if } IC = HC \end{cases} \quad (5.18)$$

and also, to verify the following condition:

$$1y \leq T^{LC} \leq T^{MC} \leq T^{HC} \leq 50y \quad (5.19)$$

The condition to perform all the retrofitting works within 50 years corresponds to the expected lifespan of wooden houses in the USA (O'Connor et al. 2004). No constraint has been considered about the minimum time for collecting premium *P* before financing retrofitting works. It means that the insurance company is supposed to have enough capital to pay the works before having collected the corresponding premium amounts ($P_{LC}$, $P_{MC}$ and $P_{HC}$).

Figure 5.11 shows the premium ratios calculated for different insurance conditions (i.e. deductible amount *F* and initial seismic design code *IC*) and retrofitting costs, according to Equations 5.11, 5.12, 5.13, 5.14, 5.15, 5.16, 5.17, 5.18 and 5.19.

For example, considering a house in Los Angeles built with a Pre-Code seismic design level (*IC=PC*) and the following retrofitting costs: $W_{LC}$=10%; $W_{MC}$=10%; $W_{HC}$=10%, Figure 5.11 shows that (tag 1) if the current earthquake insurance premium amount is equal to $P^{M}$=\$100 with a *F*=10% deductible amount, the premium decreases to *P*=\$80 (premium ratio = 80%, corresponding to the black and the white bars) under this scheme and even down to *P*=\$55 with retrofitting works (premium ratio = 55%, corresponding to the grey bar only). With a deductible amount at *F*=25% (tag 2) the premium amount is equal to *P*=\$75 under this new insurance scheme (premium ratio = 75%, corresponding to the grey bar only) but *P*=\$85 if including retrofitting works (premium ratio = 85%, corresponding to the grey and the black bars).

Results for San Francisco, shown in Figure 5.12, are similar to those for Los Angeles (Fig. 5.11). In conclusion, Figures 5.11 and 5.12 show that planning retrofitting works contribute to decrease the premium ratio compared to the allocation insurance model without retrofitting works (white bars), except when the costs are very high ($W_{LC}$, $W_{MC}$ and $W_{HC}$) or for a very high deductible amount (*F* = 25%), as materialized by black bars. When the initial seismic design code *IC* is High-Code, results stay unchanged since there is no retrofitting works to perform. Furthermore, the retrofitting works provide the largest premium decrease for a deductible amount at 5% or 10%, whatever the retrofitting costs, the location and the initial seismic design code.

When the retrofitting costs is equal to a constant value 2.5%, the premium ratio including the retrofitting works is below the threshold of 33% in optimal cases (Fig. 5.11) i.e. the new premium amount (*P*) is affordable for most of California homeowners (Chapter 3, Section 2). However, the premium ratio never reaches the target of 16% and for higher retrofitting costs, it remains significantly above 33%. To decrease the premium ratio further, the next section

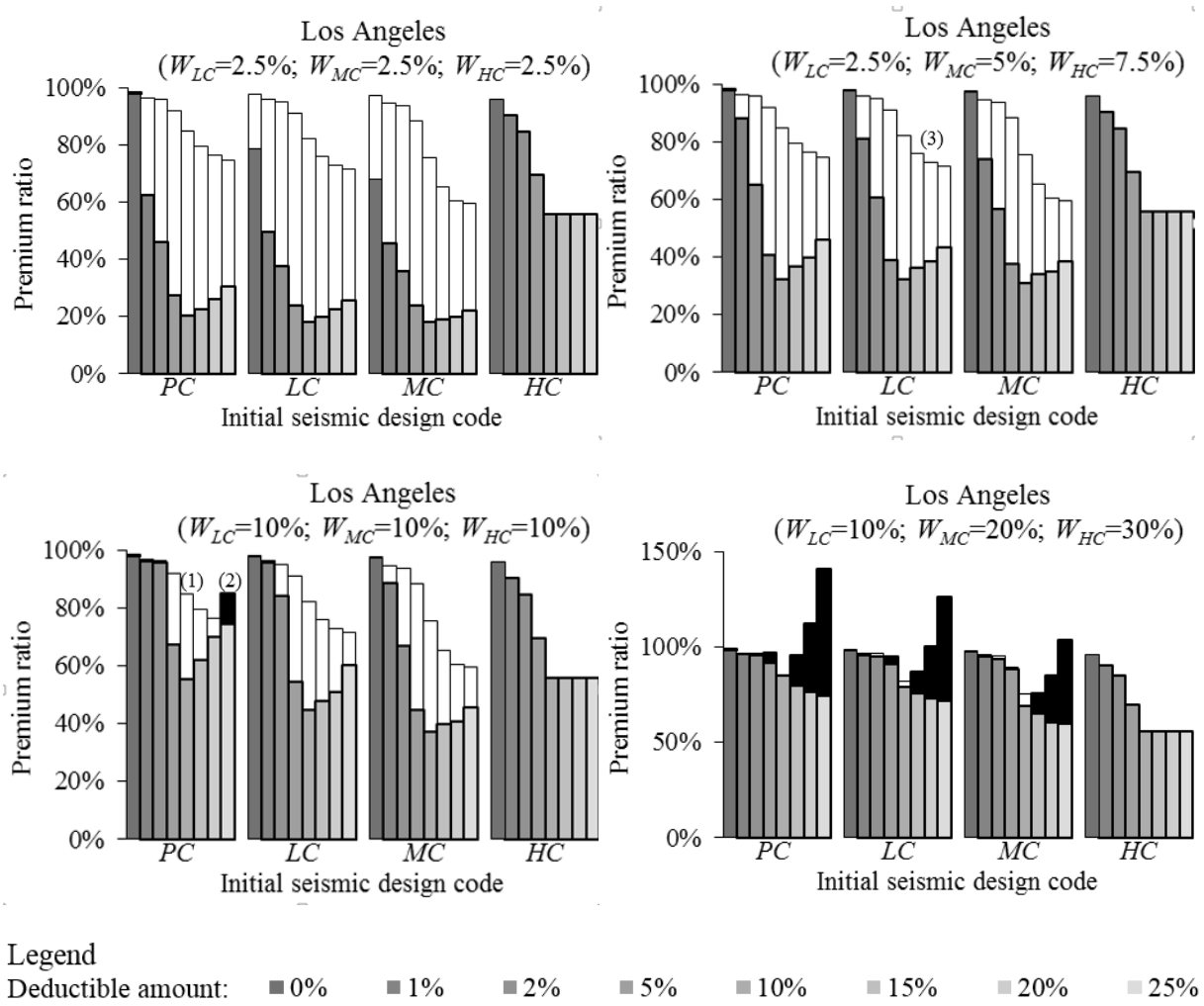


Figure 5.11: Premium ratio for the insurance cover including retrofitting works for various retrofitting costs ($W_{LC}$, $W_{MC}$ and $W_{HC}$). The insured building considered is located in Los Angeles and with different initial seismic design codes (*IC*): Pre-Code (*PC*), Low-Code (*LC*), Moderate-Code (*MC*) and High-Code (*HC*). Grey bars show the premium ratio value for different levels of deductible amount (*F*). White and black bars on the top of the grey bars show when the premium ratio including retrofitting works is lower and higher than the previous premium ratio obtained without retrofitting works (Fig. 5.10), respectively. Tags (1), (2) and (3) refer to examples described in the text.

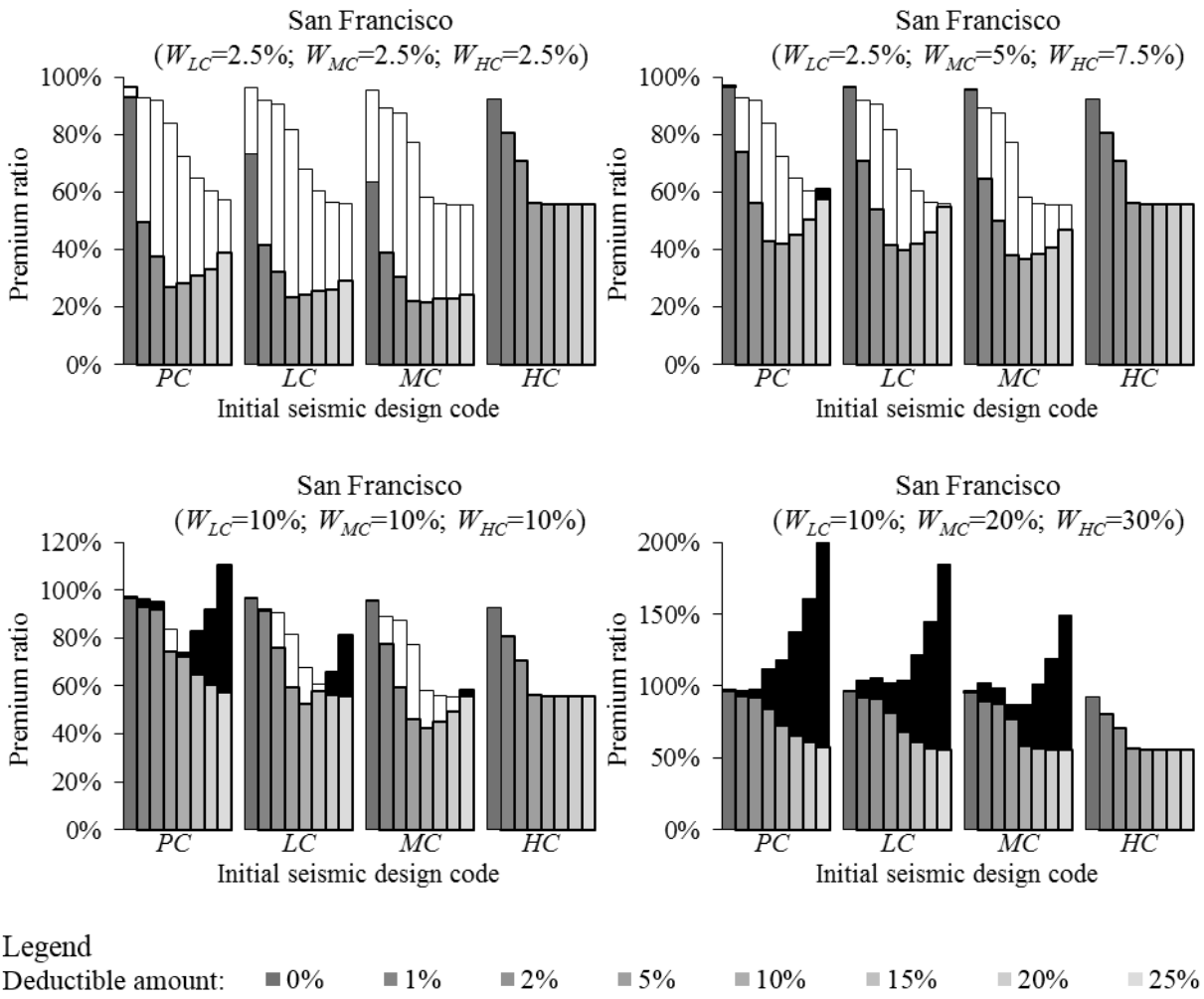


Figure 5.12: Premium ratio for the insurance cover including retrofitting works for various retrofitting costs ($W_{LC}$, $W_{MC}$ and $W_{HC}$). The insured building considered is located in San Francisco and with different initial seismic design codes (*IC*): Pre-Code (*PC*), Low-Code (*LC*), Moderate-Code (*MC*) and High-Code (*HC*). Grey bars show the premium ratio value for different levels of deductible amount (*F*). White and black bars on the top of the grey bars show when the premium ratio including retrofitting works is lower and higher than the previous premium ratio obtained without retrofitting works (Fig. 5.10), respectively.

investigates to what extent homebuilder companies can contribute to the financial effort that the annual premium amount represents.

## 5.7. Involving homebuilder companies and public authorities in the insurance scheme

The proposed earthquake insurance model gives a key role to homebuilder companies since insurance companies pays for both the repairs/reconstruction works of a damaged insured house

and retrofitting works. Therefore, such insurance model can be enhanced by a close collaboration between insurance and homebuilder companies. Homebuilder companies may be interested in taking part of this model, foremost because it opens an untapped market. Currently, 85% of Californians are not insured against earthquake risk (California Department of Insurance 2019c), and consequently, may not be able to finance repairs/reconstruction works. In addition, this could be the opportunity for a homebuilder company to benefit from the insurance's own customer network at a low cost. So, fostering earthquake insurance is then a solution for homebuilder companies to develop their business.

Among all the earthquake insurance solutions, the one introduced in this study is also very attractive for homebuilder companies. First, it is the first one scheduling seismic retrofitting works, which is an additional market for them. Next, the insurance compensation, in this model, is to perform repairs/reconstruction works instead of providing a financial amount. Consequently, the insurance compensation guarantees that adequate funds will be allocated to repairs/reconstruction works. Indeed, Marquis et al. (2017), showed that after the 2010-2011 Canterbury earthquakes most of affected people prefer to leave instead of repairing/reconstructing their house, partly because insurance compensations were lower than the cost of works. Finally, being involved in such a sustainable development collaboration can be also valuable for a homebuilder company's reputation.

The first characteristic of a financial asset is its earnings. When a homebuilder company perform repairs/reconstruction or retrofitting works, the corresponding expected earnings can be estimated by the average income rate ($b$) multiplied by the revenues:

$$\text{expected earnings} = \begin{cases} b \times W_{LC} & \text{for retrofitting works from } PC \text{ to } LC \\ b \times W_{MC} & \text{for retrofitting works from } LC \text{ to } MC \\ b \times W_{HC} & \text{for retrofitting works from } MC \text{ to } HC \\ b \times \mathbb{E}(L_{EQ}) & \text{for repairs/reconstruction works} \end{cases} \tag{5.20}$$

After the first damaging earthquake ($EQ$), the expected earnings are calculated based on the expected loss (Eq. 5.20, ($L_{EQ}$)) and not the expected insured loss (Eq. 5.1, ($L_{EQ}$) − $F$) because the policyholder is assumed to pay the deductible amount to the homebuilder company for performing the repairing works. Table 5.3 shows the average income rate ($b$) for the three biggest homebuilder companies in the USA and operating in California over the last four years (*ConstructionDive*, Nowicki 2014).

A second important variable, called the maturity ($m$) in this study, is the time to wait before receiving the first payment. In this case, the maturity is the time when, for a considered insured

Table 5.3: Average income rates for the three main homebuilder companies in the USA in 2013 according to Construction Dive (2014). Net incomes and total revenues figures are extracted from the annual reports of each company. Values outside and inside brackets are net and gross of taxes, respectively.

| Main Homebuilder companies | 2018 | 2017 | 2016 | 2015 |
|---|---|---|---|---|
| D.R. Horton Inc. | 9% (13%) | 7% (11%) | 7% (11%) | 7% (11%) |
| Pulte Group Inc. | 10% (13%) | 5% (11%) | 8% (12%) | 8% (14%) |
| Lennar Corp. | 8% (11%) | 6% (9%) | 8% (12%) | 9% (14%) |

house, the first works is undertaken (either for repairing, reconstructing or retrofitting the house). Therefore, the maturity *m* is given by the following equation:

$$m = \begin{cases} \mathbb{E}\left(\min\left(T^{LC}; Y_{EQ}\right)\right) & \text{if } IC{=}PC \\ \mathbb{E}\left(\min\left(T^{MC}; Y_{EQ}\right)\right) & \text{if } IC{=}LC \\ \mathbb{E}\left(\min\left(T^{HC}; Y_{EQ}\right)\right) & \text{if } IC{=}MC \\ \mathbb{E}\left(Y_{EQ}\right) & \text{if } IC{=}HC \end{cases} \tag{5.21}$$

The maturity *m* is calculated in Equation 5.21 with the UCERF3/HAZUS-MH MR5 model and illustrated in Figures 5.13 and 5.14 for San Francisco and Los Angeles, respectively, and different retrofitting costs, deductible amount (*F*) and initial seismic design code (*IC*). They show that, in most cases the period before the first retrofitting works is either very short (i.e. the first retrofitting works the years following the insurance policy issuance) or very long (i.e. close to 50y, the upper bound according to Eq. 5.19). In the first case, seismic retrofitting works contribute to decrease the risk and so the premium amount (*P*), despite the cost of works. As insurance company is supposed to have enough capital for financing the works, they are undertaken immediately. This expense is refunded later by the premium add-on ($P_{LC}$, $P_{MC}$ and $P_{HC}$) paid by the policyholder until the next damaging earthquake (*EQ*). As expected, the lower the retrofitting costs, the sooner the date for the retrofitting works.

At the opposite, the first retrofitting works is planned decades later (around 50y), in two cases: for vulnerable houses with a low deductible amount (Fig. 5.13, tags 1) and for resistant houses with a high deductible amount (Fig. 5.13, tags 2). For the first one, the occurrence probability of the first damaging earthquake above the deductible amount is high. This is shown in Figures 5.13 and 5.14 by an expected occurrence time of ($Y_{EQ}$) significantly below the time for the next retrofitting works ($T^{LC}$, $T^{MC}$ and $T^{HC}$). Consequently, the maturity (Eq. 5.21) is too short for collecting enough premiums for paying the retrofitting works. In such a case, this insurance model would require a higher deductible amount to be applicable.

About high deductible and high seismic design level (Fig. 5.13, tag 2), the earthquake risk covered by the insurance is not material, giving a low-priority to seismic retrofitting works.

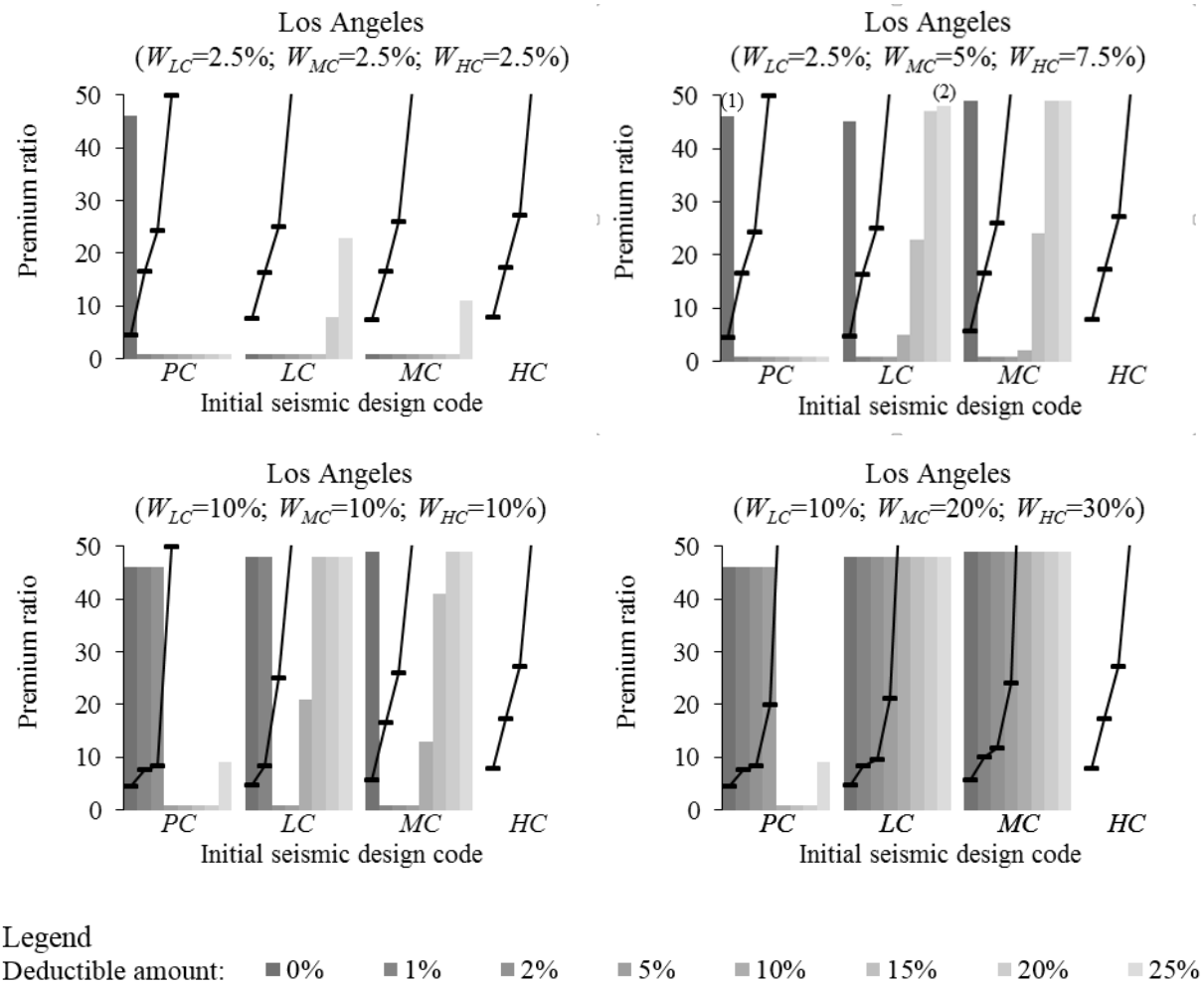


Figure 5.13: Illustration of the maturity (*m*) of repairs/reconstruction or retrofitting works for a building located in Los Angeles and different retrofitting costs ($W_{LC}$, $W_{MC}$, $W_{HC}$), deductible amount (*F*) and initial seismic design code (*IC*): Pre-Code (*PC*), Low-Code (*LC*), Moderate-Code (*MC*) and High-Code (*HC*). The black line represents $\mathbb{E}(Y_{EQ})$, the expected time before the first earthquake causing a damage above the deductible amount *F*. The histogram shows the time for the next retrofitting works (e.g. from *LC* to *MC* when the initial seismic design code is *LC*). On each graph, the maturity *m* corresponds to the minimum between the histogram and the black line. Tags (1) and (2) refer to examples described in the text.

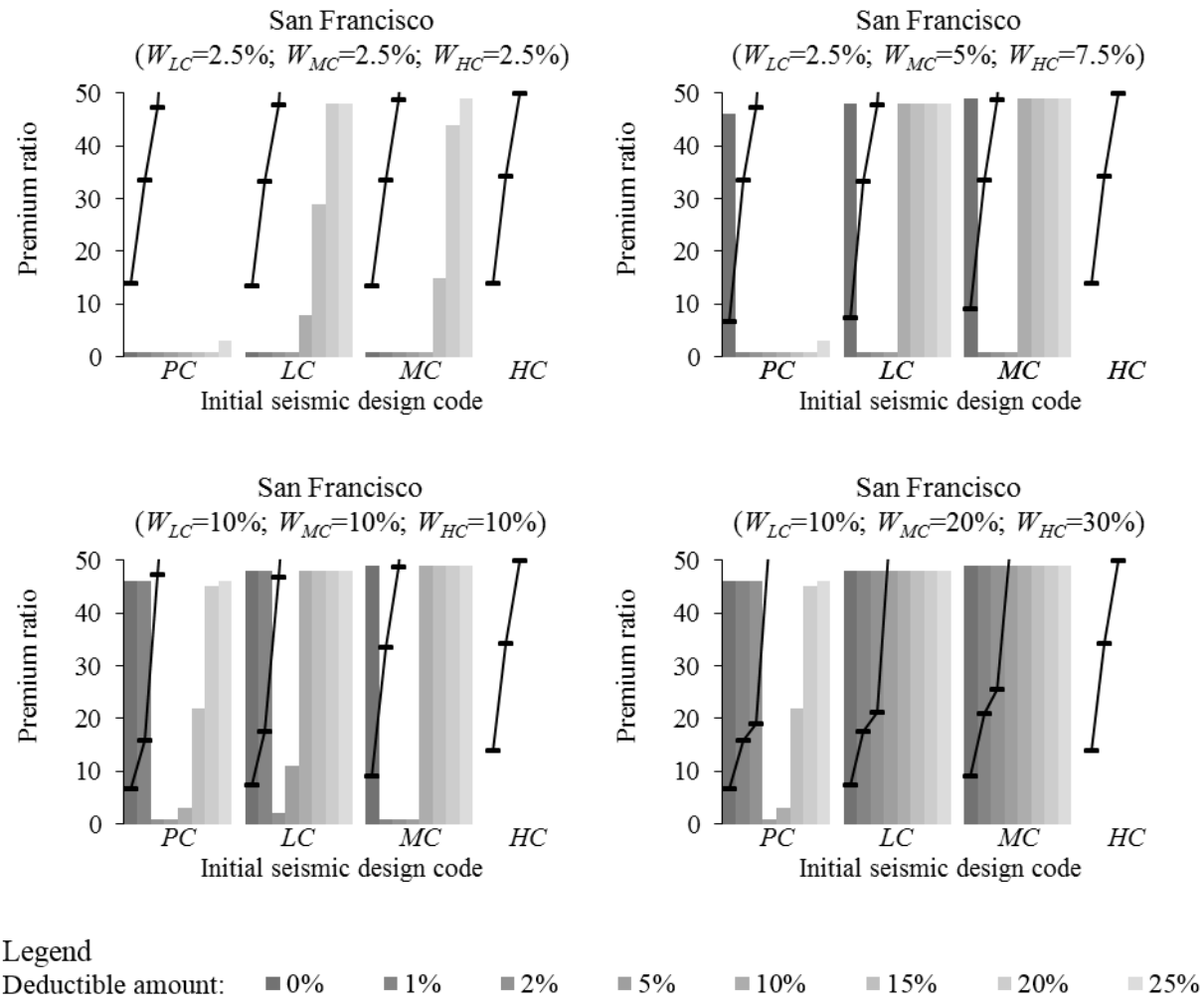


Figure 5.14: Illustration of the maturity ($m$) of repairs/reconstruction or retrofitting works for a building located in San Francisco and for different retrofitting costs ($W_{LC}$, $W_{MC}$, $W_{HC}$), deductible amount ($F$) and initial seismic design code ($IC$): Pre-Code ($PC$), Low-Code ($LC$), Moderate-Code ($MC$) and High-Code ($HC$). The black line represents $\mathbb{E}(Y_{EQ})$, the expected time before the first earthquake causing a damage above the deductible amount $F$. The histogram shows the time for the next retrofitting works (e.g. from $LC$ to $MC$ when the initial seismic design code is $LC$). On each graph, the maturity $m$ corresponds to the minimum between the histogram and the black line.

Furthermore, the expected time before the next damaging earthquake ($Y_{EQ}$) is also large (Fig.5.13 and 5.14), leading to a high maturity (Eq. 5.21). However, even in this case, this insurance model can offer a significant premium decrease (Fig. 5.11 tag 3 and Fig. 5.13 tag 2).

These results indicate that homebuilder companies can have a significant interest in the market provided by this insurance model, especially when the maturity $m$ is low (Eq. 5.21). Hence, a homebuilder can be asked for paying an annual amount as a balance. With the same methodology than for $P_{LC}$, $P_{MC}$ and $P_{HC}$ (Eq. 5.15), the contributions from a homebuilder company for the repairs/reconstruction works (called $C_1$) and for the retrofitting works from

*PC* to *LC* (called $C_{LC}$), *LC* to *MC* (called $C_{MC}$) and *MC* to *HC* (called $C_{HC}$) are derived from (Eq. 5.11, 5.14, 5.18, 5.19 and 5.20), as follows:

$$\begin{cases} \sum_{i=1}^{+\infty}\left[C_{LC} \times (1+t_H)^{i-1} \times \mathbb{P}\left(Y_{EQ} \geq i\right)\right] = \sum_{i=T^{LC}}^{+\infty}\left[b \times W_{LC} \times (1+t_H)^{i-T^{LC}} \times \mathbb{P}\left(Y_{EQ} = i\right)\right] \\ \sum_{i=1}^{+\infty}\left[C_{MC} \times (1+t_H)^{i-1} \times \mathbb{P}\left(Y_{EQ} \geq i\right)\right] = \sum_{i=T^{MC}}^{+\infty}\left[b \times W_{MC} \times (1+t_H)^{i-T^{MC}} \times \mathbb{P}\left(Y_{EQ} = i\right)\right] \\ \sum_{i=1}^{+\infty}\left[C_{HC} \times (1+t_H)^{i-1} \times \mathbb{P}\left(Y_{EQ} \geq i\right)\right] = \sum_{i=T^{HC}}^{+\infty}\left[b \times W_{HC} \times (1+t_H)^{i-T^{HC}} \times \mathbb{P}\left(Y_{EQ} = i\right)\right] \\ \sum_{i=1}^{+\infty}\left[C_1 \times (1+t_H)^{i-1} \times \mathbb{P}\left(Y_{EQ} \geq i\right)\right] = b \times \mathbb{E}\left(L_{EQ}\right) \end{cases} \quad (5.22)$$

where $t_H$ is the rate of return on investments available for the homebuilder company. It can be interpreted as the share of the profits made by the insurance company by investing the premium amount paid by the homebuilder company (Eq. 5.22, $C_1$, $C_{LC}$, $C_{MC}$ and $C_{HC}$) and redistributed to the homebuilder company.

Finally, the total annual premium *P* for the homeowner is given by incorporating both retrofitting works and a contribution from the homebuilder company:

$$P = P_1 + P_2 + P_3 + P_{LC} + P_{MC} + P_{HC} - (C_1 + C_{LC} + C_{MC} + C_{HC}) \quad (5.23)$$

For the numerical applications, the following ranges of $t_H$ and *b* have been considered:

$$\begin{cases} 0.05\% \leq t_H \leq 1.25\% \\ 0\% \leq b \leq 15\% \end{cases} \quad (5.24)$$

The rate of return on investments offered to homebuilder companies is considered strictly positive to compensate the financial effort that represents the cash flow corresponding to $C_1$, $C_{LC}$, $C_{MC}$ and $C_{HC}$. The upper bound (1.25%) is slightly lower than $t_I$ (equal to 1.3%) so that insurance company makes always a profit from investing homebuilder companies' contribution. About the average income rate (*b*), the lower bound at 0% represents the situation when homebuilder companies are not part of the insurance model (Fig. 5.11 and 5.12). The upper bound (15%) has been assessed considering market values (Tab. 5.3) and assuming that public authorities could incentivize this initiative by making free of tax the works organized within this insurance scheme. It results in an upper bound at 14% (Tab. 5.3) which is increased up to 15% for considering additional non-financial interests that a homebuilder company can also have in participating in this insurance model (strategically-based decision, e.g. access to new

customers, increase market volume, economic outlook …). Results obtained from Equations 5.11 to 5.24 are shown in Figures 5.15 and 5.16.

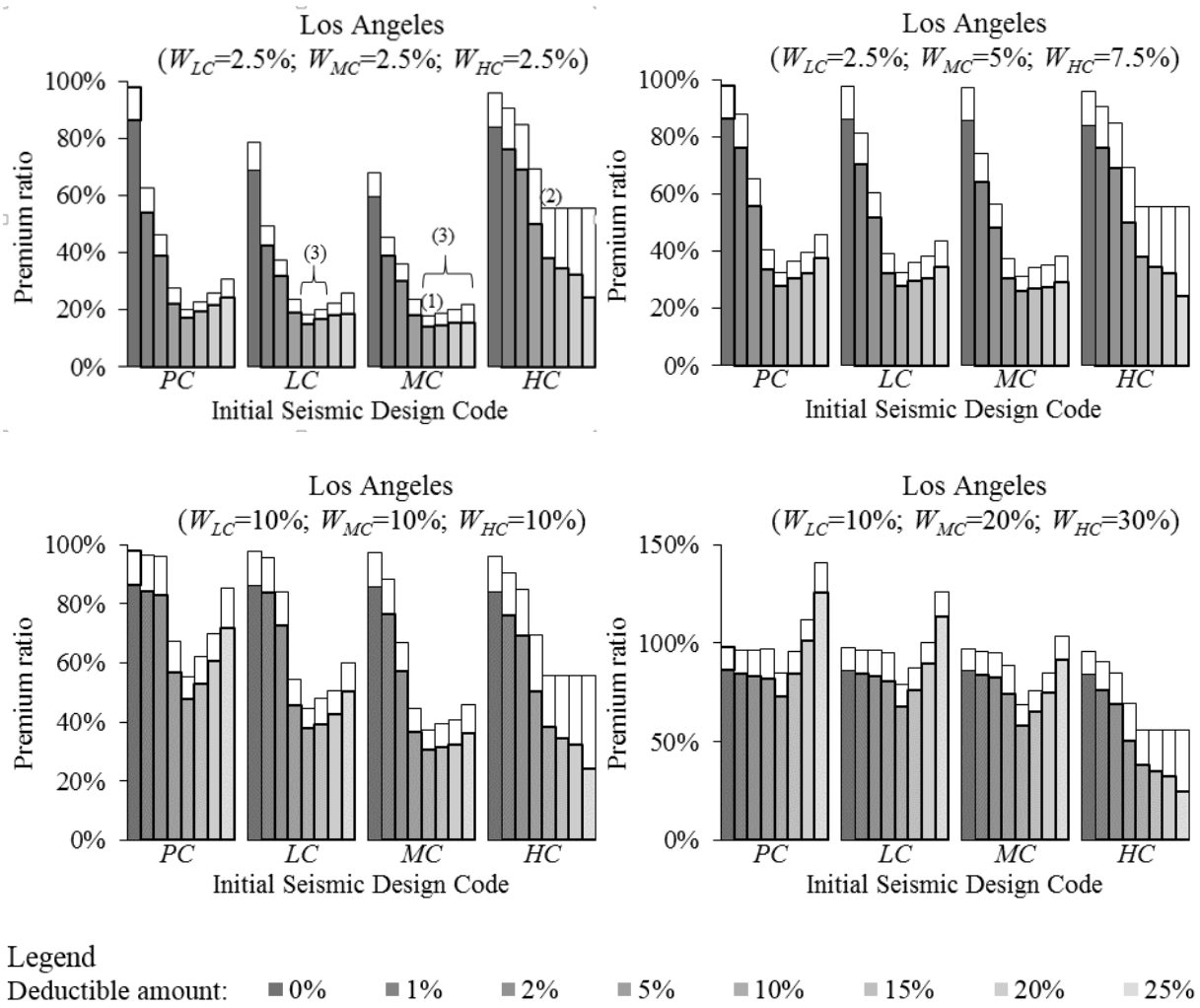


Figure 5.15: Premium ratios including the homebuilder companies' contributions ($C_1$, $C_{LC}$, $C_{MC}$ and $C_{HC}$) for having the repairs/reconstruction and the retrofitting works. Grey bars show the premium ratio value for different level of deductible amount ($F$) considering the maximum homebuilder companies' contributions, calculated with an average income rate $b$=15% and a rate of return on investment $t_H$ = 0.05%. The white bars at the top of grey bars represent the decrease of premium ratio thanks to the homebuilder companies' contributions (grey and white bars correspond to the premium ratios obtained with retrofitting works, illustrated in Fig. 5.13). The results are presented for Los Angeles, several retrofitting costs ($W_{LC}$, $W_{MC}$ and $W_{HC}$) and different initial seismic design code: Pre-Code (*IC=PC*), Low-Code (*IC=LC*), Moderate-Code (*IC=MC*) and High-Code (*IC=HC*). Tags (1), (2) and (3) refer to examples described in the text.

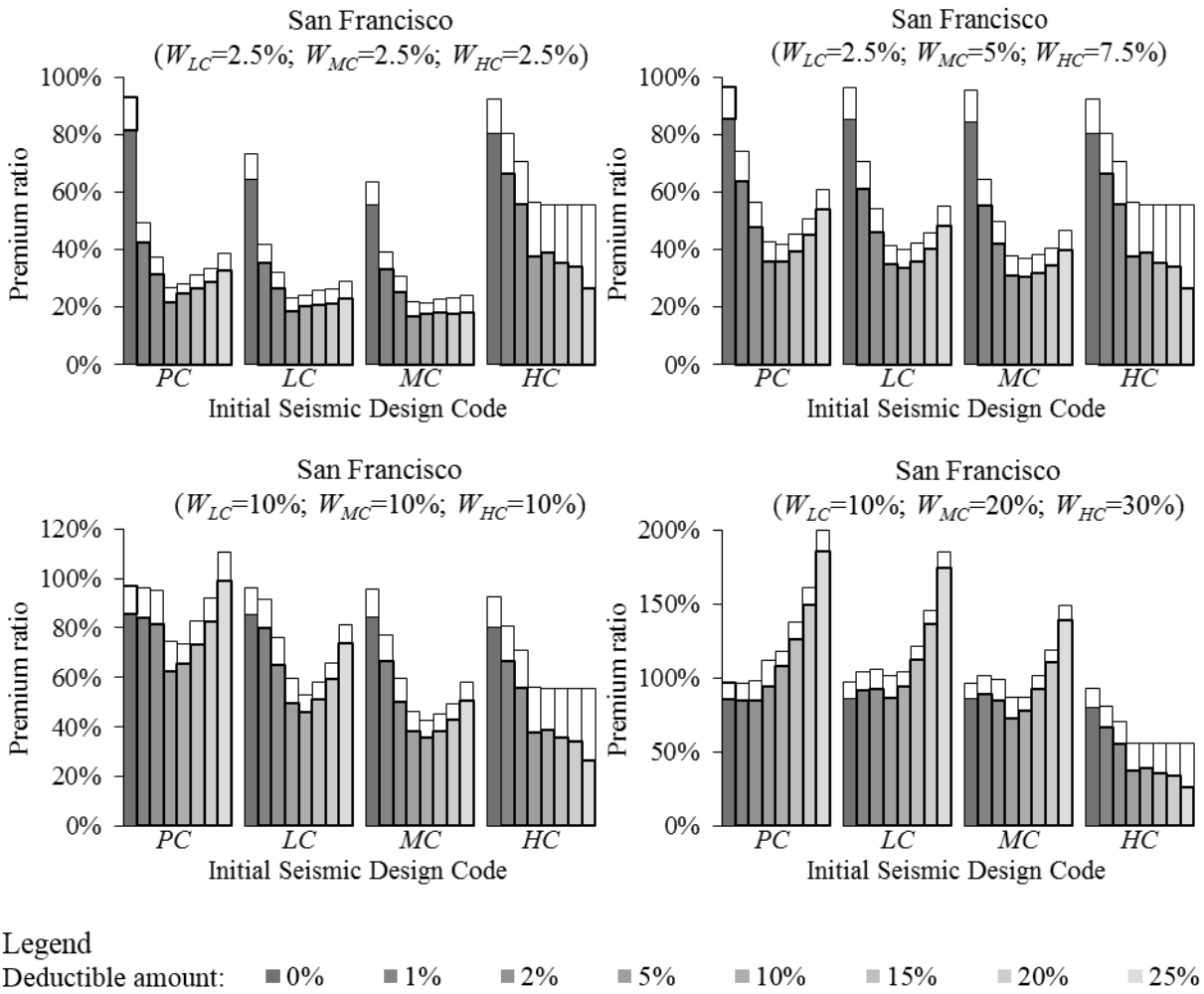


Figure 5.16: Premium ratios including the homebuilder companies' contributions ($C_1$, $C_{LC}$, $C_{MC}$ and $C_{HC}$) for having the repairs/reconstruction and the retrofitting works. Grey bars show the premium ratio value for different level of deductible amount ($F$) considering the maximum homebuilder companies' contributions, calculated with an average income rate $b$=15% and a rate of return on investment $t_H$ = 0.05%. The white bars at the top of grey bars represent the decrease of premium ratio thanks to the homebuilder companies' contributions (grey and white bars correspond to the premium ratios obtained with retrofitting works, illustrated in Fig. 5.14). The results are presented for San Francisco, several retrofitting costs ($W_{LC}$, $W_{MC}$ and $W_{HC}$) and different initial seismic design code: Pre-Code (*IC=PC*), Low-Code (*IC=LC*), Moderate-Code (*IC=MC*) and High-Code (*IC=HC*). Tags (1), (2) and (3) refer to examples described in the text.

Let us consider two houses built in Los Angeles under Moderate-Code (Fig. 5.15 tag 1) and High-Code (Fig. 5.15 tag 2). Assuming that seismic retrofitting works costs a constant 2.5%, the premium amount under this insurance scheme is equal to 18% and 67% (Fig. 5.15, tags 1 and 2, grey and white bars) of the current earthquake premium amount ($P^{M}$), respectively. Furthermore, a high contribution from homebuilder companies, including a tax-free policy, can make this premium amount decrease down to 14% and 50%, respectively (Fig. 5.15, tags 1 and 2, grey bar only).

The homebuilder companies' contribution can bring the premium amount $P$ as low as 16% in best cases (Fig. 5.15 tag 3). Such a decrease would make the premium amount affordable for all homeowners in California, according to the earthquake insurance consumption model developed in Chapter 3, Section 2. Furthermore, when the retrofitting costs do not exceed 10%, at least one deductible amount allows a premium decrease by a factor of three (Fig. 5.15 and 5.16). In such cases (i.e. a premium ratio around 33%), this insurance would be still affordable for the majority of California homeowners, according to the model developed in Chapter 3, Section 2.

Despite this study shows that a new earthquake insurance solution is possible, several issues still need to be addressed. First, the number of insurance policies issued at the same time could be limited both by homebuilder companies' financing capacity and insurance companies' claim-paying capacity. Moreover, the attractiveness of such an insurance policy for homebuilder companies can also have a large impact. The attractiveness highly depends on the profitability rate $t_H$. Furthermore, if its value is set at the start of the insurance policy and cannot be updated according to the economic fluctuations (Fig. 5.3), it must be significantly below $t_I$. Indeed, since $t_I$ fluctuates according to the market (Fig. 5.3), the profits made by the insurance company can be lower than the profits retroceded to the homebuilder company (i.e. $t_I \leq t_H$) in case of low interest rates (e.g. in 2013, Fig. 5.4). Consequently, the capital for paying the planned works (either after a damaging earthquake or the retrofitting works) could be inadequate, putting the insurance company into bankruptcy. At the opposite, a low $t_H$ can discourage homebuilder companies to invest in this insurance model if more attractive financial assets are available on financial markets.

This insurance scheme shows also several limits when looking at the evolution with time of a building and the ownership. Indeed, various events like a change in ownership, the building's level of dilapidation with time, a bankruptcy of the insurance or the homebuilder company can lapse such an insurance policy. Also, this kind of insurance policy is expected to expire at year $Y_{EQ}$ corresponding to the occurrence of the first damaging earthquake above the deductible amount. As illustrated in Figures 5.13 and 5.14, the expected value of $Y_{EQ}$ can reach in hundreds of years, and consequently be too long for an insurance policy maturity.

Last, in case of a destructive earthquake, organizing repairs/reconstruction works can also be an issue for a homebuilder company: roads may be impassable, some delays can be expected in the supply chain, or even the homebuilder company itself can be affected by the earthquake. Last but not least, if the number of repairs/reconstruction works at the charge of a homebuilder

company during the aftermath of an earthquake is too large, it can also lead to delays in the recovery process.

## 5.8. Conclusions

Based on the observation that earthquake insurance in California is unaffordable for most homeowners (California Department of Insurance database), this study introduces a new earthquake insurance solution leveraging on profits made on financial markets, retrofitting works and the participation of homebuilder companies to offer an earthquake cover at a lower price. The decrease is expected to be large enough to make this long-term property earthquake insurance affordable for most of California homeowners (Chapter 3, Section 2).

Such a low-cost insurance cover is possible foremost by considering seismic retrofitting works as a solution to significantly mitigate the vulnerability to earthquake. According to a schedule optimizing the risk reduction, retrofitting works are organized at the issuance of the insurance policy. Consequently, the capital made by insurance company from the collected premium amount is dedicated to strengthening the insured houses when it is not used for paying the claims.

This insurance scheme for reducing the earthquake insurance protection gap includes also the homebuilder companies and the public authorities as key stakeholders for risk reduction. To be affordable, part of the premium amount needs to be borne by the economic sector. For that, this model proposes to capitalize on the future revenues associated to the insurance compensation during the post-disaster repairs/reconstruction phase.

Last, developing such an earthquake insurance policy is a huge opportunity to involve all the stakeholders in the effort for reducing the protection gap and build resilient cities. Nevertheless, further studies are still necessary to make this outcome a ready-for-market insurance policy. Several variables as the homebuilder companies' available capital, the insurance company claim-paying capacity, or even the main events that could affect insured buildings have not been investigated yet. Possible connections with current earthquake mitigation plans have also to be identified to make the global risk reduction effort the most efficient. So, a larger contribution from the public authorities could be investigated, especially about co-funding seismic retrofitting works.

# CHAPTER 6: GENERAL CONCLUSIONS AND PERSPECTIVES

L'augmentation de la population et des richesses dans les zones exposées aux catastrophes naturelles a pour conséquence des événements de plus en plus dévastateurs. Dans le même temps, l'assurance n'a pas su conquérir de nouveaux marchés, et, en moyenne, la part des pertes assurées est restée constante. En 2017, plus de €100bn de dégâts causés par des catastrophes naturelles n'ont pas été pris en charge par l'assurance.

Pour le risque de tremblement de terre, les différentes solutions existantes sont le résultat d'une évolution empirique, influencée par le niveau économique du pays et la survenance des séismes passés. Ainsi, dans les pays en voie de développement, le montant de la prime dépend du temps écoulé depuis le dernier séisme destructeur : plus celui-ci est ancien, plus le montant de la prime est faible. En France, l'Etat a un rôle prépondérant dans le système assurantiel. Au titre de la solidarité nationale, il porte la responsabilité de rembourser la majorité des pertes assurées en cas d'un séisme majeur. En 1992, un système assurantiel public a également été lancé en Californie (le California Residential Earthquake Recovery program) mais a fait faillite la même année à cause de la survenance des séismes de Big Bear et Landers (Mw6.5 et Mw7.3 ; coût économique direct: $100m.) et Petrolia (Mw7.2 ; coût économique direct: $75m.). Par conséquent, le système assurantiel actuellement en vigueur en Californie repose sur des assurances privées très chères mais avec une très forte solidité financière pour faire face à des séismes extrêmes, comme celui de Northridge en 1994.

Ce tremblement de terre, tout comme celui de Tohoku (Japon) en 2011, a mis en lumière le manque de maîtrise dans l'estimation des pertes qu'ils pouvaient causer. En effet, aucun de ces deux événements n'avaient été envisagé par les assurances avant leur survenance. Cependant, le développement de modèles stochastiques de pertes plus performants nécessite au préalable de pouvoir tester et comparer ceux existants avec d'autres modèles (comme les modèles PSHA), ou des données historiques. En ce sens, les travaux menés durant cette thèse ont permis de créer deux méthodes de comparaison : l'une pour les estimations d'aléa sismique et l'autre pour les coûts de remplacement correspondant à différents niveaux d'endommagement. Néanmoins, beaucoup de travail est encore nécessaire pour interpréter les résultats de ces tests afin

d'identifier et de corriger les faiblesses dans les modèles actuels. Les analyses menées durant la thèse indiquent toutefois que cet effort devrait porter en priorité sur le développement de relations dommages-cout stochastiques. En effet, les modèles existants sont déterministes alors que l'erreur de modélisation, obtenue en les testant sur des séismes historiques, a un écart-type équivalent à un facteur 6. Cela signifie que lorsqu'une relation dommage-cout donne une perte de €100m. pour un nombre connu de bâtiments endommagés et détruits, l'intervalle correspondant à plus ou moins l'écart-type est [€16m.; €630m.]. Comme les relations sont déterministes, cette incertitude n'est pas aujourd'hui prise en compte dans les modèles stochastiques de pertes et fait donc porter un risque de sous-estimation des pertes consécutives aux séismes les plus dévastateurs.

Bien qu'une meilleure connaissance du risque sismique soit indispensable au développement de l'assurance, il n'en reste pas moins un contrat commercial. Cela implique que les clients et les compagnies d'assurance consentent mutuellement aux conditions fixées au contrat. La revue des systèmes assurantiels menée durant cette thèse a permis de montrer que dans beaucoup de systèmes assurantiels, ce consentement n'est que partiel, obligeant les pouvoirs publics à intervenir : en France, l'Etat impose un faible montant de primes aux compagnies d'assurance en échange du remboursement des pertes au-delà d'un certain seuil. En Californie, les pouvoirs publics incitent fortement les gens à souscrire une assurance pour se prémunir des conséquences malgré le prix élevé, car l'aide apportée par les pouvoirs publics après un séisme sera limitée. En outre, le principal assureur pour le risque tremblement de terre (le CEA) est dirigé par l'Etat Californien.

L'introduction d'une nouvelle police correspondant aux attentes des clients est donc une condition sine qua non au développement de l'assurance tremblement de terre. Le défi est très important car, en Californie, la baisse du montant de la prime attendue par la majorité des personnes est de 66%, soit un prix trois fois moins cher. Cependant, le montant élevé des primes d'assurance reflète le pouvoir destructeur des séismes. Pour limiter les effets d'une catastrophe, les populations ont de tout temps mis en place des mesures de prévention. Ainsi, après le tremblement de terre de 1509 qui détruisit Constantinople, les autorités Ottomanes ont imposé d'utiliser le bois comme matériau de reconstruction au détriment de la maçonnerie, à cause des dégâts constatés pour ce matériau. Encore de nos jours, les mesures de préventions sont rarement appliquées avant la survenance d'une catastrophe. Par exemple, en France, la réglementation parasismique ne concerne que les nouvelles constructions et les bâtiments faisant l'objet de travaux importants. Or, entre 30% et 50% du parc immobilier Français a été

construit avant la mise en vigueur de normes parasismiques et présente donc un risque accru en cas de tremblement de terre. L'adoption d'une politique plus proactive pour l'application des normes parasismiques permettrait donc de faire diminuer le risque et, par conséquent, le montant de la prime d'assurance.

C'est sur la base de ces observations qu'un nouveau modèle d'assurance a été développé durant la thèse. Inspiré d'un modèle de type assurance-vie, ses deux principales caractéristiques sont de planifier et de financer des travaux de renforcement parasismiques sur chaque bâtiment assuré, car le coût que cela représente est largement compensé par la diminution de la vulnérabilité et donc du montant des sinistres futurs. Le deuxième aspect innovant est la participation des entreprises en bâtiment et des pouvoirs publics. Ces acteurs ont un rôle central dans la reconstruction d'une zone sinistrée après un séisme. Or, les indemnités d'assurance versées représentent une part importante de sources de financement dont ils ont besoin. Il est donc cohérent qu'ils aient une part active dans ce nouveau système assurantiel. Le premier type de contribution identifié dans cette thèse consiste en une participation financière afin de diminuer la prime d'assurance. Cependant, bien d'autres synergies sont envisageables comme un plan de prévention conjoint entre les pouvoirs publics et les acteurs économiques, un partage des informations concernant les bâtiments exposés ou encore la création d'un vaste pôle de recherche interdisciplinaire dédiée à l'étude des conséquences d'un tremblement de terre.

Bien que les résultats obtenus en termes de réduction du montant de prime soient encourageants, beaucoup de questions quant à la mise en œuvre d'une telle solution d'assurance n'ont pas pu être traitées durant la thèse. Celles-ci sont tout d'abord d'ordre financier : les réserves financières que cela imposerait pour les compagnies d'assurance doivent être calculées afin de garantir leur solvabilité. En outre, comme le modèle prévoit l'investissement sur les marchés financiers du montant des primes, l'impact qu'auraient différents chocs financiers doit aussi être étudié. Cela permettra de connaître dans quelle mesure ce type d'assurance représente ou non un risque systémique (c'est-à-dire de déclencher une crise financière). Enfin, pour les entreprises en bâtiment, cette police d'assurance correspond à un placement financier. Par conséquent, le niveau de participation de ces entreprises dépend de l'attrait qu'elle représente par rapport à d'autres investissements, que ce soit en termes de rentabilité ou de risque de perdre tout ou partie du capital investi. Cette comparaison est d'autant plus difficile qu'au-delà d'une marge financière, la police d'assurance apporte également un intérêt économique en garantissant des marchés futurs.

A ce sujet, beaucoup d'interrogations existent aussi sur la dimension économique. La première concerne une possible inflation des coûts après le séisme : comment seraient répartis d'éventuels surcoûts dans les travaux de reconstruction ou réparation par rapport au prix décidé à l'émission du contrat d'assurance ? Ensuite, le risque de faillite de la compagnie d'assurance ou de l'entreprise en bâtiment n'est pas à négliger. En effet, cette police d'assurance prenant fin après le premier séisme destructeur, elle peut rester en vigueur pendant plusieurs années durant lesquelles d'autres événements peuvent survenir. Une autre problématique qui ne peut pas être exclue est le risque que survienne un séisme si destructeur que la compagnie d'assurance n'ait pas assez d'argent pour payer l'ensemble des travaux de reconstruction ou de réparation. Il est également possible que ce soit l'entreprise en bâtiment qui n'ait pas les ressources nécessaires pour mener l'ensemble des travaux dans un délai raisonnable.

Une autre menace économique bien connue en assurance est celle de l'anti-sélection. Le principe de l'assurance présuppose que la survenance du risque assuré soit aléatoire. Or, la plupart des personnes manifeste leur volonté de souscrire une police d'assurance lorsqu'elles sentent que le risque peut se produire rapidement. Une illustration en assurance tremblement de terre est le pic des demandes de souscription après un séisme pour être couvert au cas où une réplique causerait des dégâts. Limiter l'anti-sélection dans les contrats d'assurance souscrits est donc un paramètre important pour garantir la viabilité du modèle.

Lister les difficultés que rencontrerait la mise en œuvre d'une telle police d'assurance amène également à soulever plusieurs interrogations au sujet des droits de l'assuré. Tout d'abord, elles portent sur les conditions et le coût induit par le relogement durant les travaux après un séisme. En outre, une personne peut être amenée à déménager, faire des travaux ou subir un sinistre (par exemple dégât des eaux ou un incendie). La situation personnelle de l'assuré peut également le pousser à vouloir résilier le contrat ou à changer d'assureur ou d'entreprise en bâtiment. Ce sont là autant de changements qui doivent être prévus au contrat d'assurance.

Le volet de la responsabilité des différentes parties au contrat est aussi un point crucial, dans la mesure où le contrat d'assurance, tel que pensé dans cette thèse, inclut dans le calcul de la prime la diminution de la vulnérabilité grâce au renforcement parasismique. Dès lors, toute malfaçon mettrait en péril l'équilibre financier et pourrait entraîner pour l'entreprise en bâtiment fautive le paiement d'une compensation financière qui pourrait être problématique si elle n'est pas anticipée. Une autre source de responsabilité juridique est le délai avant le lancement des travaux de renforcement parasismique. Comme cela s'est déjà produit en Italie après le séisme de l'Aquila (2009), ou en France après la tempête Xynthia (2010) pour les pouvoirs publics, les

compagnies d'assurance et en bâtiment engagées dans une telle police d'assurance pourraient-elles voir leur responsabilité engagée pour la mise en danger de la vie de leurs assurés si un séisme meurtrier survient avant les travaux de renforcement parasismique, ou que ces derniers n'aient pas été d'une qualité suffisante ?

Enfin, pour terminer le tour d'horizon des problématiques que soulève ce nouveau type d'assurance, il faut en revenir au risque. Depuis quelques années le risque de séisme induit par l'activité humaine est pris très au sérieux, au point que des cartes d'aléa spécifiques sont produites, que les travaux exploitations du sous-sol sont surveillés en permanence par des sismomètres et que les entreprises en assurance et réassurance s'engagent auprès de la communauté scientifique dans des projets internationaux comme URBASIS. La faible fréquence annuelle des séismes destructeurs, même dans les zones les plus sismiques comme la Californie, est un paramètre indispensable pour que le modèle assurantiel proposé fonctionne. Par conséquent, l'augmentation de la fréquence que pourrait créer la sismicité induite par l'activité humaine pourrait rendre inapplicable cette solution assurantielle. De surcroît, cela renforcerait le problème de l'anti-sélection puisqu'il est envisageable que les personnes vivant à proximité d'un site industriel souscrivent massivement ce type d'assurance, s'attendant à subir les dégâts d'un séisme.

Une autre catégorie de risques à prendre en compte est celle des risques engendrés par un séisme. Ainsi, la police d'assurance doit-elle prendre en charge la réparation ou la reconstruction de bâtiments touchés par un accident nucléaire (ville de Namie au Japon à la suite du séisme de Tohoku en 2011), par un incendie (San Francisco à la suite du séisme de 1906), par un tsunami (ville de Palu en Indonésie à la suite du séisme de 2018), ou encore par un effet de liquéfaction (ville de Niigata à la suite du séisme de 1964) ? Autant de risques qui sont soit à quantifier pour adapter le calcul de la prime d'assurance, soit à exclure sur la base de critères objectifs et compréhensibles par les assurés.

Bien que nombreuses, toutes ces problématiques ne sont pas des barrières au développement d'un nouveau type d'assurance tremblement de terre mais représentent, au contraire, les défis à relever pour permettre sa commercialisation. L'enjeu est d'autant plus grand qu'elle pourrait même être, à terme, étendue à l'ensemble des risques de catastrophes naturelles. En effet, le modèle sous-jacent s'appuie d'une part sur la faible fréquence annuelle des tremblements de terre destructeurs, et d'autre part sur la possibilité de diminuer la vulnérabilité des bâtiments par des travaux. Or, ces deux caractéristiques sont partagées par la plupart des risques de

catastrophes naturelles, notamment les inondations et les tempêtes, qui sont les deux autres types d'événements les plus dévastateurs avec les séismes.

Même si cette thèse soulève plus de questions qu'elle n'apporte de réponses, nous espérons que ces travaux inspireront de nouveaux projets de recherches pour, à terme, aboutir à une solution économique dans laquelle l'ensemble des acteurs œuvreront à une société plus résiliente. Que ce soit pour protéger les biens et les personnes avant une catastrophe ou pour permettre une gestion de crise plus efficace et garantir une relance rapide de l'activité économique, un nouveau modèle économique doit émerger, dans lequel l'assurance a un rôle indispensable.

# DATA AND RESOURCES

This PhD work has been made possible by using the following open-source databases:

California Department of Insurance databases:

- Data & Reports, California Department of Insurance, www.insurance.ca.gov/0250-insurers/0600-data-reports (last accessed: 11/11/2019).
- Residential and Earthquake Insurance Coverage Study, www.insurance.ca.gov/0400-news/0200-studies-reports/0300-earthquake-study/ (last accessed: 30/07/2019).
- Summary of 1997 Residential Market Totals, California Department of Insurance Statistical Analysis Division, May 2002, www.insurance.ca.gov/0400-news/0200-studies-reports/0300-earthquake-study/ (last accessed: 19/09/2019)
- California Insurance Market Share Reports, www.insurance.ca.gov/01-consumers/120-company/04-mrktshare/2016/upload/PrmLssChartHistorical2016.pdf (last accessed: 17 / 12 / 2017).
- (1991-2015 California P&C Historical Premium and Loss, Rate Specialist Bureau, California Department of Insurance, April 30th, www.insurance.ca.gov/01-consumers/120-company/04-mrktshare/2015/ (last accessed: 04/10/2019).

CATDAT database:

- https://earthquake-report.com/ (last accessed: 12/12/2019).

CRESTA database:

- CRESTA: www.cresta.org (last accessed: 12/12/2019).

DesInventar database:

- Sendai Framework for Disaster Reduction, United Nations Office for Disaster Risk Reduction - www.desinventar.net/DesInventar/results.jsp (last accessed: 17/11/2017).

EM-DAT database:

- The Emergency Events Database - Université catholique de Louvain (UCL) - CRED, D. Guha-Sapir - www.emdat.be, Brussels, Belgium, https://www.emdat.be/emdat_db/ (last accessed: 02 / 08 / 2018).

European Commission databases:

- Schiavina, Marcello; Freire, Sergio; MacManus, Kytt (2019): GHS population grid multitemporal (1975, 1990, 2000, 2015) R2019A. European Commission, Joint Research Centre (JRC) DOI: 10.2905/42E8BE89-54FF-464E-BE7B-BF9E64DA5218 PID: http://data.europa.eu/89h/0c6b9751-a71f-4062-830b-43c9f432370f (last accessed: 12/12/2019).
- Corbane, Christina; Florczyk, Aneta; Pesaresi, Martino; Politis, Panagiotis; Syrris, Vasileios (2018): GHS built-up grid, derived from Landsat, multitemporal (1975-1990-2000-2014), R2018A. European

Commission, Joint Research Centre (JRC) DOI: 10.2905/jrc-ghsl-10007 PID: http://data.europa.eu/89h/jrc-ghsl-10007 (last accessed: 12/12/2019).

GAR database:

UNISDR 2015 Global Assessment Report (GAR2015): www.preventionweb.net/english/hyogo/gar/2015/en/home/data.php (last accessed: 12/12/2019).

GASPAR database:

- Base nationale de Gestion Assistée des Procédures Administratives relatives aux Risques (Online), www.georisques.gouv.fr/acces-aux-donnees-gaspar (last accessed: June 2019).

GEM database:

Global Earthquake Consequences Database; https://storage.globalquakemodel.org/what/physical-integrated-risk/consequences-database/ (last accessed: 12/12/2019).

Global Inventory Database:

- Jaiswal and Wald 2008: https://github.com/walshb1/gRIMM/find/UR2018 (last accessed: 12/12/2019).

GSHAP database:

Global Seismic Hazard Assessment Program, Global Map, http://static.seismo.ethz.ch/GSHAP/global/ (last accessed: 12/12/2019).

ISC database:

International Registry of Seismograph Stations: www.isc.ac.uk/registries/search/ (last accessed: 12/12/2019).

NGDC Database:

- National Geophysical Data Center / World Data Service (NGDC/WDS): Significant Earthquake Database. National Geophysical Data Center, NOAA, www.ngdc.noaa.gov/nndc/struts/form?t=101650&s=1&d=1 (last accessed: 12/12/2019).

OCHA database:

UN Office for the Coordination of Humanitarian Affairs, ReliefWeb, http://reliefweb.int/ (last accessed: 12/12/2019).

SisFrance database:

- Sismicité de la France (SisFrance): www.sisfrance.net (last accessed, October 2018).

UCERF3 databases:

- Appendix K, The UCERF3 Earthquake Catalog, by K.R. Felzer https://pubs.usgs.gov/of/2013/1165/data/ofr2013-1165_EarthquakeCat.txt (last accessed: 12/12/2019).

- UCERF3.3 Hazard Analysis Sites: https://pubs.usgs.gov/of/2013/1165/data/UCERF3_SupplementalFiles/UCERF3.3/Hazard/HazardCurves/Sites/index.html

U.S. Census Bureau databases:

- Characteristics of New Housing, www.census.gov/construction/chars/ (last accessed: 12/12/2019).
- National Population Totals and Components of Change: 2010-2017, www.census.gov/data/datasets/2017/demo/popest/nation-total.html#tables (last accessed: 10/04/2018).
- State Intercensal Tables: 1900-1990, www.census.gov/data/tables/time-series/demo/popest/pre-1980-state.html (last accessed: 10 / 04 / 2018).
- State and County Intercensal Tables: 1990-2000, www.census.gov/data/tables/time-series/demo/popest/intercensal-1990-2000-state-and-county-totals.html (last accessed: 10/04/2018).
- State Intercensal Tables: 2000-2010, www.census.gov/data/tables/time-series/demo/popest/intercensal-2000-2010-state.html (last accessed: 10/04/2018).

U.S. Department of Labor database:

- Consumer Price Index, www.dir.ca.gov/OPRL/CPI/CPIHistDataSeries.xls (last accessed: 10/04/2018).

U.S. Geological Survey (USGS) databases:

- ShakeMap database: Worden, C.B. and D.J. Wald (2016). ShakeMap Manual Online: technical manual, user's guide, and software guide, U. S. Geological Survey, https://earthquake.usgs.gov/data/shakemap/ (last accessed: 12/12/2019).
- Global slope-based Vs30 database: https://earthquake.usgs.gov/data/vs30/ (last accessed: 12/12/2019).

World Bank databases:

- World Development Indicators: Population, total: https://data.worldbank.org/indicator/SP.POP.TOTL (last accessed: 12/12/2019).
- World Development Indicators: GDP (current US$): https://data.worldbank.org/indicator/NY.GDP.MKTP.CD (last accessed: 12/12/2019).
- World Development Indicators: GDP (constant 2010 US$): https://data.worldbank.org/indicator/NY.GDP.MKTP.CD (last accessed: 12/12/2019).

# BIBLIOGRAPHY


Albarello, D. and L., Peruzza (2017). Accounting for spatial correlation in the empirical scoring of probabilistic seismic hazard estimates, Bull. Earthquake Eng., 15, 2571-2585.

Albarello, D. and V., D'Amico (2008). Testing probabilistic seismic hazard estimates by comparison with observations: an example in Italy, Geophysical Journal International, 175, pages 1088–1094.

Allen, T. I., D. J. Wald, P. S. Earle, K. D. Marano, A. J. Hotovec, K. Lin, and M. G. Hearne (2009). An Atlas of ShakeMaps and population exposure catalog for earthquake loss modelling, Bull. Earthq. Eng. 7, 701–718.

Allen, T.I. and D.J., Wald (2007). Topographic slope as a proxy for global seismic site conditions (VS30) and amplification around the globe: U.S. Geological Survey Open-File Report 2007- 1357.

Alquist, A. E. and the Seismic Safety Commission (2009). The Field Act and its Relative Effectiveness in Reducing Earthquake Damage in California Public Schools - Appendices, Seismic Safety Commission, October 2009, https://ssc.ca.gov/forms_pubs/cssc_09-02_the_field_act_report_appendices.pdf (last accessed: 16/09/2019).

Arrow, K. J. (1965). Aspects of the Theory of Risk Bearing, The Theory of Risk Aversion. Helsinki: Yrjo Jahnssonin Saatio.

Artemis (2017). Mexico confirms $150m cat bond payout for quake, October 11th, www.artemis.bm/news/mexico-confirms-150m-cat-bond-payout-for-quake/ (last accessed: 03/12/2019).

ASCE. 2010. Minimum Design Loads for Buildings and Other Structures. ASCE/SEI Standard 7-10.

Asprone, D., F., Jalayer, S., Simonelli, A., Acconcia, A., Prota and G., Manfredi (2013). Seismic insurance model for the Italian residential building stock, Struct. Saf., 70-79.

Aulady, M. F. N. and T., Fujimi (2019). Earthquake loss estimation of residential buildings in Bantul regency, Indonesia, Jàmbá Journal of Disaster Risk Studies, vol. 11, no. 1.

Bal, E, H., Crowley, R., Pinho and G., Gülay (2008). Detailed assessment of structural characteristics of Turkish RC building stock for loss assessment models. Elsevier, Soil Dynamics and Earthquake Engineering, 914–932.

Barbat, A. H., S., Lagomarsino, and L. G., Pujades (2006). Vulnerability Assessment of Dwelling Buildings, Assessing and Managing Earthquake Risk, 2, 115–134.

Barroux, E., N. A., Pino and G., Valensise (2003). Source parameters of the 11 June 1909, Lambesc (Provence, southeastern France) earthquake: a reappraisal based on macroseismic, seismological and geodetic observations, J. Geophys. Res., 108 (B9), 2454.

Båth, M. (1965). Lateral Inhomogeneities of the Upper Mantle, Tectonophysics, 2 (6), 483-514, Elsevier (1965).

Bevington, J., R., Eguchi, S., Ghosh, W., Graf, Z., Hu, P., Amyx, C., Huyck, M., Huyck, G., Esquivias, M., Eguchi and A., Vicini (2012). Indonesia Building Exposure Development. Inventory Data Capture Tools Risk Global Component, www.nexus.globalquakemodel.org/IDCT/posts/ (last accessed: 29/11/2019).

Bialik, C. (2015). USGS model suggests the Nepal earthquake death toll will keep climbing. FiveThirtyEight, April 27th, 2015.

Birkmann J., T., Welle, W., Solecki, S., Lwasa and M., Garschagen (2016). Boost resilience of small and mid-sized cities, Nature, Vol. 537, No 7622, 605-608.

Bommer, J. J., J., Douglas, F., Scherbaum, F., Cotton, H., Bungum and D., Fäh (2010). On the Selection of Ground-Motion Prediction Equations for Seismic Hazard Analysis, Vol. 81, No. 5, pp. 783-793.

Bonnefoy, N. (2019). Rapport D'information Fait Au Nom De La Mission D'Information Sur La Gestion Des Risques Climatiques Et L'Évolution De Nos Régimes D'Indemnisation, Sénat, Session Extraordinaire de 2018-2019, 628, 3 Juillet.

Born, P. H. and B. K., Klimaszewski-Blettner (2013). Should I Stay or Should I Go? The Impact of Natural Disasters and Regulation on U.S. Property Insurers' Supply Decisions, The Journal of Risk and Insurance, 2013, Vol. 80, No. 1, 1-36.

Bourguignon, D. (2014). Événements et territoires - le coût des inondations en France; analyses spatio-temporelles des dommages assurés, PhD Thesis, Université Paul Valéry – Montpellier III, France.

Brzev, S., M., Greene, C., Arnold, M., Blondet, S., Cherry, C. Comartin, D., D'Ayala, M., Farsi, S., Jain, F., Naeim, J., Pantelic, L., Samant and M., Sassu (2004). The Web-based World Housing Encyclopedia: Housing Construction in High Seismic Risk Areas of the World. 13th World Conference on Earthquake Engineering, Vancouver, BC, Canada, August 1-6, 2004.

Buffinton, P. (1961). Earthquake Insurance In The United States - A Reappraisal, Bull. Seism. Soc. Am. 51, 2, 315-329.

Burnett, B., and K., Burnett (2009). Is Quake Insurance Worth it?, SFGate, 25th March 2009, www.sfgate.com/homeandgarden/article/Is-quake-insurance-worth-it-3246888.php (last accessed: 12 / 01 / 2018).

Caisse Centrale de Réassurance (CCR) (2011). Le Régime D'indemnisation Des Catastrophes Naturelles, Caisse Centrale de Réassurance, November 17th, 2011, www.onrn.fr/site/binaries/content/assets/documents/plaquette-regime-cat-nat-2011-vf.pdf (last accessed: 23/09/2019).

Caisse Centrale de Réassurance (CCR) (2015). Natural disasters compensation scheme. www.ccr.fr/en/-/indemnisation-des-catastrophes-naturelles-en-france (last accessed: 11/11/2019).

Caisse Centrale de Réassurance (CCR) (2019a). Les Catastrophes Naturelles en France, Bilan 1982-2018, Caisse Centrale de Réassurance, https://bilancatnat.ccr.fr/ (last accessed: 03/10/2019).

Caisse Centrale de Réassurance (CCR) (2019b). Rapport Sur La Solvabilite et la Situation Financiere, Caisse Centrale de Réassurance, 31 décembre 2018, www.ccr.fr/informations-financieres (last accessed: 03/10/2019).

Caisse Centrale de Réassurance (CCR) (2019c). Groupe Caisse Centrale de Réassurance - Situation financière 2018 (www.ccr.fr/informations-financieres).

California Department of Insurance (CDI) (2015). State expands funding for incentives to protect vulnerable homes and property from earthquakes, California Department of Insurance, June 25th, 2015, www.insurance.ca.gov/0400-news/0100-press-releases/2015/release064-15.cfm (last accessed: 23/09/2019).

California Department of Insurance (CDI) (2019). Information Guides, Earthquake Insurance, www.insurance.ca.gov/01-consumers/105-type/95-guides/03-res/eq-ins.cfm (last accessed: 02 / 07 / 2019).

California Earthquake Authority (CEA) (2014). The Strength to Rebuild: Financial Foundations of the California Earthquake Authority, December 31th, www.earthquakeauthority.com/media/SiteAssets/Pages/Media-Resources/CEA\ (last accessed: 12/12/2019).

California Earthquake Authority (CEA) (2015a). The Resilient America Roundtable, July 10th, http://sites.nationalacademies.org/cs/groups/pgasite/documents/webpage/pga_167242.pdf (last accessed: 19/09/2019).

California Earthquake Authority (CEA) (2015b). Financial Report, December 31th, www.earthquakeauthority.com/whoweare/governingboard/Approved\ (last accessed: 12/12/2019).

California Earthquake Authority (CEA) (2016a). Backgrounder, California Earthquake Authority, 2016, www.earthquakeauthority.com/media/PublishingImages/Pages/Media-Resources/CEA\ (last accessed: 12/12/2019).

California Earthquake Authority (CEA) (2016b). Financial Report, California Earthquake Authority, July 31th, www.earthquakeauthority.com/whoweare/governingboard/Approved\ (last accessed: 12/12/2019).

California Earthquake Authority (CEA) (2016c). CEA Unveils Lower Rates, More Policy Options and Bigger Discounts for Earthquake Insurance, www.earthquakeauthority.com/EQA2/media/PressReleases/1-4-2016-CEA-Unveils-Lower-Rates-More-Policy-Options-Bigger-Discounts.pdf?ext=.pdf (last accessed: 29/10/2018).

California Earthquake Authority (CEA) (2017a). Retrofit Discounts and Incentives, February, http://www2.earthquakeauthority.com/earthquakerisk/Pages/Retrofit-Discounts-and-Incentives.aspx (last accessed: 20/09/2019).

California Earthquake Authority (CEA) (2017b). Our Financial Strength - More than $13 billion in claim-paying capacity, February, http://www2.earthquakeauthority.com/whoweare/financialstrength/Pages/default.aspx (last accessed: 03/10/2019).

California Earthquake Authority (CEA) (2017c). The Strength to Rebuild: Financial Foundations of the California Earthquake Authority, www.earthquakeauthority.com/Eqa/media/PDF/press-room/CEA-Financial-Overview-Documentas-of-6-30-2017.pdf (last accessed: 25/06/2019).

California Earthquake Authority (CEA) (2018a). CEA Governing Board Meeting, January 25th, 2018, www.earthquakeauthority.com/Eqa/media/Meeting-Materials/Governing-Board-Presentation-Slides.pdf (last accessed: 24/07/2019).

California Earthquake Authority (CEA) (2018b), Our Research. www.earthquakeauthority.com/About-CEA/Research-Outreach/Our-Research (last accessed: 29/10/2018).

California Earthquake Authority (CEA) (2018c). Earthquake Brace+Bolt surpasses 5,000 retrofits statewide, Press Release, June 7, 2018.

California Earthquake Authority (CEA) (2018d). CEA Governing Board Meeting, January 25th, 2018, www.earthquakeauthority.com/Eqa/media/Meeting-Materials/Governing-Board-Presentation-Slides.pdf (last accessed: 11/11/2019).

California Earthquake Authority (CEA) (2018e). Financial Statements, December 31, 2017 and 2016, www.earthquakeauthority.com/About-CEA/Financials/Financial-Statements (last accessed: 25/06/2019).

Calvi, G.M., R., Pinho, G., Magenes, J. J., Bommer, L. F., Restrepo-Vélez and H., Crowley (2006). Development Of Seismic Vulnerability Assessment Methodologies Over The Past 30 Years, ISET Journal of Earthquake Technology, Paper No. 472, Vol. 43, No. 3, pp. 75-104.

Canadian Underwriter (2016). IBC invites Quebecers to try out earthquake simulator, October 4th, www.canadianunderwriter.ca/insurance/ibc-invites-quebecers-try-earthquake-simulator-1004100958/ (last accessed: 03/12/2019).

Chen, Y. and D., Chen (2013). The review and analysis of compulsory insurance, Insurance Markets and Companies: Analyses and Actuarial Computations, Vol. 4, Issue 1.

Chiou, B. and R., Youngs (2008). An NGA model for the average horizontal component of peak ground motion and response spectra. Earthquake Spectra, 24(1), 173–215.

Choi, W., J.-W., Park and J., KIm (2019). Loss assessment of building and contents damage from the potential earthquake risk in Seoul, South Korea, Nat. Hazards Earth Syst. Sci., 19, 985–997.

CIMNE and INGENIAR (2015). Update on the Probabilistic Modelling of Natural Risks at Global Level: Global Risk Model, Global Earthquake and Tropical Cyclone Hazard Assessment. Disaster Risk Assessment at Country Level for Earthquakes, Tropical Cyclones (Wind and Storm Surge), Floods, Tsunami and Volcanic Eruptions; Centro Internacional de Métodos Numéricos en Ingeniería (CIMNE), Barcelona, Spain; Ingeniería para el Análisis del Riesgo Ingenieros Consultores (INGENIAR), Bogotá, Colombia; Prepared for the 2015 Global Assessment Report on Disaster Risk Reduction; www.preventionweb.net/english/hyogo/gar/2015/en/home/index.html (last accessed: 24 / 06 / 2018).

Clyde & Co LLP (2018). Parametric Insurance: closing the protection gap, Clyde & Co, Resilience, January 2018, www.clydeco.com/resilience/download (last accessed: 25/06/2019).

Consumers Union (1997). California Earthquake Authority to Consider Rate Decreases at Closed Session, Consumers Union, July 17th, 1997, http://consumersunion.org/1997/07/california_earthquake_authority_to_consider_rate_decreases_at_closed_session/ (last accessed: 19/09/2019).

Dan, M. B. (2018). Decision Making Based on Benefit-Costs Analysis: Costs of Preventive Retrofit versus Costs of Repair after Earthquake Hazards, Sustainability 2018, 10, 1537.

Dani, S. (2012). Building Regional Framework for Earthquake Risk Management, EAS, India Workshop, Global Facility for Disaster Reduction and Recovery, New Delhi, https://nidm.gov.in/easindia2012/PDF/Pres/Ses4/Pres1.pdf (last accessed: 13/01/2017).

Daniel, W. W. (1990). Applied nonparametric statistics, 2. ed. Boston: PWS-KENT.

Daniell, J. (2009). Comparison and production of open source earthquake loss assessment packages. Master degree, Università degli Studi di Pavia, Italy.

Daniell, J. and F., Wenzel (2014). The production of a robust worldwide rapid socio-economic loss model for earthquake economic loss and fatality estimation: success from 2009-2014. Australian Earthquake Engineering Society 2014 Conference, Nov 21-23, Lorne, Vic.

Daniell, J., B., Khazai, F., Wenzel and A., Vervaeck (2011). The CATDAT damaging earthquakes database. Natural Hazards Earth System Sciences, 11, 2235–2251.

Dixon, L. (2014). Catastrophic Risk in California Are Homeowners and Communities Prepared?, RAND Corporation, Testimony, www.rand.org/content/dam/rand/pubs/testimonies/CT400/CT417/RAND_CT417.pdf, (last accessed: 21/11/2018).

Dong, W. (2002). Engineering models for catastrophe risk and their application to insurance, Earthquake Engineering and Engineering vibration, Vol 1. No 1., 145-152, June 2002.

Douglas, J. (2019). Ground motion prediction equations 1964-2019, www.gmpe.org.uk/gmpereport2014.pdf (last accessed: 03/12/2019).

Dunbar, P. K., R. G., Bilham and M.J., Laituri (2003). Earthquake Loss Estimation for India Based on Macroeconomic Indicators, Risk Science and Sustainability Science for Reduction of Risk and Sustainable Development of Society (eds. Beer, T. & Ismail-Zadeh, A.) vol. 112 163–180 (Springer Netherlands).

Earthquake Brace+Bolt (2016). Homeowners Can Receive Up to $3,000 for an Earthquake Retrofit, Earthquake Brace+Bolt, 2016, www.ci.san-bernardino.ca.us/civicax/inc/blobfetch.aspx?BlobID=19904 (last accessed: 23/09/2019).

Earthquake Brace+Bolt (2017). Strengthen Your House - 2017 Homeowner Registration Is Open, Earthquake Brace+Bolt website, www.earthquakebracebolt.com/HomeownerRegistration (last accessed: 05/05/2017).

Egert, B. and D., Mihaljek (2007). Determinants of house prices in central and eastern Europe, BIS Working Papers, No 236, Monetary and Economic Department, Bank for International Settlements, www.bis.org/publ/work236.pdf (last accessed: 27/11/2019).

Eguchi, R., J., Goltz, C., Taylor, S., Chang, P., Flores, L., Johnson, H., Seligson and N., Blais (1998). Direct Economic Losses in the Northridge Earthquake: A Three-Year Post-Event Perspective, Earthquake Spectra, 14, 2.

Eleftheriadou, A. K. and A. I., Karabinis (2008). Damage Probability Matrices Derived From Earthquake, 14th World Conference on Earthquake Engineering, October 12-17, Beijing, China.

Ellis, V. (2000). Quackenbush Rejected Steep Fines for Insurers, Los Angeles Times, April 02, 2000.

Eren, C. and H., Lus (2014). Impact Of Risk Based PML Estimation On Earthquake Insurance Rates For Industrial Buildings In Turkey, Second European Conference on Earthquake Engineering and Seismology, Istanbul, Aug. 25-29, 2014.

Ericson, A. and C., Mitas (2012). RMS Model Use & Uncertainty, CAMAR, 10/10/2012, www.casact.org/community/affiliates/camar/1012/uncertainty.pdf (last accessed: 03/12/2019).

Federal Emergency Management Agency (FEMA) (1999). Earthquake loss estimation methodology earthquake HAZUS99 Service Release 2 (SR2) technical manual. Washington

Federal Emergency Management Agency (FEMA) (2010). HAZUS-MH MR5, Earthquake Loss Estimation Methodology. Federal Emergency Management Agency, Washington, DC, U.S.A.

Federal Emergency Management Agency (FEMA) (2017). Hazus Estimated Annualized Earthquake Losses for the United States. Federal Emergency Management Agency, FEMA P-366, Washington, DC, U.S.A. www.fema.gov/media-library-data/1497362829336-7831a863fd9c5490379b28409d541efe/FEMAP-366_2017.pdf (last accessed: 11/11/2019).

Fédération Française de l'Assurance (FFA) (2017). L'assurance des Catastrophes Naturelles en 2015, Etude – janvier 2017, www.mrn.asso.fr/wp-content/uploads/2018/01/2017-chiffres-assurance-des-catastrophes-naturelles-en-2015-ffa.pdf (last accessed: 11/12/2019).

Field, E. H., G. P., Biasi, P., Bird, T. E., Dawson, K. R., Felzer, D. D., Jackson, K. M., Johnson, T. H., Jordan, C., Madden, A. J., Michael, K. R., Milner, M. T., Page, T., Parsons, P. M., Powers, B. E., Shaw, W. R., Thatcher, R. J., Weldon and Y., Zeng (2013) Uniform California earthquake rupture forecast, version 3 (UCERF3) – The time-independent model, US Geological Survey Open-File Report 2013-1165, California Geological Survey Special Report 228, and Southern California Earthquake Center Publication 1792, p. 97.

Field, E. H., P. M., Powers, Y., Zeng, B. E., Shaw, W. R., Thatcher, R. J., Weldon, R. J., Arrowsmith, G. P., Biasi, D. D., Jackson, P., Bird, A. J., Michael, T. E., Dawson, T., Parsons, K. R., Felzer, M. T., Page, K. M., Johnson, K. R., Milner, T. H., Jordan and C., Madden (2014). Uniform California Earthquake Rupture Forecast version 3 (UCERF3)—The Time-Independent Model Uniform California Earthquake Rupture Forecast, Bulletin of the Seismological Society of America 104, 1122–1180.

Field, E. H., P. M., Powers, Y., Zeng, T., Parsons, B. E., Shaw, R. J., Weldon, G. P., Biasi, D. D., Jackson, P., Bird, T. E., Dawson, K. R., Felzer, M. T., Page, K. M., Johnson, K. R., Milner, T. H., Jordan, C., Madden, A. J., Michael and W. R., Thatcher (2015). Uniform California Earthquake Rupture Forecast version 3 (UCERF3) – Long-Term Time-Dependent Probabilities for the UCERF3, Bulletin of the Seismological Society of America 105, 511–543.

Franco G., G., Tirabassi, M., Lopeman, D. J., Wald and W. J. ,Siembieda (2018).Increasing Earthquake Insurance Coverage In California Via Parametric Hedges, 11th National Conference in Earthquake Engineering, Los Angeles, California.

Franco, G. and B., Shen-Tu (2009). From 1755 to Today—Reassessing Lisbon's Earthquake Risk, AIR Worldwide, July 15th, www.air-worldwide.com/Publications/AIR-Currents/From-1755-to-Today (last accessed: 12/12/2019).

Frécon, J.C., and F., Keller (2009). Rapport d'information N°39 fait au nom du groupe de travail sur la situation des sinistrés de la sécheresse de 2003 et le régime d'indemnisation des catastrophes naturelles constitué par la commission des finances, Session ordinaire de 2009-2010, Sénat.

Freeman, J. (1932). Earthquake Damage And Earthquake Insurance, Mc Graw-Hill Book Company Inc., New York and London, First Edition.

Fujiwara, H., N., Morikawa, Y., Ishikawa, T., Okumura, J., Miyakoshi, N., Nojima and Y., Fukushima (2009). Statistical comparison of national probabilistic seismic hazard maps and frequency of recorded JMA seismic intensities from the K-NET strong-motion observation network in Japan during 1997–2006, Seismol. Res. Lett., 80, 458–464.

Fuller, T. (2018). In Quake-Prone California, Alarm at Scant Insurance Coverage, New York Times, Aug. 31, 2018.

Fuller, T. and I., Kang (2018). California Today: Who Owns the Risk for Earthquakes?, New York Times, September 11th, 2018.

Garamendi, J. (2003). California Earthquake Zoning And Probable Maximum Loss Evaluation Program, An Analysis Of Potential Insured Earthquake Losses From Questionnaires Submitted To The California Department Of Insurance By Licensed Property/Casualty Insurers In California For 1997 To 2001, California Department of Insurance, www.insurance.ca.gov/0400-news/0200-studies-reports/upload/EQ_PML_RPT_1997_2001.pdf (last accessed: 19/09/2019).

Garamendi, J., R., Roth, S., Sam, and T., Van (1992). California Earthquake Zoning And Probable Maximum Loss Evaluation Program: An Annual Estimate Of Potential Insured Earthquake Losses From Analysis Of Data Submitted By Property And Casualty Companies In California, California Department of Insurance, Los Angeles, California, Diane Pub Co, 1992.

Gardner, J. and L., Knopoff (1974). Is the sequence of earthquakes in southern California, with aftershocks removed, Poissonian?, Bulletin of the Seismological Society of America, No.465, Vol. 64, pages 1363-1367, October 1974.

Garratt, R. and J. M., Marshall (2003). Equity Risk, Conversion Risk, and The Demand For Insurance, The Journal of Risk and Insurance, 2003, Vol. 70, No. 3, 439-460.

Geschwind, C. (1997). 1920s Prediction Reveals Some Pitfalls of Earthquake Forecasting, Eos, 78, 38, 401-412.

Geschwind, C. (2001). California Earthquakes: Science, Risk & the Politics of Hazard Mitigation, The Joins Hopkins University Press.

Ghesquiere, F. and O., Mahul (2010). Financial Protection of the State against Natural Disasters: A Primer, Policy Research Working Paper, 5429, the World Bank, Latin American and the Caribbean Region Finance and Private Sector Development Sustainable Development Network, September.

Giardini, D., G., Grünthal, K., Shedlock and P., Zhang (1999). The GSHAP Global Seismic Hazard Map, Annali di Geofisica, Vol. 42, No. 6, pages 1225-1230, December 1999.

Gilbert, G. K. (1909). Earthquake Forecasts. Science, New Series, Vol. 29, No. 734, pp. 121-138.

Gioncu, V. and F. M., Mazzolani (2011). Earthquake Engineering for Structural Design, Spon Press, 2011, www.sadra.ac.ir/images/userfiles/files/03.pdf (last accessed: 18/09/2019).

Goltz J. D. and the Southern California Earthquake Preparedness Project (1985). Earthquake Insurance: A Public Policy Dilemma, Earthquake Hazards Reduction Series 7, FEMA.

Goltz, J. D. (1985). Earthquake Insurance: A Public Policy Dilemma, Earthquake Hazards Reduction Series 7, Federal Emergency Management Agency, Southern California Earthquake Preparedness Project, www.fema.gov/media-library-data/20130726-1600-20490-8046/fema_68.pdf (last accessed: 17/09/2019).

Graizer, V. and E., Kalkan (2016). Summary of the GK15 Ground-Motion Prediction Equation for Horizontal PGA and 5% Damped PSA from Shallow Crustal Continental Earthquakes, Bulletin of the Seismological Society of America, Vol. 106, No. 2, pages 687-707.

Grossi, P., W., Dong and A., Boissonnade (2008). Evolution of Earthquake Risk Modeling, The 14th World Conference on Earthquake Engineering, October 12-17, 2008, Beijing, China.

Grünthal, G., R.M.W., Musson, J., Schwarz, M., Stucchi and the ESC Working Group "Macroseismic Scales". (1998). European Macroseismic Scale 1998, EMS-98, Cahiers du Centre Européen de Géodynamique et de Séismologie, Volume 15, Luxembourg 1998.

Guettiche A., Guéguen P., Mimoune M. (2018). Economic and human loss empirical models for earthquakes in the Mediterranean region, with particular focus on Algeria. International Journal of Disaster Risk Science.

Gustin, P. (2008). How Federal Disasters are Declared, Episcopal Relief & Development, www.episcopalrelief.org/uploads/EducationFileModel/60/file/FACT-Fed-Disaster-Declaration.pdf (last accessed: 03/10/2019).

Haddad, E. (2017). Les notions de contrat d'assurance. Droit. Université Panthéon-Sorbonne - Paris I, 2017.

Harrell, F. E. (2015). Regression Modeling Strategies. Cham: Springer International Publishing.

Harvey P, A., Stoddard, A., Harmer and G., Taylor (2010). The state of the humanitarian system, assessing performance and progress, a pilot study. Active Learning Network for Accountability and Performance in Humanitarian Action.

Hazewinkel, M., Ed. (1988). Encyclopaedia of mathematics: an updated and annotated translation of the Soviet Mathematical encyclopaedia, Dordrecht ; Boston : Norwell, MA, U.S.A: Reidel ; Sold and distributed in the U.S.A. and Canada by Kluwer Academic Publishers.

Hill, M. and T., Rossetto (2008a). Do Existing Damage Scales meet the needs of seismic loss estimation? The 14th World Conference on Earthquake Engineering.

Hill, M. and T., Rossetto (2008b). Comparison of building damage scales and damage descriptions for use in earthquake loss modelling in Europe, Bull Earthquake Eng, 6, 335-365.

Holt, C., and S., Laury (2002). Risk Aversion and Incentive Effects, Am. Econ. Rev., 92, 5, 1644-1655.

Holzheu, T. and G., Turner (2018). The Natural Catastrophe Protection Gap: Measurement, Root Causes and Ways of Addressing Underinsurance for Extreme Events, the Geneva Papers, 2018, 43, 37-71.

Iervolino, I. (2013). Probabilities and Fallacies: Why Hazard Maps Cannot Be Validated by Individual Earthquakes, Earthquake Spectra, Vol. 29, No. 3, pages 1125–1136, August 2013.

IFSO (2017). Homeowners face insurance shortfalls after earthquakes: Do you have enough cover?, Insurance and Financial Services Ombudsman, February 16, 2017, http://ifso.nz/news-and-publications/media-releases/homeowners-face-insurance-shortfalls-after-earthquakes-do-you-have-enough-cover/ (last accessed: 04/10/2019).

Insurance Information Bureau of India (2001). Circular FT/1/2001: All India Fire Tariff - Revision of Petrochemical Tariff, Insurance Information Bureau of India, January 31th 2001, https://iib.gov.in/IIB/tac/circulars/fcir2001.htm (last accessed: 03/10/2019).

Insurance Information Institute (2016). Earthquakes: Risk and Insurance Issues, Insurance Information Institute, www.iii.org/issue-update/earthquakes-risk-and-insurance-issues (last accessed: 18/09/2016).

Insurance Information Institute (2018). The San Francisco earthquake of 1906: An insurance perspective, www.iii.org/article/san-francisco-earthquake-1906-insurance-perspective (last accessed: 29/10/2018).

Insurance Journal (2017). California Homeowner Registration Starts for 2017 Brace + Bolt Program, Insurance Journal, January 26th, 2017, www.insurancejournal.com/uncategorized/2017/01/26/440011.htm?print (last accessed: 23/09/2019).

Irsyam, M., S., Widiyantoro, D., Natawidjaja, I., Meilano, A., Rudyanto, S., Hidayati, W., Triyoso, N., Hanifa, D., Djarwadi, L., Faizal and S.T. M.T., Sunarjito (2017). Peta Sumber Dan Bahaya Gempa Indonesia Tahun (2017), Pusat Penelitian dan pengembangan perumahan dan permukiman, Badan Penelitian dan Pengembangan, Kementerian Pekerjaan Umum dan Perumahan Rakyat, http://geotek.lipi.go.id/wp-content/uploads/2018/02/BUKU-PETA-GEMPA-2017.pdf (last accessed: 24 / 06 / 2018).

Irwansyah, E. and S., Hartati (2014). Assessment of Building Damage Hazard Caused by Earthquake: Integration of FNN and GIS, IERI Procedia, vol. 10, pp. 196–202.

Jaffee, D. M. and T., Russell (1997). Catastrophe Insurance, Capital Markets, and Uninsurable Risks, the Journal of Risk and Insurance, 1997, Vol. 64, No. 2, 205-230.

Jaiswal, K. S. and D. J., Wald (2008). Creating a global building inventory for earthquake loss assessment and risk management. U.S. Geological Survey Open-File Report 2008-1160, 103 p.

Jaiswal, K. S. and D. J., Wald (2011). Rapid estimation of the economic consequences of global earthquakes: U.S. Geological Survey Open-File Report 2011-1116, 47 p.

Jaiswal, K. S., D., Bausch, J., Holub, S., McGowan and J., Rozelle (2017). Estimated Annualized Earthquake Losses for the United States, FEMA P-366, FEMA, USGS and PDC, April 2017.

Jergler, D. (2017). Exclusive: California Broker Plans Parametric Quake Product That Pays Even If No Damage, Insurance Journal, July 21, 2017.

Jones, C. I. (2016). The Facts of Economic Growth, In Handbook of Macroeconomics, 2:3–69. Elsevier.

Jones, D., G., Yen and the Rate Specialist Bureau of the Rate Regulation Branch (2012). California Earthquake Zoning And Probable Maximum Loss Evaluation Program, An Analysis Of Potential Insured Earthquake Losses From Questionnaires Submitted To The California Department Of Insurance By Licensed Property/Casualty Insurers In California For 2002 To 2010, California Department of Insurance, May 2012, www.insurance.ca.gov/0400-news/0200-studies-reports/upload/EQ_PML_RPT_2002_2010.pdf (last accessed: 17 / 12 / 2017).

Jones, L. M., R., Bernknopf, D., Cox , J., Goltz, K., Hudnut, D., Mileti, S., Perry, D., Ponti, K., Porter, M., Reichle, H., Seligson, K., Shoaf, J., Treiman, and A., Wein (2008). The ShakeOut Scenario, U.S. Geological Survey Open-File Report 2008-1150 and California Geological Survey Preliminary Report 25.

Kaas, R., M., Goovaerts, J., Dhaene and M., Denuit (2008) Collective risk models. In: Modern Actuarial Risk Theory. Springer, Berlin, Heidelberg.

Kappos, A. J., G., Panagopoulos, C., Panagiotopoulos and G. Penelis (2006). A hybrid method for the vulnerability assessment of R/C and URM buildings. Bulletin of Earthquake Engineering. 4(4): 391-413.

Knowles, D. (1997). 1995-1996 Legislative Summary, California Legislature Assembly Committee on Insurance, April 24th, 1997, http://digitalcommons.law.ggu.edu/cgi/viewcontent.cgi?article=1381&context=caldocs_assembly (last accessed: 19/09/2019).

Kovacevic, R. M. and G. C., Pflug (2011). Does Insurance Help To Escape The Poverty Trap? - A Ruin Theoretic Approach, The Journal of Risk and Insurance, 2011, Vol. 78, No. 4, 1003-1027.

KPMG (2016). Insurance in Indonesia: Opportunities in a Dynamic Market, KPMG, April, https://assets.kpmg.com/content/dam/kpmg/id/pdf/id-ksa-insurance-in-indonesia.pdf (last accessed: 03/10/2019).

Krieger, L. M. (2017). California may give you $3,000 to protect your home from earthquake, The Mercury News, January 25th, 2017, www.mercurynews.com/2017/01/25/state-may-give-you-3000-to-protect-your-home-from-earthquake/ (last accessed: 23/09/2019).

Kunreuther, H. (2015). Reducing Losses from Extreme Events, Insurance Thought Leadership, August 11th, 2015, http://insurancethoughtleadership.com/tag/earthquake/ (last accessed: 19/09/2019).

Kunreuther, H., N., Doherty and A., Kleffner (1992). Should Society Deal with the Earthquake Problem?, Regulation, The CATO Review of Business & Government, Spring 1992, 60-68.

Kunreuther, H., R., Ginsberg, L., Miller, P., Sagi, P., Slovic, B., Borkan and N., Katz (1978). Disaster Insurance Protection, Wiley-Interscience Publication, John Wiley & Sons, New York.

Kunreuther, H., R., Roth, J., Davis, K., Gahagan, R., Klein, E., Lecomte, C., Nyce, R., Palm, E., Pasterick, W., Petak, C., Taylor and E., VanMarcke (1998). Paying the Price: The Status and Role of Insurance Against Natural Disasters in the United States. Washington, DC: Joseph Henry Press.

Lagomarsino, S. and S., Giovinazzi (2006). Macroseismic and mechanical models for the vulnerability and damage assessment of current buildings. Bulletin of Earthquake Engineering 4:415-443.

Lagorio, H., R., Olson, S., Scott, K., Goettel, K., Mizukoshi, M., Miyamura, Y., Miura, T., Yamada, M., Nakahara and H., Ishida (1992). Multidisciplinary Strategies for Earthquake Hazard Mitigation - Earthquake Insurance, California Universities for Research in Earthquake Engineering, Kajima Corporation, Final Project Report, Report No. CK 92-04, February 15th, 1992.

Lang, D. (2012). Earthquake Damage and Loss Assessment – Predicting the Unpredictable. PhD Thesis, the University of Bergen, Norway.

Lange, G.-M., Q., Wodon, and K., Carey, eds. (2018). The Changing Wealth of Nations 2018: Building a Sustainable Future. Washington, DC: World Bank.

Latourrette, T., J., Dertouzos, C., Steiner and N., Clancy (2010). The Effect Of Catastrophe Obligation Guarantees On Federal Disaster-Assistance Expenditures In California, RAND Corporation, www.rand.org/content/dam/rand/pubs/technical_reports/2010/RAND_TR896.pdf (last accessed: 07/12/2017).

Laux, C., G., Lenciauskaite and A., Muermann (2016). Foreclosure and Catastrophe Insurance, Preliminary Version, www.google.fr/url?sa=t&rct=j&q=&esrc=s&source=web&cd=4&ved=2ahUKEwiV-MLm8oPfAhXILFAKHVoKCBkQFjADegQIBxAC&url=https%3A%2F%2Fwww.aeaweb.org%2Fconference%2F2017%2Fpreliminary%2Fpaper%2F3ANB85Z9&usg=AOvVaw2prQoPn4ZrFaZsLVW8fs40 (last accessed: 03/12/2018).

Les Furets (2016). Combien coûte l'assurance habitation en France? LesFurets.com, October 13th, 2016, www.lesfurets.com/assurance-habitation/actualites/combien-coute-lassurance-habitation-france (last accessed: 03/10/2019).

Lin II, R. G. (2015). California budget will fund 1,000 single-family home retrofits, Los Angeles Times, June 26th, 2015.

Lin, X. J. (2013). The Interaction between Risk Classification and Adverse selection: Evidence from California's Residential Earthquake Insurance Market, Preliminary Version, University of Wisconsin-Madison, http://citeseerx.ist.psu.edu/viewdoc/download?doi=10.1.1.386.7172&rep=rep1&type=pdf (last accessed: f25/06/2019).

Lin, X. J. (2015). Feeling Is Believing? Evidence from Earthquake Insurance Market, World Risk and Insurance Economics Congress, www.wriec.net/wp-content/uploads/2015/07/1G2_Lin.pdf (last accessed: 07/12/2017).

Lloyds (2019). Instant claims for earthquake damage, www.lloyds.com/~/media/files/news-and-insight/risk-insight/2019/lloydsparametric_case_studiesv3part1.pdf (last accessed: 11/11/2019).

MacDonalds, L. (2017). Small town homeowners under-insured for Kaikoura quake rebuilds, Stuff, February 17th, 2017, www.stuff.co.nz/business/89289928/small-town-homeowners-underinsured-for-kaikoura-quake-rebuilds (last accessed: 04/10/2019).

Marquis F., J. J., Kim, K. J., Elwood and S. E., Chang (2017). Understanding post-earthquake decisions on multi-storey concrete buildings in Christchurch, New Zealand, Bull Earthquake Eng, 15, 731–758.

Marshall, D. (2017). The California Earthquake Authority, Discussion paper, Resources for the Future, Wharton university of Pennsylvania, Resources for the future, RFF DP 17-05, February, www.soa.org/Files/Research/Projects/2017-02-discussion-california-earthquake-authority.pdf (last accessed: 11/11/2019).

Marshall, D. (2018). An Overview Of The California Earthquake Authority, Risk Management and Insurance Review, 21, 1, 73-116.

McAlister, A. (1984): California Legislature 1983–84, Assembly Bill No. 2865, Regular Session, available at: http://leginfo.ca.gov/pub/95-96/bill/asm/ab_1351-1400/ab_1366_cfa_950719_145442_sen_floor.html (last accessed: 11/11/2019), 13 February 1984.

Melecky, M. and C., Raddatz (2011). How Do Governments Respond after Catastrophes? Natural-Disaster Shocks and the Fiscal Stance, Policy Research Working Paper 5564, The World Bank, Europe and Central Asia Region, Private & Financial Sectors Development Sector Unit.

Meltsner, A. (1978). Public Support For Seismic Safety: Where Is It In California?, Mass Emergencies, 3, 167-184, Elsevier.

Meroni, F., T., Squarcina, V., Pessina, M., Locati, M., Modic and R. Zoboli (2017). A Damage Scenario for the 2012 Northern Italy Earthquakes and Estimation of the Economic Losses to Residential Buildings. Springer.

Milutinovic, Z. and G., Trendafiloski (2003). An advanced approach to earthquake risk scenarios with applications to different European towns. European Commission; RISK-UE; WP4 Vulnerability of current buildings, No. of pages 110 (Figs. 18, Tables 48, Appendices 2).

Miyazawa, M. and J., Mori (2009). Test of Seismic Hazard Map from 500 Years of Recorded Intensity Data in Japan, Bulletin of the Seismological Society of America, Vol. 99, No. 6, pp. 3140–3149.

Molesky, M. (2016) This Gulf of Fire: The Great Lisbon Earthquake, or Apocalypse in the Age of Science and Reason, Vintage; Reprint edition.

Monning, W. W. and the Senate Committee on Insurance (2014). Informational Hearing: Catastrophic Risk in California: Are Homeowners and Communities prepared?, California State Senate, May 14th, 2014.

Moudi, M., S., Yan, B., Bahramimianrood, X., Li and L., Yao (2019). Statistical model for earthquake economic loss estimation using GDP and DPI: a case study from Iran, Quality & Quantity 53:583–598.

Mouroux, P., B., Le Brun, S., Depinois E., Bertrand and P., Masure (2004) – Projet européen RISK-UE: application à la ville de Nice. Rapport BRGM/RP-53202, 137 p., 43 ill., 3 Annexes.

Muir-Wood, R. (2016a). How strong is 'disaster culture' in earthquake-prone L.A.?, Los Angeles Times, October 16th, 2016.

Muir-Wood, R. (2016b). The Cure for Catastrophe: How We Can Stop Manufacturing Natural Disasters, Oneworld Publiations 2016.

Mukherji, S. (2011). The Capital Asset Pricing Model's Risk-Free Rate, The International Journal of Business and Finance Research, Volume 5, Number 2, 2011.

Mulligan, T. S. (1994). Fair Plan Earthquake Insurance Detailed, Los Angeles Times, November 9th, 1994.

Mullin, J. R. (1992). The reconstruction of Lisbon following the earthquake of 1755: a study in despotic planning, The Journal of the International History of City Planning Association, 45.

Musson, R. M., W., G. Grünthal and M., Stucchi (2009). The comparison of macroseismic intensity scales. Journal of Seismology, Springer Verlag, 14 (2), pp.413-428.

Narahari, Y. (2012). Game Theory: Chapter 7: Von Neumann-Morgenstern Utilities, Department of Computer Science and Automation Indian Institute of Science, August 2012, http://lcm.csa.iisc.ernet.in/gametheory/ln/web-ncp7-utility.pdf (last accessed: 02/07/2019).

Natural Hazards Observer (2006). The 1906 Earthquake and Public Policy, Natural Hazards Center, University of Colorado, May 2006.

Neumayer, E. and F., Barthel (2011). Normalizing economic loss from natural disasters: A global analysis, Global Environmental Change 21, 1, 13-24.

Nowicki, A. (2014). The top 10 residential construction companies, ConstructionDive, September 12th, 2014, www.constructiondive.com/news/the-top-10-residential-construction-companies/298164/ (last accessed: 24/06/2019).

Noy, I., A., Kusuma and C., Nguyen (2017). Insuring disasters: A survey of the economics of insurance programs for earthquakes and droughts. University of Wellington, Victoria Business School, Working Papers in Economics and Finance.

O' Connor, J. and the Forintek Canada Corp. (2004). Survey on actual service lives for North American buildings, Woodframe Housing Durability and Disaster Issues conference, Las Vegas, October 2004, http://cwc.ca/wp-content/uploads/2013/12/DurabilityService_Life_E.pdf (last accessed: 24/06/2019).

OECD (2018). Financial Management of Earthquake Risk, www.oecd.org/finance/Financial-Management-of-Earthquake-Risk.htm (last accessed: 24/06/2019).

O'Mara, K. (2016). How to Apply for 'Earthquake Brace and Bolt' Retrofit Funding, KQED News, January 21th, 2016. https://ww2.kqed.org/news/2016/01/21/how-to-apply-for-earthquake-brace-and-bolt-retrofit-funding/ (last accessed: 23/09/2019).

Osteraas, J. D. and A., Gupta (2008). Order Out Of Chaos: Application of Earthquake Damage Assessment and Repair Guidelines, The 14thWorld Conference on Earthquake Engineering, October 12-17, 2008, Beijing, China.

Ousley, A. and J., Wilkinson (2016). EBB Opens Registration for $3,000 Grants to Strengthen Older California Homes against Earthquakes, California Earthquake Authority, January 20th, 2016, www.earthquakeauthority.com/media/Lists/Press\

Palm, R. (1995). The Roepke Lecture in Economic Geography Catastrophic Earthquake Insurance: Patterns of Adoption, Georgia State University, Geosciences Faculty Publications, https://scholarworks.gsu.edu/cgi/viewcontent.cgi?referer=https://www.google.fr/&httpsredir=1&article=1008&context=geosciences_facpub (last accessed: 10/04/2018).

Palm, R. and M., Hodgson (1992a). Earthquake Insurance: Mandated Disclosure and Homeowner Response in California, Georgia State University, Geosciences Faculty Publications, https://pdfs.semanticscholar.org/5dc9/191ddb964e99a5def2060dad57ce0e96ab45.pdf (last accessed: 07/12/2017).

Palm, R. and M., Hodgson (1992b). After a California Earthquake: Attitude and Behavior Change, The University of Chicago, Geography Research Paper No. 223, 1992.

Papadimitriou, E. E. and B. C., Papazachos (1994). Time Dependent Seismicity in the Indonesian Region, J. Geophys. Res., 99(B8), 15387– 15398.

Patmore, N. (2008), Using Insurance Catastrophe Models to Investigate the Economics of Climate Change Impacts and Adaptation, Risk Management Solutions, http://docplayer.net/9253809-Using-insurance-catastrophe-models-to-investigate-the-economics-of-climate-change-impacts-and-adaptation.html, (last accessed: 03/12/2019).

Patton, B. (2014). Square pegs and round holes: A history of earthquake insurance in California and a look towards the future, California Earthquake Authority, May 15th, 2014, www.casact.org/community/affiliates/sccac/0514/Earthquake_insurance.pdf (last accessed: 19/09/2019).

Pereira, A. (2009). The Opportunity of a Disaster: The Economic Impact of the 1755 Lisbon Earthquake, The Journal of Economic History, Vol. 69, No. 2, pp. 466-499.

Petersen, M., D.J., Dewey, S., Hartzell, C., Mueller, S., Harmsen, A.D., Frankel and K., Rukstales (2004). Probabilistic seismic hazard analysis for Sumatra, Indonesia and across the Southern Malaysian Peninsula, Tectonophysics, 390, p. 141-158.

Petersen, M., S., Harmsen, C., Mueller, K., Haller, J., Dewey, N., Luco, A., Crone, D., Lidke and K., Rukstales (2007). Documentation for the Southeast Asia Seismic HazardMaps, Administrative Report September 30, 2007, U.S. Geological Survey.

Petseti, A., and M., Nektarios (2012). Proposal for a National Earthquake Insurance Programme for Greece, The Geneva Papers on Risk and Insurance - Issues and Practice, 37, 377-400.

Phadnis, S. (2016). Koyna earthquakes triggered by reservoir, claim seismologist, The Times of India, February 2nd, 2016.

Polacek, A. (2018). Catastrophe bonds: A primer and retrospective, Chicago Fed Letter.

Pomeroy, G. (2010). Approaches to Mitigating and Managing Natural Catastrophe Risk: H.R.2555, The Homeowners' Defense Act, https://docplayer.net/10442644-Testimony-of-glenn-pomeroy-chief-executive-officer-california-earthquake-authority.html (last accessed: 29/10/2018).

Popov, E. P. (1994). Development of US Seismic Codes, Journal of Constructional Steel Research, 29, 191-207.

Porter K. A., J. L., Beck, R. V., Shaikhutdinov, S., Kiu Au, K., Mizukoshi, M., Miyamura, H., Ishida, T., Moroi, Y., Tsukada and M., Masuda (2004). Effect of Seismic Risk on Lifetime Property Value, Earthquake Spectra, Vol 20, No 4, pp 1211-1237.

Porter, K. A., C. R., Scawthorn and J. L., Beck (2006). Cost-Effectiveness of Stronger Woodframe Buildings, Earthquake Spectra 22, 1, 239-266.

Pratt, J. W. (1964). Risk Aversion in the Small and in the Large. Econometrica. 32 (1–2): 122–136

Reich, K. (1996a). Quackenbush Limits Access to Fair Plan, Los Angeles Times, May 23th 1996.

Reich, K. (1996b). 2 Insurers to Resume Sale of New Home Policies, Los Angeles Times, October 30th, 1996.

Reich, K. (1996c). Earthquake Insurance Agency Is Born, Los Angeles Times, September 28, 1996.

République Française (2016). Indemnisation des victimes des inondations, République Française, June 2016, www.gouvernement.fr/indemnisation-des-victimes-des-inondations-5104 (last accessed: 03/10/2019).

Rey, J., C., Beauval and J., Douglas (2018). Do French macroseismic intensity observations agree with expectations from the European Seismic Hazard Model 2013?, J Seismol, 22, 589- 604.

Riedel, I. (2015). Seismic vulnerability analysis of existent buildings. Loss estimation and uncertainty analysis for deterministic earthquake scenarios. PhD Thesis, Université Grenoble Alpes, France.

Riedel, I. and P., Guéguen (2018). Modeling of damage-related earthquake losses in a moderate seismic-prone country and cost–benefit evaluation of retrofit investments: application to France, Journal of the International Society for the Prevention and Mitigation of Natural Hazards, 2018, vol. 90, issue 2, 639-662.

Riedel, I., P., Guéguen, M. D., Mura, E., Pathier, T., Leduc and J., Chanussot (2015). Seismic vulnerability assessment of urban environments in moderate-to-low seismic hazard regions using association rule learning and support vector machine methods, Natural Hazards, vol. 76, no. 2, pp. 1111–1141.

RMS (2004). Northridge Earthquake 10-year Retrospective, Risk Management Solutions, https://forms2.rms.com/rs/729-DJX-565/images/eq_northridge_ca_eq.pdf (last accessed: 18/09/2019).

Rodrigues, L. L. and R., Craig (2008), Recovery amid Destruction: Manoel da Maya and the Lisbon Earthquake of 1755, Libraries & the Cultural Record, Vol. 43, No. 4, pp. 397-410.

Roger, A. (2019). Post-Apocalyptic Insurers Try Out a New 'Make it Rain' Strategy, Wired, February 28, 2019, www.wired.com/story/post-apocalyptic-insurers-are-trying-out-a-cash-bomb-strategy (last accessed: 11/11/2019).

Rokach, L. and O., Maimon (2005). "Clustering Methods," in Data Mining and Knowledge Discovery Handbook, O. Maimon and L. Rokach, Eds. New York: Springer-Verlag, pp. 321–352.

Roth, R. J. (1997). Insurance: What are the Principles of Insuring Natural Disasters?, Earthquake Basic Brief, No 3, Earthquake Engineering Research Institute, April 1997.

Ruffle, S., J., Smith and Stride Design Ltd, Cambridge UK (2012). GEM Earthquake Damage Database specification. GEM Technical Report, GEM Foundation.

Sanchez, J. (1996). Homeowners Rush for State Quake Coverage, Los Angeles Times, May 31th 1996.

Sands, S. P. and E. G., Brown Jr (2014). Contractors Wanted: Earthquake Brace + Bolt Expands in 2015, California State Licence Board, 2014, www.cslb.ca.gov/Newsletter/2014-Fall/bracebolt.asp (last accessed: 23/09/2019).

Scotti, O., D., Baumont, G., Quenet and A., Levret (2004). The French macroseismic database SISFRANCE: objectives, results and perspectives, Annals of geophysics 47(2/3) 571-581.

Sergeant, J. (2016). 'Sum Insured' cover for household insurance - what are the risks?, The Treasury New Zealand, May 9th, 2016, www.treasury.govt.nz/publications/research-policy/staff-insights/sum-insured-cover-household-insurance (last accessed: 04/10/2019).

Sergeant, J., D., Watts, J., Beard, B., English, S., Joyce and P., Bennett (2015). Home Insurance – Implications of Sum Insured Cover, The Treasury New Zealand, June 23th, 2015, https://treasury.govt.nz/sites/default/files/2017-11/oia-20160145.pdf (last accessed: 04/10/2019).

Shenhar, G., I., Radomislensky, M., Rozenfeld and K., Peleg (2015). The Impact of a National Earthquake Campaign on Public Preparedness: 2011 Campaign in Israel as a Case Study, Disaster Medicine and Public Health Preparedness, 9 2, 138-144.

Shiller, R. J. (2015) Real Building Cost Index, www.quandl.com/data/YALE/RBCI-Historical-Housing-Market-Data-Real-Building-Cost-Index (last accessed: 20/07/2018).

Shiller, R. J. (2015). Irrational Exuberance: Revised and Expanded Third Edition, 3rd Edition, Princeton University Press, Broadway book.

Shiver Jr, J. (1991). Earthquake Insurance: Is It Worth the Price?, Los Angeles Times, June 29th, 1991, http://articles.latimes.com/1991-06-29/news/mn-1185_1_earthquake-insurance (last accessed: 17/07/2018).

Silva, V., H., Crowley, K., Jaiswal, A. B., Acevedo, M., Pittore and M., Journey (2018). Developing A Global Earthquake Risk Model, 17 European Conference on Earthquake Engineering, Thessaloniki.

Slud, E. V. (2001). Actuarial Mathematics and Life-Table Statistics, Statistics Program, Mathematics Department, University of Maryland, College Park (USA), www.math.umd.edu/~slud/s470/BookChaps/01Book.pdf (last accessed : 07/10/2019).

Snyder, J. A. (1995). Drop Quake-Coverage Mandate, Up Rates: Insurance: Both steps are needed to maintain the industry's stability, not profits, Los Angeles Times, April 3rd, 1995.

Spence, R., E., So, and C., Scawthorn, eds. (2011). Human Casualties in Earthquakes. Advances in Natural and Technological Hazards Research. Springer Netherlands.

Steinbrugge, K., H., Lagorio, and S., Algermissen (1980). Earthquake insurance and microzoned geologic hazards; United States practice. Proceedings of the World Conference on Earthquake Engineering 7, Vol 9, Id 321, www.iitk.ac.in/nicee/wcee/article/7_vol9_321.pdf (last accessed: 17/12/2017).

Stirling, M. and M., Gerstenberger (2010). Ground Motion–Based Testing of Seismic Hazard Models in New Zealand, Bulletin of the Seismological Society of America, Vol. 100, No. 4, pages 1407-1414.

Stoer, J. and R., Bulirsch (2002). Introduction to numerical analysis, 3rd ed., Texts in applied mathematics. Springer, New York.

Strasser, F. O., N. A., Abrahamson and J. J., Bommer (2009). Sigma: Issues, Insights, and Challenges, Seismological Research Letters, Vol. 80, No. 1, pp. 40-56.

Tabucchi, T. H. P. and P., Grossi (2012). 2011 Tohoku, Japan Earthquake Catastrophe Modeling Response, 15th World Conference on Earthquake Engineering, Lisbon.

Tang, Y., Y., Yin, K., Hill, V., Katiyar, A., Nasseri and T., Lai (2012), Seismic Risk Assessment of Lisbon Metropolitan Area under a Recurrence of the 1755 Earthquake with Tsunami Inundation, 15th World Conference on Earthquake Engineering, Lisbon.

Tasan, H., C., Beauval, A., Helmstetter, A., Sandikkaya and P., Guéguen (2014). Testing probabilistic seismic hazard estimates against accelerometric data in two countries: France and Turkey, Geophysical Journal International, 198, pages 1554-1571.

Thevenin, L. (2017). Catastrophes naturelles: un déficit de protection abyssal, Les Echos, January 1st, 2017.

Thevenin, L., G. Maujean and N., Barré (2018). Thomas Buberl: « La France est en pleine renaissance », Les Echos, January 11th, 2018.

Tijms, H. C. (2003). A First Course in Stochastic Models, John Wiley and Sons, Chichester (England).

Tyagunov, S., L., Stempniewski, G., Grünthal, R., Wahlstrom and J., Zschau (2004). Vulnerability and risk assessment for earthquake prone cities. 13th World Conference on Earthquake Engineering.

UN-Habitat and AXA (2019). Supporting Safer Housing Reconstruction after Disasters, Planning and Implementing Technical Assistance at Large Scale, http://urbanresiliencehub.org/housingreconstruction/ (last accessed: 03/12/2019).

Von Neumann, J. and O., Morgenstern (1944), Theory of Games and Economic Behavior, Princetown University Press.

Vranes, K. and R. Jr., Pielke (2009). Normalized Earthquake Damage and Fatalities in the United States: 1900–2005, Natural Hazards Review, 10(3), 84–101.

Wachtendorf, T. and X., Sheng (2002). Influence Of Social Demographic Characteristics And Past Earthquake Experience On Earthquake Risk Perceptions, Disaster Research Center, University of Delaware, www.drs.dpri.kyoto-u.ac.jp/us-japan/cd-2/TriciaWachtendorf.pdf (last accessed: 27/12/2016).

Wald, D. J. and T. I., Allen (2007). Topographic slope as a proxy for seismic site conditions and amplification, Bulletin of the Seismological Society of America, 97, no. 5, 1379-1395.

Wald, D. J., C. B., Worden, V., Quitariano, and K., Pankow (2005). ShakeMap manual: Users guide, technical manual, and software guide, U.S. Geol. Surv. Techniques and Methods 12–A1; U.S. Geol. Surv. available at http://pubs.usgs.gov/tm/2005/12A01/ (last accessed: June 2018).

Wald, D.J., K., Jaiswal, K., Marano, P., Earle and T.I., Alen (2009). Advancements in Casualty Modeling Facilitated by the USGS Prompt Assessment of Global Earthquakes for Response (PAGER) System, Second International Workshop on Disaster Casualties, 15-16 June 2009, University of Cambridge, UK.

Wei, X., J., Liu, X., Guodong, W., Ying, L., Lianyou and S., Peijun (2016). Natural disasters in China. Springer, Berlin Heidelberg.

Weiss, N. A., P. T., Holmes, and M., Hardy (2006). A course in probability. Boston: Pearson Addison Wesley.

Werland, D. L. and J. W., Pitts (1997). Pricing Earthquake Exposure Using Modeling, Journal of Actuarial Practice 1993-2006. 105.

Wiley, K. and the Seismic Safety Commission (2000). Twenty-five Years of Protecting Life and Property From Earthquake Threats in California, Living Where the Earth Shakes, A History of the California Seismic Safety Commission, California Senate Office of Research.

World Bank (2019). World Bank Catastrophe Bond Transaction Insures the Republic of Philippines against Natural Disaster-related Losses Up to US$225 million, November 25th, www.worldbank.org/en/news/press-release/2019/11/25/world-bank-catastrophe-bond-transaction-insures-the-republic-of-philippines-against-natural-disaster-related-losses-up-to-usd225-million (last accessed: 03/12/2019).

Xia, R. and R. G., Lin II (2016). Registration begins for $3,000 grants to retrofit homes against earthquakes, Los Angeles Times, January 20th, 2016.

Yeats, R. S. (2001). Living with Earthquakes in California: A Survivor's Guide, Oregon State University Press, 2001.

Yeats, R. S. (2004). Living with Earthquakes in the Pacific Northwest, Oregon State University Press Corvallis, 2nd edition, 2004, http://oregonstate.edu/instruct/oer/Earthquake.pdf (last accessed: 17/09/2019).

Yucemen, M. S. (2005). Probabilistic Assessment of Earthquake Insurance Rates for Turkey, Nat. Hazards, 35, 291-313.

Zhao, J., J., Zhang, A., Asano, Y., Ohno, T., Oouchi, T., Takahashi, H., Ogawa, K., Irikura, H., Thio, P., Somerville, Y., Fukushima and Y., Fukushima (2006). Attenuation relations of strong ground motion in Japan using site classification based on predominant period; Bulletin of the Seismological Society of America, 96(3), 898–913.

# APPENDIX

## A. The Expected Utility theory

The Expected Utility theory (also called the Von Neumann-Morgenstern Utilities), was introduced in 1947 by Von Neumann and Morgenstern. It models a decision-maker's preference from a *basket of goods* (materialized by the function *g*), according to his *utility*. Under this framework, the *utility* is defined as the satisfaction that a decision-maker retrieves from the goods he gets. The *utility* is measured by a *utility function*, $U_i$, where *i* is the name of the decision-maker. The function $U_i$ is defined by the Von Neumann-Morgenstern (1944) theorem which is based on several axioms that could be split in six parts (Narahari 2012). For the two firsts, let us considering a basket of three goods: $b=\{g_1; g_2; g_3\}$. Then, the two first axioms state that:

1. **Completeness**: the decision-maker can always compare two goods (e.g. $g_1$ and $g_2$) and decide which one he prefers or if the both are equal.
2. **Transitivity**: If the decision-maker prefers $g_1$ to $g_2$ and $g_2$ to $g_3$, then he also prefers $g_1$ to $g_3$.

Let us now considering that the decision-maker does not select a good from a basket of goods $b=\{g_1; g_3\}$ but instead participates to a lottery $l_1$ on *b*. We introduce $p_1$ and $1 - p_1$ as the probability for the decision-maker to win the good $g_1$ and $g_3$, respectively. Similarly, $l_2$ is the lottery on *b* with the probabilities $p_2$ and $1 - p_2$. Here, the decision-maker can choose between two different lotteries. On this basis, the four remaining axioms are:

3. **Substitutability**: The decision-maker has no preference between $l_1$ and the same lottery where $g_1$ is changed by $g_4$ if the decision-maker has no preference between $g_1$ and $g_4$.
4. **Decomposability**: The decision-maker has no preference on the way to carry on the lottery $l_1$, as long as long as the probabilities ($p_1$ and $1 - p_1$) remain the same.
5. **Monotonicity**: Between $l_1$ and $l_2$, the decision-maker always prefer the one with the higher chance to win its favourite good (i.e. if he prefers $g_1$ to $g_3$, then the decision-maker prefers $l_1$ to $l_2$ when $p_1 > p_2$, and reciprocally).

6. **Continuity**: If the decision-maker prefers $g_1$ to $g_2$ and $g_2$ to $g_3$, it exists a value of $p_1$ for which the decision-maker has no preference between having $g_2$ and participating at $l_1$.

According to the Von Neumann-Morgenstern theorem, a utility function associates to a good $g_1$ a level of utility $U_i(g_1)$ for the decision-maker $i$. When the good $g_1$ is replaced by a lottery $l_1$, this theorem states that the level of utility is the weighted average: $U_i(l_1) = p_1 \times U_i(g_1) + (1 - p_1) \times U_i(g_3)$.

The first property of $U_i$ is to be strictly increasing (i.e. its first derivative $U_i'$ is strictly positive). When $g_1$ corresponds to the decision-maker's wealth, like in this study, it means that the decision-maker always wants to increase his level of wealth. At the opposite, the sign of the second derivative, $U_i''$, can be positive (i.e. $U_i$ is convex) or negative (i.e. $U_i$ is concave). It represents the decision maker's behaviour: when $U_i''<0$, the decision maker is risk averse, meaning that the difference of utility between $g_1$ and $g_1+1$ is decreasing when $g_1$ increases. Still considering that $g_1$ is the decision-maker's wealth, it means that increasing the wealth by + €100 provides a higher utility for a decision-maker with a wealth $g_1$ = €1,000 than for one with a wealth $g_1$ = €1,000,000. In terms of insurance, a risk-averse decision maker wants to be covered. Indeed, assuming that the decision-maker can be protected against losing $g_1$ with a probability $p_1$ when paying a premium amount $P_N = p_1 \times g_1$. Since the utility function is concave, the following equation is verified:

$$U_i(0) \times p_1 + U_i(g_1) \times (1 - p_1) < U_i(g_1 - P_N) \qquad (A.1)$$

Conversely, when $U_i''>0$, the decision-maker is risk-loving and behave in the opposite way.

Depending on the choice of $U_i$, this behaviour (risk-averse or risk-loving) can change depending on $g_1$. To represent it, the Arrow-Pratt measure of relative risk aversion (named after Pratt 1964 and Arrow 1965) is used:

$$RRA(g_1) = g_1 \times \frac{-U_i''(g_1)}{U_i'(g_1)} \qquad (A.2)$$

when *RRA* is decreasing, increasing or constant, it means that the decision-maker is less, more, or indifferently risk averse with the value of the good $g_1$.

The utility function $U_i$ used in this study has been developed by Holt and Laury (2002).

$$U_i(g_1) = \begin{cases} \frac{{g_1}^{1-\beta_i}}{1-\beta_i} & \text{if } \beta_i \neq 1 \\ \ln(g_1) & \text{else} \end{cases} \qquad (A.3)$$

Where $\beta_i$ is the *level of relative risk aversion* and materializes the decision-maker's risk behaviour from highly risk loving to highly risk averse. Indeed, one can verify that the *RRA* measure for the Holt and Laury (2002) utility function is: $RRA(g_1) = \beta_i$. Therefore, this function belongs to the Constant Risk Relative Aversion utility function family. It means that for a decision-maker behaviour is supposed uncorrelated to his wealth level ($g_1$). Furthermore, the parameter $\beta_i$ controls the decision-maker behaviour (Tab. A1).

Table A.1. Risk preference scale depending on the parameter $\beta_i$. Source: Holt and Laury (2002).

| Risk preference classification | Range of relative risk aversion |
|---|---|
| highly risk loving | $\beta i < -0.95$ |
| very risk loving | $-0.95 < \beta i < -0.49$ |
| risk loving | $-0.49 < \beta i < -0.15$ |
| risk neutral | $-0.15 < \beta i < 0.15$ |
| slightly risk averse | $0.15 < \beta i < 0.41$ |
| risk averse | $0.41 < \beta i < 0.68$ |
| very risk averse | $0.68 < \beta i < 0.97$ |
| highly risk averse | $0.97 < \beta i < 1.37$ |
| stay in bed | $1.37 < \beta i$ |

# B. Solution of the expected utility maximization equation

Let us consider the following mathematical problem in (Eq. 3.2.14):

$$t_N^{Estimated} = \underset{0 \le t_N \le 1}{\operatorname{argmax}} \mathbb{E}\left(U\left(g_N(t_N)\right)\right) \tag{3.2.14}$$

The function $f(t_N) = \mathbb{E}\,[U(g_N(t_N))]$ can be rewritten by detailing the expression of the expected utility $\mathbb{E}$:

$$f(t_N) = U\left(g_N(t_N)\right) \times \mathbb{P}\left(\mathcal{B}_{EQ}(r_N) = 0\right) + U\left(g_N(t_N)\right) \times \mathbb{P}\left(\mathcal{B}_{EQ}(r_N) = 1\right) \tag{B.1}$$

Introducing the definition of $g_N(t_N)$ (Eq. B.1) gives:

$$\begin{aligned} f(t_N) = {} & U(K - t_N \times P_N) \times \mathbb{P}\left(\mathcal{B}_{EQ}(r_N) = 0\right) \\ & + U\left(K - t_N \times P_N - K \times (1 - t_N)\right) \times \mathbb{P}\left(\mathcal{B}_{EQ}(r_N) = 1\right) \end{aligned} \tag{B.2}$$

Using next the definition of the function $U$ (Eq. 3.2.12), $f(t_N)$ becomes:

$$\begin{aligned} f(t_N) = {} & \left(\frac{(K - t_N \times P_N)^{1-\beta}}{1-\beta}\right) \times \mathbb{P}\left(\mathcal{B}_{EQ}(r_N) = 0\right) \\ & + \left(\frac{\left(t_N \times (K - P_N)\right)^{1-\beta}}{1-\beta}\right) \times \mathbb{P}\left(\mathcal{B}_{EQ}(r_N) = 1\right) \end{aligned} \tag{B.3}$$

$$f(t_N) = \frac{1}{1-\beta} \times \left((1 - r_N) \times (K - t_N \times P_N)^{1-\beta} + r_N \times (K - P_N)^{1-\beta} \times {t_N}^{1-\beta}\right)$$

Furthermore, the derivative of $f(t_N)$ is equal to:

$$\begin{cases} \dfrac{\delta f(t)}{\delta t_N} = (-P_N) \times (1 - r_N) \times (K - t_N \times P_N)^{-\beta} + r_N \times (K - P_N)^{1-\beta} \times {t_N}^{-\beta} \\ \dfrac{\delta f(0)}{\delta t_N} = +\infty \\ \dfrac{\delta f(1)}{\delta t_N} = (K - P_N)^{-\beta} \times (K \times r_N - P_N) \end{cases} \tag{B.4}$$

Thus, when $\delta f(1)/\ \delta t_N < 0$; $t_N^{Estimated}$ is equal to (otherwise, $t_N^{Estimated} = 1$):

$$\frac{\delta f\left(t = t_N^{Estimated}\right)}{\delta t_N} = 0 \Leftrightarrow \left(\frac{K}{t_N^{Estimated}} - P_N\right)^{-\beta} \times P_N \times (1 - r_N) = r_N \times (K - P_N)^{1-\beta} \tag{B.5}$$

$$t_N^{Estimated} \Leftrightarrow \frac{K \times X}{K - P_N + P_N \times X}$$

where:

$$X = \left(\frac{r_N \times (K - P_N)}{P_N \times (1 - r_N)}\right)^{\frac{1}{\beta}} \quad \text{(B. 6)}$$

As the expression of $t_N^{Estimated}$ is complex, it can be simplified using the approximation: $P_N/K \approx 0$:

$$t_N^{Estimated} = X \quad \text{(B. 7)}$$

$$t_N^{Estimated} = \left(\frac{r_N \times (K - P_N)}{P_N \times (1 - r_N)}\right)^{\frac{1}{\beta}}$$

$$t_N^{Estimated} = \left(\frac{r_N}{(1 - r_N)} \times \frac{K}{P_N}\right)^{\frac{1}{\beta}} \times \left(1 - \frac{P_N}{K}\right)^{\frac{1}{\beta}}$$

$$t_N^{Estimated} = \left(\frac{r_N}{(1 - r_N)} \times \frac{K}{P_N}\right)^{\frac{1}{\beta}}$$

## C. Expression of the premium amount $P_1$ when considering the date of retrofitting works

The premium amount $P_1$ is defined by (Eq. 5.7):

$$\sum_{i=1}^{+\infty}\left[P_1 \times (1+t_I)^{i-1} \times \mathbb{P}\left(Y_{EQ} \geq i\right)\right] = \frac{36\%}{81\%} \times \left(\mathbb{E}\left(L_{EQ}\right) - F\right) \tag{5.7}$$

The left-hand term of Equation 5.7 can be split according to the four periods: [1; $T^{LC}$]; ]$T^{LC}$; $T^{MC}$]; ]$T^{MC}$; $T^{HC}$]; and ]$T^{HC}$; +∞[ standing for the Pre-Code, Low-Code, Moderate-Code and High-Code vulnerability profile. Using the Law of Total Probability (Tijms 2003), the probability $\mathbb{P}\left(Y_{EQ} \geq i\right)$ is equal to:

$$\begin{aligned}\mathbb{P}\left(Y_{EQ} \geq i\right) = {} & \mathbb{P}\left(Y_{EQ} \geq i | Y_{EQ} \leq T^{LC}\right) \times \mathbb{P}\left(Y_{EQ} \leq T^{LC}\right) \\ & + \mathbb{P}\left(Y_{EQ} \geq i | T^{LC} < Y_{EQ} \leq T^{MC}\right) \times \mathbb{P}\left(T^{LC} < Y_{EQ} \leq T^{MC}\right) \\ & + \mathbb{P}\left(Y_{EQ} \geq i | T^{MC} < Y_{EQ} \leq T^{HC}\right) \times \mathbb{P}\left(T^{MC} < Y_{EQ} \leq T^{HC}\right) \\ & + \mathbb{P}\left(Y_{EQ} \geq i | T^{HC} < Y_{EQ}\right) \times \mathbb{P}\left(T^{HC} < Y_{EQ}\right)\end{aligned} \tag{C.1}$$

The expression of the expected total amount of $P_1$ becomes (left-hand term in Eq. 5.7):

$$\begin{aligned}&\sum_{i=1}^{+\infty}\left[P_1 \times (1+t_I)^{i-1} \times \mathbb{P}\left(Y_{EQ} \geq i\right)\right] \\ &= \sum_{i=1}^{+\infty}\left[P_1 \times (1+t_I)^{i-1} \times \mathbb{P}\left(Y_{EQ} \geq i | Y_{EQ} \leq T^{LC}\right) \times \mathbb{P}\left(Y_{EQ} \leq T^{LC}\right)\right] \\ &+ \sum_{i=1}^{+\infty}\left[P_1 \times (1+t_I)^{i-1} \times \mathbb{P}\left(Y_{EQ} \geq i | T^{LC} < Y_{EQ} \leq T^{MC}\right) \times \mathbb{P}\left(T^{LC} < Y_{EQ} \leq T^{MC}\right)\right] \\ &+ \sum_{i=1}^{+\infty}\left[P_1 \times (1+t_I)^{i-1} \times \mathbb{P}\left(Y_{EQ} \geq i | T^{MC} < Y_{EQ} \leq T^{HC}\right) \times \mathbb{P}\left(T^{MC} < Y_{EQ} \leq T^{HC}\right)\right] \\ &+ \sum_{i=1}^{+\infty}\left[P_1 \times (1+t_I)^{i-1} \times \mathbb{P}\left(Y_{EQ} \geq i | T^{HC} < Y_{EQ}\right) \times \mathbb{P}\left(T^{HC} < Y_{EQ}\right)\right]\end{aligned} \tag{C.2}$$

Then, noticing that:

$$\begin{cases} \sum_{i=T^{LC}+1}^{+\infty} \left[P_1 \times (1+t_I)^{i-1} \times \mathbb{P}\left(Y_{EQ} \geq i | Y_{EQ} \leq T^{LC}\right) \times \mathbb{P}\left(Y_{EQ} \leq T^{LC}\right)\right] = 0 \\ \sum_{i=T^{MC}+1}^{+\infty} \left[P_1 \times (1+t_I)^{i-1} \times \mathbb{P}\left(Y_{EQ} \geq i | T^{LC} < Y_{EQ} \leq T^{MC}\right) \times \mathbb{P}\left(T^{LC} < Y_{EQ} \leq T^{MC}\right)\right] = 0 \\ \sum_{i=T^{HC}+1}^{+\infty} \left[P_1 \times (1+t_I)^{i-1} \times \mathbb{P}\left(Y_{EQ} \geq i | T^{MC} < Y_{EQ} \leq T^{HC}\right) \times \mathbb{P}\left(T^{MC} < Y_{EQ} \leq T^{HC}\right)\right] = 0 \end{cases} \quad (C.3)$$

Equation C.2 can be simplified as follows:

$$\sum_{i=1}^{+\infty} \left[P_1 \times (1+t_I)^{i-1} \times \mathbb{P}\left(Y_{EQ} \geq i\right)\right] \quad (C.4)$$

$$\begin{aligned} &= \sum_{i=1}^{T^{LC}} \left[P_1 \times (1+t_I)^{i-1} \times \mathbb{P}\left(Y_{EQ} \geq i | Y_{EQ} \leq T^{LC}\right)\right] \times \mathbb{P}\left(Y_{EQ} \leq T^{LC}\right) \\ &+ \sum_{i=1}^{T^{MC}} \left[P_1 \times (1+t_I)^{i-1} \times \mathbb{P}\left(Y_{EQ} \geq i | T^{LC} < Y_{EQ} \leq T^{MC}\right)\right] \times \mathbb{P}\left(T^{LC} < Y_{EQ} \leq T^{MC}\right) \\ &+ \sum_{i=1}^{T^{HC}} \left[P_1 \times (1+t_I)^{i-1} \times \mathbb{P}\left(Y_{EQ} \geq i | T^{MC} < Y_{EQ} \leq T^{HC}\right)\right] \times \mathbb{P}\left(T^{MC} < Y_{EQ} \leq T^{HC}\right) \\ &+ \sum_{i=1}^{+\infty} \left[P_1 \times (1+t_I)^{i-1} \times \mathbb{P}\left(Y_{EQ} \geq i | T^{HC} < Y_{EQ}\right)\right] \times \mathbb{P}\left(T^{HC} < Y_{EQ}\right) \end{aligned}$$

Finally, Equation C.4 gives a new expression of the expected total amount of $P_1$ actualised, where each term corresponds to a different period delineated by the dates of retrofitting works.

## D. Calculating the premium amount in case of time independent earthquake model

Let us suppose that the year of occurrence of the next damaging earthquake, $Y_{EQ}$, is distributed according to an Exponential distribution. Therefore, Equation 5.11 can be simplified using the memoryless property of the Exponential distribution. Equation 5.11 is given by:

$$\sum_{i=1}^{+\infty}\left[P_1 \times (1+t_I)^{i-1} \times \mathbb{P}\left(Y_{EQ} \geq i\right)\right] \tag{5.11}$$

$$= \sum_{i=1}^{T^{LC}}\left[P_1 \times (1+t_I)^{i-1} \times \mathbb{P}\left(Y_{EQ} \geq i | Y_{EQ} \leq T^{LC}\right)\right] \times \mathbb{P}\left(Y_{EQ} \leq T^{LC}\right)$$

$$+ \sum_{i=1}^{T^{MC}}\left[P_1 \times (1+t_I)^{i-1} \times \mathbb{P}\left(Y_{EQ} \geq i | T^{LC} < Y_{EQ} \leq T^{MC}\right)\right] \times \mathbb{P}\left(T^{LC} < Y_{EQ} \leq T^{MC}\right)$$

$$+ \sum_{i=1}^{T^{HC}}\left[P_1 \times (1+t_I)^{i-1} \times \mathbb{P}\left(Y_{EQ} \geq i | T^{MC} < Y_{EQ} \leq T^{HC}\right)\right] \times \mathbb{P}\left(T^{MC} < Y_{EQ} \leq T^{HC}\right)$$

$$+ \sum_{i=1}^{+\infty}\left[P_1 \times (1+t_I)^{i-1} \times \mathbb{P}\left(Y_{EQ} \geq i | T^{HC} < Y_{EQ}\right)\right] \times \mathbb{P}\left(T^{HC} < Y_{EQ}\right)$$

It can be rewritten as follows:

$$\sum_{i=1}^{+\infty}\left[P_1 \times (1+t_I)^{i-1} \times \mathbb{P}\left(Y_{EQ} \geq i\right)\right] = E_{LC} + E_{MC} + E_{HC} + E_{+\infty} \tag{D. 1}$$

where:

$$\begin{cases} E_{LC} = \sum_{i=1}^{T^{LC}}\left[P_1 \times (1+t_I)^{i-1} \times P\left(Y_{EQ} \geq i | Y_{EQ} \leq T^{LC}\right)\right] \times P\left(Y_{EQ} \leq T^{LC}\right) \\ E_{MC} = \sum_{i=1}^{T^{MC}}\left[P_1 \times (1+t_I)^{i-1} \times P\left(Y_{EQ} \geq i | T^{LC} < Y_{EQ} \leq T^{MC}\right)\right] \times P\left(T^{LC} < Y_{EQ} \leq T^{MC}\right) \\ E_{HC} = \sum_{i=1}^{T^{HC}}\left[P_1 \times (1+t_I)^{i-1} \times P\left(Y_{EQ} \geq i | T^{MC} < Y_{EQ} \leq T^{HC}\right)\right] \times P\left(T^{MC} < Y_{EQ} \leq T^{HC}\right) \\ E_{+\infty} = \sum_{i=1}^{+\infty}\left[P_1 \times (1+t_I)^{i-1} \times P\left(Y_{EQ} \geq i | T^{HC} < Y_{EQ}\right)\right] \times P\left(T^{HC} < Y_{EQ}\right) \end{cases} \tag{D. 2}$$

As $Y_{EQ}$ follows an Exponential distribution, $E_{MC}$ becomes:

$$
\begin{aligned}
E_{MC} = {} & \mathbb{P}\left(T^{LC} < Y_{EQ} \le T^{MC}\right) \\
& \times \left( \sum_{i=1}^{T^{LC}} \left[ P_1 \times (1+t_I)^{i-1} \right] \right. \\
& \left. + \sum_{i=T^{LC}+1}^{T^{MC}} \left[ P_1 \times (1+t_I)^{i-1} \times \mathbb{P}\left(Y_{EQ} \ge i \middle| T^{LC} < Y_{EQ} \le T^{MC}\right) \right] \right) \\
= {} & \mathbb{P}\left(T^{LC} < Y_{EQ} \le T^{MC}\right) \\
& \times \left( P_1 \times \frac{(1+t_I)^{T^{LC}} - 1}{t_I} \right. \\
& \left. + \sum_{i=1}^{T^{MC}-T^{LC}} \left[ P_1 \times (1+t_I)^{i+T^{LC}-1} \times \mathbb{P}\left(Y_{EQ} \ge i + T^{LC} \middle| T^{LC} < Y_{EQ} \le T^{MC}\right) \right] \right) \\
= {} & \mathbb{P}\left(T^{LC} < Y_{EQ} \le T^{MC}\right) \times P_1 \times \frac{(1+t_I)^{T^{LC}} - 1}{t_I} \\
& + \left( \sum_{i=1}^{T^{MC}-T^{LC}} \left[ P_1 \times (1+t_I)^{i+T^{LC}-1} \times \mathbb{P}\left(i + T^{LC} \le Y_{EQ} \le T^{MC}\right) \right] \right) \\
= {} & \mathbb{P}\left(T^{LC} < Y_{EQ} \le T^{MC}\right) \times P_1 \times \frac{(1+t_I)^{T^{LC}} - 1}{t_I} \\
& + \left( \sum_{i=1}^{T^{MC}-T^{LC}} P_1 \times (1+t_I)^{i+T^{LC}-1} \times \left[ \mathbb{P}\left(Y_{EQ} \ge i + T^{LC}\right) - \mathbb{P}\left(Y_{EQ} > T^{MC}\right) \right] \right) \\
= {} & \mathbb{P}\left(T^{LC} < Y_{EQ} \le T^{MC}\right) \times P_1 \times \frac{(1+t_I)^{T^{LC}} - 1}{t_I} \\
& + \left( \sum_{i=1}^{T^{MC}-T^{LC}} P_1 \times (1+t_I)^{i+T^{LC}-1} \right. \\
& \times \left[ \mathbb{P}\left(Y_{EQ} \ge i + T^{LC} \middle| Y_{EQ} \ge T^{LC}\right) \times \mathbb{P}\left(Y_{EQ} \ge T^{LC}\right) - \mathbb{P}\left(Y_{EQ} > T^{MC} \middle| Y_{EQ} \ge T^{LC}\right) \right. \\
& \left. \left. \times \mathbb{P}\left(Y_{EQ} \ge T^{LC}\right) \right] \right)
\end{aligned}
\tag{D.3}
$$

$$E_{MC} = \mathbb{P}\left(T^{LC} < Y_{EQ} \leq T^{MC}\right) \times P_1 \times \frac{(1+t_I)^{T^{LC}} - 1}{t_I} + \left( \sum_{i=1}^{T^{MC}-T^{LC}} P_1 \times (1+t_I)^{i+T^{LC}-1} \times \left[\mathbb{P}\left(Y_{EQ} \geq i\right) \times \mathbb{P}\left(Y_{EQ} \geq T^{LC}\right) - \mathbb{P}\left(Y_{EQ} > T^{MC} - T^{LC}\right) \times \mathbb{P}\left(Y_{EQ} \geq T^{LC}\right)\right] \right)$$

$$= \mathbb{P}\left(T^{LC} < Y_{EQ} \leq T^{MC}\right) \times P_1 \times \frac{(1+t_I)^{T^{LC}} - 1}{t_I} + \left( \mathbb{P}\left(Y_{EQ} \geq T^{LC}\right) \times (1+t_I)^{T^{LC}} \times \sum_{i=1}^{T^{MC}-T^{LC}} P_1 \times (1+t_I)^{i-1} \times \left[\mathbb{P}\left(Y_{EQ} \geq i\right) - \mathbb{P}\left(Y_{EQ} > T^{MC} - T^{LC}\right)\right] \right)$$

$$= \mathbb{P}\left(T^{LC} < Y_{EQ} \leq T^{MC}\right) \times P_1 \times \frac{(1+t_I)^{T^{LC}} - 1}{t_I} + \mathbb{P}\left(Y_{EQ} \geq T^{LC}\right) \times (1+t_I)^{T^{LC}} \times \left( \sum_{i=1}^{T^{MC}-T^{LC}} P_1 \times (1+t_I)^{i-1} \times \mathbb{P}\left(i \leq Y_{EQ} \leq T^{MC} - T^{LC}\right) \right)$$

Replacing $T^{LC}$ by 1 and $T^{MC}$ by $T^{LC}$ in Equation D.3 gives the new expression of $E_{MC}$. Similarly, $E_{HC}$ and $E_{+\infty}$ can be obtained by replacing $(T^{LC}; T^{MC})$ by $(T^{MC}; T^{HC})$ and $(T^{HC}; +\infty)$ in Equation D.3, respectively. Finally, $P_1$ is solution of this new equation when $Y_{EQ}$ is distributed according to an Exponential distribution:

$$\sum_{i=1}^{+\infty} \left[P_1 \times (1+t_I)^{i-1} \times \mathbb{P}\left(Y_{EQ} \geq i\right)\right] \tag{D.4}$$

$$= \left[ \left( \sum_{i=1}^{T^{LC}} P_1 \times (1+t_I)^{i-1} \times \mathbb{P}\left(T^{LC} \geq Y_{EQ} \geq i\right) \right) \right] + \left[ \mathbb{P}\left(T^{LC} < Y_{EQ} \leq T^{MC}\right) \times P_1 \times \frac{(1+t_I)^{T^{LC}} - 1}{t_I} + \mathbb{P}\left(Y_{EQ} \geq T^{LC}\right) \times (1+t_I)^{T^{LC}} \times \left( \sum_{i=1}^{T^{MC}-T^{LC}} P_1 \times (1+t_I)^{i-1} \times \mathbb{P}\left(T^{MC} - T^{LC} \geq Y_{EQ} \geq i\right) \right) \right]$$

$$+\left[\mathbb{P}\left(T^{MC} < Y_{EQ} \leq T^{HC}\right) \times P_1 \times \frac{(1+t_I)^{T^{MC}}-1}{t_I} + \mathbb{P}\left(Y_{EQ} \geq T^{MC}\right) \times (1+t_I)^{T^{MC}}\right.$$
$$\left.\times\left(\sum_{i=1}^{T^{HC}-T^{MC}} P_1 \times (1+t_I)^{i-1} \times \mathbb{P}\left(T^{HC}-T^{MC} \geq Y_{EQ} \geq i\right)\right)\right]$$
$$+\left[\mathbb{P}\left(T^{HC} < Y_{EQ}\right) \times P_1 \times \frac{(1+t_I)^{T^{HC}}-1}{t_I} + \mathbb{P}\left(Y_{EQ} \geq T^{HC}\right) \times (1+t_I)^{T^{HC}}\right.$$
$$\left.\times\left(\sum_{i=1}^{+\infty} P_1 \times (1+t_I)^{i-1} \times \mathbb{P}\left(Y_{EQ} \geq i\right)\right)\right]$$